

adaptive fabric façade for a high-rise in paris



p5 report | July 2017



antigoni lampadari-matsa | 4516907



adaptive fabric façade for a high-rise in paris

antigoni lampadari-matsa | 4516907

p5 report | July 2017



MSc Architecture, Urbanism and Building Sciences | Building Technology track

main mentor: Prof.dr.ing. U. Knaack
second mantor: Dr. R.M.J. Bokel
delegate examiner: Dr. ir. A. Koutamanis

acknowledgments

Time flies...I can confirm this "saying" after seven months of being fully occupied with my graduation project. It was a challenging and interesting experience, through which I gained a great amount of knowledge on a topic that I hadn't dealt with before. Of course, as it happens with every thesis, I wouldn't have made it on my own.

At this point I would like to thank my mentors, Prof. dr. ing. U. Knaack and Dr. R.M.J. Bokel, who both provided me with helpful knowledge, comments and questions in order to understand the problems that occurred throughout the whole graduation process and come up with prosperous solutions. With their encouragement and support I managed to bring this project to a successful end. Furthermore, I would like to thank Dr. ing. Marcel Bilow for the valuable and practical help in the matter of materials and fabrication methods he provided for the construction of the model for the acoustic test, despite the fact that he was not part of my mentors' team. Moreover, I would like to express my gratitude to Dr.ir. M.J. Tenpierik, who

was the reason for the realisation of the acoustic test, as he provided the knowledge and the required equipment, as well as the software needed for the processing of the measured results.

Also, I would like to thank Mitchell Everts for his collaboration, mainly for the accomplishment of the acoustic test and also in general, as he dealt with a similar topic and the exchange of knowledge and ideas between us was really helpful to comprehend better the specific topic.

Additionally, I would like to thank my friends for supporting me during these two years and of course for sharing unforgettable experiences together. Along with this, I would like to thank a special friend that has changed my life to a better extent.

Finally, a special thanks goes to my family who has been supporting me all these years, and no matter the distance, is always there to encourage my efforts and achievements.

The topic of this graduation project is the design of an adaptive fabric façade for a high-rise in Paris. The stimulus for this choice was the turn of nowadays towards lightweight materials and constructions, a trend that is growing tremendously. Glass façades always remain popular and are frequently used in all kinds of buildings. For instance, a great quantity of glass is used in curtain walls. Therefore, following the need of research for lightweight materials, alternatives for glass are being investigated and membranes can be an interesting solution. They offer a number of possibilities and have many advantages, such as a variety of transparency levels and the fact that they are extremely lightweight materials. Furthermore, this graduation project concerns an office building, which is a rather demanding building type, as it requires a building envelope that offers a high level of indoor comfort, in terms of thermal and acoustical insulation, as well as efficient solar control.

Thus, taking all the above into account and the global growing interest towards membranes, which are mostly used as roof components until now, the decision of exploring the potential of such materials as the main part of a building envelope for an open-plan office building in Paris was taken.

The graduation research has an experimental character, as it tackles several issues of a possible membrane façade element and it tries to answer the questions that are being raised throughout of the development of this thesis. Firstly, a literature research is conducted on the available materials, their physical and mechanical properties, their production and connection methods, their advantages and drawbacks in general. Subsequently, design aspects are taken into consideration concerning the building envelope and physical models are constructed in order to visualise the design. Furthermore, hand calculations are conducted for the thermal and acoustical performance of the under study membrane façade element and then software simulations are made in order to validate the results. Moreover, an actual acoustical test is attempted with several difficulties, though, that will be described later on. Finally, conclusions are drawn concerning the whole research and design. As it is evident in the end, although the proposed solution is proved to be rather successful, there is still space for improvement, as well as further research and development.



0

table of
content

1. fabrics	13	festo ag technology centre	60	conclusions and further steps	144	9.conclusions	211
		olympic shooting venue	62			overall assessment	212
introduction	14	3. climate	65	7. case study	149	further development	214
research framework	16	4. high-rises	69	8. final design	155	10. references	217
fibres	20	height limit	70	position of the new façade	156	11. appendix	225
fabrics	22	problems	70	design experiments	157	A. time planning	226
coatings	24	reference projects	72	vacuum experiments	159	B. design builder settings	227
membrane-integrated photovoltaics	26	façade types	74	design concept	160	C. reduction factors for PV calculations	232
phase change materials (PCMs)	28	unitised element façade	76	façade patterns	166	D. wind and vacuum forces calculations	233
fabrication and connections	30	5. preliminary design concepts	83	façade configurations	168	E. preliminary details	234
connection details	32	chosen concepts	92	indicative elevations	169		
recycling	34	final concept	97	sections	170		
materials	36	6. building physics	99	structural concept	174		
table of materials	38	thermal hand calculations	100	forces calculations	176		
summary of comparison conclusion	40	acoustic hand calculations	107	max. deflection calculations	180		
2. reference projects	43	hand calculations conclusions	116	spacers	186		
beijing national aquatics centre	44	acoustics test	118	details 1.5	188		
gerontology technology centre	46	THERM calculations	130	assmby concept	194		
suvarnabhumi international airport	48	comparison hand calculations and simulations	134	lines of defense	198		
burj al arab	50	design builder	136	3D detail impression	199		
olympic stadium / roof reconstruction	52			3D impressions	200		
icarus house / solar decathlon	54			physical model	206		
german pavilion / shanghai expo	56			safety & maintenance	208		
centre pompidou - metz	58						



1

fabrics

introduction

Designing an adaptive fabric façade for a high-rise in Paris can be a very interesting and challenging topic, but at the same time a number of doubts and questions is generated. Nowadays, sustainability plays an important role and of course it influences the construction domain as well. There is a need for the reduction of the energy consumption, which means also the reduction of the energy demands. As the construction sector is responsible for a rather high percentage of the world's energy consumption, it becomes essential to decrease this factor. During the construction process, large amounts of materials are usually wasted and the high levels of embodied energy of the materials' production and the buildings' erection lead to the research for more eco-friendly solutions.

The weight of the structures has also a great impact on their ecological footprint. Therefore, lightweight constructions are preferred in order to reduce the structural loads and consequently the materials used for the load-bearing structures. Fabrics are very lightweight materials that can replace certain heavier ones, such as glass. A primary fabric structure constitutes the traditional tent, introduced many years ago. Since then, technological evolution has achieved remarkable results, concerning new fibres (natural and synthetic) and therefore fabrics, as well as improvements in the manufacturing processes. The durability, the energy

efficiency and the recycling properties that characterise fabrics render them a challenging and competitive material of our days.

advantages of fabrics

- » lightweight
- » flexible / foldable
- » high tensile and tear strength
- » variety of transparency levels
- » possible printing
- » recyclability

Since in this project fabrics will be used as a façade element they have to fulfill the requirements of a building envelope.

façade requirements

- » daylight levels
- » glare control
- » solar heat gain
- » thermal insulation
- » ventilation
- » water management
- » sound and pollution control



research framework

research objectives

main objective

To design an adaptive fabric façade for a high-rise in Paris

sub objectives

- » To research the properties of different fabrics/textiles
- » To investigate their properties in terms of thermal and acoustical insulation, as well as transparency levels, UV protection, water and airtightness, reaction to fire, soiling behaviour, recyclability levels
- » To explore the kind of the desired adaptivity (light-sun/temperature-heat/air-wind)
- » To research the problems of high-rises that occur in the chosen location
- » To define the façade requirements that need to be fulfilled

research question

main research question

- » How can an adaptive, lightweight and flexible fabric façade be designed, a façade that will be responsible for meeting the requirements and improving the indoor comfort in

terms of thermal and acoustical insulation, as well as shading and sun control in a high-rise in Paris?

sub questions

- » Which are the main problems of high-rises that should be tackled? Which among them occur in the chosen location?
- » Which are the most suitable fabrics/textiles as a solution to the above problems? Do they meet the building envelope requirements?
- » Which is the most effective façade design that meets all the requirements?
- » How can the desired adaptivity be achieved? With what kind of mechanisms?

method description

literature survey

The first part of the project consists of a literature survey concerning the various types of fabrics/textiles and more specifically their properties. In addition, the available coatings are mentioned and their advantages, as well as some new technologies, which are being integrated gradually to fabrics (photovoltaic films, PCMs). The recycling parameter is also

taken into consideration at a certain extent. Subsequently, a comparison table of fabrics is produced depending on their properties, their advantages and disadvantages. Then, a list of reference projects is mentioned, in which fabrics/textiles are used, either as roof -which concerns usually most of the cases- or as façade components.

Furthermore, the climate conditions of Paris are examined (diffuse and direct radiation, average temperature, wind direction and speed, humidity levels, precipitation etc.), as well as the building regulations that apply for Paris are investigated.

Moreover, a research is conducted concerning high-rise buildings. The main problems of such buildings are explored and then a couple of reference projects are mentioned focusing on the ways architects and engineers dealt with the highlighted problems. Also, the unitised façade system will be analysed, along with examples of reference projects.

Lastly, a number of design concepts is presented -based mainly on façade principles- that could be applied to high-rises and are suitable for dealing with the already mentioned problems.

analysis and conclusions

After the completion of the literature review, all the gathered information is analysed and as a first step a certain number of fabrics/textiles are highlighted according to their durability, as well as their good thermal and acoustical properties, transparency levels, UV protection, water and airtightness, reaction to fire, soiling behaviour, recyclability level. Secondly, four design concepts are chosen in order to be developed further. This choice is based on their adaptivity, feasibility, flexibility, thermal and acoustical insulation properties, transparency and shading, air and water tightness, reaction to fire, soiling behaviour. Finally, a case study is selected onto which the façade concepts will be applied.

design phase

The chosen designed concepts mentioned above are developed further. The design becomes more detailed and physical models in scale are constructed as well. Subsequently, calculations are conducted concerning their thermal and acoustical performance. Afterwards, the one with the best performance that meets all the requirements is finally chosen. This final concept is analysed once again and designed further with detailed drawings and calculations. A final physical model is

constructed in scale (1:10). Also, an acoustic test is conducted concerning the acoustic properties and behaviour of a vacuum system that is elaborated later on. Finally, conclusions about the designed proposal are drawn and suggestions are made for further research and in order to avoid possible mistakes and failures in the future as well.

relevance

Designing an adaptive fabric/textile façade for a high-rise can have many advantages in terms of sustainability. The protection of the environment and the reduction of the energy consumption constitute two main goals of the sustainable design. Such façade elements can be rather lightweight, which has a great impact on the structural elements of the rest of the building that can be reduced and thus less material is used. Another aspect, which should be taken into account, is that of recycling. Nowadays, technology has been significantly developed towards this direction. For instance, the French company “Serge Ferrari” has developed a procedure named “Texyloop” (which will be analysed further later) that renders membranes recyclable and also it aims to create new materials, which can then be reintroduced into the membrane

fabrication process. Furthermore, the properties of fabrics concerning their transparency, translucency, insulation and solar protection, as well as coatings, such as low-e coatings, applied onto them, can be rather beneficial for creating low energy buildings. Consequently, such design solutions could be considered an innovative sustainable idea in the building domain that will also be responsible for reducing construction costs.

fibres

When we are referring to textiles usually we are referring to coated and uncoated woven fabrics, to polymer foils and also to thin metal sheets. Fabrics consist of fibres whose properties depend on the raw material from which they have emerged and of course on the production method that was followed. But first it would be useful to state the definition of fibre according to the Oxford Dictionary.

“Fibre is a thread or a filament from which a vegetable tissue, a mineral substance or a textile is formed.”

Fibres have certain characteristics that are worth mentioning. They are flexible, versatile in their use and processing and they have a rather high strength. They can be divided into four categories: inorganic fibres, whose base is glass or carbon, organic fibres (polymers), which are synthetic, metal and natural fibres.

» Inorganic synthetic fibres

Glass
Carbon
Basalt
Ceramic

» Organic synthetic fibres (polymers)

Polyethylene (PE)
Polyethylene Terephthalate (PET)
Polyamide (PA)
Polyimide (PI)
Polyacrylonitrile (PAN)
Polytetrafluoroethylene (PTFE)
Aramid

» Metal fibres

Steel
Aluminium
Cooper

» Natural fibres

Flax
Sisal
Hemp
Jute
Ramie
Banana

As mentioned before, the fibres' properties depend on their raw material and therefore not all of them are suitable for architectural applications. More specifically, fibres with high elastic modulus and subsequently minimum elongation are usually preferred. For example, the elastic modulus of carbon fibres is higher than that of glass-fibres. Consequently, the strength of carbon-fibre-reinforced polymers (CFRP) is much higher than that of glass-fibre-reinforced polymers (GFRP). Moreover, metal fibres' smooth surface renders them unsuitable, as an adequate bond cannot be achieved with the polymer. In addition, the low self-weight of natural fibres makes them suitable for lightweight structures. Also, they can be used for façade components or interior applications due to their good acoustical properties. Nevertheless, the fact that they absorb moisture and the possible scattering of their mechanical properties rules them out from being used for load-bearing elements.

Another interesting group of materials is that of biopolymers. They are produced from starch or cellulose and they can be biodegradable. More specifically, Polylactide (PLA) has the ability to be recycled without going through the procedure of downgrading. PLA presents certain characteristics worth mentioning. It is waterproof, scratch-resistant, transparent

and has good mechanical properties comparable to those of Polyethylene Terephthalate (PET) and Polypropylene (PP). In addition, it is air-permeable, UV resistant and suitable for printing (Knippers 2011).

After having mentioned some advantages and disadvantages of fibres, the following chapter concerns the fabrics, which are produced from fibres.



Figure 1: rope made from natural hemp fibres

source:

1. Knippers, Cremers, Gabler, Lienhard, (2011), Construction manual for polymers + membranes : materials semi-finished products form-finding design, Basel, Boston, Berlin, Birkhauser Verlag GmbH

fabrics

categories of fabrics

In order to choose the most suitable fabric, one of the main reasons that should be looked into is its load-bearing behaviour. The orientation of the fibres, their waviness (undulation) and the weight per unit area (g/m²) are the factors that determine the load-bearing behaviour.

Fabrics can be divided into three categories according to their production method: **woven**, **knitted** and **non-woven**. Their definitions are the following:

» **Woven fabric** is a textile formed by weaving. It is produced on a loom, and made of many threads, woven on a warp (direction in which the fabric is manufactured) and a weft (perpendicular to warp's direction). (Wikipedia)

» **Nonwoven fabric** is a fabric-like material made from long fibers, bonded together by chemical, mechanical, heat or solvent treatment. (Wikipedia)

» **Knitted fabric** is a textile that results from knitting, which means forming loops or stitches. Its properties are distinct from those of woven fabric in the sense that it is more flexible and can be more readily constructed into smaller pieces (Wikipedia). The manufacturing process is essentially similar

to knitting by hand. As these textiles do not have a dominant direction, their suitability as reinforcement for polymers is limited. They are primarily used as backing materials for other reinforcing fibres or for fixing those fibres. Their very good drapeability, though, makes them suitable for uses involving very small radii (Knippers 2011).

Woven fabrics are produced from systems of threads crossing at right-angles. The warp threads run parallel to the longitudinal direction of the fabric (they are fixed to the weaving loom) and the weft threads are interwoven perpendicular to these with shuttles or a jet of air. The weft threads generally undulate, i.e. pass above and below the warp threads. When the material is loaded this leads to different strains in the textile in the warp and weft directions, depending on the type of weave. Different arrangements of raised warp threads during the weft insertion (floating) produce different types of weave that exert a considerable influence on the mechanical properties. The three main types of weave are **plain**, **twill** and **satin** weave. The smallest repetitive unit of a weave is known as the rapport. Woven fabrics can obtain higher strengths and stability than the other structures and this is the reason why they are preferred in the textile manufacturing (Knippers 2011).

drapeability of woven fabrics

» **Plain weave** is a style of weave in which the weft alternates over and under the warp. It is usually used for lightweight membrane types and uncoated fabrics. However, coated fabrics provide more stiffness as the weft threads are pretensioned during the weaving process.

» **Twill weave** (croisé) the weft thread passes once above and then at least twice below the warp thread. Twill is a type of textile weave with a pattern of diagonal parallel ribs (in contrast with a satin and plain weave). It is also stronger than plain weave as the strain in the warp direction is lower and its drapeability is better than that of plain weave.

» **Satin weave** is a method of weaving where the weft threads initially passes under a warp thread and then above more than two warp threads. It has very good drapeability and is usually used in fibre-reinforced polymers in order to achieve smoother surfaces.

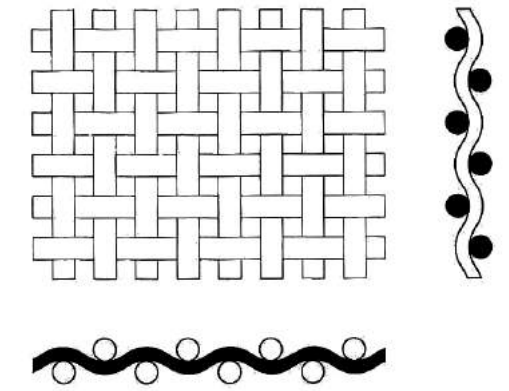


Figure 2: plain weave

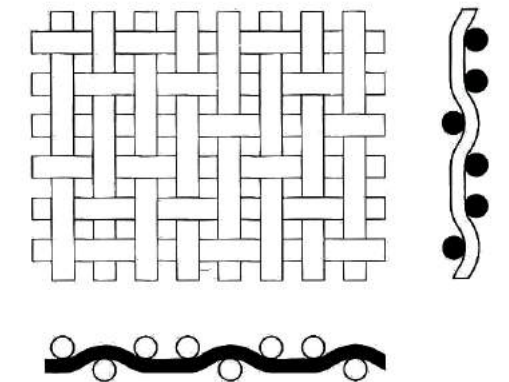


Figure 3: twill weave

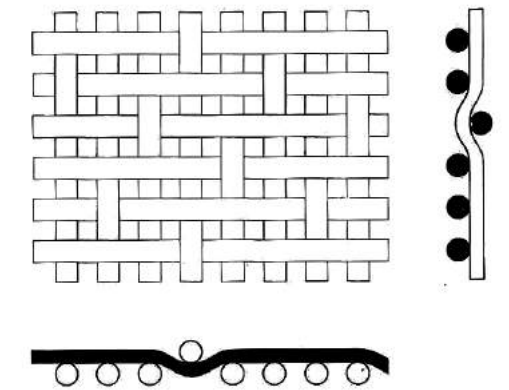


Figure 4: satin weave

source:

1. Knippers, Cremers, Gabler, Lienhard, (2011), Construction manual for polymers + membranes : materials semi-finished products form-finding design, Basel, Boston, Berlin, Birkhauser Verlag GmbH

coatings

Coatings provide a protective, waterproofing function and produce the desired surface finish of a fabric. The membranes usually used in architectural applications are a combination of woven fabrics and one or more coating layers. Uncoated woven fabrics are preferred mostly for sun shading structures or room acoustics purposes.

The role of coatings is to protect the fabric from moisture, UV radiation, fire and attack by microbes and bacteria. In addition, the durability of the fabric is increased and its mechanical properties are influenced as well. More precisely, coatings have an impact on the following fabrics' properties:

- » strain and shear stiffness
- » weldability
- » UV protection
- » watertightness
- » fire resistance
- » light transmittance
- » light reflectance
- » scattering of the incoming light
- » soiling behaviour
- » colouring
- » heat radiation

Thermoplastic coatings (PVC, PTFE) are the most common ones and with their use the connection of separate pieces of fabrics can be realised. Another group of coatings constitute the elastomers (silicone rubber) and the thermosets (silicone resin).

application method of coatings

There are two ways of applying coatings to fabrics.

- » Doctor blade method
- » Dip coating method

Doctor blade method is used for PVC and silicone coatings. It consists of a PVC powder dispersed in a plasticier that are then chemically bonded. Usually the coating is applied on both sides of the fabric so the procedure is repeated twice. In the end, top coatings are applied in order to ensure the protection of the plasticier from UV radiation and also influence the soiling behaviour of the fabric.

Dip coating is usually applied to PTFE coatings and it consists of PTFE particles on the fabric that are coated on both sides. The process is repeated several times until the desired thickness is achieved. Also, this kind of coatings can only be applied to woven fabrics with very high melting point as high temperatures are reached during this process.

examples of coatings

A very common and popular category of coatings are the **low-emissivity** coatings that have the ability to reduce the heat radiation effect and can be applied to many fabrics. Since the latter have very low specific mass radiation it is crucial for their thermal behaviour. More specifically, during winter thermal radiation is reflected, but in the summer the fabric heats up due to sunlight. However, the fabric does not emit thermal radiation towards the interior because of the existence of the low-e coating. Additionally, in the summer the cold radiation is reflected and therefore the coating contributes to the air-conditioning system.

Another category constitute the **transparent selective functional** coatings that are able to reduce the near infrared part of the sun's spectrum while still transmitting most of the visible spectrum.

Titanium dioxide coating is worth mentioning as it can be applied to flexible architectural fabrics. It is based on nanotechnology and it decomposes nitrogen oxide (air pollution due to traffic) when exposed to UV radiation. It has self-cleaning properties due to its high hydrophobic properties. Furthermore, it contributes to the increase of the light reflectance of the membrane that is applied onto.

PVDF is another coating material that can be found in two forms: weldable and non-weldable. It is a fluoropolymer lacquer and the weldable one has better UV resistance than acrylics. Nevertheless, it is usually combined with acrylics in order to reduce the cost. The non-weldable PVDF, on the other hand, has a better resistance against soiling as it less compound with acrylics.

Lastly, another coating that draws the attention constitutes the "**Lotusan**" produced by the company *STO Corp*. It is inspired by the micro-structure of the Lotus plant, which is characterised by its nanometric structure that is responsible for trapping the air and thus making the surface hydrophobic. Like the plant, the coating uses this way rainwater to clean its surface and so it can render the fabric, on which it is applied, dirt-repellent.



source :1. Knippers, Cremers, Gabler, Lienhard, (2011), Construction manual for polymers+membranes: materials semi-finished products form-finding design, Basel, Boston, Berlin, Birkhauser Verlag GmbH

membrane-integrated photovoltaics

PV flexibles (PTFE/ETFE)

The use of photovoltaics in the buildings constitutes a growing trend in our days. Integrating them into the building envelope can have many advantages: they don't need additional structure, they can be used as shading systems in transparent or semi-transparent applications, reducing thus the solar heat gains and contributing to the reduction of cooling demands in the summer. According to a report of the International Energy Agency (IEA), an estimation of approximately 1000 GWp at a low average efficiency of 5% is given for the building-integrated photovoltaic potential of 23 billion square metres.¹

Up to nowadays, there are several examples of integrated photovoltaics into membranes, but they concern only transparent PVC membranes, which are unfortunately unsuitable for long-term structures. Therefore, there is a need for applying photovoltaics into other materials that are more durable, such as fluoropolymers PTFE and ETFE.

The University of Neuenburg in Switzerland developed this technology. It is a process of manufacturing amorphous silicon thin-film photovoltaic cells on a thin polymer film. Roll-to-roll technique is used in order to place the PV cells in a multi-layer process on the polymer. The result is a very thin and lightweight film, which is rather flexible and suitable for integration in



Figure 6: First photovoltaic tensile structure at the 'Under the Sun' exhibition at the Cooper-Hewitt National Design Museum, New York, 1998, designed by FTL Design Engineering Studio.

membranes structures.

As far as the lamination process is concerned, the PV film is

sources:

1. Pohl, G., (2010), Textiles, Polymers and Composites for Buildings, Woodhead Publishing
2. Gumm, M., (2008). Integrating Photovoltaics Building Envelope Onto Surfaces (Retrieved from <http://rci-online.org/wp-content/uploads/2008-12-gumm.pdf>)

embedded between two ETFE films in order to be protected from mechanical stresses, humidity, weathering. The dimensions of the final product depend on the lamination machine (3.5x2m). The position of the PV film on the outer layer of a cushion is preferable, as if placed in the middle it will have limited power output due to refraction and heating effects. The laminated modules do not permit any light transmission, as they are opaque, but the light diffusion is decreased as perceived from underneath.

PV thin-films VS traditional silicon modules:

- » Thin-film PV modules generate less power per m² (lower power density) compared to crystalline silicon and can produce up to 5% more power in a solar day. Crystalline silicon's peak power production is between 10:00 a.m. and 3:00 p.m., while thin-film modules can generate power throughout the day.
- » Thin-film PVs produce more power during low-light (early morning and late afternoon) and overcast conditions compared to crystalline silicon. A solar module peak-power output is measured at noon with the sun directly overhead.
- » Thin-film PVs produce 55 to 110 watts of power per m² on average, depending on the type of semiconductor material used.
- » High rooftop operating temperature has less effect on thin-film solar power output compared to standard crystalline silicon. Crystalline silicon modules start losing power output once PV module temperature exceeds 25°C.
- » Thin-film modules' power output is less affected by solar shading than crystalline silicon.²



Figure 7: Fully flexible a-Si PV on polymer substrate



Figure 8: PV flexibles: ETFE embedded a-Si PV

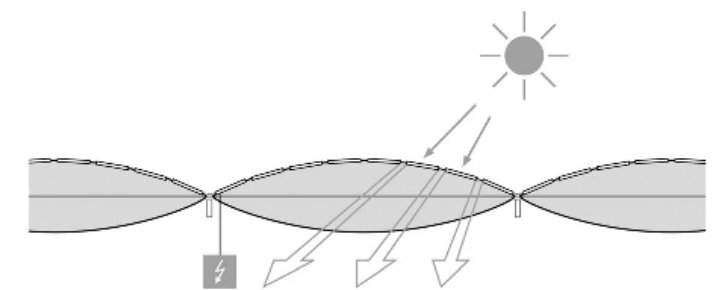


Figure 9: Principle of PV flexibles integrated in the top layer of an ETFE cushion, providing shading and electrical power.

phase change materials (PCMs)

Recently, there have been conducted several researches on the improvement of the thermal performance of membranes. One solution constitutes the integration of phase change materials (PCM), substances that absorb and release large amounts of latent heat while changing physical state (from solid to liquid and vice versa). During the heating process, after the PCM reaches a certain temperature, it starts melting and absorbing latent heat without any temperature change. On the other hand, during the cooling process, the PCM starts solidifying again, after reaching a certain temperature, while releasing the absorbed heat. Once again the temperature of the material remains constant during the whole process.

The most common PCMs are paraffins, salt hydrates, organic materials and eutectics. Salt hydrates are the most suitable ones for the application on membranes, as they can absorb and store a large amount of latent heat and also they are incombustible, meeting thus the fire-resistant requirements (A2 category). Usually, it is necessary, though, to add stabilizing chemicals in order to avoid an irreversible melting or freezing.

As far as the application of PCMs on a fabric is concerned, it has to be ensured that the dissolution of the material during its liquid phase will be prevented. Therefore, a silicone rubber

is used for this purpose. Firstly, the salt hydrate PCM is mixed with the silicone rubber matrix and then this mixture is applied on the fabric, after a primer has already been applied. Subsequently, it is cured at 100°C and afterwards a top coat is added to protect the fabric from soiling and mechanical stresses. Different parts of this final product can be connected with each other with the use of silicone-based adhesive tape.

As mentioned before, the temperature of the PCM remains constant when changing physical state. This has as a result the stable state of the membrane structure and therefore the prevention of the interior's overheating.

In figure 10, we can see the comparison between a PVC-coated polyester membrane without PCM (PVC/PES) and PCM/silicone rubber-coated fibreglass fabric (PCM/SR/FG). In both cases a single-layer membrane is used. It can be confirmed from the figure that the temperature differences between the two structures reaches the 6°C, indicating a delay in the increase of temperature during the day, because of the existence of the PCM.

Another aspect worth mentioning constitutes the translucency

source:
1. Llorens, J., (2015), *Fabric Structures in Architecture*, Woodhead Publishing

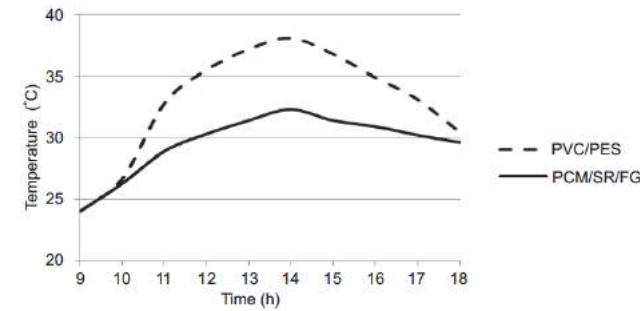


Figure 10: Temperature development of two model structures

of the PCMs. More specifically, the levels of translucency of the PCM/silicone rubber-coated fibreglass fabric (PCM/SR/FG) are higher than other membrane materials, as it can be seen in figure 11.

Most of the PCMs are opaque in their solid state and transparent in their liquid one and the silicone rubber coating is also transparent. When changing physical state, the PCM and thus

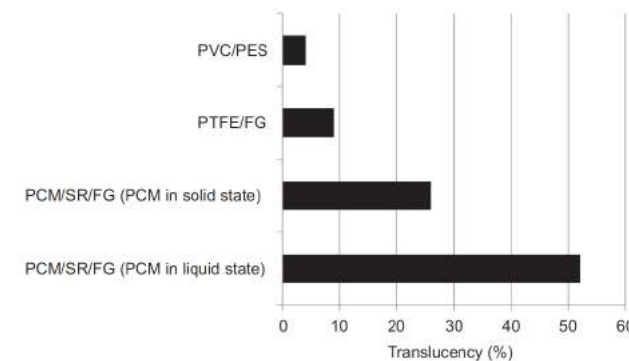


Figure 11: Light transmission of different materials

the membrane become gradually more or less translucent. In the liquid state, which is during the day, the transparency reaches the 53%, while during the night (solid state) is maximum 26% and it also reflects the light from sources of the interior, rendering it more efficient.

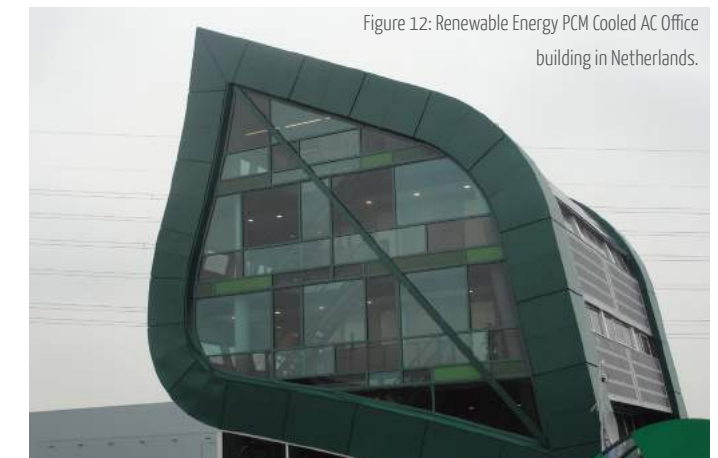


Figure 12: Renewable Energy PCM Cooled AC Office building in Netherlands.



Figure 13: Floating Balls of Rotterdam cooled (Air Conditioned) by PCM.

fabrication and connections

fabrication process

The fabrication process of a fabric consists of the following steps:

- » preparing the cutting pattern (with the cutting plotter)
- » welding the different pieces together
- » welding or folding over the edges incorporating keders or sewing belts
- » attaching corner fittings if necessary
- » folding / rolling and packing

connection methods

There are several ways of connecting different pieces of fabric:

welding

Welding is the process applied to thermoplastic coatings in order to be fused with heat and pressure. After the welded seam has cooled down it can reach up to 90% of the strength of the parent material.

There are three types of welding:

- » *High-frequency welding:* it is also known as radiofrequency welding (RF) and it's used mostly for thermoplastics with a polar molecular structure, like PVC. It is a fast connection method.

- » *hot-plate and impulse welding:* it is applied to join the membrane coating with an intermediate foil from thermoplastic fluoropolymer. It is suitable for PTFE-coated materials that cannot be joined with the first method. After the seam has cooled down, with the application of pressure once again, it can reach up to 90% of the parent material's strength.

- » *welding on site:* it is used for large membrane structures, usually for finishing clamped joints and open corner details. It must be ensured, though, that the joining can be achieved on site.

gluing

It is used mostly for polyester-PVC membranes, but the strength of the seams has a much lower value than that of welding process. However, glass-silicone membranes use this method as they cannot be welded. Silicone can be vulcanised by adding adhesive silicone strips to the seams. Another alternative is the two-part adhesives method where the surfaces are joined with a cross-linking adhesive.

source:

1. Knippers, Cremers, Gabler, Lienhard, (2011), Construction manual for polymers + membranes : materials semi-finished products form-finding design, Basel, Boston, Berlin, Birkhauser Verlag GmbH

stitching

Due to the high speed and high strength values of welding, stitching method is limited to non-weldable materials, like PTFE or glass-silicone. In order to avoid high production costs and lack of waterproofing, special adhesives are used.

Some details that should be taken into consideration during the joining process are the following:

intersections

When joining together different parts of membranes multiple connections of seams can be formed. On the one hand, these parts are thicker, which could lead to loading problems, but on the other hand, usually it is preferable in terms of aesthetics.

overlapping membrane sections

Membranes overlapping can cause many problems if not dealt properly. Run-off water should always drain from the upper part towards the lower one to prevent leaking. Also, if the

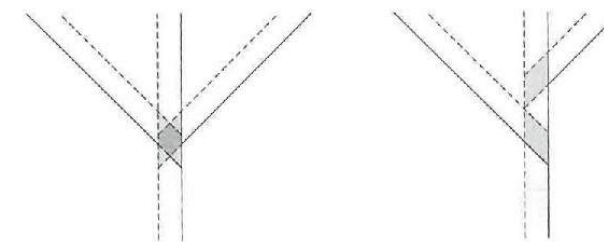


Figure 14: Overlapping membrane intersections

arrangement of the membrane section is reversed, dirt and dust can stick into the seams.

It is necessary to divide the details of a membrane structure according to the loads (liner or point loads). Linear loads occur at **edges** and **seams** and point ones at the **corners**. Moreover, it is important to take into account that big membrane structures undergo large deformations and thus the necessary tolerances should be considered, during erection as well. Lastly, all metal parts used additionally for structural and joining reasons should be rounded off in order not to damage the fabrics.

assembling and packaging

After the membrane is cut and joined, it has to be either folded or rolled up, so as to be transported to the construction site. To protect the material from being damaged, foils or textiles are placed between the layers of the membrane.

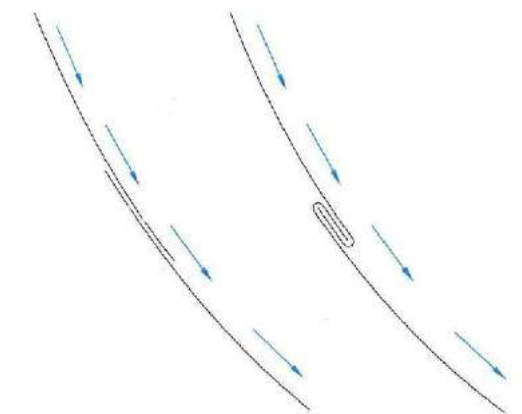


Figure 15: Overlapping seams in the direction of water run-off

connection details

seams

As mentioned before there are three ways of connecting the different pieces of fabrics: welding, stitching and gluing. This applies also to the connection of the fabric itself at the edges.

There can be discerned two categories of seams:

- » *Permanent seams*: factory-made junctions between two membranes.
- » *Detachable seams*: connections made during erection so that the prefabricated sections of the membranes can be assembled on site.

keders

In the edges of every cushion the membranes are joined with the help of keders (beading) in order to form structural, interlocking connections. Keders are usually made of Polypropylene (PP), PVC monofilaments and Polyurethane (PUR). They can be welded into strips along the edges of the foils. The advantage of a polymer keder (PVC) is the fact that it has similar elongation properties with the membranes and thus stresses or temperature-related restraint stresses are avoided. (Knippers, 2011)

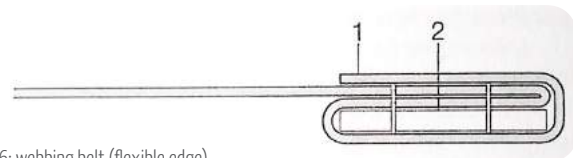


Figure 16: webbing belt (flexible edge)

edges

All membranes are clamped together along their edges or held in place by either edge cables or webbing belts. Usually, extruded sections from anodised aluminum are used for clamping the edges of the membrane cushions. The edges can also be divided into two categories:

- » *Flexible edges*: curved edges where cables or belts carry the membrane stresses perpendicular to the edge and transfer these to the corners as tensile forces (figure 16)
- » *Rigid edges*: connection of the membrane to a rigid linear component (e.g. steel section)

simple edge clamp detail

There is a distinction between clamping with simple flat bars and clamping with extruded aluminum. In the first case, the keder is placed behind the clamping bar and the fixing screws and bolts are passing through the membrane material, which could lead to its damage (figure 17a). In the second situation, the keder is held in place with the extruded aluminum sections and is placed in front of the fasteners, avoiding thus any possible damage of the foil (figure 17b, c) (Knippers, 2011).

source:

1. Knippers, Cremers, Gabler, Lienhard, (2011), Construction manual for polymers + membranes : materials semi-finished products form-finding design, Basel, Boston, Berlin, Birkhauser Verlag GmbH

edge clamp detail with factory-fitted polymer edge bead

In this case, the keder is already welded to the membrane and placed together into a polymer edge bed, usually made out of EPDM. Then, the polymer edge bed is clamped into a two-part aluminum section (figure 17d). This type of connection presents several advantages compared to the simple edge clamp:

1. faster erection
2. protection of the membrane edge
3. lower stress peaks at the edge
4. ability to allow for thermal expansion because the EPDM is clamped in the two-part aluminum section

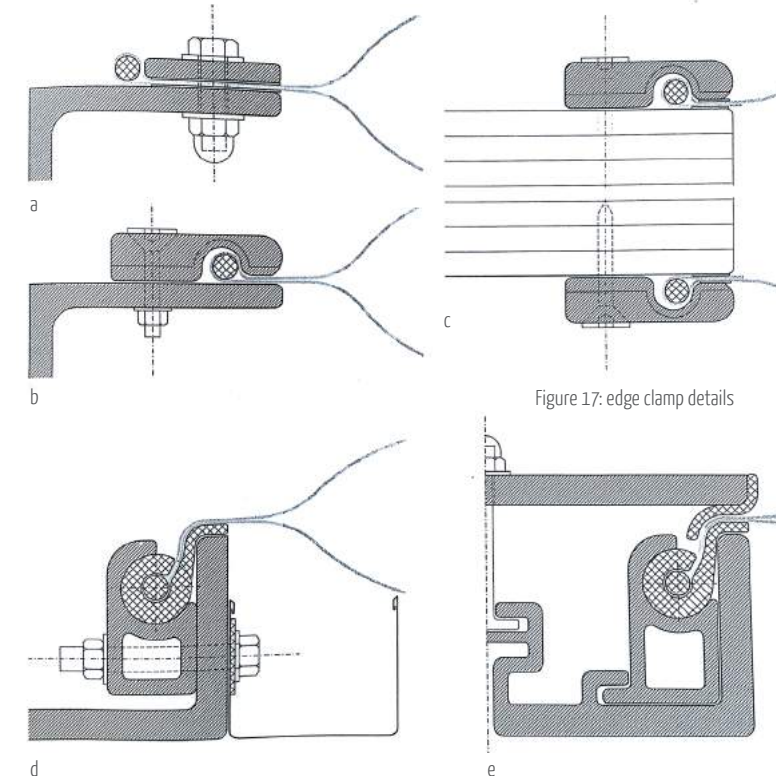


Figure 17: edge clamp details

edge clamp detail with erection aid

The last category concerns separate clamping bars that can be integrated into the extruded section in order to simplify the installation of the cushions. These separate bars are clipped into the sections attached to the loadbearing structure without the need of any screws or bolts and are either fitted directly to the keder or clamped to a polymer edge bed (figure 17e) (Knippers, 2011).

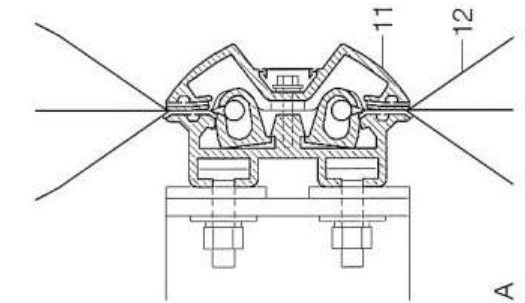


Figure 18: edge clamp detail of Beijing National Aquatic Centre

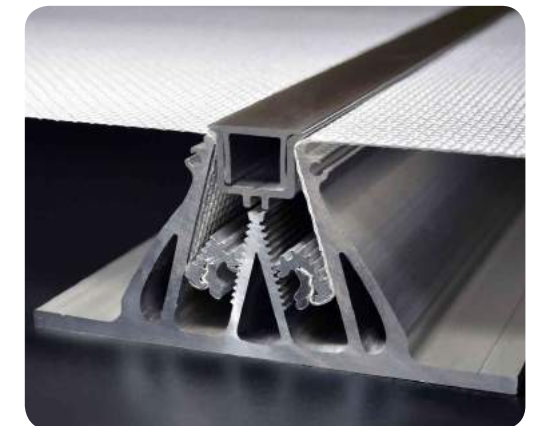


Figure 19: edge clamp detail of FACID, the first textile façade of Schüco

recycling

texyloop / Serge Ferrari

In the context of sustainability, the company *Serge Ferrari* developed in 2000 a recycling procedure for composite textiles named "Texyloop". It is actually a cycle, as not only does it enable membranes to be recycled, but also it aims for the creation of new materials. 90% of the company's products can be recycled at the industrial recycling plant that was built in Italy in 2000.

Serge Ferrari is not the only company that turned towards that direction. Later, in 2007, recycling initiatives were taken from other companies as well, like *Freitag* in Switzerland and *Reversible* in France.

The challenge was to invent a technology that can separate the components of the flexible composite materials in order to create single raw materials. The Serge Ferrari® Group, together with Solvay, developed this technology and created a prototype unit to recycle the flexible composite materials (figure 20).

A Lifecycle Analysis (LCA) showed that the extraction and the production of raw materials are responsible for the main environmental impact (80%). Thus, the recycling of products and the creation of new raw materials play a significant role in the reduction of the environmental impact. The lifetime of materials influence the energy savings, as well.



Figure 20: Separation of the components of the flexible composite materials in order to create single raw materials

source:

1. Motro, R., (Ed.), (2013), *Flexible Composite Materials in Architecture, Construction and Interiors*

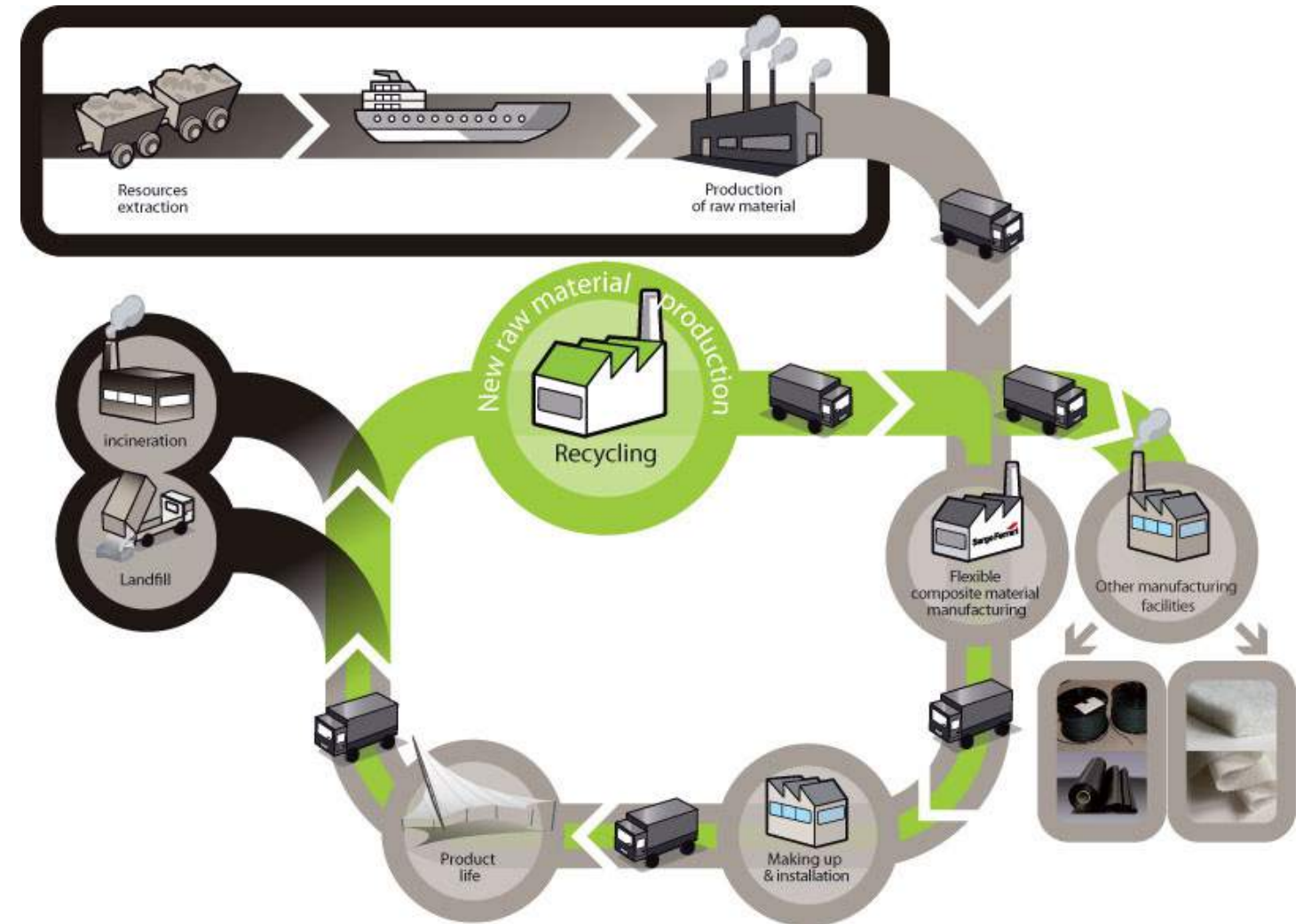


Figure 21: Texyloop recycling cycle

materials

In order to choose the right material(s) for the project, a comparison of their properties was necessary to be made. Therefore, a number of membranes, foils and fabrics were studied and compared according to various properties, such as:

- » tensile strength
- » UV-resistance
- » reaction to fire
- » light transmittance
- » sensitivity to soiling
- » resistance to external factors
- » necessity of a top coat
- » price
- » levels of transparency / translucency
- » service life
- » possibility of recycling

The materials that were investigated can be seen in the next page.

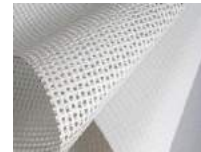
PVC-coated polyester



PVC-Birdair



PTFE



uncoated PTFE



PVC/PTFE-coated aramid fibre



ETFE



Tenara fabric (Architen Landrell) - ePTFE (fluoropolymer composite)



KEVLAR® PARA-ARAMID (DuPont™)



NOMEX® PARA-ARAMID (DuPont™)



PTFE-coated glass-fibre



TENSOTHERM™ with nanogel® (layers with PTFE fiberglass)



VECTRAN® liquid crystal polymer (Kuraray™)



PTFE/ETFE/PVDF coated with fluoropolymer



Texlon® ETFE Vector Foiltech



ZYLON® PBO (Toyobo™)



THV coated polyester/ETFE



PLA



TECHNORA® (Teijin™)



Silicone-coated glass-fibre



PU coated nylon



UHMWPE (Honeywell™)



PTFE laminated glass-fibre mesh



PVDF (Polyvinylidene fluoride)



coated PTFE

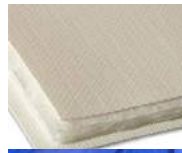


Silicone leather



table of materials

	material	tensile strength	UV resistance	reaction to fire	light transmittance	sensitivity to soiling	resistance to external factors	top coat	cost	transparency / translucency	disadvantages	service life	Recycling
	PVC - coated polyester	3 000 - 10 000 N/5	good	not readily flammable (B1)	5 - 15 %	not very good but can be improved with the addition of top coats from fluoride lacquer	a low-wick substance is required in order to prevent moisture, dust and dirt, water resistant	acrylate or polyvinylidene fluoride lacquers (PVDF) or polyvinyl fluoride laminates (PVF)	low	translucency 0.8 - 4%		15 - 20	yes
	PVC - Birdair		low	not readily flammable (B1)	80 - 95%					transparency 100%			
	PTFE fabric	2 390 - 4 470 N/5	very good	excellent resistance (A2)						transparency up to 37%			
	PTFE - coated glass fibre fabric	3 500 - 8 000 N/5	very good	non - flammable	8 - 20 %	self-cleaning	resistant to chemical substances and mould, water resistant	required in order to improve the anti-adhesive characteristics and weldability		translucency up to 13%, limited printed possibilities	<ul style="list-style-type: none"> • folds have 2 consequences: 1) breaking of the coating and thus water penetration and 2) fracture which leads to reduction of the membrane's capacity 	> 25	no
	PTFE, ETFE or PVDF fabric coated with fluoropolymer		very good	non - flammable		self-cleaning	water resistant						no
	THV - coated polyester fabric	3 500 - 5 000 N/5	very good	not readily flammable (B1)	15 - 23 %	self-cleaning	excellent protection against weathering				sometimes it has relatively high weight per unit area		
	THV - coated ETFE fabric	1 200 N/5	very good	not readily flammable (B1)						translucency up to 90%		> 25	
	Silicone-coated glass-fibre fabric	2 500 - 8 000 N/5	good	excellent resistance (A2)	25 - 30 %				high	translucency up to 25%	the surface charges up statically and attracts dirt	> 20	yes
	PTFE - laminated glass-fibre mesh	4 500 N/5	good		43 - 65 %	self-cleaning but dirt and dust can stick onto uneven surfaces	water resistant				limited stretchability and formability	> 25	
	Coated PTFE fabric	1 600 - 4 000 N/5	very good	non - flammable	20 - 40 %	good resistance	water resistant		high price of raw materials	pure PTFE is transparent but it becomes white in process / translucency 20 - 40%		> 25	
	Uncoated PTFE fabric	2 000 - 4 000 N/5	very good	non - flammable	35%	good resistance	water resistant		high price of raw materials	pure PTFE is transparent but it becomes white in process / translucency 20 - 40%		> 30	
	PVC or PTFE - coated aramid-fibre fabric	7 00 - 24 000 N/5	low	B1 for PTFE and A2 for PVC	0%				high	opaque as aramid is sensible to UV light coating need to cover it completely		> 20	
	ETFE foil		very good	not readily flammable (B1)	> 90 %	self-cleaning				transparent, dyed white, various colours, possible printing			yes

	material	tensile strength	UV resistance	reaction to fire	light transmittance	sensitivity to soiling	resistance to external factors	top coat	cost	transparency / translucency	disadvantages	service life	Recycling
	TENSOTHERM™ with nanogel® (layers with PTFE fiberglass)		good				water repellent, resists mold and mildew			translucency 0 - 50%			no
	Texlon® ETFE Vector Foltech		very good	not readily flammable (B1)	88 - 95 %								
	PLA	5 300 - 6 000 N/5	good	flame retardant, self-extinguishing			acceptable water resistance			opaque			yes (biodegradable)
	PU coated nylon fabric				high		good levels of airtightness						
	PVDF (Polyvinylidene fluoride) fabric		very good	flame retardant	up to 95%, scattering light up to 96%		high weathering resistance, low permeability to most gases and liquids			transparent, white with 40% translucency, printable			yes
	Silicone leather		good	flame retardant		easy to clean	mold proof, weatherproof, anti-bacterial			opaque			
	Tenara fabric (Architen Landrell) - ePTFE (fluoropolymer composite)		good	very good			water resistant, easily foldable		high	translucency up to 40%			no
	KEVLAR® PARA-ARAMID (DuPont™)		low	good			prosperity to absorb moisture						
	NOMEX® PARA-ARAMID (DuPont™)		very good	good									
	VECTRAN® liquid crystal polymer (Kuraray™)		low	good									
	ZYLON® PBO (Toyobo™)		low	good									
	TECHNORA® (Teijin™)		low	good									
	UHMWPE (Honeywell™)		good	low									

summary of comparison | conclusion

excellent UV resistance	good UV resistance	fire resistance	transparent	translucent	opaque	self-cleaning properties	possible printing	recyclable	high price
coated & uncoated PTFE PTFE-coated glassfibre PTFE/ETFE/PVDF coated with fluoropolymer ETFE THV coated polyester/ETFE Texlon ETFE Vector Foiltech PVDF NOMEX® PARA-ARAMID (DuPont™)	PVC-coated polyester Silicone-coated glassfibre PTFE laminated glassfibre mesh TENSOTHERM™ with nanogel® (layers with PTFE fiberglass) PLA Silicone leather Tenara fabric (ePTFE) UHMWPE	PVDF NOMEX® PARA-ARAMID (DuPont™) PTFE Silicone-coated glassfibre PVC/PTFE-coated aramid fibre Tenara fabric (ePTFE)	ETFE PVC Birdair Texlon ETFE Vector Foiltech PV coated nylon PVDF	coated & uncoated PTFE Silicone-coated glassfibre THV coated polyester/ETFE PTFE-coated glassfibre PVC-coated polyester TENSOTHERM™ with nanogel® (layers with PTFE fiberglass) Tenara fabric (ePTFE)	PVC/PTFE-coated aramid fibre PLA Silicone leather	ETFE PTFE-coated glassfibre PTFE/ETFE/PVDF coated with fluoropolymer THV coated polyester/ETFE PTFE laminated glassfibre mesh	ETFE PTFE-coated glassfibre PVDF	ETFE PVDF PVC-coated polyester Silicone-coated glassfibre	Silicone-coated glassfibre coated & uncoated PTFE PVC/PTFE-coated aramid fibre Tenara fabric (ePTFE)

After the comparison of the materials was made, based on the aspects mentioned previously, this table was created with the most important properties the chosen material should possess. From this, certain materials seemed to belong to the majority of the categories, with ETFE membrane being one

of them, which consists the final choice as well. The reason for this was based on the fact that ETFE has, firstly, a rather high tensile strength compared to the other membranes, Furthermore, it offers a light transmittance of 90% and above and thus it is transparent, important factor in a multi-layer

component. In addition, it has an excellent UV-resistance, with the suitable coatings it can be completely watertight and also it has self-cleaning properties, important aspect concerning its maintenance. Lastly, it offers the possibility of printing, something that can be used for sun shading for instance.

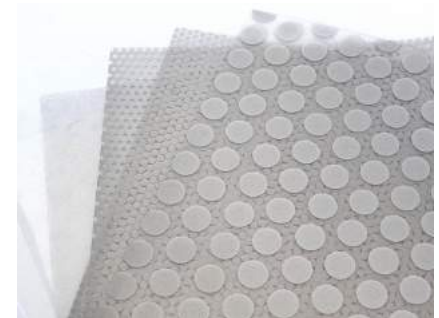


Figure 22: ETFE foil different printed patterns



2

reference
projects

beijing national aquatics center

PTW Architects, Arup
2008, Beijing Olympic Games

translucent ETFE cushions

The building's distinctive appearance is inspired by soap bubbles. The façade and the roof are constructed from translucent ETFE cushions (ethylene tetrafluoroethylene), a tough, recyclable material, in order to achieve the desired organic look. Enclosed within the bubble walls are five swimming pools (including a wave machine and rides), a restaurant and seating and facilities for 17,000 spectators.

Arup's designers and structural engineers realised that a structure based on this unique geometry would be highly repetitive and buildable, while appearing organic and random. There are 4,000 ETFE bubbles constituting the "Water Cube's" cladding, as it is also called, with some as large as nine meters across. The roof is made from seven different bubbles and the walls from fifteen bubbles. Despite this repetition, the eye perceives a random pattern.

Each pillow is permanently inflated by a low power pump. This internal air pressure transforms a 0.2-millimetre-thick plastic into a cladding panel capable of spanning relatively large distances. ETFE weighs just 1% of glass and is a better thermal insulator. Around 20% of solar energy is trapped and used for

heating. The bubble cladding lets in more light than glass and cleans itself with every rain shower.

The "Water Cube" is specifically designed to act as a greenhouse. This allows high levels of natural daylight into the building, like mentioned above and as swimming pools require a lot of heating, the power of the sun is being harnessed to passively heat the building and the pool water. Arup estimated that this sustainable concept has the potential to reduce the energy consumption of the leisure pool hall by 30%, equivalent to covering the entire roof in photovoltaic panels. More specifically, the daylight allowed into the cube saves up to 55% on the lighting energy required for the leisure pool hall.



Figure 23: general external view

sources:

1. <https://www.dezeen.com/2008/02/06/watercube-by-chris-bosse/>
2. http://www.arup.com/projects/chinese_national_aquatics_center
3. <http://www.e-architect.co.uk/beijing/watercube-beijing>
4. <http://architectureau.com/articles/practice-23/>



Figure 24: construction phase



Figure 25: internal view

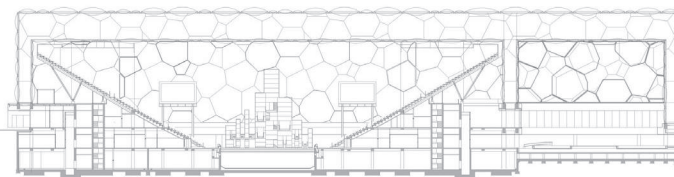


Figure 26: section

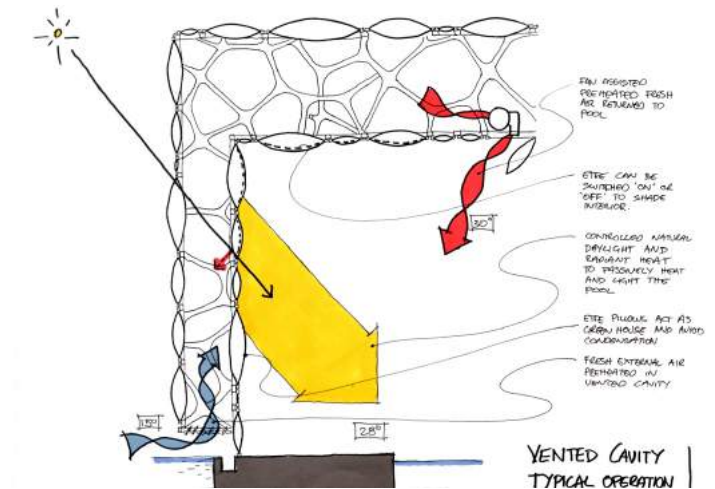
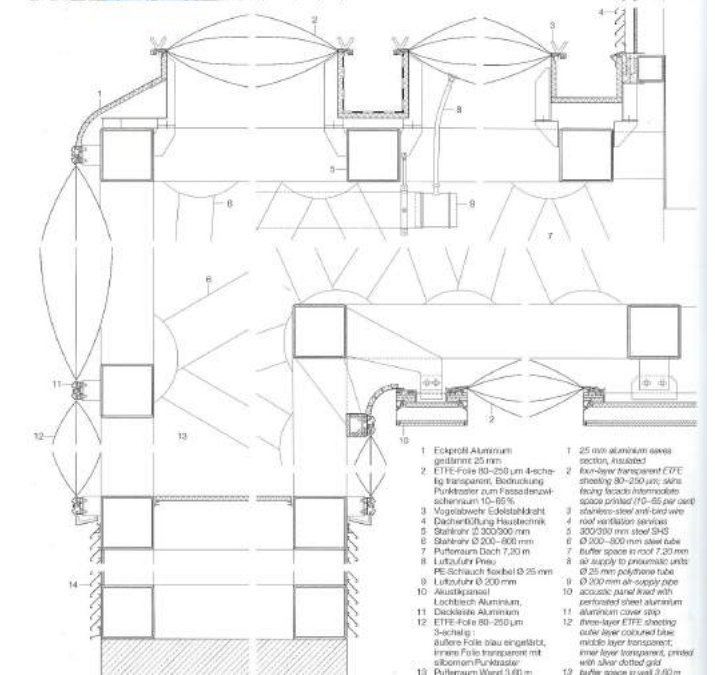
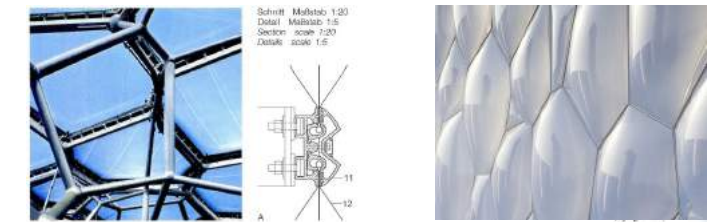


Figure 27,28: façade details

gerontology technology centre

D.J. Siegert, Wörsching Steelbuildings
2004, Bad Tölz, Germany

The Gerontology Technology Centre (GTC) uses a single layer of transparent ETFE film for its façade. Also, the double curvature of the façade gives to the building a new perspective and presents a challenge to conventional design perceptions. It has a spiral shape in plan and it was designed in order to house the new Innovations Centre. The geometrically complex building evolves like a ramp from the three storeys at the start of the spiral till the four storeys at its end. Additionally, behind the façade each storey is drawn back so as to reveal an open walkway at each level. These walkways connect the individual offices with the retail units and can be used for exhibitions and presentations, as well as seating areas.

The external envelope of these walkways consists of transparent ETFE film curving in two directions. The film spans the whole height of the building, it provides protection against the weather and it is responsible for the indoor climate. It also forms a buffer zone between the interior and the exterior. In winter, spring and autumn, this buffer zone stores solar radiation and therefore reduces the heating demands of the building. In the summer, on the other hand, the printing pattern on the film and the screens on the inside provide protection against the sun. Furthermore, sensor-controlled vents open

at night to ensure the exchange of air. The stack effect in the multi-storey void between the walkways and the façade ensures the airflow, which replaces the warm interior air with cold night air. Moreover, the storage capacity of the solid floor slabs contributes to the reduction of daytime temperature peaks. In addition, as the façade is fully transparent energy costs for artificial lighting is minimised. Lastly, the façade's load-bearing structure consists of steel circular hollow sections on which the film is stretched.



Figure 29: external view

sources:

1. Garbe, T., editors: Lang, W., McClain, A., Tents, Sails, and Shelter: Innovations in Textile Architecture, (based on a presentation by Dr. Jan Cremers)
2. Jeska, S., (2008), Transparent Plastics, Design and technology, Basel, Boston, Berlin, Birkhäuser
3. Knaack, U., Klein, T., (2010), The future envelope 3: façades - the making of, IOS Press and the Authors
4. Krippners, Herzog, R., Lang, T., Werner, (2004), Façade Construction Manual, Birkhäuser Verlag GmbH

transparent ETFE film

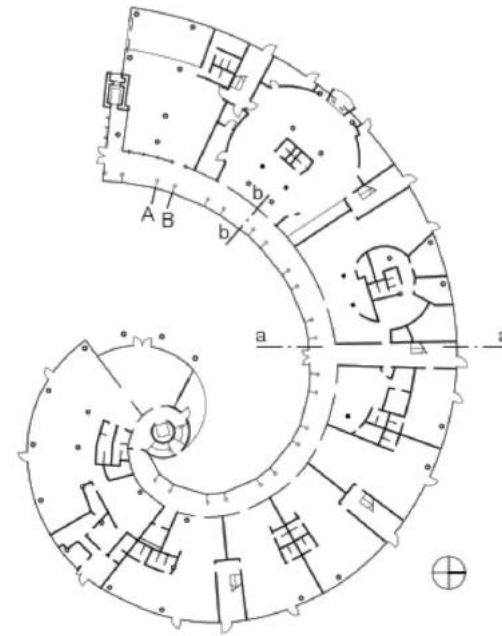


Figure 30: plan



Figure 31: external view

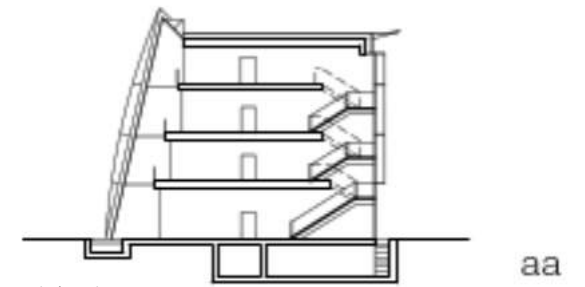


Figure 32: vertical section

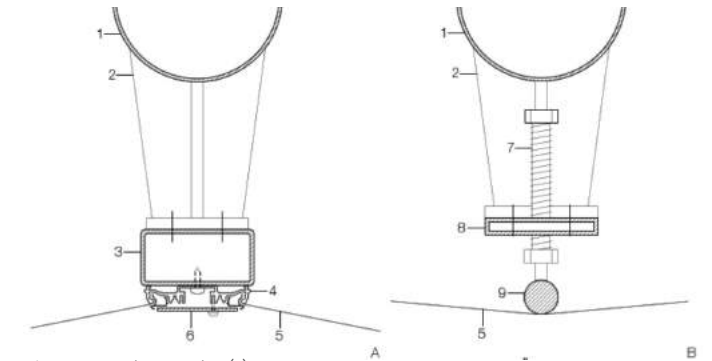


Figure 33: membrane anchor (A) and tensioning (B) point

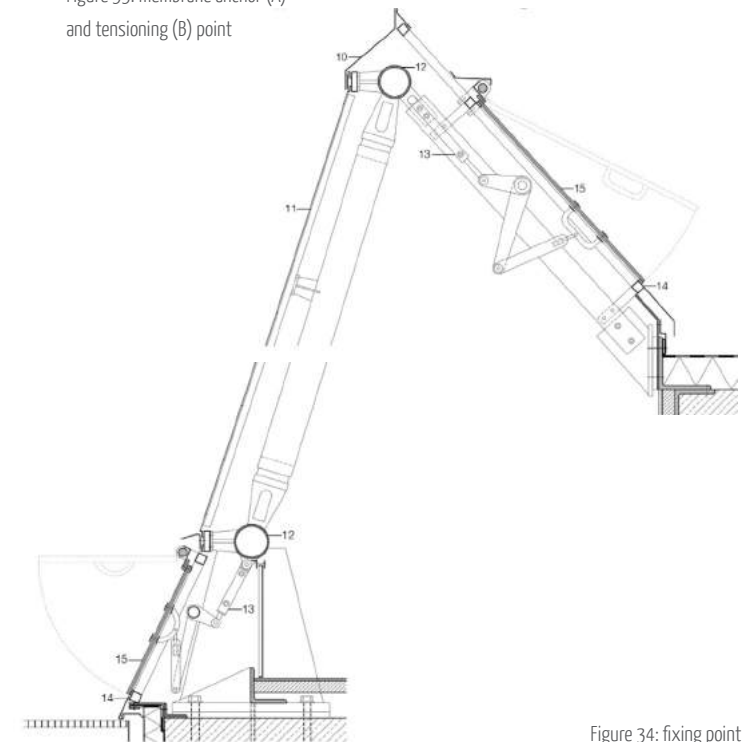


Figure 34: fixing point

suvarnabhumi international airport

Murphy/Jahn, Chicago
2004, Bangkok, Thailand

The Suvarnabhumi airport site covers an area of 3,100 hectares with a current capacity for 45 million passengers, but there are long-term plans for 2 main terminals and 2 satellite buildings with an eventual capacity of up to 100 million passengers and 6.4 million tones of cargo. The main passenger terminal has 7 storeys and a basement giving a total floor area of more than 500,000 square meters, making it the largest in the world.

The first application of low-E coated membrane material on a large scale has been applied to this airport. The new material development and the membrane structure were executed by *Hightex* based on an energy concept of *Transsolar GmbH, Munich*. According to this concept the amount of energy used for the air conditioning of the huge interior space of the airport's concourses (span width 42 m, total length 3 km) has been reduced by limiting the air-conditioned zone to the floor area with a height of approximately 2.5 m, which is the only part of the space used by people. This has been achieved by floor cooling and displacement ventilation close to the frequented circulation areas on the floor.

Additionally, no U-value requirements for the building envelope have been set. The result is constant temperature

low-e coating on PTFE/glass layer

stratification in the concourses (figure 34), as a result of a dynamic CFD simulation. The image shows that there are very high temperatures under the top of the roof, which would lead to severe heat radiation from the roof back to the interior (like a huge radiator). To reduce this effect, a low-E surface has been successfully developed for the interior PTFE/glass layer. As thereby this coated inner liner also mirrors the cold floor temperatures back to the people, the interior comfort is improved even further. The real advantage of PTFE over glass in this case is that it does not gather any dirt, and therefore its reflectivity remains constant over the lifetime of the product.

The high and lasting solar reflection of 70% of the outer waterproof PTFE/glass layer is also an important feature. To improve the acoustic properties of the roof, an additional middle layer has been included, which consists of a cable net covered with translucent polycarbonate (PC) sheets. This, in conjunction with the translucent inner membrane liner, acts as a baffle. All these constitute the complex three-layer membrane of Bangkok Airport's membrane roof.

sources:

1. Pohl, G., (2010), *Textiles, Polymers and Composites for Buildings*, Woodhead Publishing
2. Knaack, U., Klein, T., (2010), *The future envelope 3: façades - the making of*, IOS Press and the Authors
3. Garbe, T., editors: Lang, W., McClain, A., *Tents, Sails, and Shelter: Innovations in Textile Architecture*, (based on a presentation by Dr. Jan Cremers)



Figure 35: internal view of the passengers' terminal

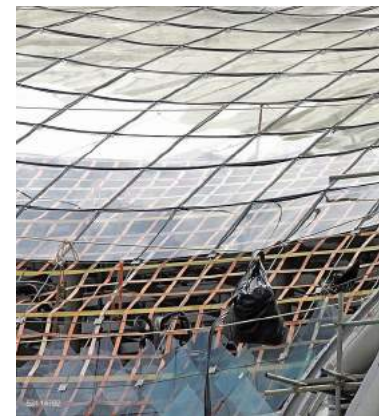


Figure 36: under construction



Figure 37: connection of the roof with the load-bearing structure



Figure 38: general external view

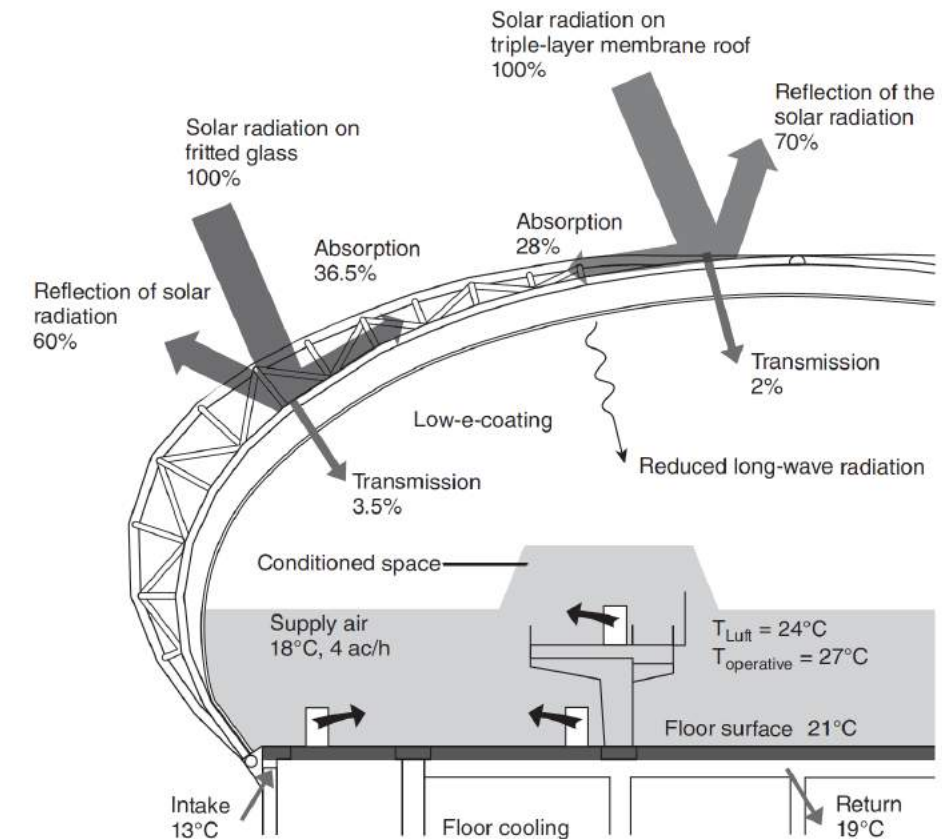


Figure 39: energy concept bt Transsolar

burj al arab

Tom Wright (WKK Architects), Atkins
1999, Dubai

This extraordinary 321m tower is entirely unique in design, fulfilling the clients desire for a landmark building in Dubai. It is the 15th tallest building in the world, and the tallest single structure hotel, standing on a man-made island, Designed in the shape of a giant sail on a triangular plan, the Burj al Arab Hotel is characterised by its simplicity and clarity.

It is a super luxury 7 star All Suite hotel accommodating 202 No. 1, 2, 3 bedroom suites, currently the tallest hotel in the world, with 28 double-storey floors. The Burj al Arab offers three richly decorated restaurants, a 27th floor sky-view Restaurant, a 1st floor all-day dining restaurant and an underwater restaurant housing a high density of indigenous fish in 1150m³ in 3 reef aquariums accessible only via a submarine styled ride.

The mainly in-situ concrete structure of the tower, with exposed diagonal steel wind bracing, is triangular in plan founded on 250 concrete piles, which penetrate the sea floor to a depth of more than 40 meters. Its accommodation wings enclose two sides of a huge triangular atrium that runs up the full height of the accommodation floors. The third side, facing

two-layer PTFE glass-fibre membrane

the shore, is enclosed by a double skinned, Teflon (PTFE) coated woven glass fibre screen (each piece of fabric measuring 2500 meters square); the first time such technology has been used vertically in this form and to this extent. Its textile envelope has become iconic, relating the building to an Arabic tent at a vast scale. Lastly, dichroic lights illuminating the exterior of the Burj al Arab Tower in varying colours throughout the night.

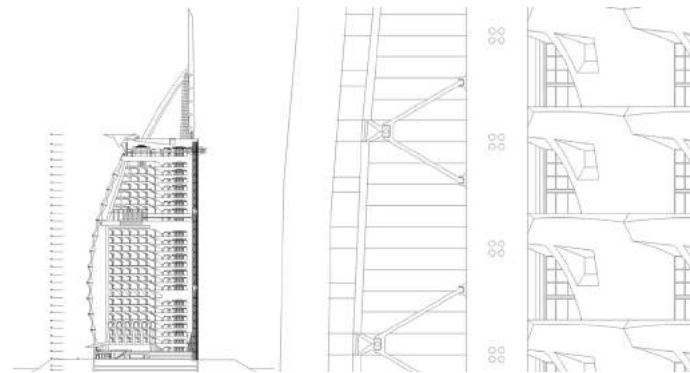


Figure 40: sections

sources:

1. Garbe, T., editors: Lang, W., McClain, A., Tents, Sails, and Shelter: Innovations in Textile Architecture, (based on a presentation by Dr. Jan Cremers)
2. <http://www.e-architect.co.uk/dubai/burj-al-arab>



Figure 41: view of the atrium



Figure 42: general external view

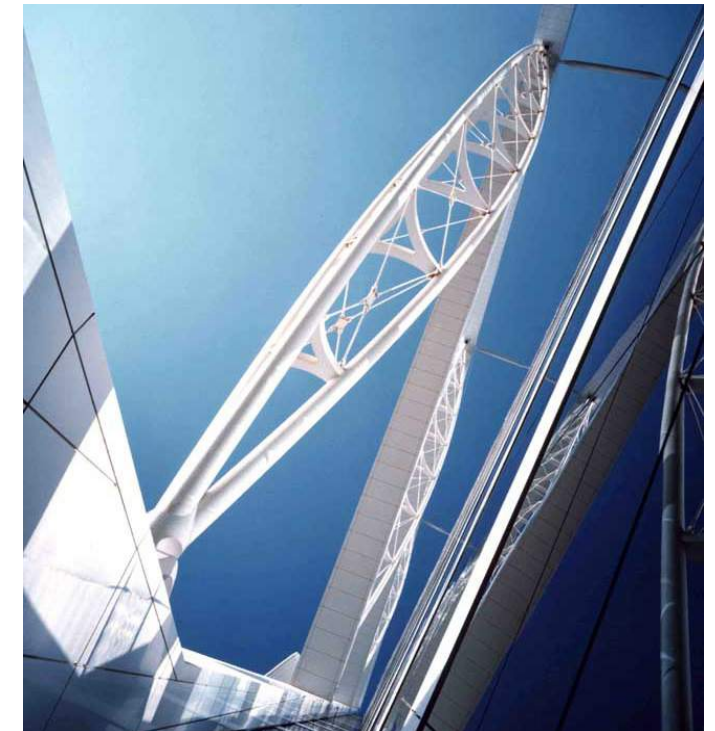


Figure 43: external view

olympic stadium/roof reconstruction

Hans-Georg Esch, Oliver Schwabe

2004, Berlin, Germany

The stadium is conceived as a uniform entity relating to the entire spatial context. The master plan proposed by Werner March in 1936 remains under urban historic preservation, with the new plans emphasizing the quality of the original structure. All necessary additions have been placed underground, outside of the stadium, to prevent obvious visual intervention to the stadium's appearance.

The new roof structure, with its open-ended ring towards the Marathon Gate, sets itself apart from stadium typology with its simple construction and choice of surface material, emphasizing the urban axis from the Olympic Square to the Bell tower. The roof is designed as a light cantilevering steel construction with an upper and lower membrane. The total length of the steel truss-work functioning as the main support is reaches the 68 metres and is visible through the translucent membrane.

The construction height is minimised in the inner and outer edges so that the parapet of the stadium is accompanied by a minimally visible, low horizontal. This way, the roof construction does not dominate the stadium and the architecture of its historical façades remains intact. From the interior, the roof

double layer of PTFE-coated glass fabric

rests on 20 steel columns, which each has a slim profile of 25 cm in diameter, allowing as little obstruction to spectator view as possible. The necessary constructions to bear the roof loads are integrated into the upper tier construction, hidden underneath the natural stone facing.

A special installation integrates the field lights with the stadium's acoustics close to the inner roof edge and omits the use of unsightly floodlight and loud speaker masts. The new stadium roof will illuminate itself and become a recognisable icon.

The stadium received an innovative new membrane roof as part of a retrofit for the latest world cup. *Von Gerkan, Marg & Partner* specified a double layer of PTFE-coated glass fabrics for this purpose. The two layers are separated by a 4.5m gap for technical equipment, while the outermost layer acts as a rain screen. The lightweight outer membrane is only 1.5 mm thick, yet is sturdy enough to support human occupation for construction and repair.

sources:

1. <http://www.gmp-architekten.com/projects/olympic-stadium-reconstruction-and-roofing.html>
2. <http://www.e-architect.co.uk/berlin/olympic-stadium-building>
3. Knippers, Cremers, Gabler, Lienhard, (2011), Construction manual for polymers + membranes : materials semi-finished products form-finding design, Basel, Boston, Berlin, Birkhäuser Verlag GmbH

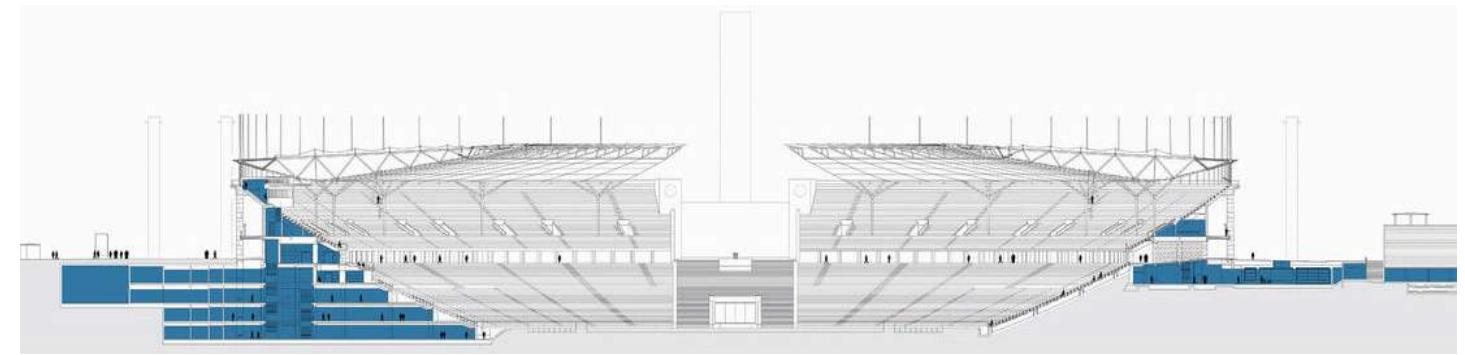


Figure 44: section



Figure 45: view below the roof



Figure 46: view above the roof

icarus house | solar decathlon

Solanext AG, Hightex Group, Georgia Institute of Technology, 2007

Because of the low material thickness of membrane structures and the high levels of light transmission frequently desired, high thermal insulation has previously been difficult to achieve with membranes. The most promising solution is the use of translucent silica-aerogel. Aerogel is a highly efficient thermal insulator, which also transmits light well.

Solanext AG and Hightex Group worked with the Georgia Institute of Technology on their "Solar Decathlon Entry of 2007" to design a roof that was highly insulating and allowed for high light-levels within the structure. The solution was to create an ETFE pillow structure filled with aerogel that is divided into two functional levels. The lower level, which is the ceiling, consists of nine insulated panels (4x1.5m). Aerogel-filled ETFE foil spans between the timber frames to these panels and this has as a result a luminous ceiling that achieves 15% light transmittance. The upper level is an ETFE-covered arch arrangement for weather protection. This layer is independent from the insulating layer and spans only a short distance.

The east and south walls of the house incorporate cellular polycarbonate panels that let in sunlight while being thermally

ETFE structure with aerogel

efficient, as aerogel insulation has been incorporated also into them. The photovoltaic modules above the roof act as sunshades and block most of the solar radiation.

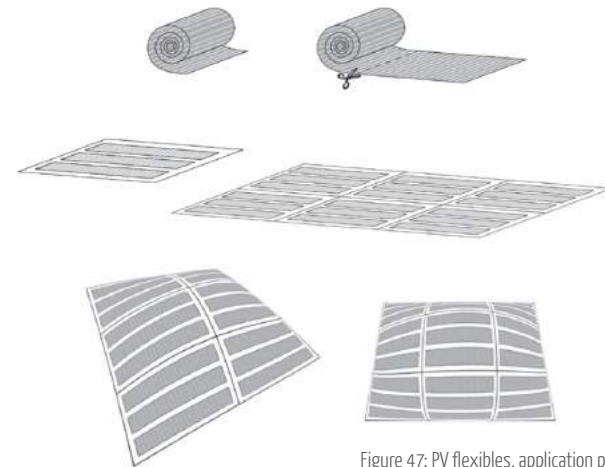


Figure 47: PV flexibles, application process

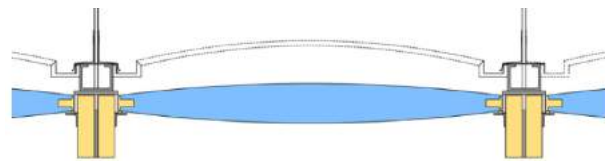


Figure 48: section of translucent aerogel-filled ETFE cushion

sources:

1. http://www.solardecathlon.gov/past/pdfs/07_talking_points/07_georgia_tech.pdf
2. Knaack, U., Klein, T., (2010), The future envelope 3: façades - the making of, IOS Press and the Authors
3. Garbe, T., editors: Lang, W., McClain, A., Tents, Sails, and Shelter: Innovations in Textile Architecture, (based on a presentation by Dr. Jan Cremers)
4. Pohl, G., (2010), Textiles, Polymers and Composites for Buildings, Woodhead Publishing



Figure 49: external view during the day



Figure 50: external view during the night

german pavilion | shanghai expo

Shmidhuber + Kaindl
2010, Shanghai Expo, China

The pavilion is called “balancity” and represents “a city in balance between renewal and preservation, innovation and tradition, urbanity and nature, society and its individuals, work and recreation, and finally globalisation and national identity”.

The four large exhibition buildings, intertwined with each other, provided a symbol of solidarity. Individually each structure would be in equilibrium, but interacting they attain perfect harmony. This interdependence highlights the connections between the interior and exterior spaces, the exchange of light and shade, of building and nature. The choice of *Stamisol FT371* by *Serge Ferrari* (polyester mesh fabric with vinyl coating) an eco-designed, sustainable and 100% recyclable textile for the façade is a decisive element for the project’s coherence.

The silver fabric is flexible and covers the whole building as a second skin. It has the ability to reflect the ambient light. While a great part of the fabric is opaque, areas with transparent textile reveal nice views of the outside space.

polyester mesh fabric with vinyl coating

As far as the recyclability of the material is concerned, after the deconstruction of the pavilion some of the fabric could be re-used at the German School in Shanghai and the rest could be recycled by being transported back to the manufacturer’s *Texyloop* plant in Ferrara. There fabrics are fully recycled with 70% used as PVC granulate and 30% as polyester fibres, raw material for new products.

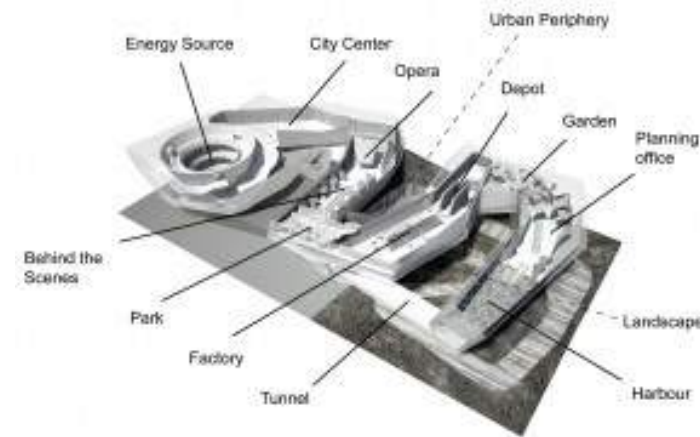


Figure 51: functions

sources:

1. Motro, R. (Ed.), (2013), *Flexible Composite Materials in Architecture, Construction and Interiors*, Basel, Birkhäuser Verlag GmbH
2. <https://www.dezeen.com/2010/04/27/german-pavilion-by-schmidhuber-partner/>
3. <http://www.e-architect.co.uk/shanghai/shanghai-expo-german-pavilion>



Figure 52: construction phase



Figure 53: façade detail

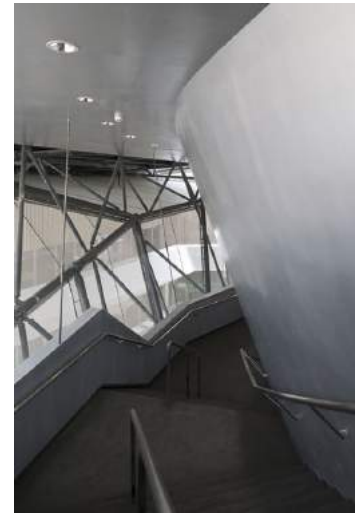


Figure 54: interior view



Figure 55: external view

centre pompidou-metz

Shigeru Ban

2010, Metz, France

The Centre Pompidou-Metz is a vast modular structure around a central spire rising 77m above ground, a nod to the Centre Pompidou, opened in 1977. The hexagonal roof structure covers the building with a total surface area of 10,700 sq. m, including 5,000 sq m of gallery space. Other areas such as the Forum, the restaurant terrace and the garden provide further opportunities to exhibit works.

The main shell of the third gallery at the Centre Pompidou-Metz was completed in December 2008 and a new phase of construction began, with the building of the wooden roof structure by the German firm *Holzbau Amann*.

It took ten months to prepare and four months to install the wooden mesh, which comprises 18 kilometres of glue-laminated timber beams. Every single beam was CNC-machined to unique proportions. This enabled both the production of multi-directional curves and the perforations for the final assembly (node points, pins and braces).

The 8,000 sq. m textile membrane that covers the wooden

PTFE-fibreglass with Titanium Dioxide coating

mesh was made in Japan by *Taiyo*, and it was installed by its German subsidiary, *Taiyo Europe*. Covering the whole building, it protects the wooden frame from rain, sun and wind. The membrane is made of fibreglass and Teflon (PTFE, or polytetrafluoroethylene). The overhanging roof, up to 20 metres in places, protects the walls from the elements. The membrane is translucent, letting through 15% of the light to reveal the hexagonal roof structure at night when the building is lit from the inside.

The membrane is also covered with titanium dioxide coating (TiO_2). This coating is based on nano-technology and it decomposes nitrogen oxide (air pollution due to traffic) when exposed to UV radiation. It has self-cleaning properties due to its high hydrophobic properties. Furthermore, it contributes to the increase of the light reflectance of the membrane that is applied onto.

sources:

1. <http://www.archdaily.com/490141/centre-pompidou-metz-shigeru-ban-architects>
2. <https://www.dezeen.com/2010/02/17/centre-pompidou-metz-by-shigeru-ban/>
3. Llorens, J., (2015), *Fabric Structures in Architecture*, Cambridge UK, Woodhead Publishing

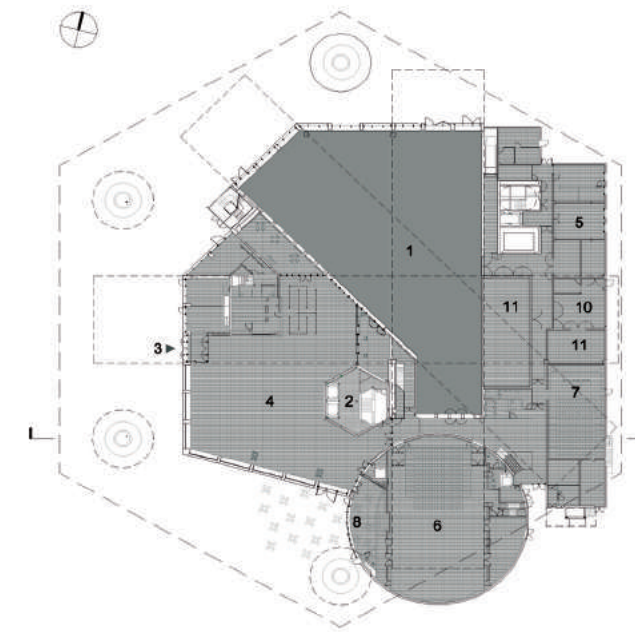


Figure 56: floor plan

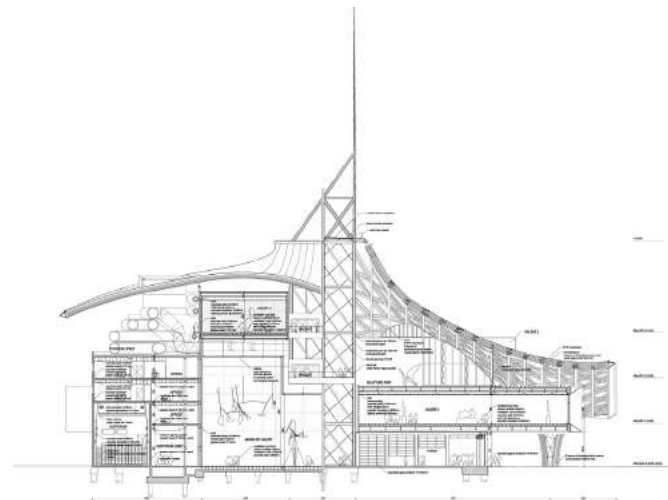


Figure 57: vertical section



Figure 58: general external view



Figure 59: internal view of the canopy



Figure 60: general external view at night

festo ag technology centre

Jaschek & Partner

2002, Esslingen, Germany

three-layer ETFE membrane cushions with integral sunshading

The new Technology centre of the Festo company in Esslingen features spacious atria with roofs of pneumatic membrane constructions from ETFE. The plastic membranes enclose non-air-conditioned conservatories, which act as buffer zones and are intrinsic to the energy concept.

The transparent cushions are 2.5m wide and are placed on a grid of steel elements. They are composed of three layers of plastic film which are welded together airtight along the edges and stretched between an aluminum frame. A fan maintains a marginal overpressure inside the cushions in order to keep their form.

The special feature worth mentioning as well is the integral, pneumatically adjustable sun shading. The middle and the upper layer are printed with a chessboard-type pattern, but with the black squares offset. A fully automatic control mechanism regulates the pressures in the two chambers of the cushions depending on the sun's position and thus it changes the position of the middle layer. It is possible to vary the degree of sun shading from 50-93%.

The layer of air is also responsible for the insulation properties of the structure. In addition, large fabric "sails" in front of the atrium façades provide shade when required.

In terms of energy, the atria with the membrane roofs function as fully glazed conservatories. This effect is due to the solar gains and the layer of air inside the cushions. The "sails" mentioned above contribute to avoid overheating and also air can be pumped through the cushions to prevent a built-up of heat. Permanent ventilation and night-time cooling are ensured by the louver openings above the edges of the roofs to the adjoining office blocks. Lastly, the water-filled solid components of the adjoining concrete walls and the gallery floors provide additional cooling.

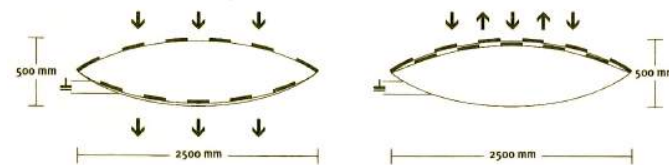


Figure 61: ETFE cushions

Sources:

1. Jeska, S., (2008), Transparent Plastics, Design and technology, Basel, Boston, Berlin, Birkhäuser
2. <https://www.festo.com/net/SupportPortal/Files/8574>



Figure 62: view from the atrium

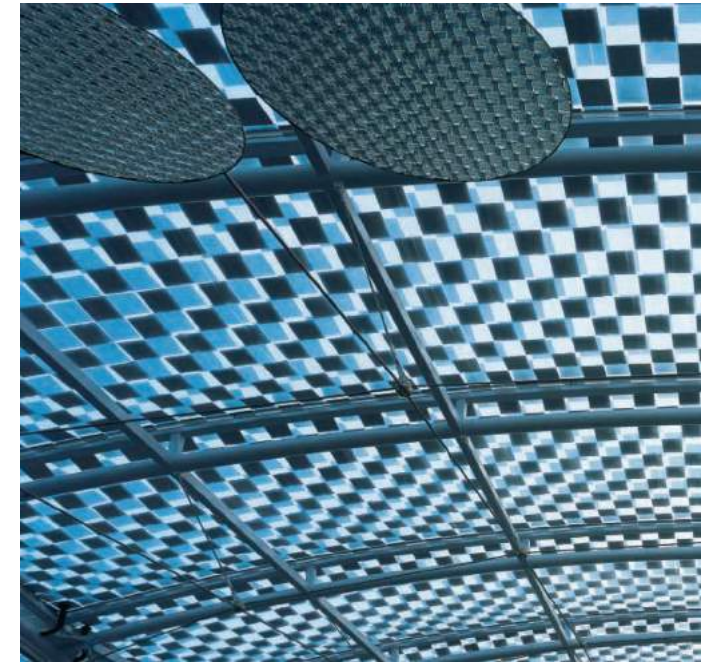


Figure 63: printed patterns on the ETFE membrane

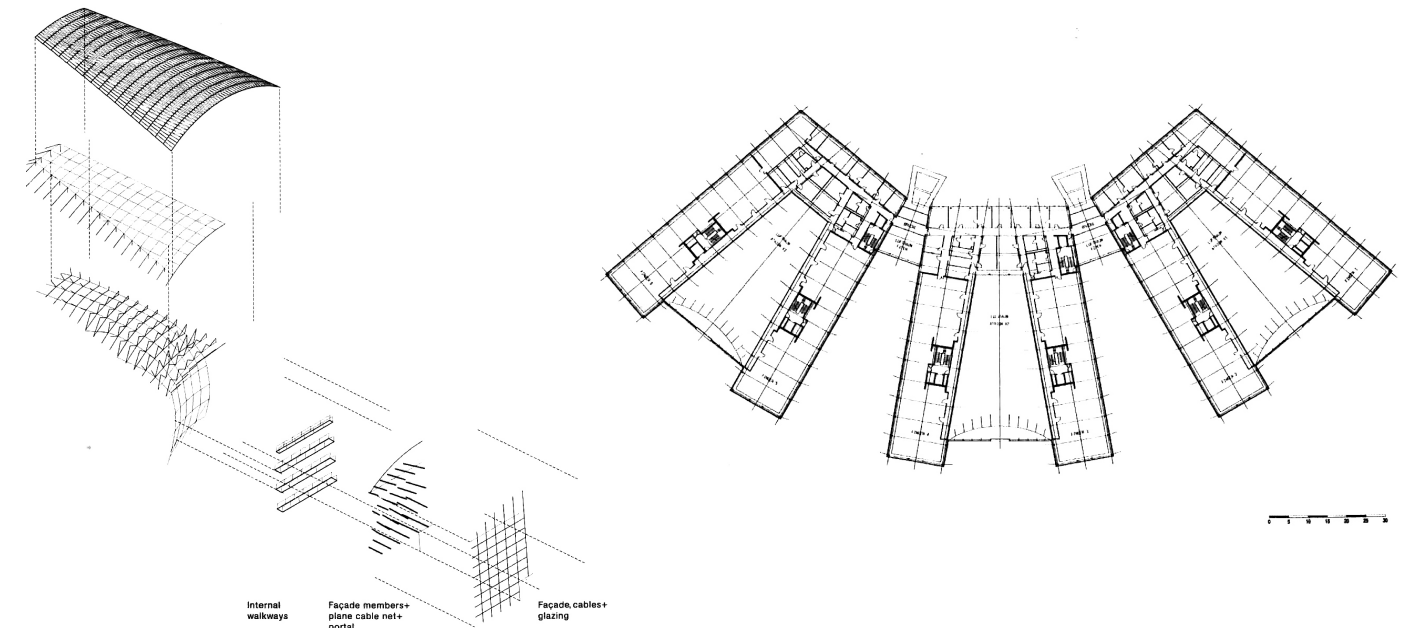


Figure 64: atrium construction

Figure 65: typical floor plan

olympic shooting venue

Magma architecture, Berlin

2011, London, Woolwich, Arsenal Station

The London Shooting Venue accommodated the events in 10, 25 and 50 m Sport Shooting at the 2012 Olympic and Paralympic Games in the southeast London district of Woolwich. The temporary facility consists of three halls, forming an urban ensemble on the former training area.

The building construction is completely covered in a white membrane with bright easy-to-focus-on discs of colour set into high and low points, creating undulations in the façades. These openings structure the building envelope as well as allowing natural ventilation. They are arranged according to their function as main entrances or ventilation inlets, and serve to maintain the necessary tension in the membrane.

Some natural light permeates this PVC membrane, while the entrances are contained inside all the spots that meet the ground.

Meeting the demanding sustainability criteria set by the client ODA (Olympic Delivery Authority) made the design of the venue particularly challenging. Important goals included minimising

polyester mesh fabric with vinyl coating

material usage and energy consumption. The construction, furthermore, had to be easy stored, transported and reused.

The foundations of the buildings, which do not have any basements, constitute a pure steel construction. The support loads are transferred to foundation piles in the ground via cross-shaped steel plates. The steel pipe piles were made out of recycled oil pipes.

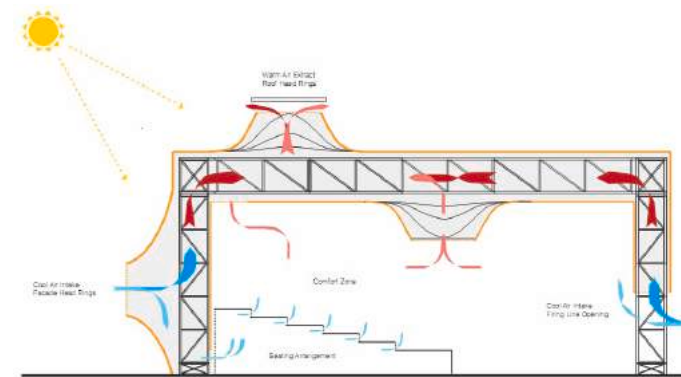


Figure 66: climate concept diagram

sources:

1. <http://www.detail-online.com/article/london-2012-olympic-shooting-venues-16398/>
2. <https://www.dezeen.com/2012/06/12/olympic-shooting-venue-by-magma-architecture/>
3. <http://www.archdaily.com/244370/olympic-shooting-venue-magma-architecture>

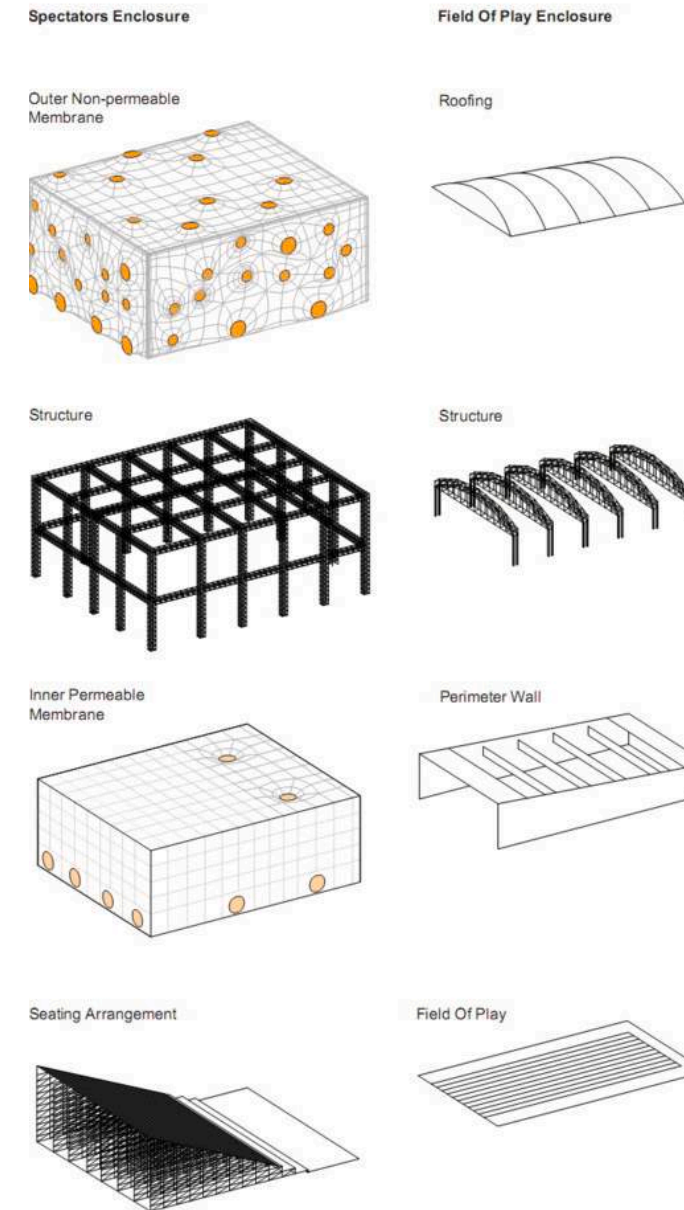


Figure 67: structure diagram

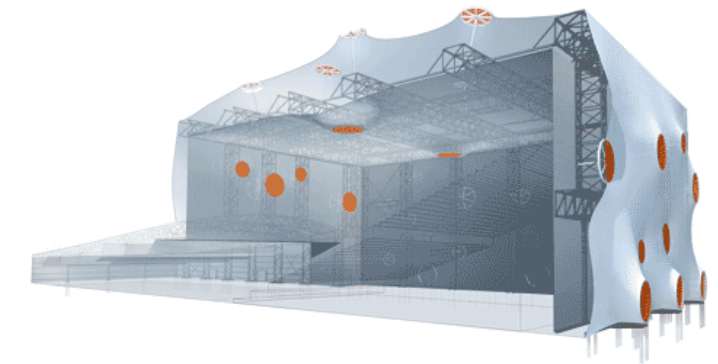


Figure 68: perspective section rendering



Figure 69: external façade component

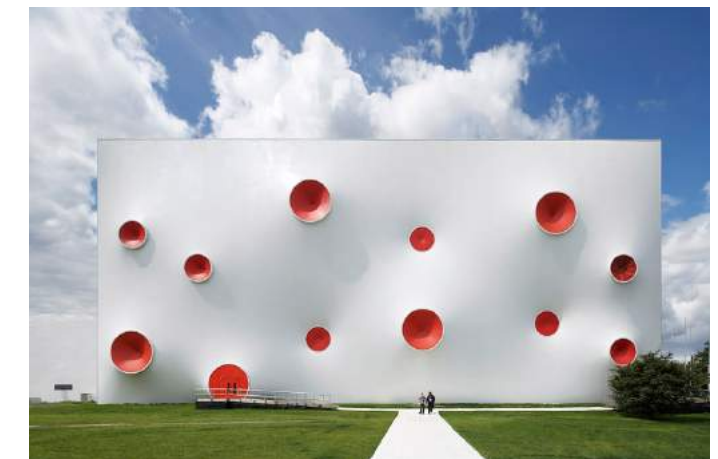


Figure 70: external façade view



3

climate

paris, france

The chosen location for the project is Paris, France. In order to decide which material, among those described in the literature review, is the most suitable one as a solution to the problems high-rises face, it is necessary to conduct a research on the climate conditions of the specific location, as well as take into consideration the required indoor comfort.

The climate in Paris, according to the Köpen-Geiger classification, is oceanic (Cfb), which is warm temperate climate and typical of the west coasts in higher middle latitudes of continents. London and Amsterdam have similar climate. It is moderate and influenced by the sea. It is rather humid with cool summers and mild to cool (but not cold) winters. The annual average temperature is 11°C, with a minimum of 3°C in January and 19°C in July and August. Also, it rains rather frequently all times of the year, with May being the most wet month (60mm) and April the driest (44mm). The annual average of the sky coverage is 62%, with the lowest value in August (47%) and the highest in January (73%). The sun's angle reaches the 18° in winter and 65° in the summer. Lastly, the wind's direction is mainly west/south-west with an annual average speed of 3.58m/s.

Using the Climate Consultant software we can collect various data, like the ones above and subsequently draw several conclusions. These data concern the daylight hours, the wind's

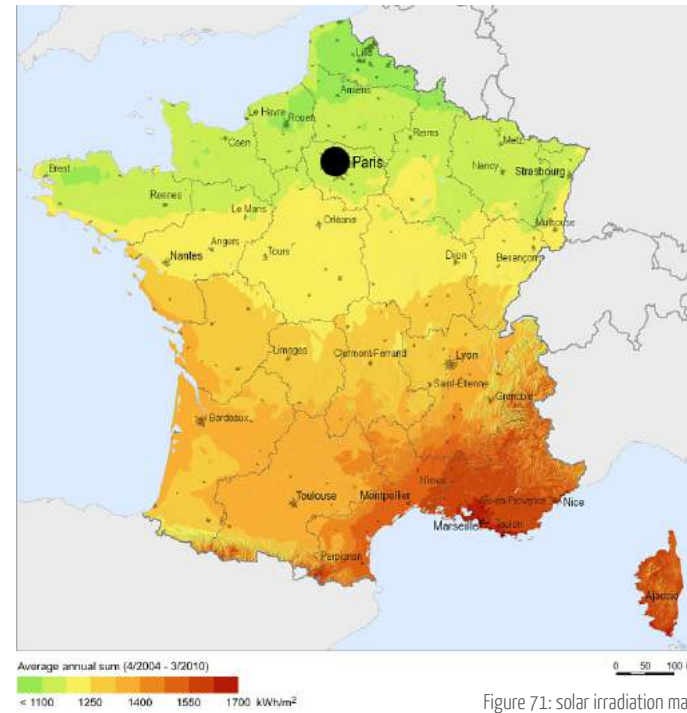


Figure 71: solar irradiation map

speed and direction, the average temperature in different times of the year, the sky cover range etc. Furthermore, according to European standard EN15251 we can collect data about the indoor comfort requirements. The lowest comfort temperature in winter is 20°C and the highest 24°C, as for the summer, the highest is 26°C and the maximum humidity reaches 84.6%, as calculated by the Predicted Mean Vote (PMV) model. The indoor comfort consists of various aspects that should be taken into account, some of which are the thermal, acoustical and visual comfort.

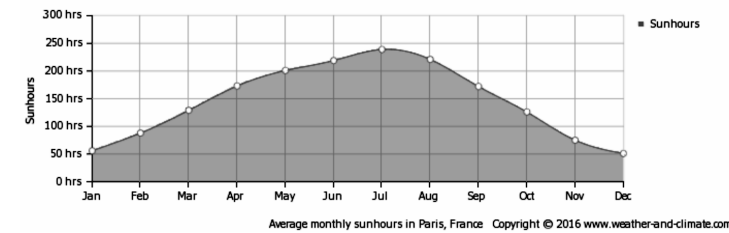


Figure 72: average monthly sunhours

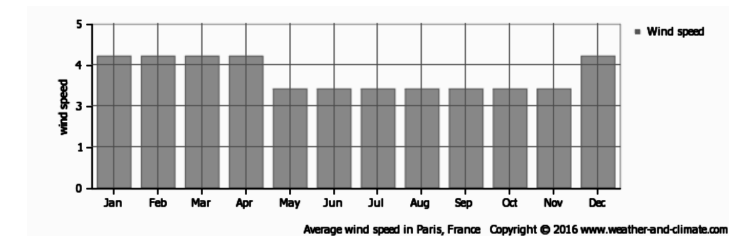


Figure 73: average wind speed

Lastly, the new façade design should follow certain requirements according to building regulations of the chosen location. France appertains to RT2012 (Réglementation thermique) and also follows the EN15251_2007 of the European Regulations.

sources:

1. Climate Consultant software
2. https://fr.wikipedia.org/wiki/Climat_de_Paris
3. <https://weather-and-climate.com/average-monthly-Rainfall-Temperature-Sunshine,Paris,France>
4. NEN-EN 15251:2007: Indoor environmental input parameters for design and assessment of energy performance of buildings addressing indoor air quality, thermal environment, lighting and acoustics
5. <http://www.rt-batiment.fr/batiments-neufs/reglementation-thermique-2012/presentation.html>

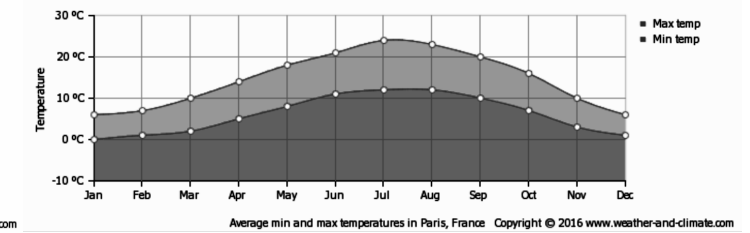


Figure 74: average min and max temperature

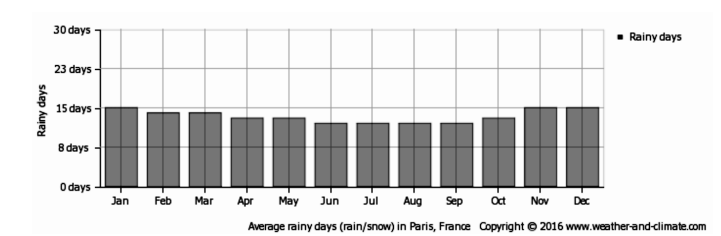


Figure 75: average rainy days

building regulations (RT 2012+EN15251_2007)

thermal:

- » U-value (max): 1.2 - 1.5 W/m²K
- » Solar transmittance factor > 0.35

acoustics:

- » values in offices for equivalent levels: 33 - 45 dB
- » values in offices for instantaneous levels: 35-50 dB



high-rises

high-rises

height limit

In Europe, there is no official general law restricting the height of structures. There are, however, height restriction laws in many cities, often aimed to protect historic skylines. As far as Paris is concerned, where the case study will be located, the tallest structure remains the Eiffel Tower in the 7th arrondissement, 300 meters high, completed in 1889 as the gateway to the 1889 Paris Universal Exposition. The tallest building, though, is the “Tour First”, reaching the 231 meters and is located in the area of *La Défense*. The second one is the “Tour Montparnasse”, reaching the 210 meters and located in the 15th arrondissement. Lastly, the “Hermitage Plaza” is a project consisting of a podium and 6 buildings, including two towers, designed by *Foster+Partners* for the Paris-La Défense business district. After its completion in 2021, the two 323 metres tall towers with 93 and 91 floors respectively will be the tallest buildings in the European Union.

problems

The most common structural factors that all high-rises have to deal with are earthquakes, wind, vibrations (traffic), explosions and airplane impact. As far as the indoor comfort is concerned, it is rather challenging to satisfy the occupants

of such buildings. More specifically, wind and traffic can be both experienced as unpleasant and even unhealthy in many cases.

effects of the wind

The wind constitutes one of the main problems of high-rises that should be tackled. On the one hand, it affects the indoor comfort, as mentioned above, near the ground and it is responsible for the spread of pollutants. Therefore, high local speed can be developed near the buildings' corners causing discomfort. On the other hand, the horizontal wind forces have a great impact on the structure of the building, even more than the vertical gravity forces. In addition, wind can cause extreme noise disturbance that should be reduced by rounding off the profiles of the façade elements for example.

1. https://en.wikipedia.org/wiki/List_of_tallest_buildings_and_structures_in_the_Paris_region
2. <http://www.citylab.com/design/2013/09/could-city-light-become-city-height/6953/>
3. <http://parispropertygroup.com/blog/2015/rise-paris-city-center-skyscrapers/>
4. Eisele, J., Kloft, E., (2003), *High-Rise Manual: Typology and Design, Construction and Technology*, Basel, Boston, Berlin, Birkhäuser
5. Gräwe, C., Cachola Schmal, P., (2007), *Contemporary highrise architecture and the international highrise award 2006*, Jovis
6. Hemel, M., Kuit, B., (2010), *Supermodel: making one of the world's tallest tower*, nai010 publishers

façade structures

As mentioned above, the wind can create significant loads towards the building envelope. The façade should be divided into zones based on the wind's force. Thus, the joints between the façade elements play an important role. The greater the height of the façade and the distance between the different elements, the greater the joints' size.

High-rise façade types can be divided according to the following structural criteria:

- » standing / suspended
- » location in relation to the primary structure
- » non load-bearing / load-bearing (as primary component)

Subsequently, a couple high-rises examples will follow in order to explore certain solutions given to the above problems by architects and engineers.

Figure 76: Canton TV tower - Guangzhou Tower, Mark Hemel and Barbara Kuit



reference projects

Canton TV tower, Guangzhou, China Mark Hemel & Barbara Kuit, 2010

In towers with smooth façade surfaces the wind sticks on the one façade and at the other side of the building it starts pulling. On the contrary, a rough surface has the ability to reduce vortex shedding. All the different elements reflect the wind towards various directions producing, thus, an overall neutralizing effect.

Three characteristics of the Canton TV tower (600m height) are responsible for the reduction of the wind loads on the building envelope:

- » **slenderness** --> less surface is available for the wind to catch onto
- » **openings** --> the wind can flow through the building having a minimum resistance
- » **roughness of the skin** --> redirection of the wind towards different ways and reduction of the vortex shedding

1. Hemel, M., Kuit, B., (2010), Supermodel: making one of the world's tallest tower, nai010 publishers

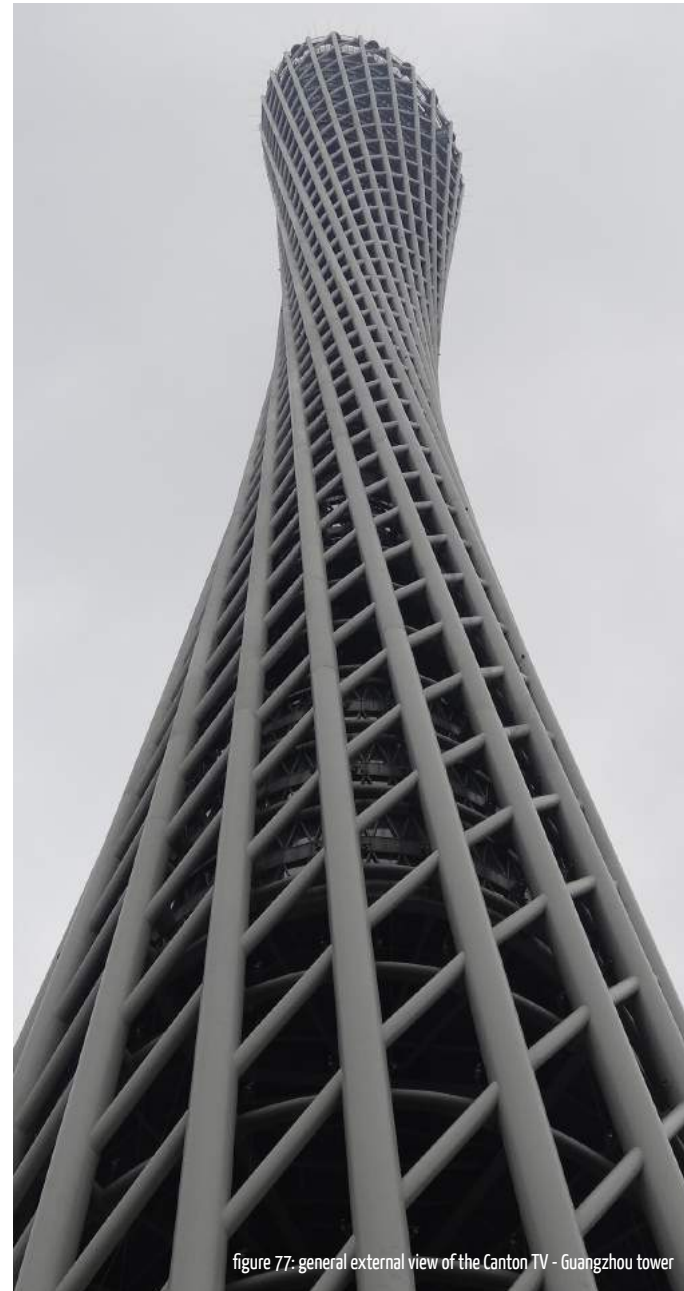


figure 77: general external view of the Canton TV - Guangzhou tower



figure 78: general external view of the Turning Torso tower

Turning Torso, Malmö, Sweden Santiago Calatrava, 2005

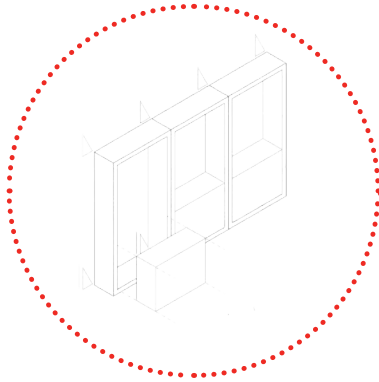
The idea is based on one of Calatrava's sculptures. It is 190m high and it consists of nine cubes, each one containing five floors. Each cube is rotated 90 degrees clockwise from the one below. A concrete core constitutes the main load-bearing structure, around which square rooms are arranged. Attached to them, triangular rooms are supported by a curved steel frame on the outside.

As far as wind loads are concerned, the twisted form can be very effective, alleviating the effects of vortex-shedding induced by lateral wind loads and minimizing the wind loads from prevailing direction. Also, giant pins attached to the ground were then implemented, decreasing the movement during severe storms, which is nearly unnoticeable.

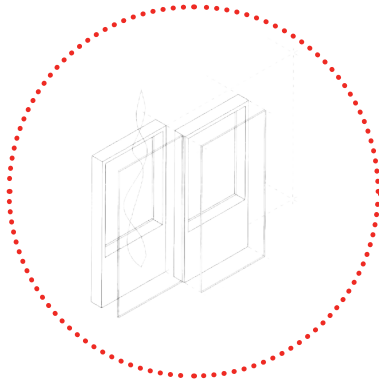
1. Contemporary highrise architecture and the international highrise award 2006, C. Gräwe, P. Cachola Schmal, Jovis, 2007
2. http://faculty.arch.tamu.edu/media/cms_page_media/4433/TurningTorso.pdf

façade types

There are a lot of different façade types that can be found and implemented in various buildings. A short reference will be made here in these types¹ and then the one(s) that will be followed for the design later on will be mentioned.

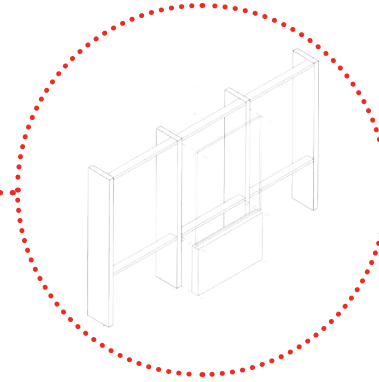


2. curtain wall façade

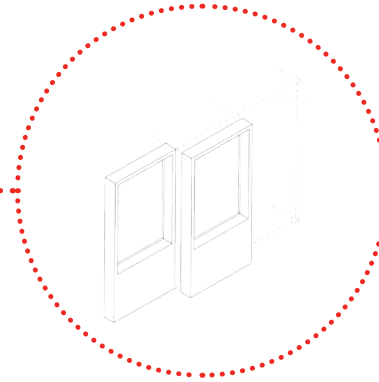


4. double façade

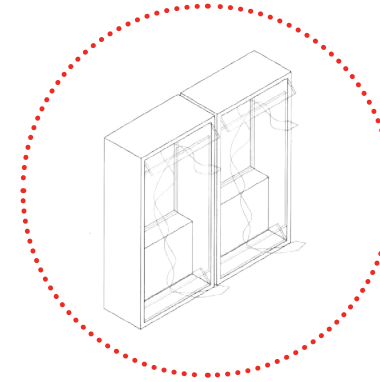
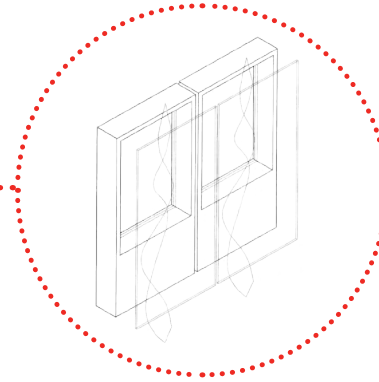
1. post-and-beam façade



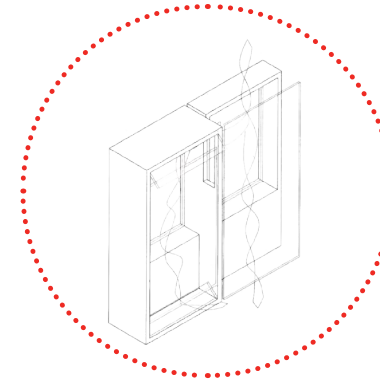
3. system façade



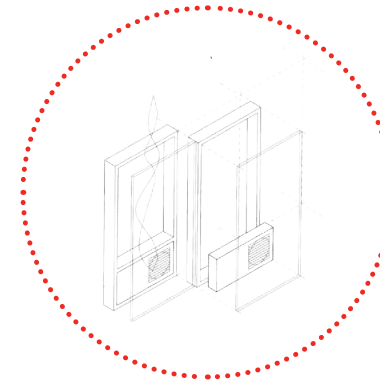
5. second-skin façade



6. box-window façade

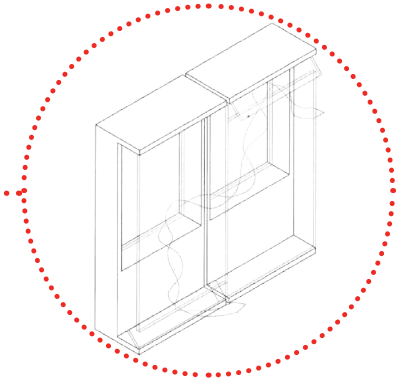


8. shaft box façade

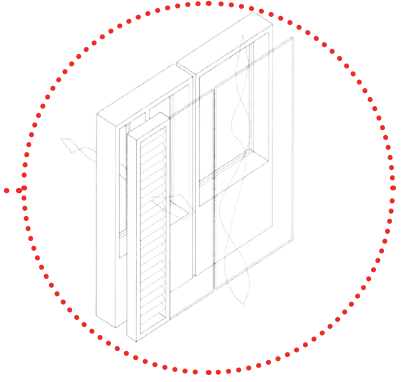


10. integrated façade

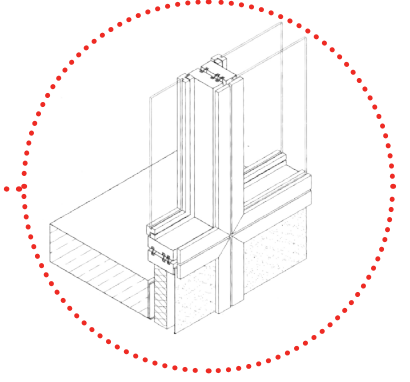
7. corridor façade



9. alternate façade



11. unit system façade



source:

1. Knaack, U., Klein, T., Bilow, M., Auer, T., (2007), Façades: Principles of Construction, Birkhäuser

unitised element façade

From the façade types mentioned above, the last one (unit system façade) will be investigated and elaborated on for the design project. Unitised façades are completely prefabricated elements that are most of the times one store high and they need to be transported to the building site and then positioned onto the building. They have a load bearing framework in which the glazing or the desired cladding is placed. Usually, the elements are suspended at the top and connected at the bottom. This way, they can be easily placed consecutively on top of each other. Furthermore, the unitised façade performs several functions simultaneously: it should be able to provide thermal and acoustical insulation, as well as weatherproofing.

As already mentioned, since they are prefabricated elements and they need to be transported and positioned on site it is required that they are rather rigid in order to avoid any possible damage, as well as watertight and airtight in advance. This has as a result the fast and cost-efficient installation with limited manpower and equipment in comparison with the traditional curtain walls. As for the high-rises, which is the case in this graduation project, this way of construction allows for building tolerances to be taken into account and for the chance to build floor by floor, from the bottom to the top, while permitting at the same time constructions in the inside of the building.

The fact that a great number of possibilities is available makes the element façade rather unique. There are several standard solutions that can be applied to many situations, but a lot of times the projects require custom-made solutions combining different types and aspects together, such as ventilated façades, double skin, sunshading, operable windows, insulation materials etc. A number of examples are shown in the following pages concerning buildings with unitised façades.

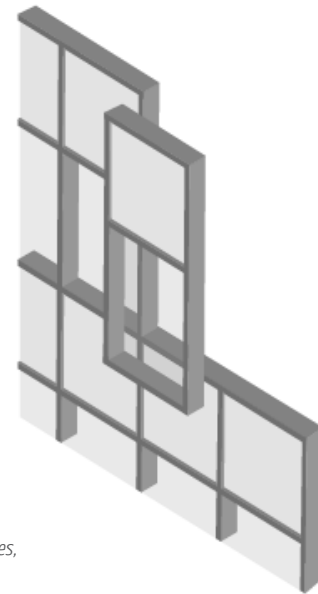


Figure 79: unitised façade
(source: *Unitised Element Façades*, REYNAERS aluminium)

source:
1. Knaack, U., Klein, T., Bilow, M., Auer, T., (2007), *Façades: Principles of Construction*, Birkhäuser
2. *Unitised Element Façades*, REYNAERS aluminium

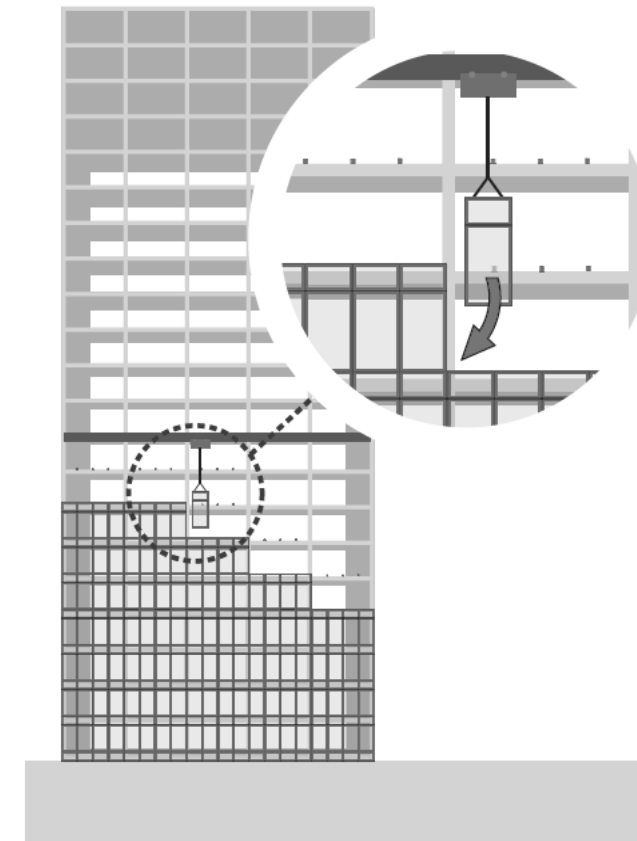


Figure 80: installation solution (source: *Unitised Element Façades*, REYNAERS aluminium)

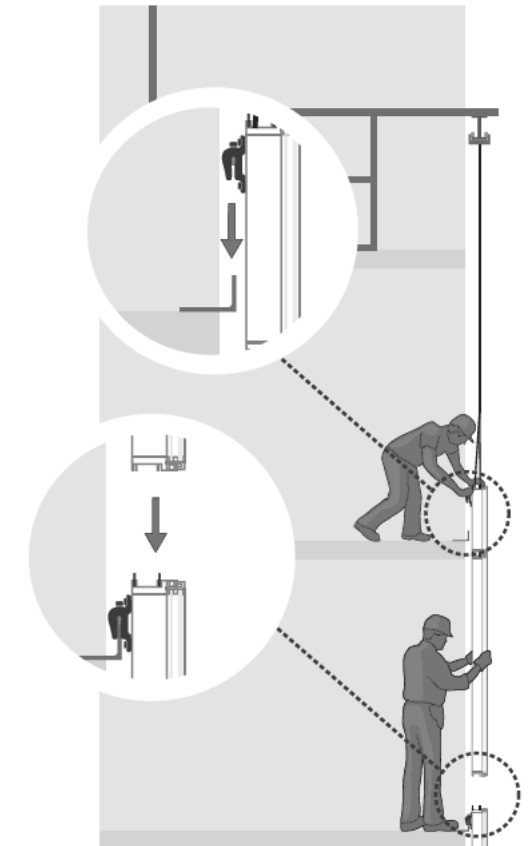


Figure 81: standard element installation
(source: *Unitised Element Façades*, REYNAERS aluminium)

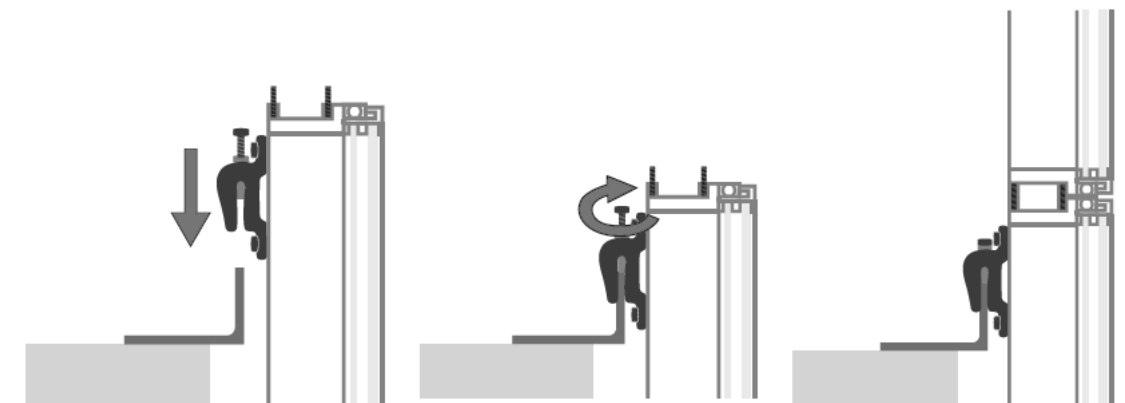


Figure 82: detail of standard bracket functionalities (source: *Unitised Element Façades*, REYNAERS aluminium)

unitised element façade

Etopia centre for art and technology

The challenge for this façade design was to maintain the same narrow 65mm width. The panels span from floor to floor and a special anchor was designed in order to connect the elements with a hook bracket in front of the floor slabs. As for the windows, when they open their frames disappear completely behind the fixed frames.

PROJECT INFORMATION

GENERAL INFORMATION

Location : Zaragoza, Spain
 Architect : MCBAD/Colomer Dumont, Paris-Valencia
 Investor : Ayuntamiento de Zaragoza
 Contractor : UTE Sacyr, S.A.U.- Marcor Ebro, S.A., Zaragoza
 Fabricator : Euroscá, Huesca
 Reynaers systems : CW 65-EF bespoke solution, CW 50-SC, CS 77, CS 68-HV

MAIN ELEMENTS

- 2,800 m² exhibition hall divided into 2 show-rooms & an Art Lounge
- Individual workshops
- Media Lab
- Meeting rooms, 4 company workshops, 4 fabrication laboratories and an electronics laboratory
- Training rooms for up to 100 people

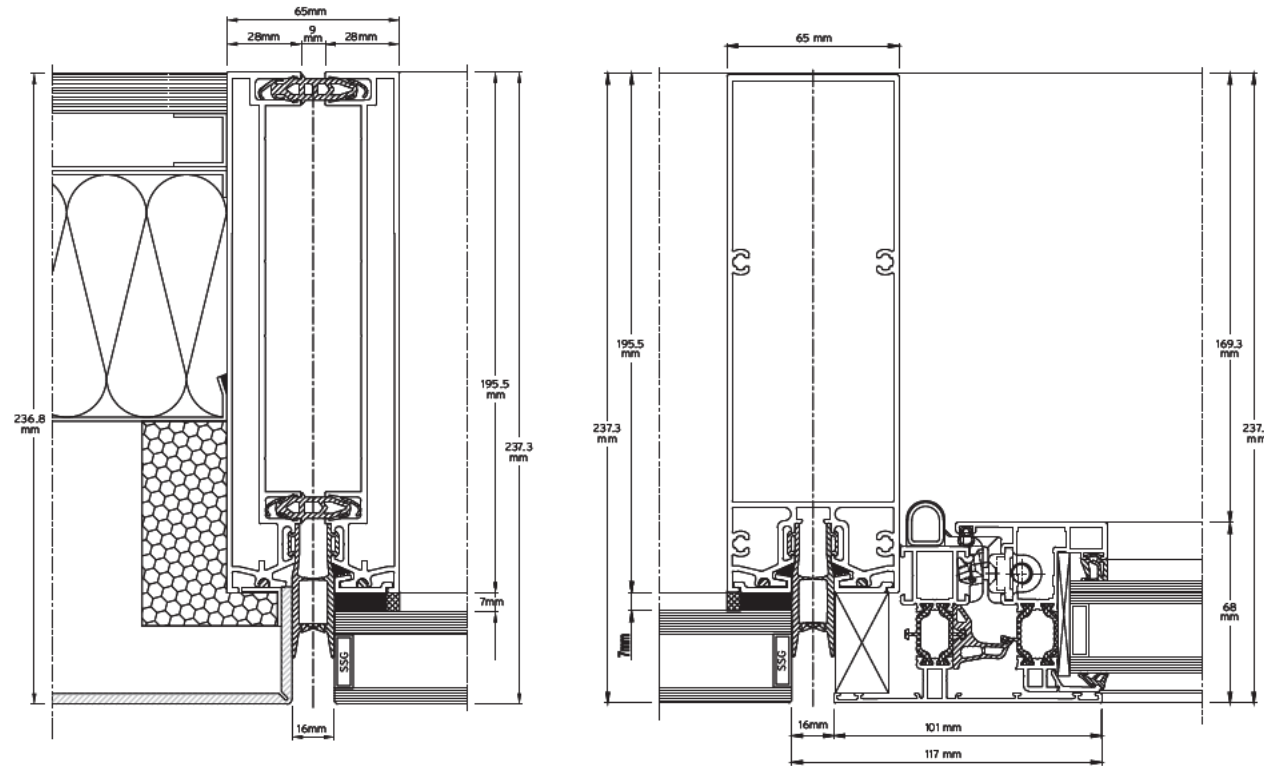


Figure 83: unitised façade horizontal details
 (source: Unitised Element Façades, REYNAERS aluminium)

source:
 1. Unitised Element Façades, REYNAERS aluminium

Lazurniye Nebesa

The building is designed as the most eco-friendly building in Kazan and it was equipped with 52 mm 3-glass elements. Due to complex space-planning decisions and the constructive features of the building, special solutions for corner profiles as well as mullions and transoms along with pressure plates and glazing beads were developed.

The process of building a 122 meter circular building, with different corners ranging from 90 & 137 to 151 & 177 degrees, requires excellent engineering capabilities. Employees and engineers of the involved companies took on, parallel with works, training courses on assembly of full-size elements.

PROJECT INFORMATION

GENERAL INFORMATION

Location : Kazan, Russia
 Architect : LLC Aghai, Kazan
 Investor : RosInterBank
 Contractor : LLC Stroitel'naya Kompania, Kazan
 Fabricator : LLC Element Façade, Chelyabinsk
 Reynaers systems : CW 65-EF/HI

MAIN ELEMENTS

- 37 floors, 122 metres
- 1 Helicopter platform
- 33 Residential floors with apartments
- 2 Office floors
- 3 Parking floors, 275 parking spaces

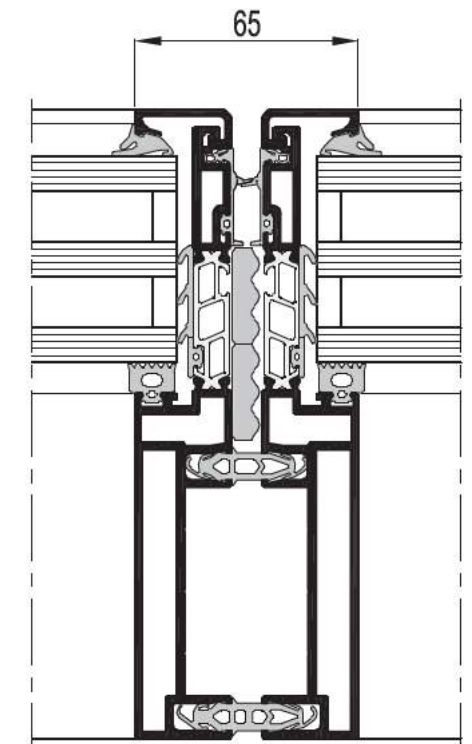


Figure 84: unitised façade horizontal detail of the 3-glass element
 (source: Unitised Element Façades, REYNAERS aluminium)

source:
 1. Unitised Element Façades, REYNAERS aluminium

unitised element façade

HÖFÐATORG

Four different façade elements were developed based on a 1.5x3.5m module: elements with vertical glass and top-hung windows over the total width of the element, elements with sloped glass parts, either fixed or with top-hung windows and corner elements of 64 and 116 degrees. For the sharp and obtuse corners of the tower, special elements were fabricated with custom-made vertical T-profiles to achieve the desired visual effect. For the sloped glass parts, a new unitised curtain wall system was developed. It consists of a main frame, with the requested structural elements, fixed to the concrete structure of the building. Inside this frame, a fixed glass frame or top-hung frame supporting the glass was installed. All top-hung windows are motor-operated, and the motor is integrated inside the system.

Lastly, a 250 mm deep thermal broken outer frame construction was developed with horizontal and vertical transoms to support the glass frames. The 250 mm deep system was required to withstand the expected high wind speeds of up to 280 kilometres per hour.

source:
1. Unitised Element Façades, REYNAERS aluminium

i PROJECT INFORMATION

GENERAL INFORMATION	PROJECT SOLUTIONS
Location : Reykjavik, Iceland	• Ground floor: structural clamped solution
Architect : PK Arkitektar, Reykjavik & LWW Architekten, Berlin	• Tower: structural sealed inclined glass parts integrated into the unitized system
Contractor : Eykt ehf., Reykjavik	• A 250 mm deep thermal broken outer frame
Façade consultant : IFFT - Karlotto Schott	• SSG stepped glass units
Fabricator : Gluggar & ASF, Akureyri	• All top hung windows are motor operated, integrated inside the system
Reynaers systems : CW 50-SC, CW 86-EF bespoke solution	• Corner elements were fabricated with special vertical T-profiles to obtain the requested look

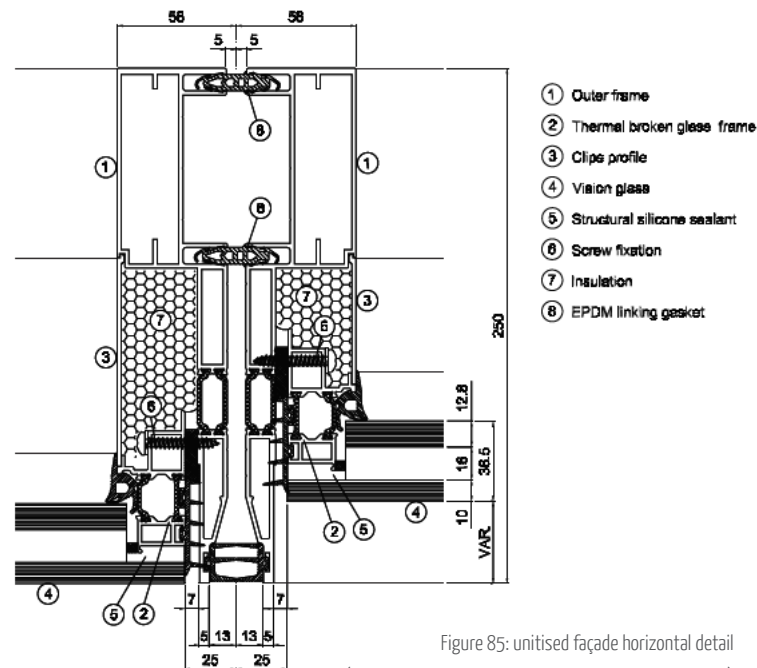


Figure 85: unitised façade horizontal detail
(source: Unitised Element Façades, REYNAERS aluminium)

Ferrari World

funnel:

- Two major parts, funnel and shield
- Additional walkway
- The funnel was installed via a 3D space frame
- The shield's curtain wall was uniquely anchored to the outside steel
- Different colours for outside and inside parts
- The steel walkway has a large aluminium ball nose accepting light fixtures and a custom-made sunscreen solution
- The roof is molded after Yas Island's logo

curtain wall:

- Curtain walls were installed via a 3D space frame to allow movement prompting proper dilatation adjustments
- The mullion's shape was fixed (visual architectural aspect) but the final size was determined through inertia calculations
- Strong fixation of heavy elements to the frame
- Panels are mostly trapezoidal and 3D shapes

source:
1. Unitised Element Façades, REYNAERS aluminium

i PROJECT INFORMATION

GENERAL INFORMATION	PROJECT STAGES
Location : Abu Dhabi, United Arab Emirates	• First design meeting : February 2008
Architect : Benoy Architects, London	• Funnel die drawing finished : August 2008
Façade Team : Besix Global Façade Org., Belgium	• Shield die drawing finished : September 2008
Fabricator : Jungbluth Alu Partners Ltd., Belgium	• Funnel element testing : November 2008
Contractor : SixConstruct	• Shield element testing : December 2008
Investor : Aldar Properties, United Arab Emirates	• Final delivery of materials : April 2009
Client : Yas Island, United Arab Emirates	• Last Shield element install : June 2009
Reynaers systems : CW 86-EF bespoke solution	• Last Funnel element install : July 2009

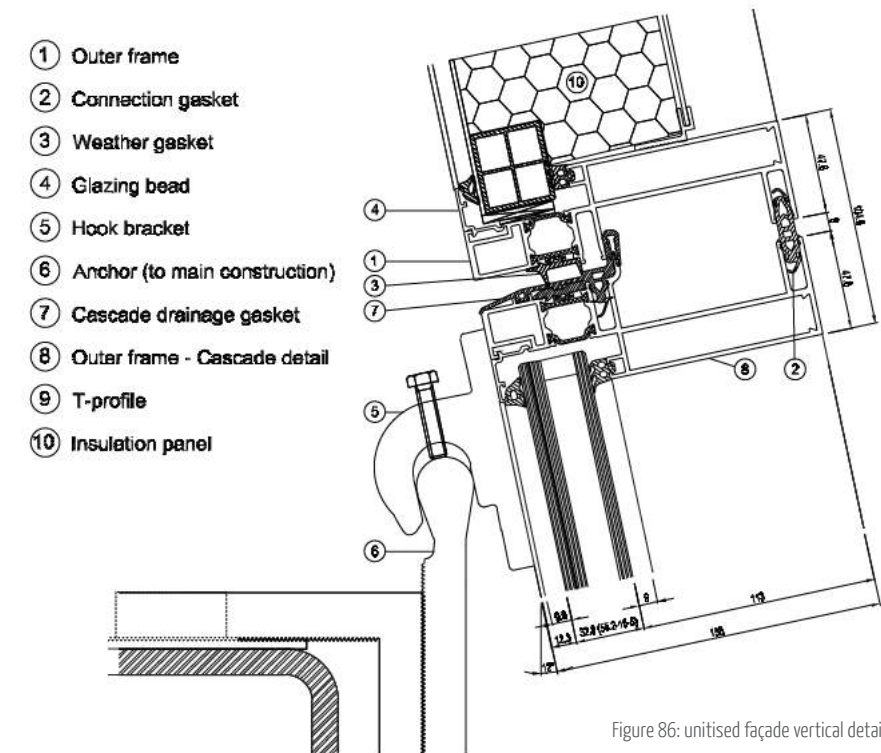


Figure 86: unitised façade vertical detail of the hook bracket and the anchor connection
(source: Unitised Element Façades, REYNAERS aluminium)

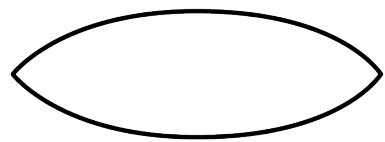
preliminary
design
concepts

design concepts

There are three main categories in which fabric structures can be divided: **inflatable**, **deflateable** and **multi-layer** structures. Furthermore, as described in the literature part, membranes can be combined with **PV films**, **silica-aerogel** and **phase change materials (PCMs)** in order to improve their thermal insulation. Based on these categories and combinations the first preliminary designs, concerning an adaptive fabric façade of a high-rise building in Paris, were created. They are mainly based on design principles that take into account certain parameters.

inflatable (cushions)

[pressure difference]



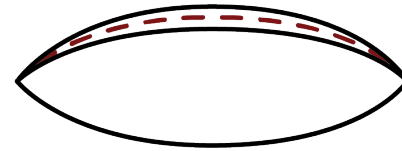
horizontal sections

deflateable (vacuum system)

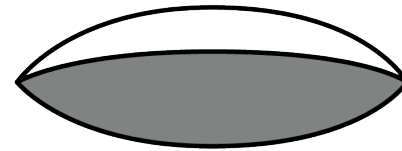
[pressure difference]



PV flexibles



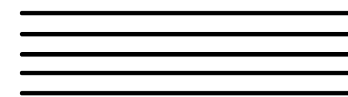
silica-aerogel



PCMs



multi-layers



vertical sections

1.

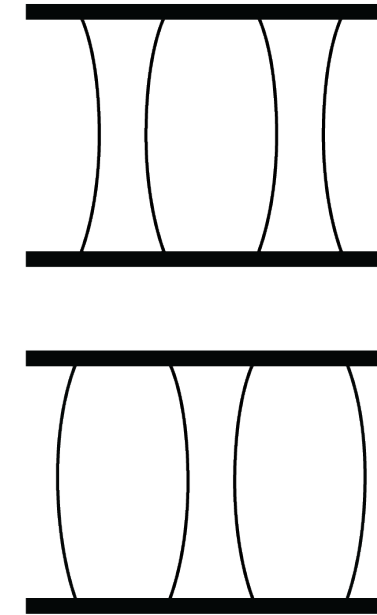
1 a



vertical section

1a. Inflated and deflated elements: create a rough façade and prevent vortex shedding.

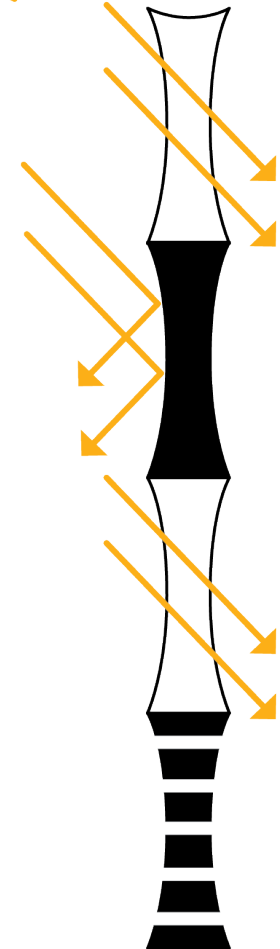
1 b



vertical section

1b. Inflated and deflated elements: using both inflated cushions and vacuum system in a multilayer façade element for thermal and acoustical insulation.

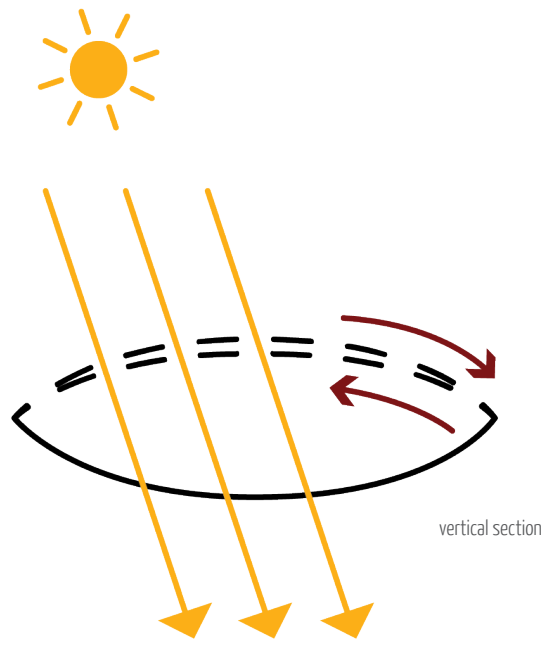
2.



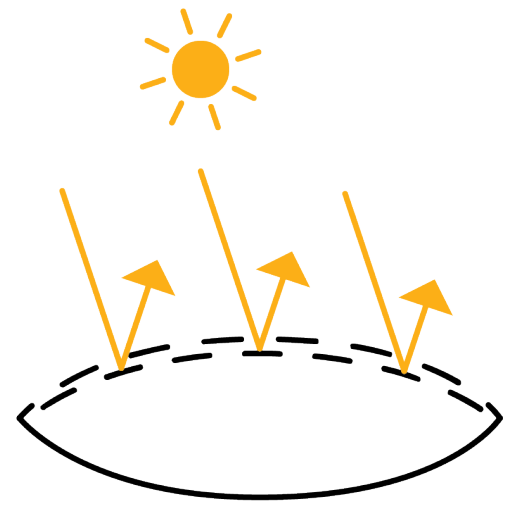
vertical section

Combination of different transparency levels (opaque/transparent/semi-transparent).

3.



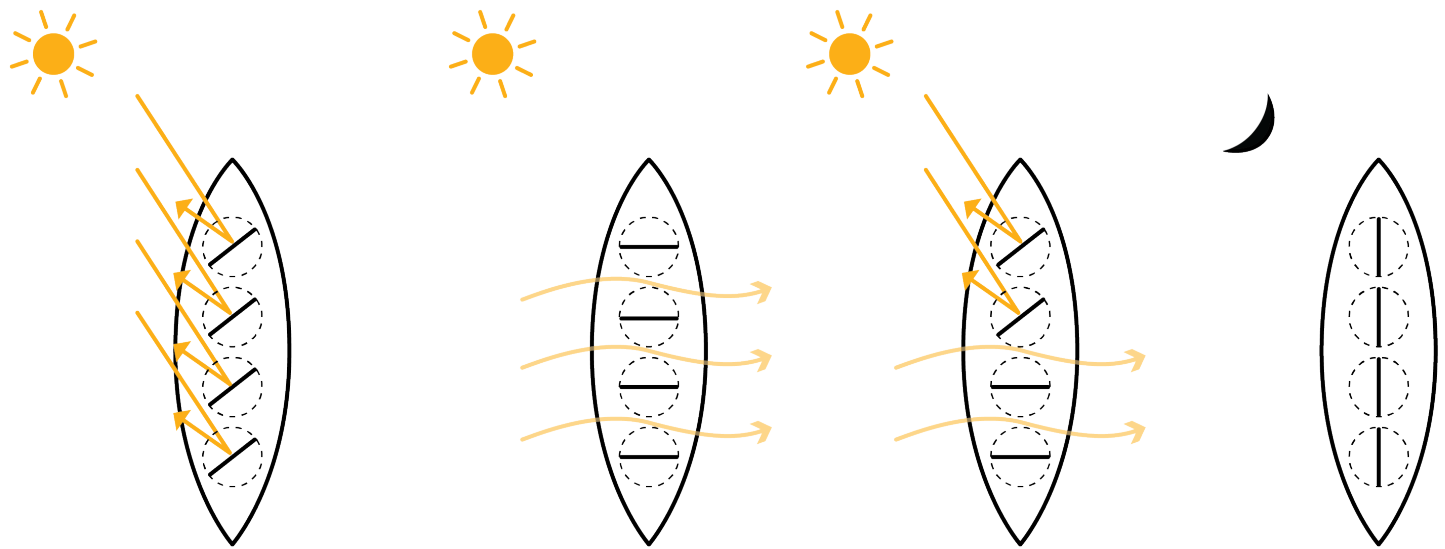
vertical section



vertical section

Integration of PV films or printed patterns on an inflated cushion // the two upper layers are adjustable to sun's position in order to provide shading when needed.

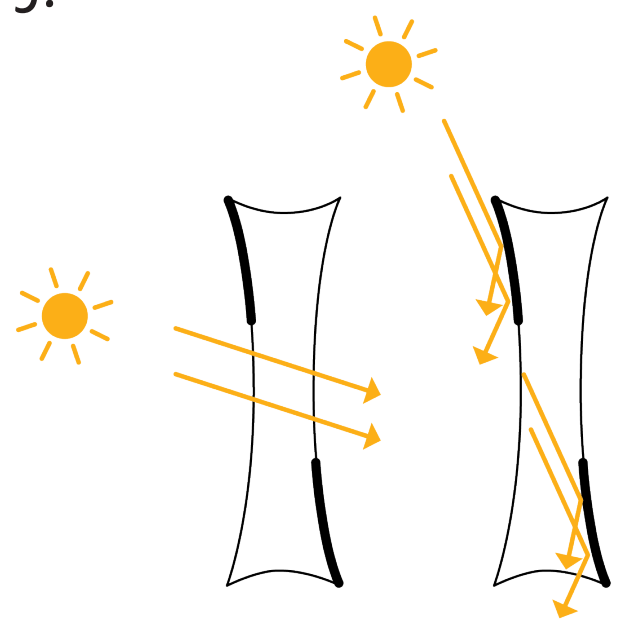
4.



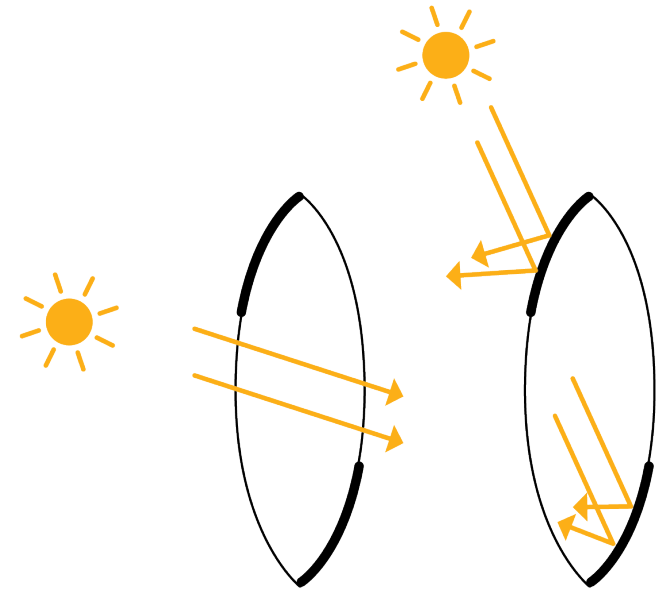
vertical sections

Integration of a shading system into an inflated structure // the shading system is adaptable and adjustable to sun's position.

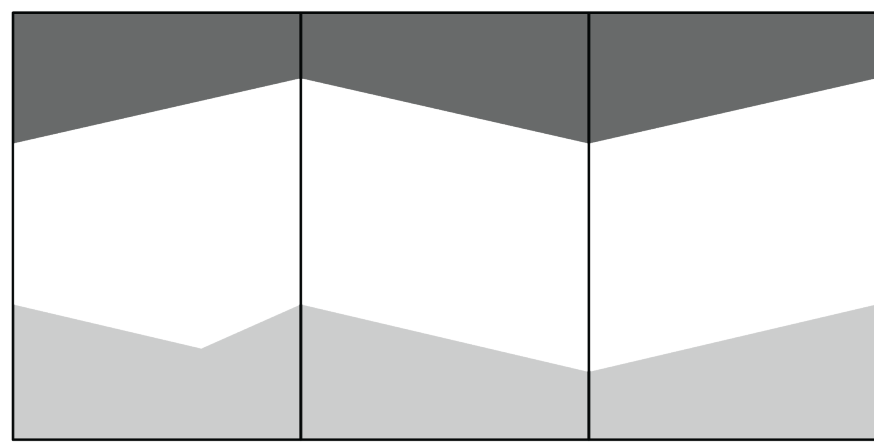
5.



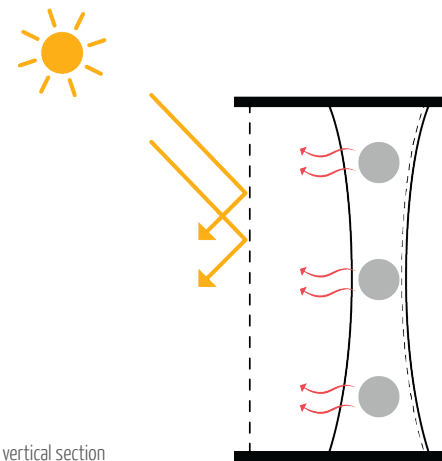
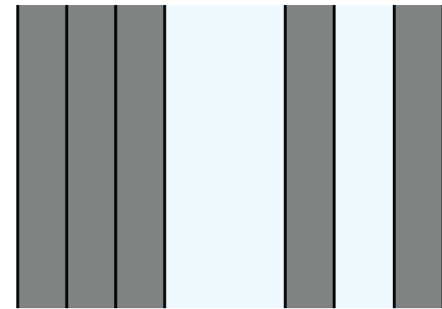
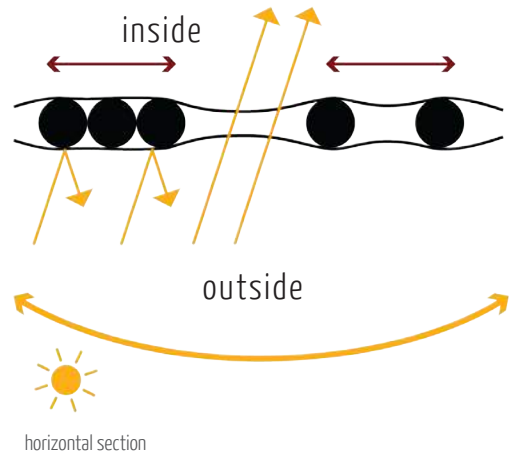
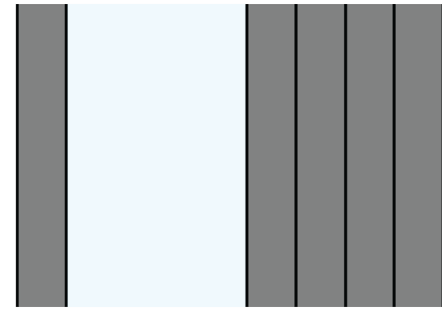
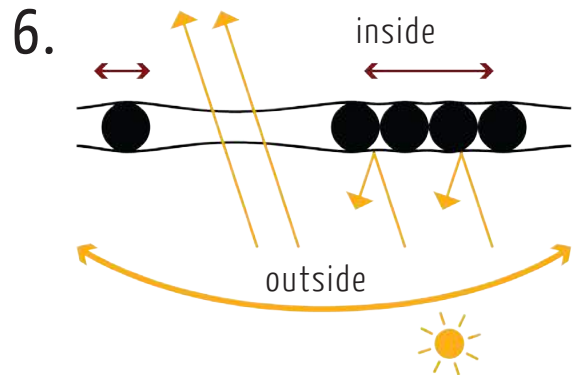
vacuum system_vertical section



inflated system_vertical section

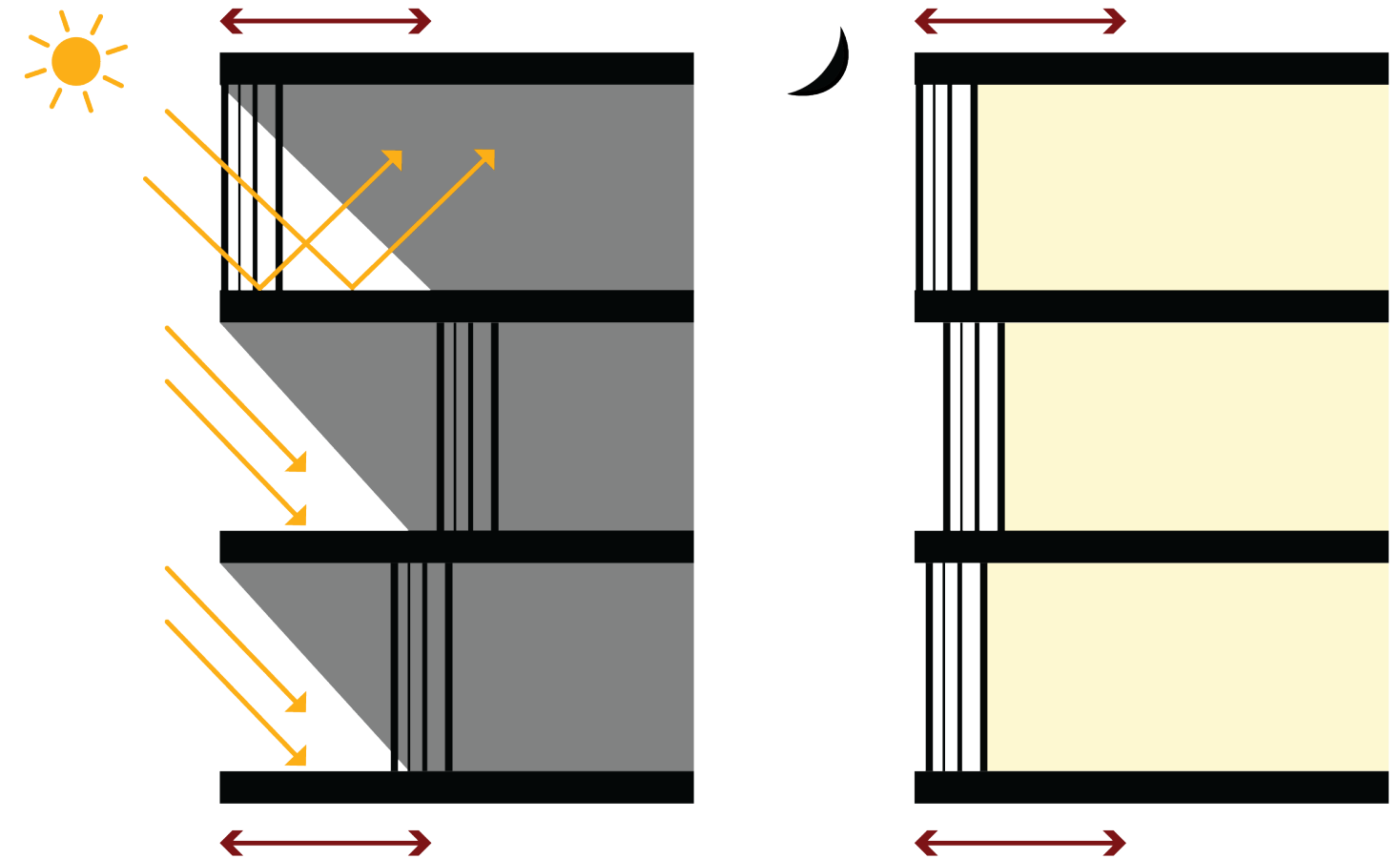


Combination of fabrics with **different transparency levels** on the same façade element (opaque/transparent/semi-transparent): **shading** and creation of an **interesting pattern** on the façade.

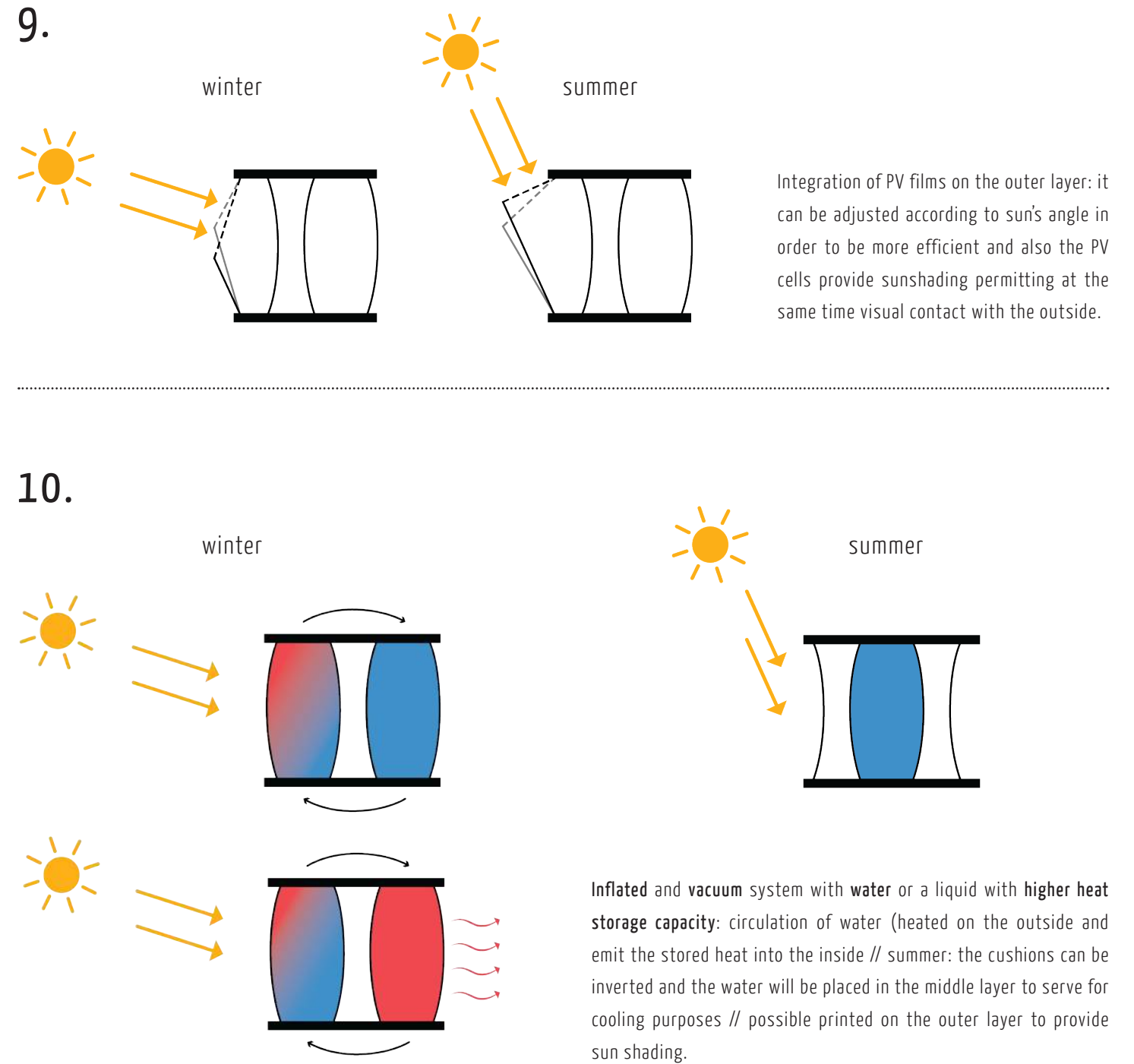
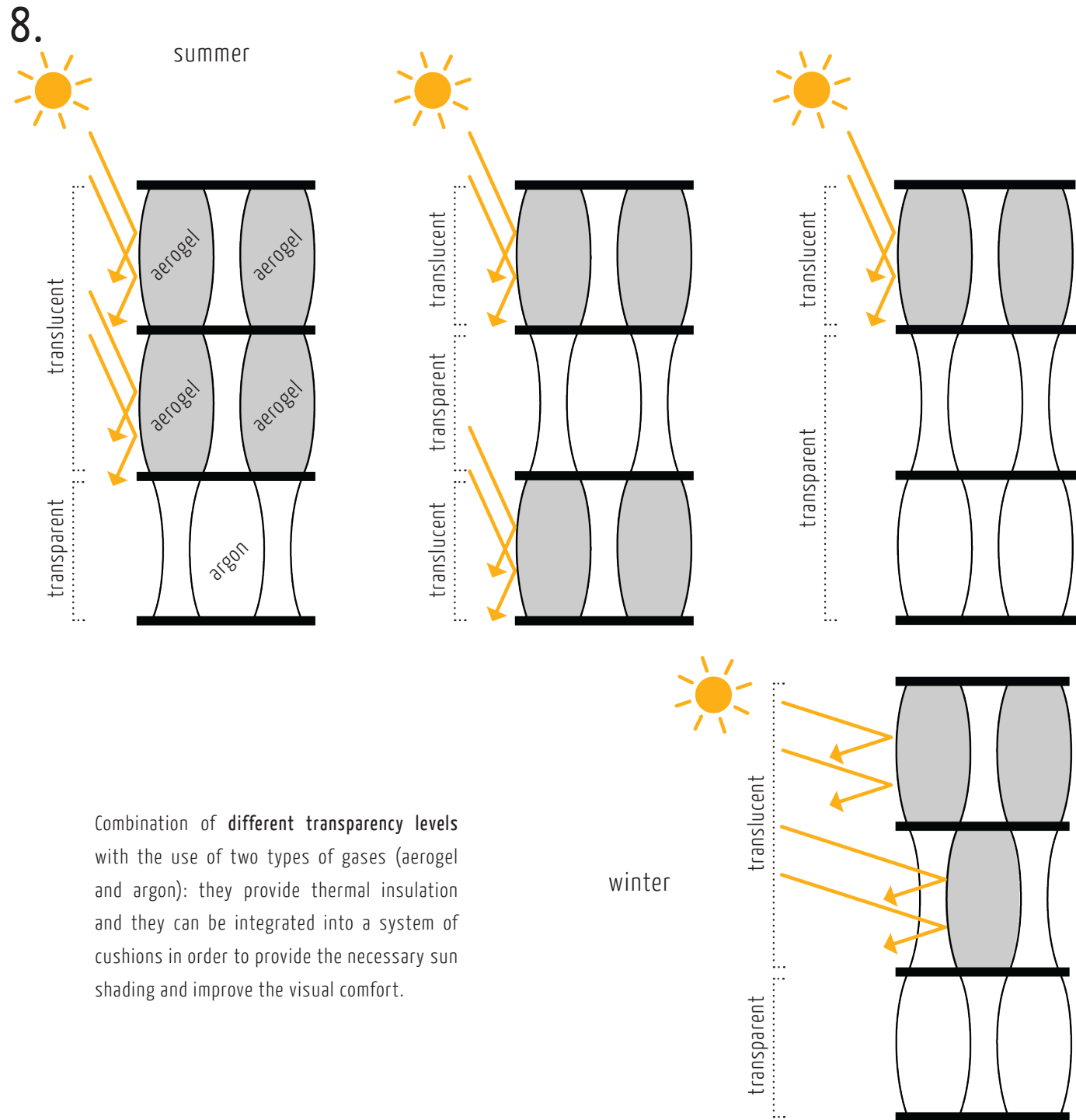


Two layers of fabric (internal and external) and a solid material in between in the form of vertical or horizontal elements (possible PCM integration) that are movable and adjustable to the sun // the vacuum system is used here // this system can improve the thermal and acoustical insulation of a façade, as the absence of a medium results in heat transferring only by radiation (no convection neither conduction) // sound waves also need a medium to be transmitted, so if there is no medium no sound transmission will occur.

7.



Movable façade elements that are adjustable to the sun's position and also they have the chance to improve the visual comfort when placed on the external limit of the building.



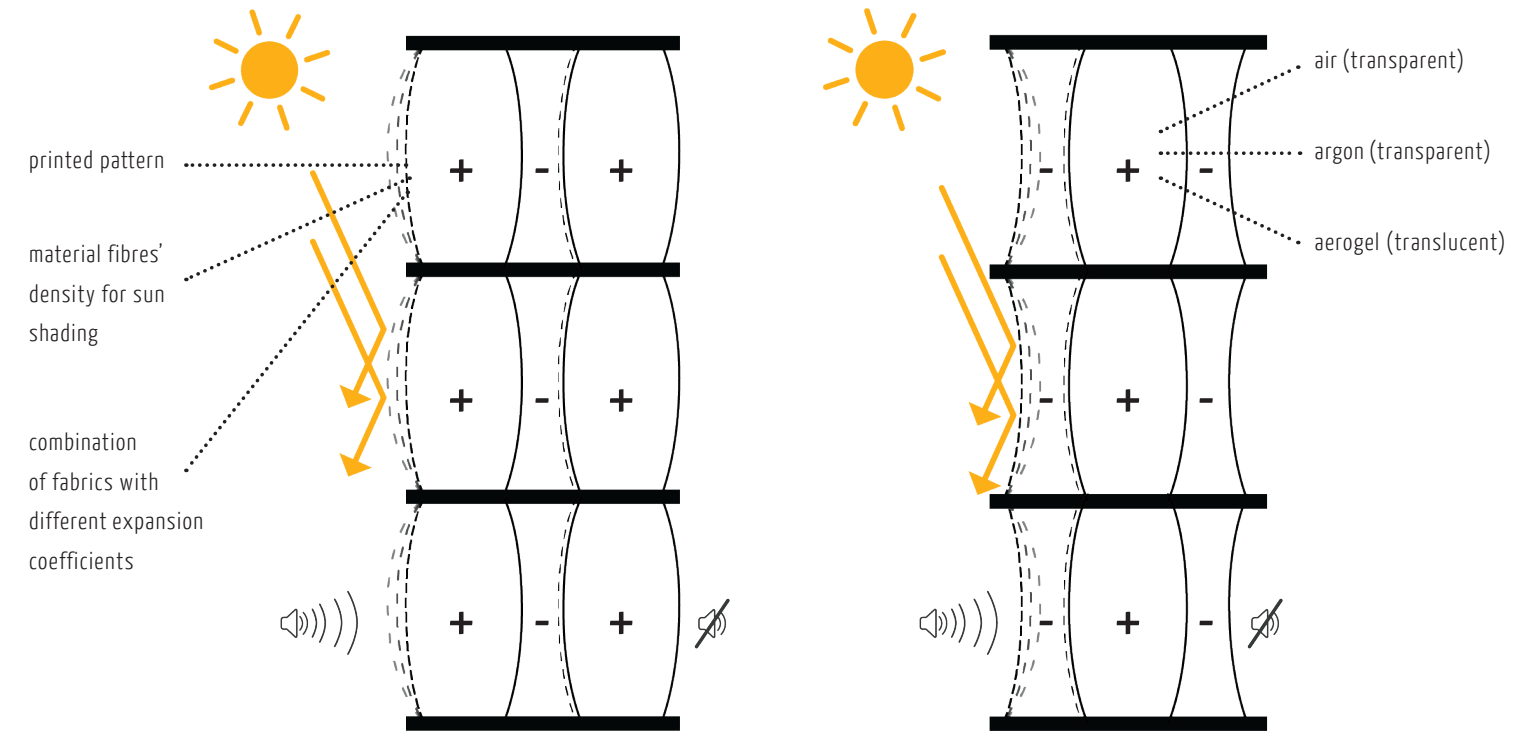
chosen concepts

Having defined these ten concepts already described, the next step was to eliminate the choices in order to conclude to the final design. Therefore, several concepts were rejected immediately for the following reasons.

More specifically, the concept (4) with the rotating shading system integrated into an inflated cushion is at risk of overheating, since the cavity inside the cushion cannot be ventilated and also a large amount of energy would be consumed for the adjustment of the louvers. Furthermore, the concept (7) with the movable façade elements adjustable to the sun's position is creating a lot of useless and unexploited space and a waste of energy responsible for the movement of the elements. Lastly, the final concept (10) with the inflated and the vacuum system along with the water filling (or a liquid with higher heat storage capacity) consists a -non-compatible with fabrics- idea, as the liquid cannot be easily sealed into the membrane system and thus leaks would probably occur.

Hence, four new concepts were created from the merge of several characteristics of the 7 remaining concepts mentioned previously and they are all based on either an inflated system, or a vacuum one or a combination of both.

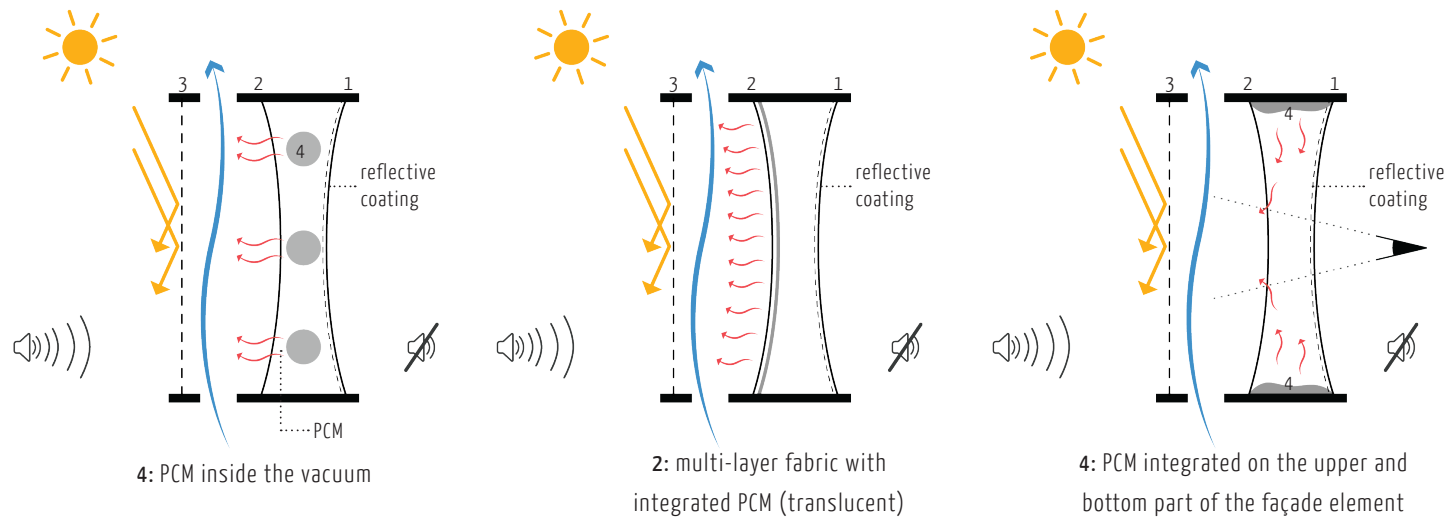
1. multi-layered inflated_vacuum system



This concept is based on the combination of an inflated cushion and a vacuum system placed one after the other so as to form a multi-layered façade element in order to improve the thermal and the acoustical insulation of the whole building envelope. More specifically, the use of two cushions and a vacuum element or one cushion in the middle and two vacuum ones on each side, take advantage of the multiple air cavities that are being created and thus the thermal insulation is improved. In addition, as mentioned before, the absence of a medium (air) results in heat transferring only by radiation and therefore neither convection, nor conduction occur in an ideal

vacuum situation or in a more realistic scenario they are being dramatically reduced. Sound waves also need a medium to be transmitted, so if there is no medium, no sound transmission occurs either. Lastly, the outside layer could be used for sun shading in the three following ways: a) with a printed pattern on it, b) depending on the density of the material's fibers (more inflation, less dense, more light penetration and vice versa) and c) with the combination of fabrics having different expansion coefficients (when one expands, the other one shrinks and thus the light transmission levels vary).

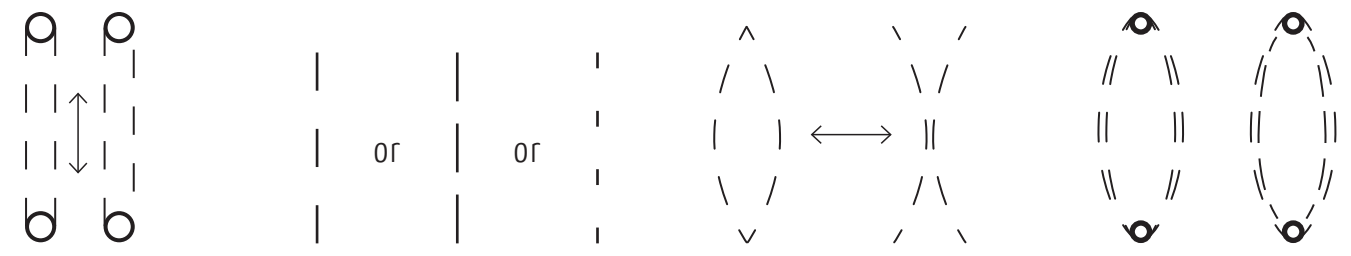
2. vacuum system & PCM



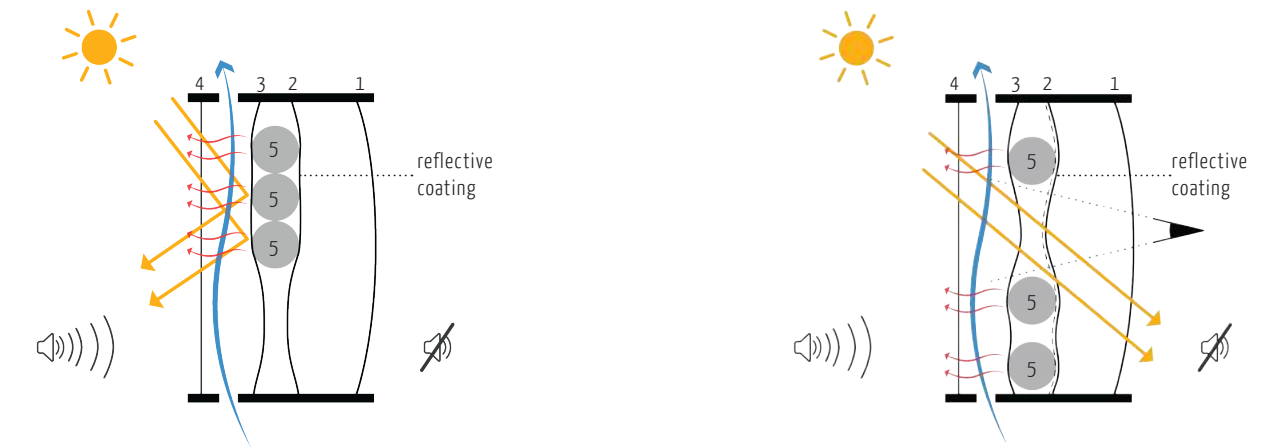
- 1-2: vacuum with a reflective coating on the inner layer so radiation can be reflected back to the outside
- 2-3: ventilated cavity for cooling purposes
- 3: outer layer --> shading // in case of rain it can be loosened up to avoid the effect of drums

The shading system can consist of the following options:

- a) 2-layered printed pattern moving parallel to each other // possible use of bi-metals
- b) 2 fabrics with different expansion coefficient moving with the use of bi-metals or acting like bi-metals
- c) inflation and deflation of the cushion with printed pattern
- d) 4-layered cushion with printed pattern on all layers // inner layer rotating



3. inflated_vacuum system & PCM

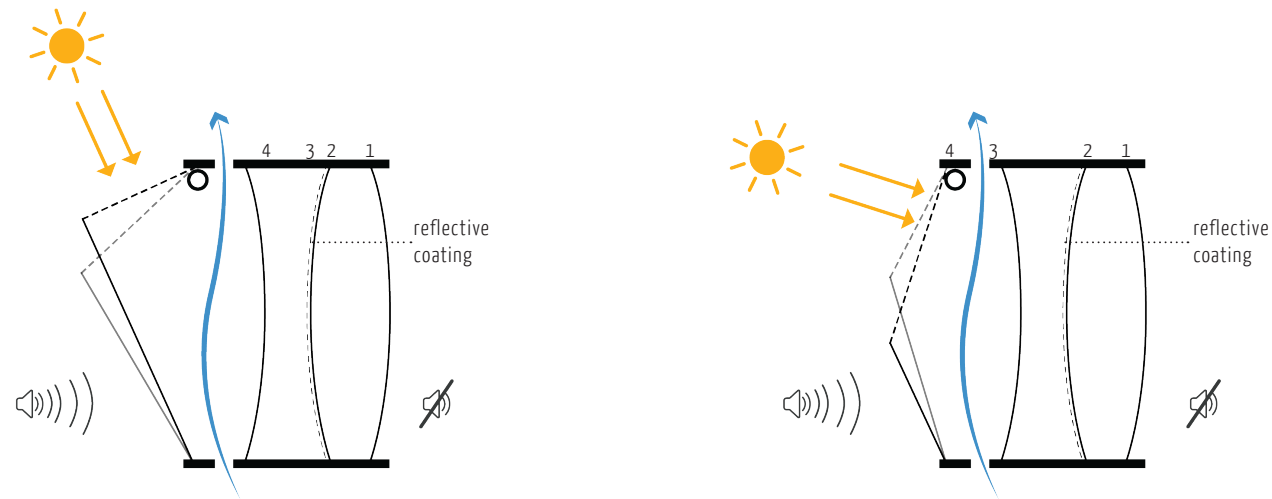


- 1-2: inflated cushion filled with either aerogel (translucent) or argon gas (transparent)
- 2-3: vacuum with a reflective coating on the inner layer // cylinders with PCM that reduce the cooling loads and they can be moved vertically (upwards and downwards) to provide sun shading
- 3-4: ventilated cavity for cooling purposes
- 4: outer layer --> protective layer that can be loosened up in case of rain to avoid drums (low-e coating is also possible)

Several issues emerged from these two concepts though. Firstly, the matter of transparency and visual comfort constitutes a main one, as with having the PCM, for example, integrated into the layer 2 of the membrane, it blocks immediately any view to the outside. The same applies for the aerogel as a filling of the inflated cushion. Also, the use of the PCM for cooling purposes, since for heating it is not sufficient,

causes a few problems as well. As in the vacuum system neither convection nor conduction occur the latent heat of the PCM is transferred and stored only by radiation. This means that it is much less than if the PCM was placed outside the vacuum system. Lastly, the integration of the shading system into the vacuum has a high risk of damaging the membrane in the end because of the movement and friction.

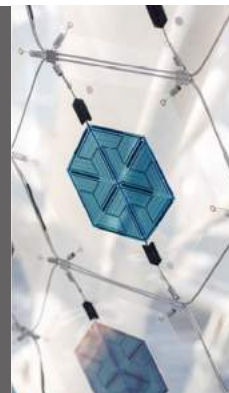
4. vacuum system & PV cells



- 1-2: inflated cushion filled with either aerogel (translucent) or argon gas (transparent)
- 2-3: vacuum with a reflective coating on the inner layer so radiation can be reflected back to the outside
- 3-4: ventilated cavity for cooling purposes
- 4: sun shading layer --> integration of PV films on the outer layer // it can be adjusted according to sun's angle in order to be more efficient and at the same time it can act as sun shading

Flexible Organic Photovoltaic modules

- made out of sustainable, carbon-based, "organic" materials
- roll-to-roll manufacturing process
- different shapes, colours and degrees of transparency
- compatibility with membrane architecture
- sun's angle independent
- power efficiency under diffuse light conditions



[source: www.opvius.com]

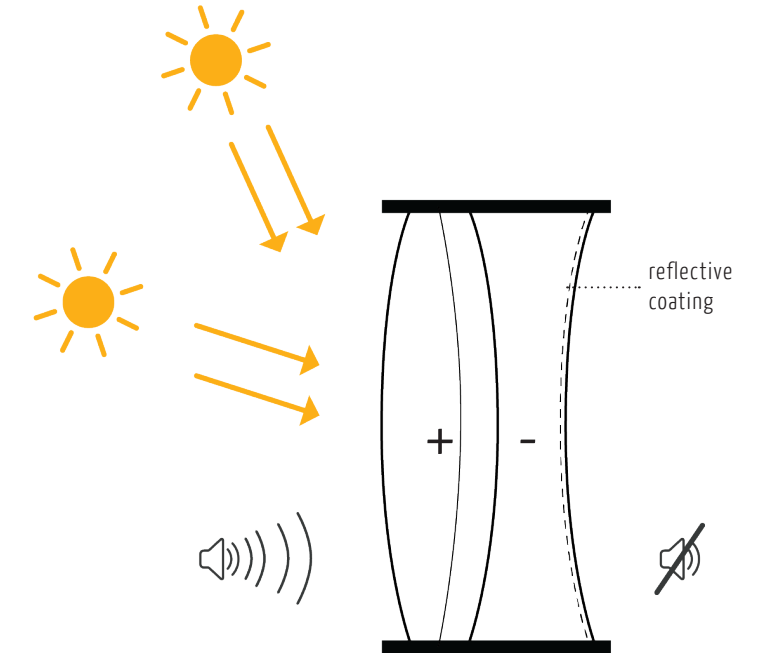
final concept

Having eliminated the number of the concepts, one final design had to be chosen. The selection was based on both the advantages and disadvantages of each one. Therefore, the final design concept consists of an inflated cushion on the outside and a vacuum system element on the inside. The reasons for this choice were, first of all, the thermal and acoustical improvement possibilities that the combination of these two systems offers. Furthermore, my personal wish and curiosity concerning the potential of the vacuum element was another determining factor. Finally, I wanted to investigate how an inflated and a vacuum system could be combined in order to form a complete and sufficient façade element of a high-rise building.

The next step was to define and answer several questions:

- » how many layers of fabric are required for both elements (inflated and vacuum)
- » what would be the cavity filling (air, aerogel, argon)
- » how low can the pressure of the vacuum system become
- » which sun shading system will be used and how can it be integrated

inflated cushion + vacuum system



A black and white photograph of a waterfall, showing multiple streams of water falling into a pool. The water is captured in motion, creating a blurred, dynamic effect. The background is dark, making the white water stand out. In the top right corner, there is a large, white, sans-serif number '6'.

6

building
physics

thermal hand calculations

Having chosen the final design concept, the building physics aspect had to be taken into account. For this reason, a number of hand calculations were conducted, under the scope of thermal and acoustics performance, both for the inflated and the vacuum system. Various different versions were investigated, depending on the number of the membrane layers and thus the number of cavities, the cavity's filling and width and of course the different pressure levels.

Fistly, the theory of Building Physics chapter 2: "Glazing properties and their effect on the insulation and heat admittance in a building" will be presented, along with the formulas that will be used for the calculations.

For the thermal calculations, the total **U-value** of the construction element had to be calculated.

$$U = 1/R \quad (1)$$

The total thermal resistance (R) of the construction element, which constitutes a fabric façade element in this case, has to be calculated first.

$$R = r_e + R_{\text{cushion}} + r_i \quad (2)$$

The heat resistances for inside and outside are standardised in the European regulations and they are:

$$r_e = 0.04 \text{ m}^2\text{K/W}$$

$$r_i = 0.13 \text{ m}^2\text{K/W}$$

The thermal resistance of the membrane cushion depending on the number of membrane layers and the number of cavities that are formed is given by the formula:

$$R_{\text{cushion}} = r_1 + r_{\text{cav1}} + r_2 + r_{\text{cav2}} + r_3 + r_{\text{cav3}} + \dots \quad (3)$$

Now the resistance of each layer of membrane has to be determined, as well as the resistance of every cavity.

The heat resistance (r) of each membrane layer can be calculated if the thickness (d) of the material and its heat conduction coefficient (λ) are known.

$$r_{\text{cond}} = d/\lambda \quad (4) \quad \text{and} \quad a_{\text{cond}} = 1/r_{\text{cond}} \quad (5)$$

The heat conduction coefficients (λ) for the materials that compose the under study façade element are the following:

$$\text{air: } \lambda_{\text{air}} = 0.0248 \text{ W/mK}$$

$$\text{argon: } \lambda_{\text{argon}} = 0.016 \text{ W/mK}$$

$$\text{ETFE: } \lambda_{\text{ETFE}} = 0.238 \text{ W/mK}$$

The heat resistance of each cavity is given by:

$$r_{\text{cav}} = 1/(a_{\text{cond(cav)}} + a_{\text{conv(cav)}} + a_{\text{rad(cav)}}) \quad (6)$$

where:

$$a_{\text{cond(cav)}} = 1/r_{\text{cond(cav)}} \quad (7) \quad (\text{concerns the cavity filling})$$

The $a_{\text{conv(cav)}}$ can be taken as **1 W/m²K** as the cavities that are investigated are 50mm and above. More specifically, as it can be seen in the figure 87 below, the heat transfer coefficient for convection is dependent on the cavity width until a certain value and after this width (50mm) remains stable around 1 W/m²K.

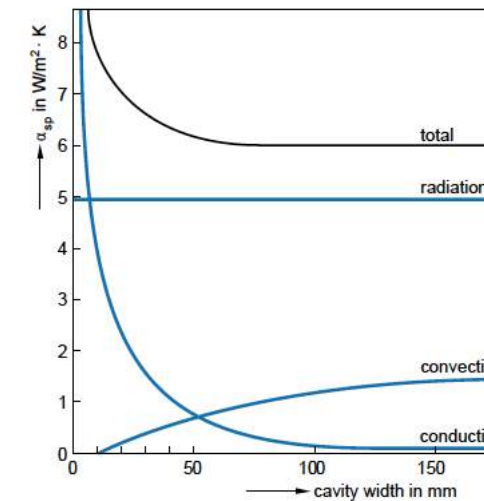


Figure 87: Heat transport through vertical air cavities through conduction, radiation and convection, depending on width of cavity: approximate indication of transfer coefficient a_{sp} (source: van der Linden, A.J., *Bouw fysica - Engels, Chapter 1. Heat, heat transport, thermal insulation, p. 7*)

The heat transfer coefficient for radiation ($a_{\text{rad(cav)}}$) is dependent on the emissivity of the two surfaces of the cavity.

$$a_{\text{rad(cav)}} = [\epsilon_{\text{res}} * \sigma * (T_1^4 - T_2^2)] / (T_1 - T_2) \quad (8)$$

where

σ : Stefan-Boltzmann constant ($=5.67*10^{-6} \text{ W/m}^2\text{K}^4$)

T_1 : surface 1 temperature [K]

T_2 : surface 2 temperature [K]

With an average temperature of the two surfaces around 300K ($=27^\circ\text{C}$) the previous equation can be simplified to:

$$a_{\text{rad(cav)}} = 6 * \epsilon_{\text{res}} \quad (9)$$

$$1/\epsilon_{\text{res}} = (1/\epsilon_1) + (1/\epsilon_2) - 1 \quad (10)$$

where

ϵ_1 : emission coefficient of one surface

ϵ_2 : emission coefficient of second surface

source:

equations 1-10 were taken from: Building Physics - Chapter 2: "Glazing properties and their effect on the insulation and heat admittance in a building, p. 4-17, 14-23

inflated system

Firstly, the two systems were investigated separately. The inflated one was considered as a double and a triple layered system. In addition, several possibilities for the cavity filling were examined and thus air, argon and aerogel were used. Furthermore, reflective coatings were applied to the inner layers of certain cavities in order to reduce the radiation values.

As far as the triple layered system is concerned, although the aerogel gave the best results for the double layered system, its high price renders it less desired for use. Therefore, the version with argon as a cavity filling was examined with the combination of a reflective coating on the middle layer.

So, in the two tables on the next page, the results of the R and U-values of the cushions from the excel file with the hand calculations are presented, for both the double and the triple layered system.

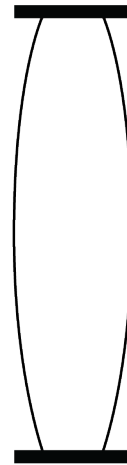


Figure 88: double layered inflated cushion



Figure 89: triple layered inflated cushion

double layer system	AIR	ARGON	AEROGEL	AIR with coatings	ARGON with coatings	AEROGEL with coatings
λ_{gas_cav} (W/mK)	0.0248	0.016	0.012	0.0248	0.016	0.01349
λ_{fabric} (W/mK)	0.238	0.238	0.238	0.238	0.238	0.238
d_{cav} (m)	0.1	0.1	0.1	0.1	0.1	0.1
d_{fabric} (m)	0.0003	0.0003	0.0003	0.0003	0.0003	0.0003
Te (C)	11	11	11	11	11	11
Ti (C)	24.5	24.5	24.5	24.5	24.5	24.5
a_{cond} (gas) (W/m ² K)	0.248	0.16	0.12	0.248	0.16	0.1349
a_{conv} (air) (W/m ² K)	1	1	1	1	1	1
$\epsilon 1$	0.9	0.9	0.9	0.9	0.9	0.9
$\epsilon 2$	0.9	0.9	0.9	0.2	0.2	0.2
a_{rad} 2 (W/m ² K)	4.56	4.56	4.56	1.09	1.09	1.09
a_{cav} (W/m ² K)	6.16	6.07	6.03	2.42	2.33	2.31
$r_{cushion}$ (m ² K/W)	0.165	0.167	0.168	0.415	0.431	0.436
R (m²K/W)	0.335	0.337	0.338	0.585	0.601	0.606
U (W/m²K)	2.986	2.965	2.955	1.708	1.664	1.651

triple layer system	1st cavity	2nd cavity	1st cavity	2nd cavity
λ_{gas_cav} (W/mK)	0.016	0.016	a_{conv} (gas) (W/m ² K)	1
λ_{fabric} (W/mK)	0.238		$\epsilon 1$	0.9
d_{cav} (m)	0.05	0.05	$\epsilon 2$	0.2
d_{fabric} (m)	0.0003	0.0001	a_{rad} 2 (W/m ² K)	1.09
Te (C)	11	11	a_{cav} (W/m ² K)	2.41
Ti (C)	24.5	24.5	$r_{cushion}$ (m ² K/W)	0.83
a_{cond} (gas) (W/m ² K)	0.32	0.32	R (m²K/W)	1.00
			U (W/m²K)	1.00

Figure 90: results from excel file with the calculations for the inflated system

vacuum system

For the vacuum system the situation was a bit different. It was considered as a double layer system with one cavity filled with air, but because of the change in the pressure level the new thermal conductivity value for the air had to be defined. There is a formula that relates the thermal conductivity to the pressure level.

More specifically, according to the Low Pressure Theory (the so-called Slip Flow Theory) the formula described above is:

$$K_e/K_0 = 1/(1+C/PP)^1$$

where

Ke: the new thermal conductivity of air in lower pressure [W/mK]

Ko: the thermal conductivity of air at 1 bar (10⁵ Pascal) [W/mK]

C: constant equal to 7.6*10⁻⁵ [mK/N]

PP: pressure parameter P*d/T [N/mK]

P: pressure [Pa]

d: plate distance [m]

T: absolute temperature [K]

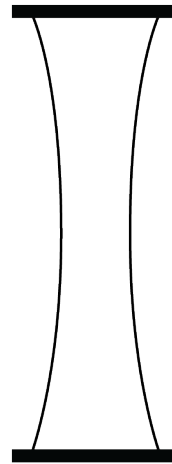


Figure 91: double layer vacuum system

When the pressure level changes from 10⁵ Pascal (1 bar), which consists the atmospheric pressure, till 10³ Pascal (10⁻² bar) there is no evident change in the thermal conductivity value. However, from 100 Pascal (10⁻³ bar) and below a difference starts to appear. In the next page, the values for the new thermal conductivity of air in 100, 10 and 1 Pascal (10⁻³, 10⁻⁴ and 10⁻⁵ bar respectively) are presented, as well as the corresponding R and U-values of the vacuum system of 5cm membranes' distance in these pressure levels. Lastly, no reflective coatings were applied to the surfaces, as the purpose was to examine the influence only of the pressure level change in the thermal performance of the component. The results are unfortunately not the desired ones, as even at the pressure of 1 Pa (which is a very low value and unrealistic at least for a façade element) the difference in the U-value compared with the atmospheric pressure is insignificant.

100 Pa (10 ⁻³ bar)		10 Pa (10 ⁻⁴ bar)		1 Pa (10 ⁻⁵ bar)	
P (Pa)	100	P (Pa)	10	P (Pa)	1
d (m)	0.05	d (m)	0.05	d (m)	0.05
T (K)	290.75	T (K)	290.75	T (K)	290.75
PP (N/mK)	0.0171969	PP (N/mK)	0.00171969	PP (N/mK)	0.00017197
C (mK/N)	0.000076	C (mK/N)	0.000076	C (mK/N)	0.000076
λ₀ (thermal conductivity at 1 bar)	0.0248	λ₀ (thermal conductivity at 1 bar)	0.0248	λ₀ (thermal conductivity at 1 bar)	0.0248
λ_{gas}	0.0247	λ_{gas}	0.0238	λ_{gas}	0.0172
λ_{fabric} (W/mK)	0.238	λ_{fabric} (W/mK)	0.238	λ_{fabric} (W/mK)	0.238
d_{air} (m)	0.05	d_{air} (m)	0.05	d_{air} (m)	0.05
d_{fabric} (m)	0.0003	d_{fabric} (m)	0.0003	d_{fabric} (m)	0.0003
Te (C)	11	Te (C)	11	Te (C)	11
Ti (C)	24.5	Ti (C)	24.5	Ti (C)	24.5
Te (K)	284	Te (K)	284	Te (K)	284
Ti (K)	297.5	Ti (K)	297.5	Ti (K)	297.5
a_{cond} (air) (W/m²K)	0.49	a_{cond} (air) (W/m²K)	0.48	a_{cond} (air) (W/m²K)	0.34
a_{conv} (air) (W/m²K)	1	a_{conv} (air) (W/m²K)	1	a_{conv} (air) (W/m²K)	1
ε1	0.9	ε1	0.9	ε1	0.9
ε2	0.9	ε2	0.9	ε2	0.9
a_{rad 2} (W/m²K)	4.56	a_{rad 2} (W/m²K)	4.56	a_{rad 2} (W/m²K)	4.56
a_{cav} (W/m²K)	6.40	a_{cav} (W/m²K)	6.38	a_{cav} (W/m²K)	6.25
r_{cushion} (m²K/W)	0.15870	r_{cushion} (m²K/W)	0.15916	r_{cushion} (m²K/W)	0.16244
R (m²K/W)	0.3287	R (m²K/W)	0.3292	R (m²K/W)	0.3324
U (W/m²K)	3.0423	U (W/m²K)	3.0380	U (W/m²K)	3.0080

Figure 92: results from excel file with the calculations for the vacuum system

1. source: <https://www.electronics-cooling.com/2002/11/the-thermal-conductivity-of-air-at-reduced-pressures-and-length-scales/>

combination

Subsequently, a combination of the two systems was investigated. More specifically, a 5-layered element consisting of a 3-layered inflated cushion 10cm wide in total, a vacuum element 5cm wide with 100Pa (10⁻³ bar) pressure level and a 6cm distance (air cavity) between them. According to the separate calculations, the vacuum's cavity width doesn't play an important role to the thermal performance of the element as the minimum cavity width is 5cm (see figure 92, page 105) -only a slight reduction of the U-value was noticed- so the 5cm cavity width was preferred in order to diminish the total width of the façade element. Also, a reflective coating was placed on the 3rd layer (inner layer of the inflated cushion), so as to reduce the radiation levels.

	1st cavity	2nd cavity	3rd cavity	4th cavity
$\lambda_{\text{gas_cav}}$ (W/mK)	0.016	0.016	0.0248	0.0247
λ_{fabric} (W/mK)	0.238	0.238	0.238	0.238
d_{cav} (m)	0.05	0.05	0.06	0.05
d_{fabric} (m)	0.0003	0.0001	0.0003	0.0003
T_1 (C)	11	14.375	17.75	21.125
T_2 (C)	14.375	17.75	21.125	24.5
r_{cond} (gas) (m ² K/W)	3.13	3.13	2.42	2.02
a_{cond} (gas) (W/m ² K)	0.32	0.32	0.41	0.50
a_{cond} (fabric) (W/m ² K)	793.33	2380.00	793.33	793.33
a_{conv} (gas) (W/m ² K)	1	1	1	1
ϵ_1	0.9	0.9	0.9	0.9
ϵ_2	0.9	0.2	0.9	0.9
a_{rad} 2 (W/m ² K)	4.33	1.07	4.64	4.80
a_{cav} (W/m ² K)	5.65	2.39	6.05	6.30
r_{cushion} (m ² K/W)	0.92			
R (m²K/W)	1.09			
U (W/m²K)	0.91			

Figure 93: results from excel file with the calculations for the combination of the inflated and the vacuum system

acoustics hand calculations

In order to examine the acoustical performance of the façade element, once again the two components were researched separately. Firstly, the inflated cushion was investigated as a double and a triple layered structure with both air and argon as cavity fillings. Then, three different cavity widths (5, 10 and 15cm) of the vacuum system were considered, each one of them with 3 different pressure levels (10⁴ Pa, 10³ Pa and 100 Pa).

Mass-spring resonance frequency (f_{ms})

$$f_{ms} = (C_{\text{air}}/2\pi \cos\theta) * \sqrt{[(\rho_{\text{air}}/d_{\text{cav}})*(1/m_1+1/m_2)]}$$

$$R_{ms} = 20\log[(m_1/2m_2)+(m_2/2m_1)]$$

Above mass-spring resonance & below transition frequency (f_T)

$$f_T = C_{\text{air}}/(2\pi*d_{\text{cav}}*\cos\theta)$$

$$R = 20\log[(2\pi f*m_1*\cos\theta)/(2\rho_{\text{air}}*C_{\text{air}})] + 20\log[(2\pi f*m_2*\cos\theta)/(2\rho_{\text{air}}*C_{\text{air}})] + 20\log[(2*2\pi f*d_{\text{cav}}*\cos\theta)/C_{\text{air}}]$$

Above transition frequency

$$R = 20\log[(2\pi f*m_1*\cos\theta)/(2\rho_{\text{air}}*C_{\text{air}})] + 20\log[(2\pi f*m_2*\cos\theta)/(2\rho_{\text{air}}*C_{\text{air}})] + 6$$

where

C_{air} : speed of sound through the air [m/s]

ρ_{air} : density of air [kg/m³]

θ : angle of incidence

m_1, m_2 : masses of the glass/membranes (kg/m²)

f : frequency [Hz]

d_{cav} : cavity width [m]

For an immediate comparison with the performance of a glass unit, the airborne sound insulation values of a double (4-10-6) and a triple (4-5-6-5-4) layered glass systems are also presented, with both air and argon as cavity fillings, as well as different pressure levels of 10³ Pa, 100 Pa and 10 Pa. The formulas that were used are based on the acoustics theory concerning the airborne sound insulation of cavity constructions.

Below mass-spring resonance

$$R = 20\log\{[2\pi f*(m_1+m_2)*\cos\theta]/[2\rho_{\text{air}}*C_{\text{air}}]\}$$

$$R_{\text{random}} = R_{\text{normal}} - 5$$

$$R_{\text{random}} = R_{\text{normal}} - 8.5$$

Standing waves frequency

$$f_{sw} = (n*C_{\text{air}})/(2*d_{\text{cav}})$$

inflated system

glass unit

double-layered

	mass1	mass2	mass 3	cavity 1	cavity 2	
thickness	0.004	6.00E-03	1.00E-15	1.00E-01	0.00E+00	m
density	1200	1200	1200			kg/m3
Young's modulus	7.00E+09	7.00E+09	7.00E+10			N/m2
mass	4.8	7.2	1.2E-12			kg/m2
speed of air				343	343	m/s
density of air				1.21	1.21	kg/m3
loss factor	0.01	1.00E-02	1.00E-02			
angle of incidence				60		

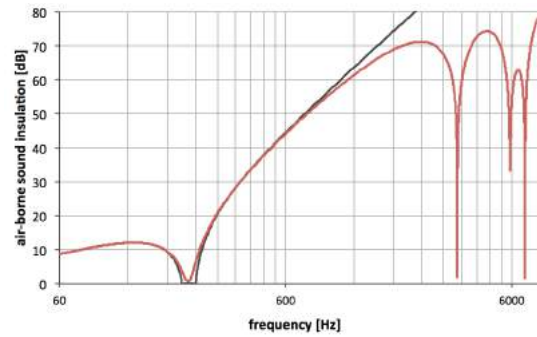


Figure 94: double glass unit filled with air

	mass1	mass2	mass 3	cavity 1	cavity 2	
thickness	0.004	6.00E-03	1.00E-15	1.00E-01	0.00E+00	m
density	1200	1200	1200			kg/m3
Young's modulus	7.00E+09	7.00E+09	7.00E+10			N/m2
mass	4.8	7.2	1.2E-12			kg/m2
speed of air				308	308	m/s
density of air				1.661	1.661	kg/m3
loss factor	0.01	1.00E-02	1.00E-02			
angle of incidence				60		

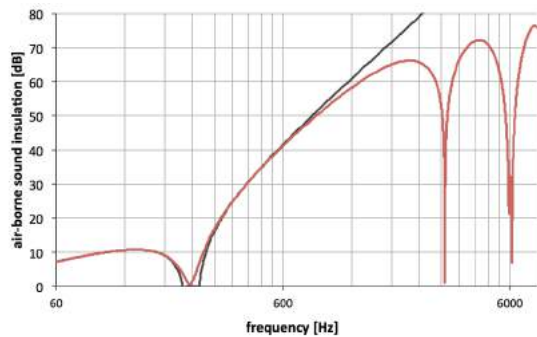


Figure 95: double glass unit filled with argon

ETFE unit

inflated double-layered

	mass1	mass2	mass 3	cavity 1	cavity 2	
thickness	0.0003	0.0003	1.00E-15	1.00E-01	0.00E+00	m
density	1750	1750	1750			kg/m3
Young's modulus	1.50E+09	1.50E+09	1.50E+09			N/m2
mass	0.525	0.525	1.75E-12			kg/m2
speed of air				343	343	m/s
density of air				1.21	1.21	kg/m3
loss factor	0.01	1.00E-02	1.00E-02			
angle of incidence				60		

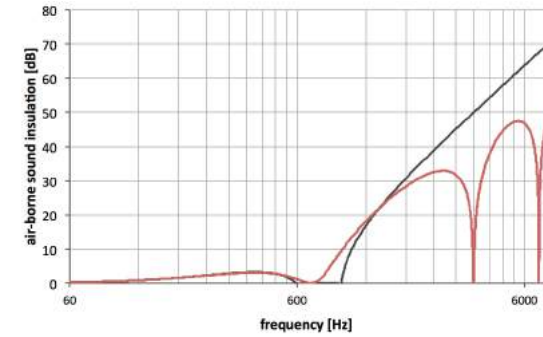


Figure 96: double layered ETFE unit with air filling

	mass1	mass2	mass 3	cavity 1	cavity 2	
thickness	0.0003	0.0003	1.00E-15	1.00E-01	0.00E+00	m
density	1750	1750	1750			kg/m3
Young's modulus	1.50E+09	1.50E+09	1.50E+09			N/m2
mass	0.525	0.525	1.75E-12			kg/m2
speed of air				308	308	m/s
density of air				1.661	1.661	kg/m3
loss factor	0.01	1.00E-02	1.00E-02			
angle of incidence				60		

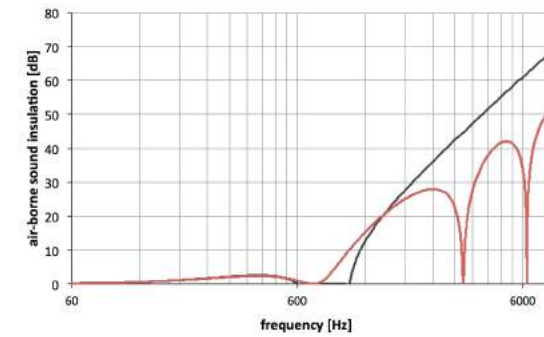


Figure 97: double layered ETFE unit with argon filling

glass unit

triple-layered

	mass1	mass2	mass 3	cavity 1	cavity 2	
thickness	0.004	6.00E-03	0.004	5.00E-02	5.00E-02	m
density	1200	1200	1200			kg/m3
Young's modulus	7.00E+09	7.00E+09	7.00E+10			N/m2
mass	4.8	7.2	4.8			kg/m2
speed of air				343	343	m/s
density of air				1.21	1.21	kg/m3
loss factor	0.01	1.00E-02	1.00E-02			
angle of incidence				60		

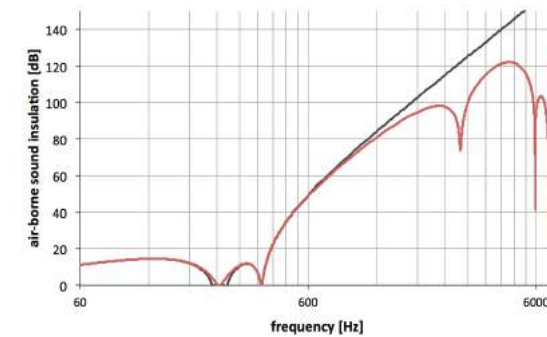


Figure 98: triple glass unit with air filling

	mass1	mass2	mass 3	cavity 1	cavity 2	
thickness	0.004	6.00E-03	0.004	5.00E-02	5.00E-02	m
density	1200	1200	1200			kg/m3
Young's modulus	7.00E+09	7.00E+09	7.00E+10			N/m2
mass	4.8	7.2	4.8			kg/m2
speed of air				308	308	m/s
density of air				1.661	1.661	kg/m3
loss factor	0.01	1.00E-02	1.00E-02			
angle of incidence				60		

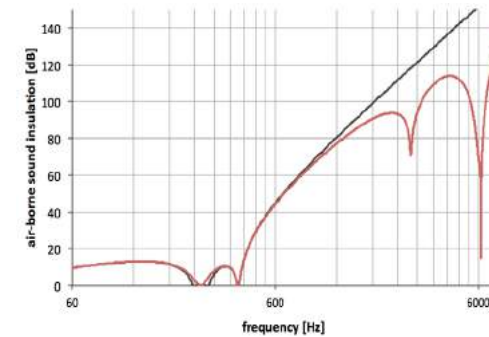


Figure 99: triple glass unit with argon filling

ETFE unit

inflated triple-layered

	mass1	mass2	mass 3	cavity 1	cavity 2	
thickness	0.0003	0.0001	0.0003	5.00E-02	5.00E-02	m
density	1750	1750	1750			kg/m3
Young's modulus	1.50E+09	1.50E+09	1.50E+09			N/m2
mass	0.525	0.175	0.525			kg/m2
speed of air				343	343	m/s
density of air				1.21	1.21	kg/m3
loss factor	0.01	1.00E-02	1.00E-02			
angle of incidence				60		

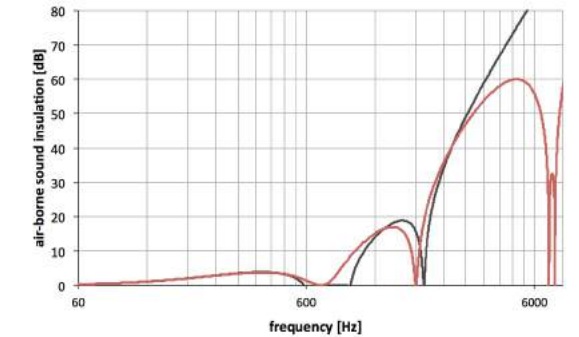


Figure 100: triple layered ETFE unit with air filling

	mass1	mass2	mass 3	cavity 1	cavity 2	
thickness	0.0003	0.0001	0.0003	5.00E-02	5.00E-02	m
density	1750	1750	1750			kg/m3
Young's modulus	1.50E+09	1.50E+09	1.50E+09			N/m2
mass	0.525	0.175	0.525			kg/m2
speed of air				308	308	m/s
density of air				1.661	1.661	kg/m3
loss factor	0.01	1.00E-02	1.00E-02			
angle of incidence				60		

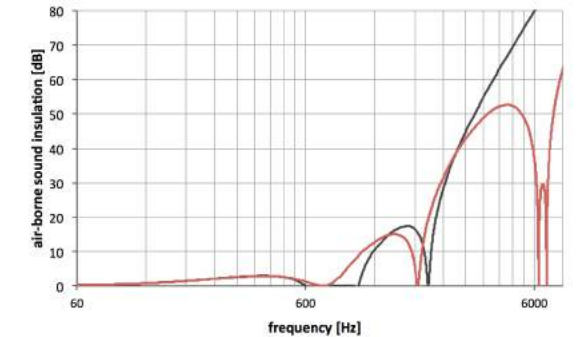


Figure 101: triple layered ETFE unit with argon filling

vacuum system

In order to calculate the airborne sound insulation of the vacuum systems, the new air density for lower pressures

According to the Ideal Gas Law (or Boyle's Law)¹:

$$P = \rho * R * T \quad (1)$$

where

P: pressure

ρ : density [kg/m³]

R: gas constant equal to 287 [J/kg/K]

T: absolute temperature [K]

For the same gas and keeping the temperature constant, equations 1 and 2 can be written as:

$$R * T = P / \rho \quad \rightarrow \quad P / \rho = P' / \rho' \quad \rightarrow \quad \rho' = P' * \rho / P$$

Now from the equation 3 we can calculate the new values of the air density at 10⁴ Pa, 10³ Pa and 100 Pa.

1: sources:

- https://en.wikipedia.org/wiki/Density_of_air
- http://www.atmo.arizona.edu/students/courselinks/fall11/atmo551a/ATMO_451a_551a_files/GasLawHydrostatic.pdf
- http://msrc.sunysb.edu/~chang/atm205/Notes/Chapter_1_txb.pdf

had to be determined first. This can be calculated using the formulas below. The speed of air remains the same as before.

and for the new pressure level and new density:

$$P' = \rho' * R * T \quad (2)$$

where

P': new pressure

ρ' : new density [kg/m³]

R: gas constant equal to 287 [J/kg/K]

T: absolute temperature [K]

glass unit

double-layered | 5cm

	mass1	mass2	mass 3	cavity 1	cavity 2	
thickness	0.004	6.00E-03	1.00E-15	5.00E-02	0.00E+00	m
density	1200	1200	1200			kg/m3
Young's modulus	7.00E+09	7.00E+09	7.00E+10			N/m2
mass	4.8	7.2	1.2E-12			kg/m2
speed of air				343	343	m/s
density of air				0.121	1.21	kg/m3
loss factor	0.01	1.00E-02	1.00E-02			
angle of incidence				60		

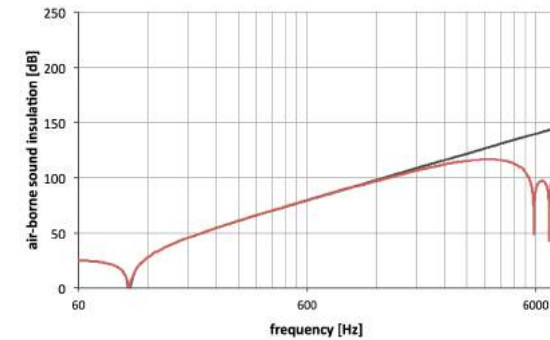


Figure 102: double glass unit 5cm at 10000 Pa

	mass1	mass2	mass 3	cavity 1	cavity 2	
thickness	0.004	6.00E-03	1.00E-15	5.00E-02	0.00E+00	m
density	1200	1200	1200			kg/m3
Young's modulus	7.00E+09	7.00E+09	7.00E+10			N/m2
mass	4.8	7.2	1.2E-12			kg/m2
speed of air				343	343	m/s
density of air				0.0121	1.21	kg/m3
loss factor	0.01	1.00E-02	1.00E-02			
angle of incidence				60		

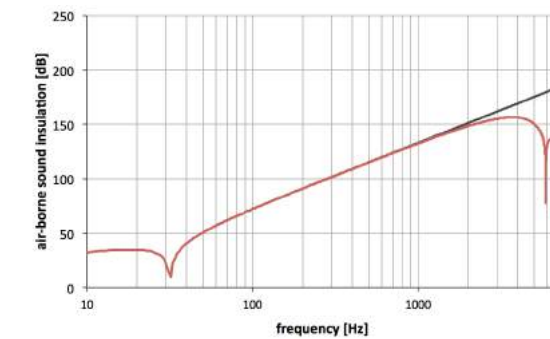


Figure 103: double glass unit 5cm at 1000 Pa

ETFE unit

vacuum | 5cm

	mass1	mass2	mass 3	cavity 1	cavity 2	
thickness	0.0003	3.00E-04	1.00E-15	5.00E-02	0.00E+00	m
density	1750	1750	1700			kg/m3
Young's modulus	1.50E+09	1.50E+09	1.50E+10			N/m2
mass	0.525	0.525	1.7E-12			kg/m2
speed of air				343	343	m/s
density of air				0.121	1.21	kg/m3
loss factor	0.01	1.00E-02	1.00E-02			
angle of incidence				60		

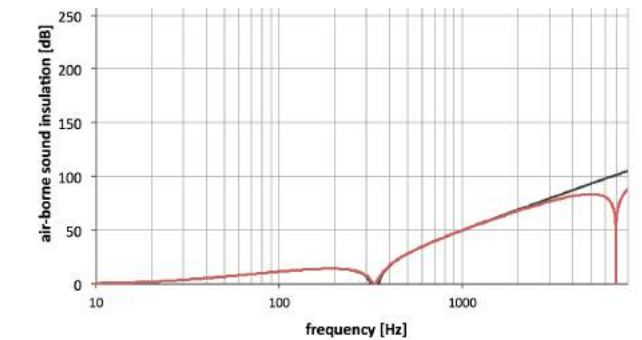


Figure 104: vacuum system 5cm at 10000 Pa

	mass1	mass2	mass 3	cavity 1	cavity 2	
thickness	0.0003	3.00E-04	1.00E-15	5.00E-02	0.00E+00	m
density	1750	1750	1700			kg/m3
Young's modulus	1.50E+09	1.50E+09	1.50E+10			N/m2
mass	0.525	0.525	1.7E-12			kg/m2
speed of air				343	343	m/s
density of air				0.0121	1.21	kg/m3
loss factor	0.01	1.00E-02	1.00E-02			
angle of incidence				60		

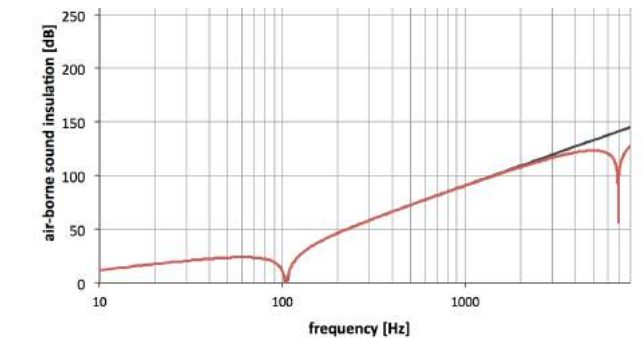


Figure 105: vacuum system 5cm at 1000 Pa

glass unit

	mass1	mass2	mass 3	cavity 1	cavity 2	
thickness	0.004	6.00E-03	1.00E-15	5.00E-02	0.00E+00	<i>m</i>
density	1200	1200	1200			<i>kg/m3</i>
Young's modulus	7.00E+09	7.00E+09	7.00E+10			<i>N/m2</i>
mass	4.8	7.2	1.2E-12			<i>kg/m2</i>
speed of air				343	343	<i>m/s</i>
density of air				0.00121	1.21	<i>kg/m3</i>
loss factor	0.01	1.00E-02	1.00E-02			
angle of incidence				60		

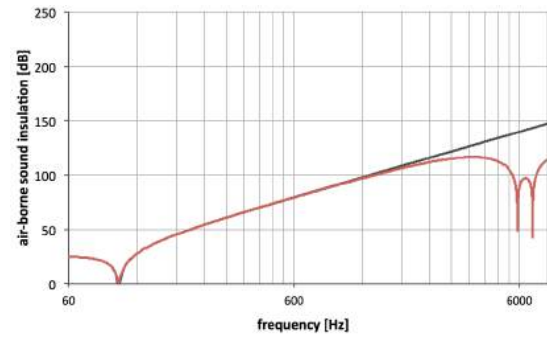


Figure 106: double glass unit 5cm at 100 Pa

ETFE unit

	mass1	mass2	mass 3	cavity 1	cavity 2	
thickness	0.0003	3.00E-04	1.00E-15	5.00E-02	0.00E+00	<i>m</i>
density	1750	1750	1700			<i>kg/m3</i>
Young's modulus	1.50E+09	1.50E+09	1.50E+10			<i>N/m2</i>
mass	0.525	0.525	1.7E-12			<i>kg/m2</i>
speed of air				343	343	<i>m/s</i>
density of air				0.00121	1.21	<i>kg/m3</i>
loss factor	0.01	1.00E-02	1.00E-02			
angle of incidence				60		

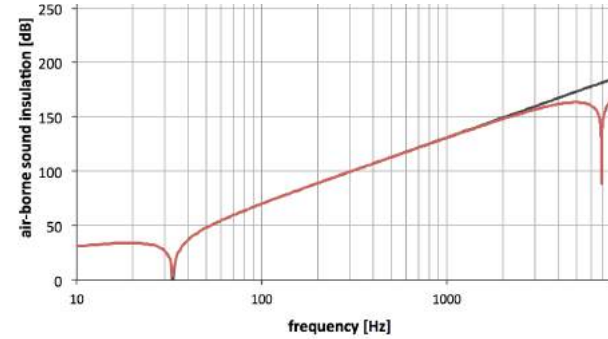


Figure 108: vacuum system 5cm at 100 Pa

glass unit

	mass1	mass2	mass 3	cavity 1	cavity 2	
thickness	0.004	6.00E-03	1.00E-15	1.00E-01	0.00E+00	<i>m</i>
density	1200	1200	1200			<i>kg/m3</i>
Young's modulus	7.00E+09	7.00E+09	7.00E+10			<i>N/m2</i>
mass	4.8	7.2	1.2E-12			<i>kg/m2</i>
speed of air				343	343	<i>m/s</i>
density of air				0.0121	1.21	<i>kg/m3</i>
loss factor	0.01	1.00E-02	1.00E-02			
angle of incidence				60		

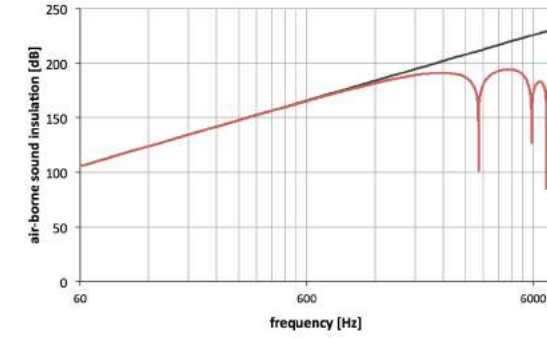


Figure 110: double glass unit 10cm at 1000 Pa

ETFE unit

	mass1	mass2	mass 3	cavity 1	cavity 2	
thickness	0.0003	3.00E-04	1.00E-15	1.00E-01	0.00E+00	<i>m</i>
density	1750	1750	1700			<i>kg/m3</i>
Young's modulus	1.50E+09	1.50E+09	1.50E+10			<i>N/m2</i>
mass	0.525	0.525	1.7E-12			<i>kg/m2</i>
speed of air				343	343	<i>m/s</i>
density of air				0.0121	1.21	<i>kg/m3</i>
loss factor	0.01	1.00E-02	1.00E-02			
angle of incidence				60		

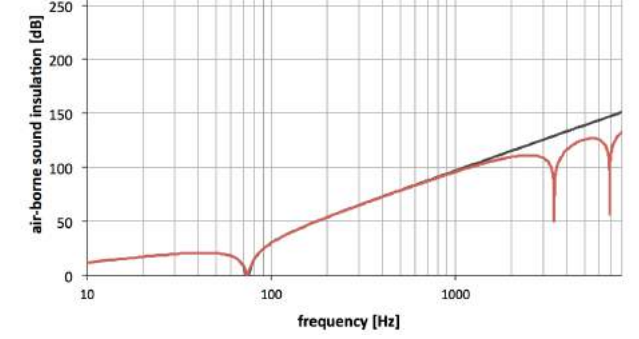


Figure 112: vacuum system 10cm at 1000 Pa

double-layered | 10cm

	mass1	mass2	mass 3	cavity 1	cavity 2	
thickness	0.004	6.00E-03	1.00E-15	1.00E-01	0.00E+00	<i>m</i>
density	1200	1200	1200			<i>kg/m3</i>
Young's modulus	7.00E+09	7.00E+09	7.00E+10			<i>N/m2</i>
mass	4.8	7.2	1.2E-12			<i>kg/m2</i>
speed of air				343	343	<i>m/s</i>
density of air				0.121	1.21	<i>kg/m3</i>
loss factor	0.01	1.00E-02	1.00E-02			
angle of incidence				60		

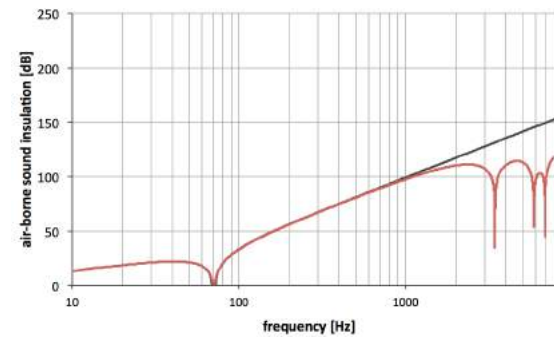


Figure 107: double glass unit 10cm at 10000 Pa

vacuum | 10cm

	mass1	mass2	mass 3	cavity 1	cavity 2	
thickness	0.0003	3.00E-04	1.00E-15	1.00E-01	0.00E+00	<i>m</i>
density	1750	1750	1700			<i>kg/m3</i>
Young's modulus	1.50E+09	1.50E+09	1.50E+10			<i>N/m2</i>
mass	0.525	0.525	1.7E-12			<i>kg/m2</i>
speed of air				343	343	<i>m/s</i>
density of air				0.121	1.21	<i>kg/m3</i>
loss factor	0.01	1.00E-02	1.00E-02			
angle of incidence				60		

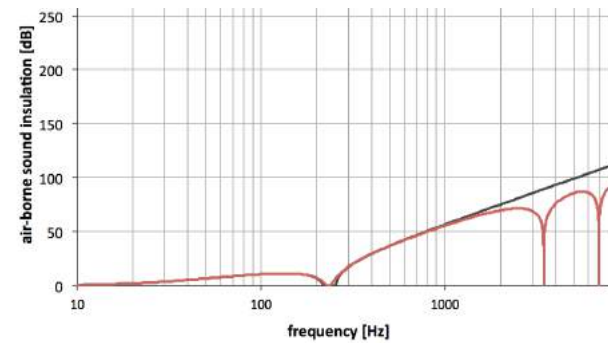


Figure 109: vacuum system 10cm at 10000 Pa

	mass1	mass2	mass 3	cavity 1	cavity 2	
thickness	0.004	6.00E-03	1.00E-15	1.00E-01	0.00E+00	<i>m</i>
density	1200	1200	1200			<i>kg/m3</i>
Young's modulus	7.00E+09	7.00E+09	7.00E+10			<i>N/m2</i>
mass	4.8	7.2	1.2E-12			<i>kg/m2</i>
speed of air				343	343	<i>m/s</i>
density of air				0.00121	1.21	<i>kg/m3</i>
loss factor	0.01	1.00E-02	1.00E-02			
angle of incidence				60		

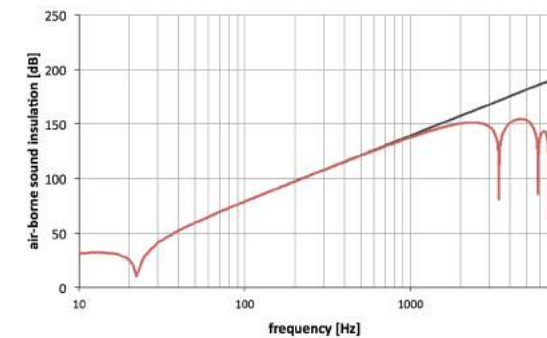


Figure 111: double glass unit 10cm at 100 Pa

	mass1	mass2	mass 3	cavity 1	cavity 2	
thickness	0.0003	3.00E-04	1.00E-15	1.00E-01	0.00E+00	<i>m</i>
density	1750	1750	1700			<i>kg/m3</i>
Young's modulus	1.50E+09	1.50E+09	1.50E+10			<i>N/m2</i>
mass	0.525	0.525	1.7E-12			<i>kg/m2</i>
speed of air				343	343	<i>m/s</i>
density of air				0.00121	1.21	<i>kg/m3</i>
loss factor	0.01	1.00E-02	1.00E-02			
angle of incidence				60		

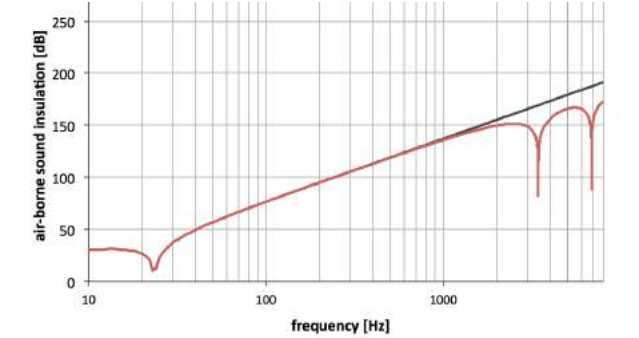


Figure 113: vacuum system 10cm at 100 Pa

glass unit

double-layered | 15cm

	mass1	mass2	mass 3	cavity 1	cavity 2	
thickness	0.004	6.00E-03	1.00E-15	1.50E-01	0.00E+00	m
density	1200	1200	1200			kg/m3
Young's modulus	7.00E+09	7.00E+09	7.00E+10			N/m2
mass	4.8	7.2	1.2E-12			kg/m2
speed of air				343	343	m/s
density of air				0.121	1.21	kg/m3
loss factor	0.01	1.00E-02	1.00E-02			
angle of incidence				60		

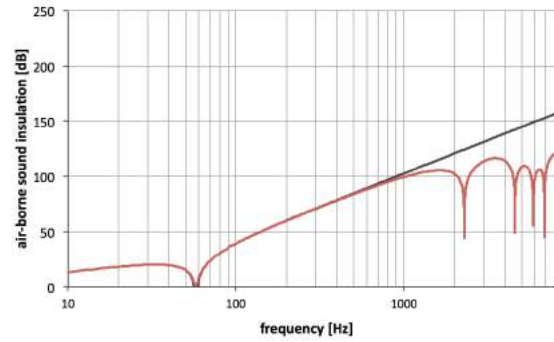


Figure 114: double glass unit 15cm at 10000 Pa

ETFE unit

vacuum | 15cm

	mass1	mass2	mass 3	cavity 1	cavity 2	
thickness	0.0003	3.00E-04	1.00E-15	1.50E-01	0.00E+00	m
density	1750	1750	1700			kg/m3
Young's modulus	1.50E+09	1.50E+09	1.50E+10			N/m2
mass	0.525	0.525	1.7E-12			kg/m2
speed of air				343	343	m/s
density of air				0.121	1.21	kg/m3
loss factor	0.01	1.00E-02	1.00E-02			
angle of incidence				60		

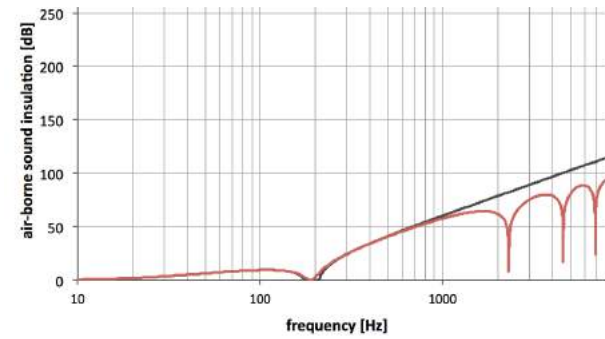


Figure 116: vacuum system 15cm at 10000 Pa

glass unit

	mass1	mass2	mass 3	cavity 1	cavity 2	
thickness	0.004	6.00E-03	1.00E-15	1.50E-01	0.00E+00	m
density	1200	1200	1200			kg/m3
Young's modulus	7.00E+09	7.00E+09	7.00E+10			N/m2
mass	4.8	7.2	1.2E-12			kg/m2
speed of air				343	343	m/s
density of air				0.00121	1.21	kg/m3
loss factor	0.01	1.00E-02	1.00E-02			
angle of incidence				60		

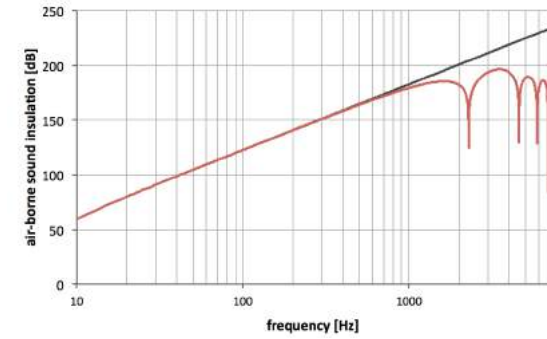


Figure 118: double glass unit 15cm at 100 Pa

ETFE unit

	mass1	mass2	mass 3	cavity 1	cavity 2	
thickness	0.0003	3.00E-04	1.00E-15	1.50E-01	0.00E+00	m
density	1750	1750	1700			kg/m3
Young's modulus	1.50E+09	1.50E+09	1.50E+10			N/m2
mass	0.525	0.525	1.7E-12			kg/m2
speed of air				343	343	m/s
density of air				0.00121	1.21	kg/m3
loss factor	0.01	1.00E-02	1.00E-02			
angle of incidence				60		

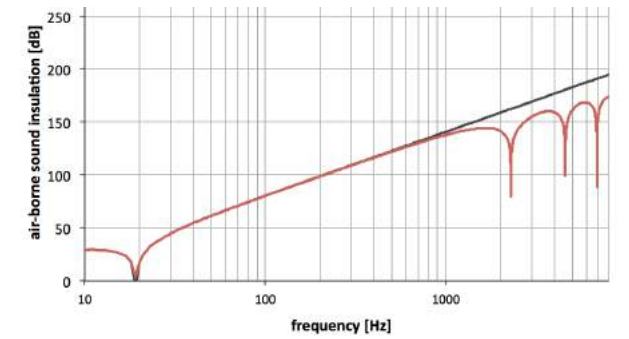


Figure 119: vacuum system 15cm at 100 Pa

	mass1	mass2	mass 3	cavity 1	cavity 2	
thickness	0.004	6.00E-03	1.00E-15	1.50E-01	0.00E+00	m
density	1200	1200	1200			kg/m3
Young's modulus	7.00E+09	7.00E+09	7.00E+10			N/m2
mass	4.8	7.2	1.2E-12			kg/m2
speed of air				343	343	m/s
density of air				0.0121	1.21	kg/m3
loss factor	0.01	1.00E-02	1.00E-02			
angle of incidence				60		

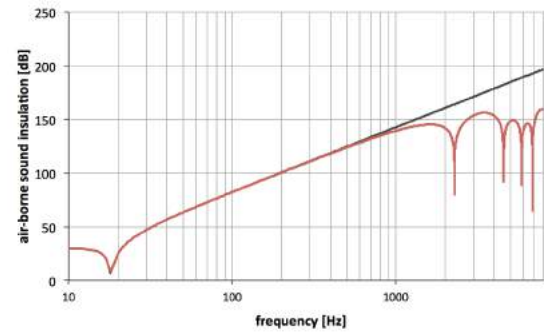


Figure 115: double glass unit 15cm at 1000 Pa

	mass1	mass2	mass 3	cavity 1	cavity 2	
thickness	0.0003	3.00E-04	1.00E-15	1.50E-01	0.00E+00	m
density	1750	1750	1700			kg/m3
Young's modulus	1.50E+09	1.50E+09	1.50E+10			N/m2
mass	0.525	0.525	1.7E-12			kg/m2
speed of air				343	343	m/s
density of air				0.0121	1.21	kg/m3
loss factor	0.01	1.00E-02	1.00E-02			
angle of incidence				60		

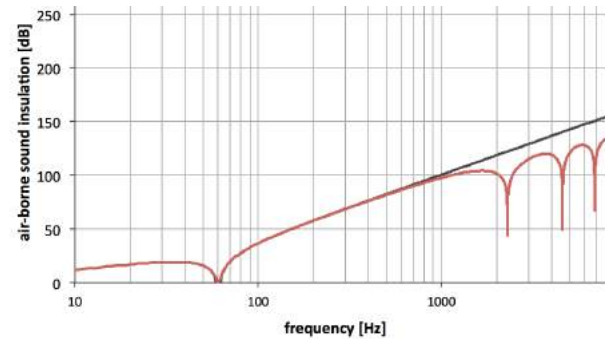


Figure 117: vacuum system 15cm at 1000 Pa

* All the graphs were made according to an excel file for hand acoustic calculations provided by Dr.ir. M.J. Tenpierik.

hand calculations conclusions

Having completed the hand calculations for the thermal and acoustical performance of the under study façade element, certain conclusions can be drawn. As far as the thermal performance is concerned, the application of reflective coatings plays a significant role in the reduction of the radiation value and thus the total U-value. In addition, the argon as a cavity filling improves a bit the thermal insulation, although the aerogel gives the best results ($U=1.65 \text{ W/m}^2\text{K}$ with coating). However, its high price doesn't render it very popular to be used for such applications. Taking these into account, the triple-layered system that consists of an argon cavity filling and a reflective coating in the middle layer gives a U-value of $1 \text{ W/m}^2\text{K}$.

As for the vacuum component, as already mentioned, when the pressure level changes from 10^5 Pascal (1 bar), which consists the atmospheric pressure, till 10^3 Pascal (10^{-2} bar) there is no evident change in the thermal conductivity value of air. However, from 100 Pascal (10^{-3} bar) and below a difference starts to appear, but the results aren't that remarkable, even at the pressure of 1 Pa ($U=3.01 \text{ W/m}^2\text{K}$). Also, the cavity's width doesn't affect significantly the thermal performance of the element.

Nevertheless, the combination of the two systems (inflated and vacuum) proved to be giving considerable results, along with the suitable coating, with a total U-value of $0.91 \text{ W/m}^2\text{K}$.

The second part concerned various calculations for the acoustical performance of the element, as the façade is supposed to prevent outside noise from entering the building. Random incidence was researched as the airborne sound insulation is usually worse in this case than in the normal incidence. Several conclusions were drawn and are the following. Firstly, argon has a negative effect in the airborne sound insulation, as the gas filling lacks attenuation of the mass-spring resonance¹. On the contrary, a lighter gas than air might have a positive impact, but this is rather difficult to contain into the cavity because of leaks and of course with the membranes this becomes almost impossible to achieve.

Another remark would be that the reduction of the pressure increases the airborne sound insulation of the cavity structure and decreases the stiffness of the cavity. Therefore the mass-spring resonance frequency (f_{ms}) shifts to lower frequencies².

This can be proved with the following formulas as well.

Stiffness of the cavity

$$S_t' = \gamma * P_{\text{gas}} / d_{\text{cav}} \quad (3)$$

Mass-spring resonance frequency

$$f_{ms} = 1/\cos\theta * \sqrt{[S_t' * (1/m_1 + 1/m_2)]} \quad (4)$$

where

S_t' : stiffness of the cavity

γ : heat capacity ratio

P_{gas} : gas pressure [Pa]

d_{cav} : cavity width [m]

θ : angle of incidence

m_1, m_2 : masses of membranes (kg/m^2)

^{1,2,3,4}: source:

Building Acoustics notes, chapter 4: Airborne sound insulation of cavity constructions, p. 4.6, 4.17

The next step would be to prove these assumptions. For this reason, an acoustic test of the vacuum element was decided to be conducted in collaboration with Mitchell Everts, who is also investigating the vacuum system's potential as a façade component. More information on this experiment will be given in the following chapter.

acoustics test

first experiment

Having completed the hand calculations for the acoustical performance of the under study façade element, an acoustic test was programmed to be conducted, as mentioned previously. After being informed from Dr. ir. M. J. Tenpierik, the test could take place in the transmission chamber at TPD, TNO in TU Delft. A couple of guidelines concerning the size of the model had to be followed though. The opening between the two chambers has specific dimensions (1.5 x 1.25 m) and this should be the size of the panel as well. So, in collaboration with Mitchell we started building the mock-up. The several steps that were taken are described here.

construction steps

A wooden frame with a cross section of 10x4cm was used. As it consists of a vacuum element, where high forces were going to be developed, the need for spacers was indispensable. The question, though, was how these spacers were going to be placed within the wooden frame and how they will remain perpendicular to the membranes without damaging them. The solution we thought of was the use of fishing wires that will be connected to the outer frame and also passing through the edge of each side of the spacers connecting them all together and thus holding them in place.

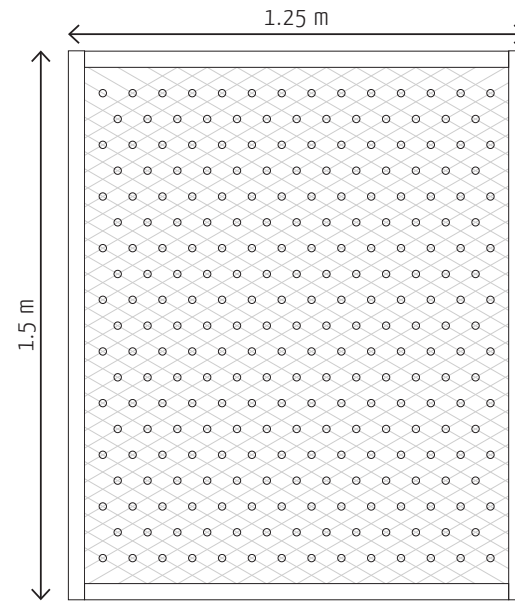


Figure 120: elevation of the model to be constructed

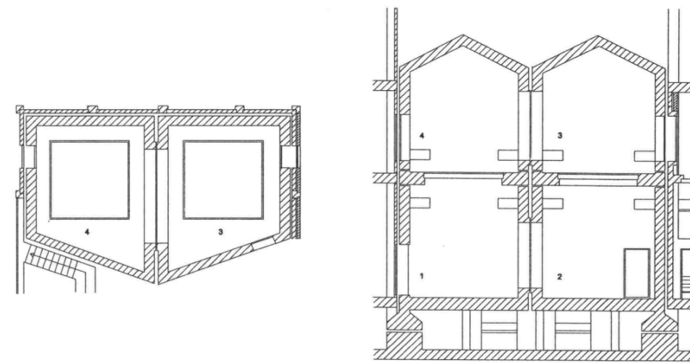


Figure 121: plan and vertical section of the transmission chamber at TPD / TNO / TU Delft

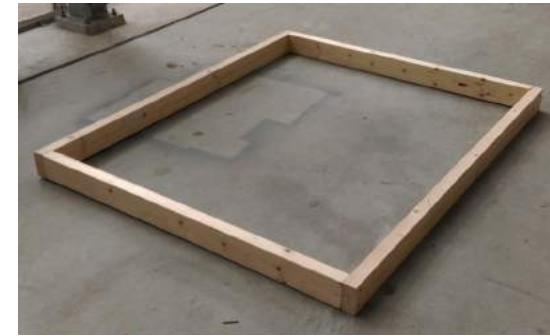


Figure 122: cutting and connecting the wooden frame



Figure 123: cutting and sanding of the spacers

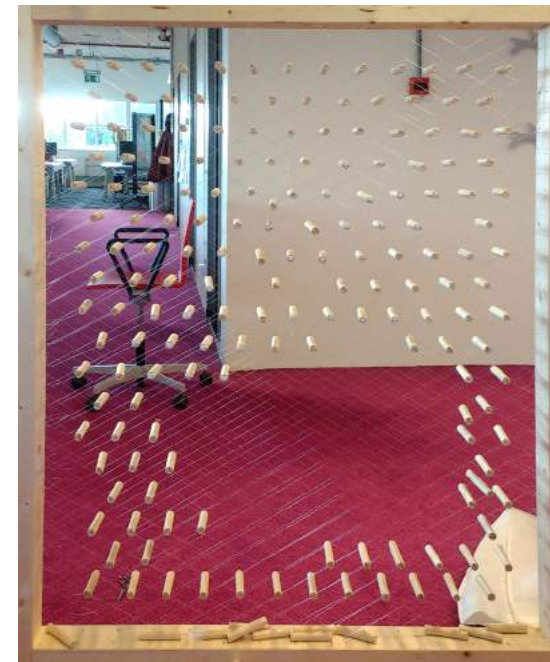


Figure 124: placement of the spacers between the wires



Figure 125: sealing the connections with silicone



Figure 126: staples for connecting the wires to the frame



Figure 127: connection of the spacers with the wires



Figure 128: sanding the rough edges of the frame

The next step was to place the two sheets of ETFE on each side. For this, double-sided tape was used and then the whole model was sealed all around with strong tape. We actually managed to avoid almost any leaks, at least to the extent that the results of the test wouldn't be affected that much.

Lastly, when the construction of the panel was complete we wanted to see if it was airtight enough and started deflating it with a hand pump. After a while we noticed that the frame started bending inwards, due to the high forces that were developed, until there was a crack. Consequently, we decided to reinforce it by placing two steel tubes in a cross in the middle of the panel and continued to deflate it.

Unfortunately, around **0.55 Bar** we heard a loud noise, which meant the damage of the ETFE and the failure of the panel to withstand the vacuum forces. This is half of the ideal vacuum we wanted to achieve. Luckily there were no leaks, as already mentioned, but some spacers that weren't aligned perfectly slid out of place and led to the collapse.

conclusions

Although it was an incomplete experiment we can draw several conclusions. Firstly, the spacers were not perfectly aligned and all perpendicular to the membranes, as the panel was rather big and it was impossible to achieve perfect alignment



Figure 129: placement of the ETFE in both sides with double-sided tape



Figure 130: crack in the frame because of vacuum forces



Figure 131: connection of the steel tube to the frame

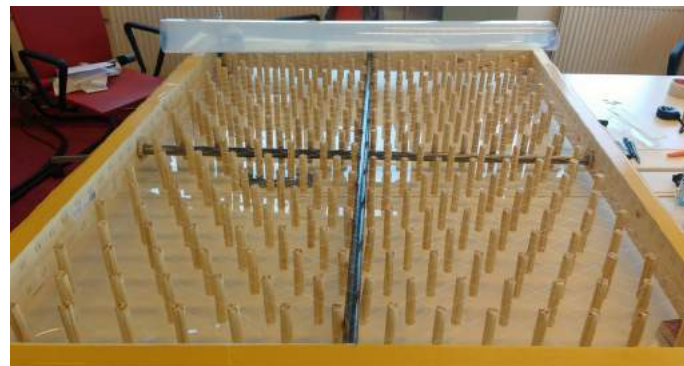


Figure 132: reinforcement of the frame with steel tubes



Figure 133: deflation after placement of the steel tubes

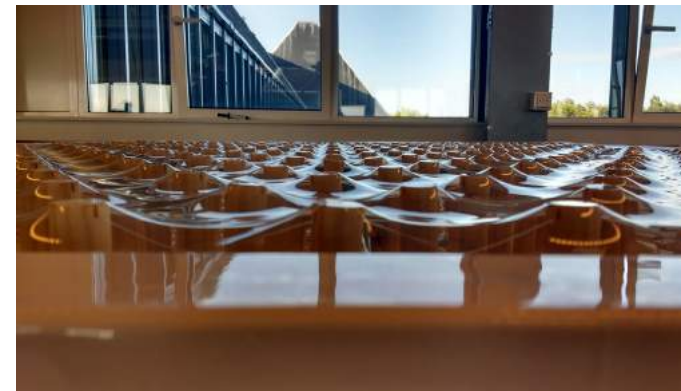


Figure 134: deflation of the panel / membrane pushing the spacers inwards



Figure 135: vacuum manometer connected to the panel



Figure 136: after the deflation and the damage of the membrane



Figure 137: damage of the ETFE membrane

connecting them with the wires only. In a professionally constructed panel, as the proposed design suggests later on, the spacers are placed into polymer "cups" that are welded onto the membrane, which constitutes a much stronger connection. In addition, the fact that the spacers were connected all together to each other through the wires led to a "domino" situation, where if one slips and falls then the rest

follow likewise. Furthermore, during the deflation the two membranes were getting closer to each other pushing inwards the wires as well. Therefore, this constitutes another reason for the displacement of a certain number of spacers.

Lastly, the ETFE foil proved to have a rather slippery surface finish, which also resulted in the collapse of the spacers and the damage of the membrane in the end.

second experiment

After the failure of testing acoustically the first model, we decided to build a second one. The latter was going to be tested in a different way and not in the transmission room that was supposed to be used for the first test. A wooden box will be used instead that has an integrated speaker on one side and an open opposite side allowing for materials placed on there to calculate how much sound is blocked through them, by measuring the sound pressure levels inside and outside of the wooden box. But first the new panel had to be constructed.

construction steps

Since the opening of the box was much smaller than the one in the transmission room, the dimensions of the new panel were also smaller. The same wooden frame was used as before, cut into shorter parts (0.50x0.48m). As for the spacers, a new approach was followed in order not to have the same results

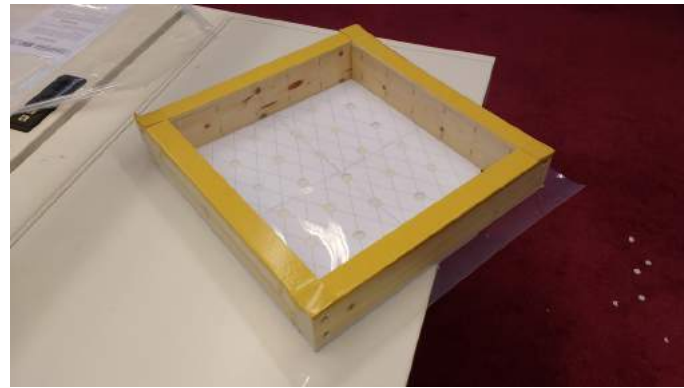


Figure 138: new wooden frame with double sided tape for the ETFE



Figure 139: new connection method of spacers

as the previous time. This time they are not connected to each other, as it was decided not to use the wires again. Instead, double-sided tape was used to connect a small piece of ETFE to both edges of the spacers and this provided more surface area for the connection of the spacers' edges with the ETFE sheets. For even stronger connection the small piece of ETFE was first nailed into the spacer and then connected with the double-sided tape to the outer membrane. In the end, the whole panel was sealed once again with strong tape to ensure airtightness.

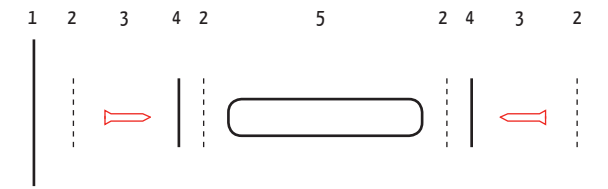


Figure 140: scheme of the new connection method of the spacers:

1. outer ETFE layer, 2. double-sided tape, 3. nail, 4. small ETFE piece, 5. spacer

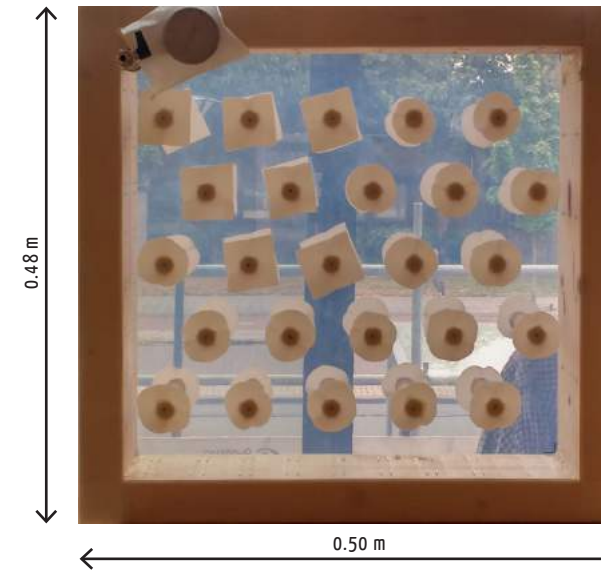


Figure 141: new constructed panel



Figure 142: new connection method of spacers

acoustic test

After completing the second panel, we were finally able to conduct the acoustic test. This took place in the PD Lab, the pavilion erected in the West entrance of the architecture faculty.

As already mentioned, an acoustic box was used with an integrated speaker on one side and an opposite open side where our panel was placed. The speaker is connected to a device that produces sound (white noise was chosen) and another device that measures the sound pressure levels was used.

Firstly, the reverberation time of the room had to be determined. For this, balloons were used that when exploded the device was triggered and started measuring the decay of the produced sound. Subsequently, because we didn't know the acoustic properties of the wooden box, an MDF plate (9mm) was measured first, as a reference, since it is easy to calculate its sound insulation. Then, the results for our



Figure 143: wooden acoustic box with integrated speaker



Figure 144: wooden acoustic box with integrated speaker with the panel placed on top



Figure 145: balloons test for measuring the reverberation time



Figure 146: first test with the 9mm MDF plate



Figure 147: measurement of the panel before deflating it

panel were going to be based on the results of the MDF plate. For each measurement, the sound pressure level inside and outside the box were measured twice to ensure the validity of the results.

After the measurement of MDF plate, the panel was placed on top of the box and was measured first without deflating it in order to take into account the existence of the spacers. The next step was to start the deflation. Initially, the hand pump was used for 0.8 bar (-0.2 bar) and the first test of 0.6 bar (-0.4 bar). Then, an electric pump was used for the rest of the 0.6 bar (-0.4 bar) measurements. Unfortunately, after the completion of these tests the pump stopped working and we couldn't continue the measurements with lower pressures. We tried once again with the hand pump but the minimum pressure that was reached was 0.55 bar (-0.45 bar).



Figure 149: electric vacuum pump



Figure 148: panel connected to the hand pump



Figure 150: measurement of the panel while deflating it with the hand pump

conclusions

After the completion of the acoustic test, the results had to be analysed in order to draw conclusions. For this, some formulas of the acoustics theory were needed. Firstly, the average of the measurements of the reverberation time for every frequency had to be calculated. Subsequently, the average of the sound pressure levels for every frequency between the two measurements had to be determined as well. Then, since each measurement lasted either one or two minutes, several sound pressure levels were recorded (specifically every 10 seconds) during each measurement. So, the average of these values had to be calculated, but this was not as simple as the mathematical average. More specifically, the energetic average of the sound pressure level for each frequency can be calculated with the following formula.

$$L_{\text{freq}} = 10 \log * \left\{ \left(\frac{1}{t_{\text{tot}}} \right) * \sum [10 \cdot (L_i / 10) * t_i] \right\}^{(1)}$$

where

L_{freq} : sound pressure level energetic average [dB]

t_{tot} : total duration of the measurement [s]

L_i : sound pressure level on a specific moment [dB]

t_i : the specific moment of time [s]

sources:

1. Provided by Dr. ir. M. J. Tenpierik

2. Building Acoustics notes, chapter 1: Definitions, Measurement Procedures and Composite Walls, p. 1.21

Afterwards, the airborne sound insulation for each frequency can be calculated, since the sound pressure levels inside and outside the box are known.

$$R = Lp_{\text{in}} - Lp_{\text{out}} + 10 \log (S/A)^{(2)}$$

where

R: airborne sound insulation [dB]

Lp_{in} : the sound pressure level inside the box [dB]

Lp_{out} : the sound pressure level outside the box [dB]

S: surface area of the specimen (panel) [m²]

A: sound absorption in the receiver room [sabin]

Having calculated the sound insulation for every frequency for the measured pressure levels (0.8, 0.6 and 0.55 bar) several graphs were made to portray these results, which are presented in the next page.

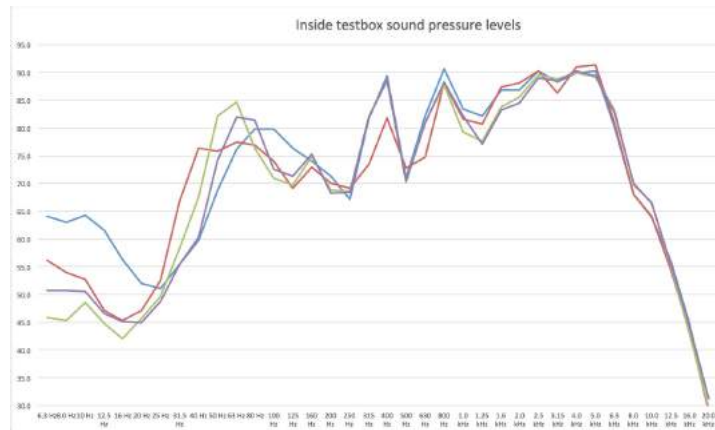


Figure 151: sound pressure levels inside the box

- MDF Outside
- 0 Bar Outside
- 0,2 Bar Outside
- 0,4 Bar Outside
- 0,45 Outside

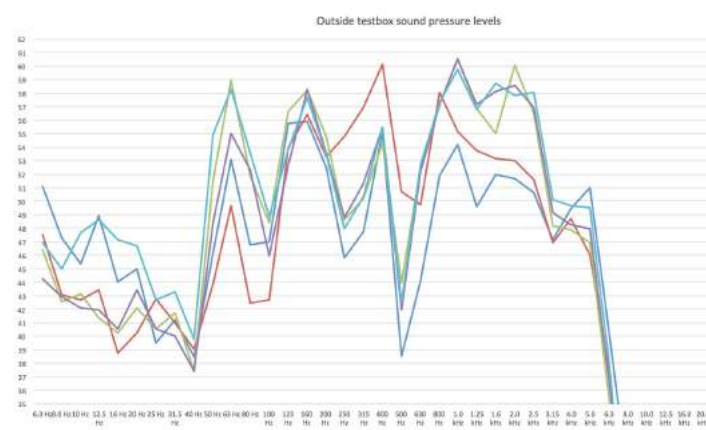


Figure 152: sound pressure levels outside the box

- MDF Inside
- 0 Bar Inside
- 0,2 Inside
- 0,4 Bar Inside



Figure 153: sound pressure levels differences compared to 9mm MDF plate

- 0 Bar
- 0,2 Bar
- 0,4 Bar
- 0,45 Bar

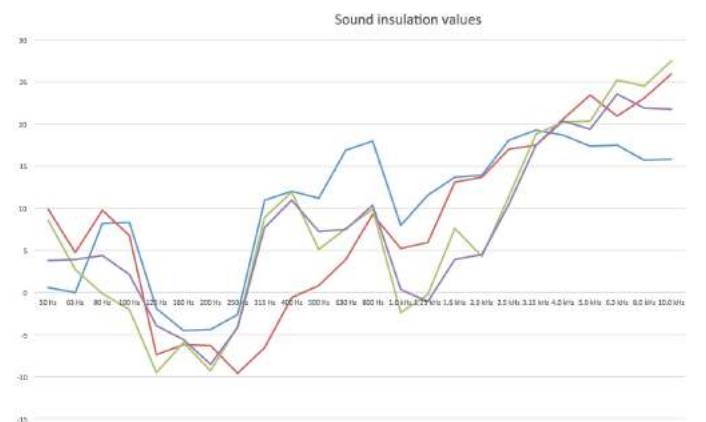


Figure 154: airborne sound insulation values

- MDF sound insulation
- 0 Bar sound insulation
- 0,2 Bar sound insulation
- 0,4 Bar sound insulation

As it can be noticed from the graphs (figures 151-154), all the curves of the sound pressure level values follow almost the same pattern, even the MDF, which doesn't help us draw

reliable conclusions. In the hand calculations described previously, the graphs (figures 155-164) showed almost no difference in the airborne sound insulation from 1 bar

pressure of air									
<i>pascal</i>		$8 \cdot 10^4$	$6 \cdot 10^4$	$5.5 \cdot 10^4$	$2 \cdot 10^4$	10000	$8 \cdot 10^3$	1000	100
<i>bar</i>		0.8	0.6	0.55	0.2	0.1	0.08	0.01	0.001
density of air (kg/m³)		0.968	0.726	0.6655	0.242	0.121	0.0968	0.0121	0.00121

Figure 155: correlation of air pressure levels and air density

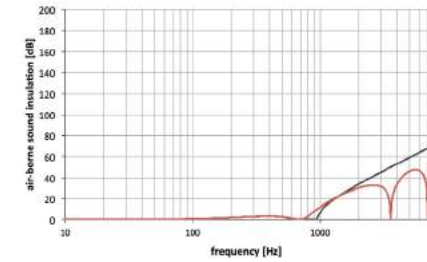


Figure 156: airborne sound insulation at 1 bar

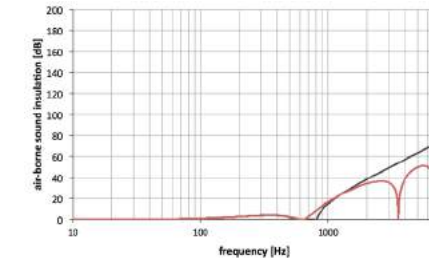


Figure 157: airborne sound insulation at 0.8 bar

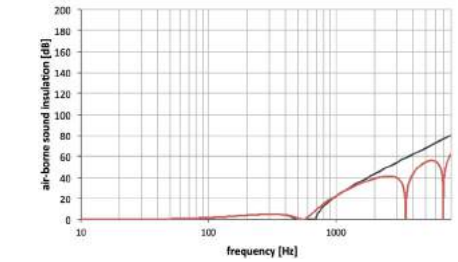


Figure 158: airborne sound insulation at 0.6 bar

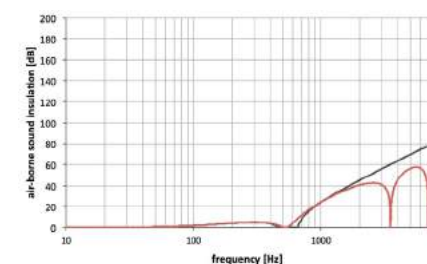


Figure 159: airborne sound insulation at 0.55 bar

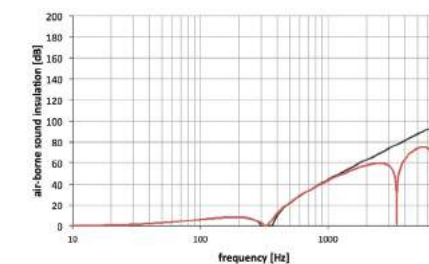


Figure 160: airborne sound insulation at 0.2 bar

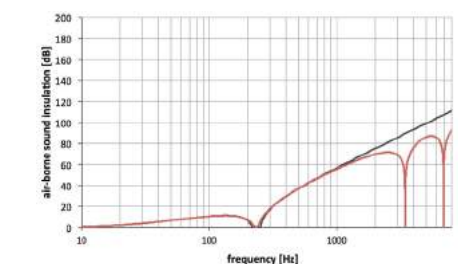


Figure 161: airborne sound insulation at 0.1 bar

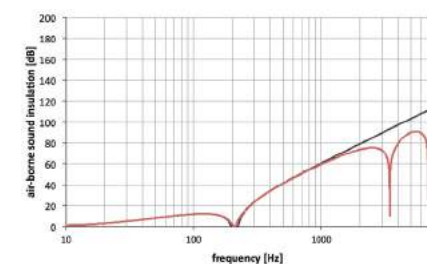


Figure 162: airborne sound insulation at 0.08 bar

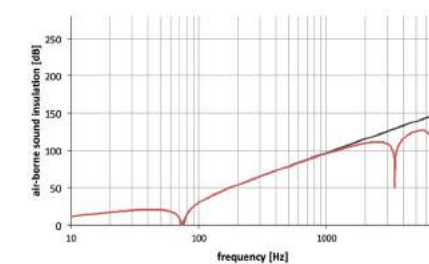


Figure 163: airborne sound insulation at 0.01 bar

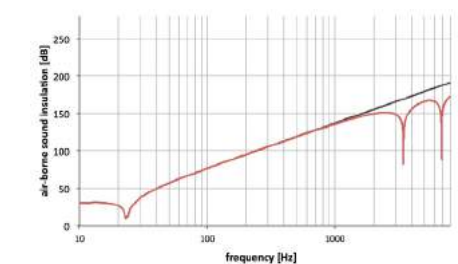


Figure 164: airborne sound insulation at 0.001 bar

(10^5 Pa) until 0.2 bar ($2 \cdot 10^4$ Pa). On the contrary, from 0.2 bar an evident increase in the airborne sound insulation starts to appear. At 0.01 bar there is a remarkable increase in the sound insulation values and the mass-spring resonance frequency (f_{ms}) drops below 100 Hz, which is a positive result. Of course, at 0.001 bar there is an even bigger increase of the sound insulation and the f_{ms} drops to even lower values. Nevertheless, these pressure levels are almost impossible to achieve due to the really high forces that are developed and especially in our case of making the specific model without any professional equipment. Unfortunately, the tested air pressure levels are included in the range where no evident difference can be noticed in the sound insulation values. Therefore, we can conclude that since the experiment stopped at 0.55 bar it can be considered incomplete, as the desired pressure of 0.2 bar was not reached in the end.

Several other remarks that are worth mentioning are the following. Firstly, from the sound insulation graph (figure 156, p. 126), we can notice a number of negative values, which don't really make sense. Furthermore, the first "drop" in the graph that represents the sudden decrease of the sound insulation value due to the occurrence of the mass-spring resonance, happens within a range of frequencies, which doesn't correspond to the theory (it should happen at a specific frequency: f_{ms}). Moreover, the wooden box that was

used for the measurements could be considered unreliable, as it is supposed to represent the source room. However, due to its small dimensions it can be considered as a big cavity, for instance, instead of a room and that could affect the results of the acoustic test. Last but not least, the ETFE could have performed differently than expected. More specifically, the membrane is supposed to be a flexible material, but with the deflation of the panel to reach lower air pressures, the ETFE was stretched significantly and this could have an impact on its acoustic properties, for example it could influence the frequency where the mass-spring resonance occurs.

In any case, these were several assumptions drawn for the incomplete acoustic test and further research is needed to obtain more accurate and reliable results.

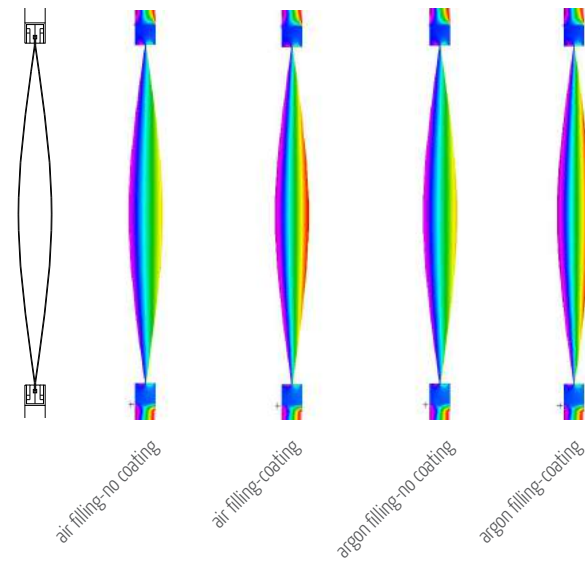
THERM calculations

Having completed the hand calculations for the thermal and acoustical performance, a number of simulations had to be conducted in order to validate or reject the results and the already drawn conclusions. Once again, the two systems (inflated and vacuum) were investigated separately at first and then in combination. The inflated element was explored both as a two-layered and a three-layered system with air, argon and aerogel cavity fillings. For the vacuum element, there was not an option to set a new thermal conductivity value for the air as a result of a lower pressure and therefore it was simulated with normal air ($\lambda = 0.0248 \text{ W/mK}$). Three different cavity's widths were taken into account for the vacuum component, as well as one with the addition of spacers, in case they are proved to be necessary for structural reasons. Subsequently, all the versions of the combinations of the inflated and the vacuum were tested.

As THERM constitutes a 2D simulation software certain simplifications and compromises had to be made. More specifically, the goal was to test the cushions themselves and especially the membranes' performance, so there was not given much attention to the frame (which unfortunately proved to be the reason for thermal losses). In addition, the whole element was placed in between of a good insulation (glass fibre) so as to avoid any losses from the rest of the wall.

inflated cushion

2-layers



3-layers // aerogel

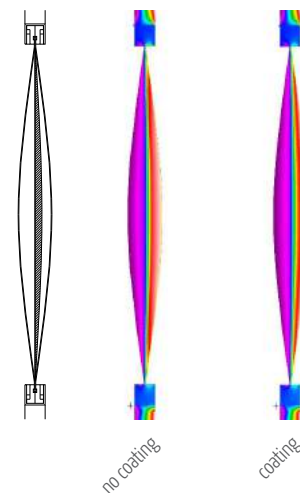
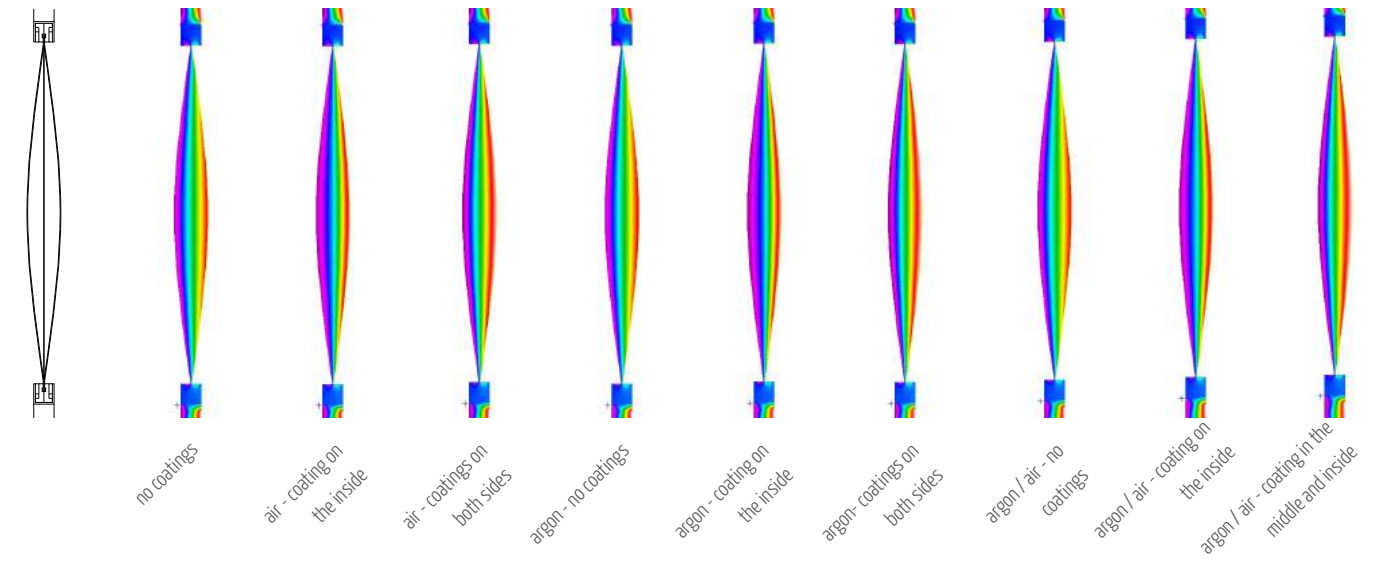


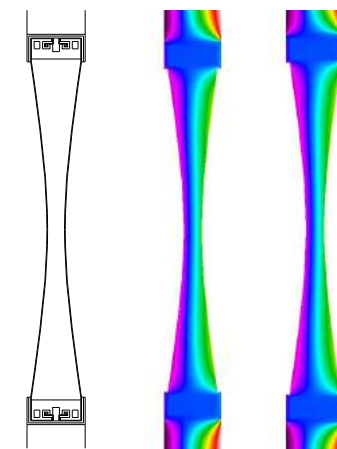
Figure 165: colour legend

3-layers // air - argon



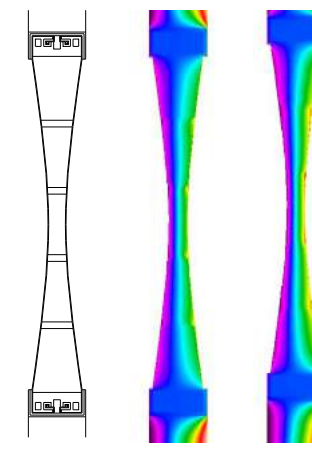
vacuum system

5 cm



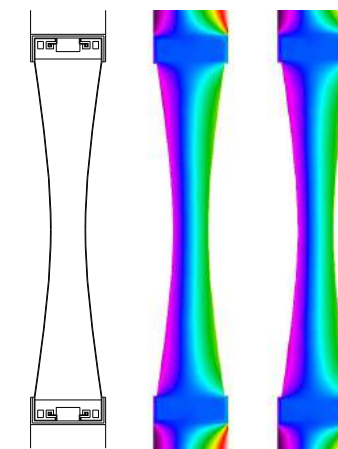
no coatings
coating on the inside

5 cm with spacers



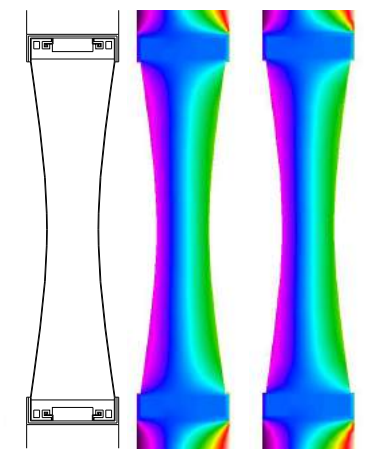
no coatings
coating on the inside

10 cm



no coatings
coating on the inside

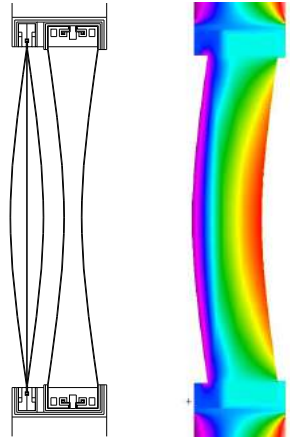
15 cm



no coatings
coating on the inside

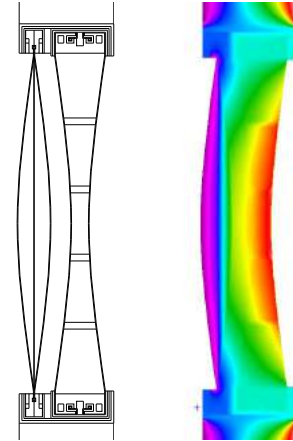
combinations

5 cm vacuum



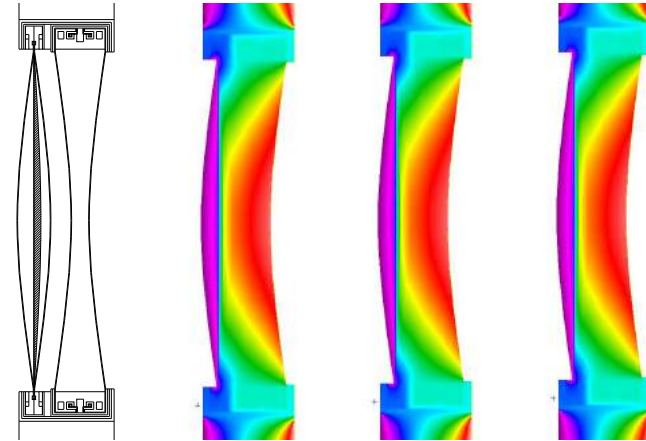
argon - coating on the middle layer of the inflated

5 cm vacuum with spacers



argon - coating on the middle layer of the inflated

5 cm vacuum with aerogel

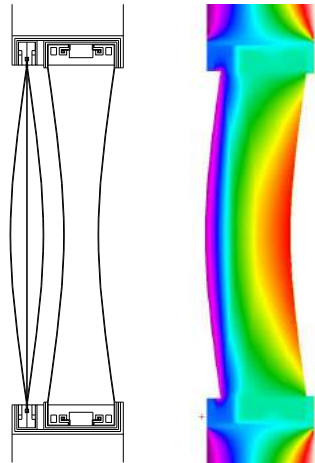


no coatings

coating on the middle layer of the inflated

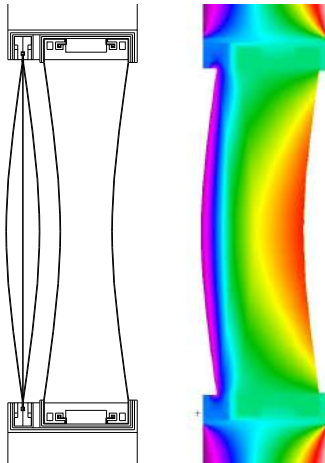
coating on the inside layer of the vacuum

10 cm vacuum



argon - coating on the middle layer of the inflated

15 cm vacuum



argon - coating on the middle layer of the inflated

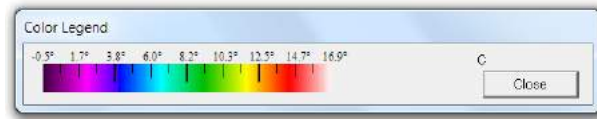


Figure 166: colour legend

U-values

	U-value (W/m²K)		U-value (W/m²K)
2layers inflated			
<i>air</i>			
air no coating	3.22	100 mm	air no coating 3.065
air coating on the inside	2.38	air coating	2.17
<i>argon</i>			
argon no coating	2.18	150 mm	air no coating 3.065
argon coating on the inside	2.17	air coating	2.225
3layers inflated			
<i>air</i>			
no coating / no coating	2.4	combinations	
no coating / coating	1.94	3layers inflated_argon no coating-argon coating	1.385
coating / coating	1.63	+50mm vacuum air no coatings	
<i>argon</i>			
no coating / no coating	2.32	3layers inflated_argon no coating-argon coating	1.335
coating / coating	1.47	+50mm vacuum with SPACERS air no coatings	
no coating / coating	1.8	3layers inflated_argon no coating-argon coating	1.415
<i>argon air</i>			
no coating / no coating	2.36	+100mm vacuum air no coatings	
coating / coating	1.54	3layers inflated_argon no coating-argon coating	1.455
no coating / coating	1.91	+150mm vacuum air no coatings	
<i>aerogel</i>			
no coating / aerogel / no coating	1.27	3layers inflated_air no coating-aerogel-air no coating	0.98085
no coating / aerogel / coating	1.17	coating+50mm vacuum air no coatings	
vacumm			
50 mm			
air no coating	3.18	3layers inflated_air no coating-aerogel-air no coating	0.98065
air coating	2.275	coating+50mm vacuum air coating	
SPACERS air no coating	2.88		
SPACERS air coating	2.3		

Figure 167: table with U-values calculated form the THERM software

conclusions

After the simulations with the THERM software we can draw several conclusions from the results presented in the previous table. Firstly, the coatings play a significant role in the reduction of the total U-value of the elements. The maximum value for the inflated cushion can be found in the two-layered component without any coating ($U = 3.22 \text{ W/m}^2\text{K}$) and the minimum in the three-layered element with a layer of 20mm aerogel in the middle and a coating on the inside layer ($U = 1.17 \text{ W/m}^2\text{K}$). As already mentioned, though, the high price of the aerogel leads to the choice of the second best option, which is the three-layered cushion with argon as a cavity filling and a coating on the inside layer, giving a U-value of $1.8 \text{ W/m}^2\text{K}$.

As for the vacuum, as it was mentioned before, it was simulated with atmospheric air pressure level at 10^5 Pascal (1 bar) as the software doesn't have the option of entering lower air pressure values. Therefore, the 5 cm cavity width with no coating gives the maximum U-value of $3.18 \text{ W/m}^2\text{K}$ and the 10 cm cavity width with a coating on the inside gives the minimum value of $2.17 \text{ W/m}^2\text{K}$.

Lastly, the combination, as expected, has the best performance

with a maximum value for the three-layered cushion with a coating on the inside and a 15 cm cavity width of the vacuum ($1.455 \text{ W/m}^2\text{K}$) and a minimum of $1.355 \text{ W/m}^2\text{K}$ for the three-layered element with argon as cavity filling, coating on the inside and a 5 cm wide cavity with spacers (fibreglass) for structural purposes.

It can be noted that the spacers have a remarkable impact on the total U-value of the component. More specifically, the 5 cm vacuum cavity without any spacers nor coatings gives a U-value of $3.18 \text{ W/m}^2\text{K}$ and with coating $2.275 \text{ W/m}^2\text{K}$. On the contrary, with the addition of spacers the value without coating drops to $2.88 \text{ W/m}^2\text{K}$ and with coating to $2.3 \text{ W/m}^2\text{K}$. As far as the combination of the systems is concerned, the version without spacers gives a value of $1.385 \text{ W/m}^2\text{K}$ and with a value of $1.335 \text{ W/m}^2\text{K}$, which shows that the spacers have still a small influence in the reduction of the total U-value.

The addition of spacers is worth mentioning as they would be expected to have a negative impact, since they are considered thermal bridges and thus they could lead to heat losses. Fortunately, the choice of fibreglass as the spacers' material gave the opposite results.

comparison hand calculations // simulations

	U-value (hand) [W/m ² K]	U-value (THERM) [W/m ² K]
2layers inflated		
<i>air</i>		
air no coating	2.986	3.22
air coating on the inside	1.708	2.38
<i>argon</i>		
argon no coating	2.965	2.18
argon coating on the inside	1.664	2.17
3layers inflated		
<i>argon</i>		
no coating /coating	1	1.8
vacumm		
<i>50 mm</i>		
air no coating	3.04	3.18
combinations		
3layers inflated_argon no coating-argon coating +50mm vacuum air no coatings	0.91	1.385

Figure 168: comparison table of the U-values obtained from the hand calculation and the THERM software

As it can be seen from the table above, the results are in accordance with each other, in terms of both hand and THERM values are being reduced proportionally. However, the results given from the hand calculations have in general lower values than the ones from the simulation. One reason for that could be that for the hand calculations simplified versions were taken into account with the assumption that all the elements have infinite height and the same cavity width all along. In the simulations, the whole component was drawn

with a specific height and also the width of the cavity was being reduced closer to the frame, which is a potential area for bigger amounts of heat loss. Another reason could be that the frame used in THERM is not the best choice after all, since it is responsible for a great amount of heat loss, as it can be confirmed from the colour range images. In the hand calculations, on the other hand, the frame was not taken into account.

design builder

simplifications

In order to perform simulations with the Design Builder software, several simplifications had to be made. Firstly, since the case study consists of 44 floors it would be time-consuming to design and simulate the whole building. For this reason separate offices would be easier to be investigated separately. For this purpose, three floors (41x53m) were designed as a sample and each one of them was divided into smaller office areas (zones) of 9.4x5.5m. As it can be seen from the floor plan, two openings correspond to each office space. The floor height is 3.65m and this dimension was taken into account for every office area as well.

For the purpose of simplicity again, the façade had to be modified too. The designed façade surrounds normally the existing building and it is placed 70cm in front of it. As this would make things more complicated for the simulation and probably more time would be necessary for its completion, it was decided to place the membrane façade inside the existing openings (3x2.1m). Also, the idea of the design is a wider rectangular structural element of 2.9x3.65m that would span from floor to floor and it would be divided into smaller irregular shapes where the cushions' systems would be placed. As it can be seen from the figure 110 the shapes of the cushions were also simplified into triangles since Design Builder recognises rectangular and triangular openings.

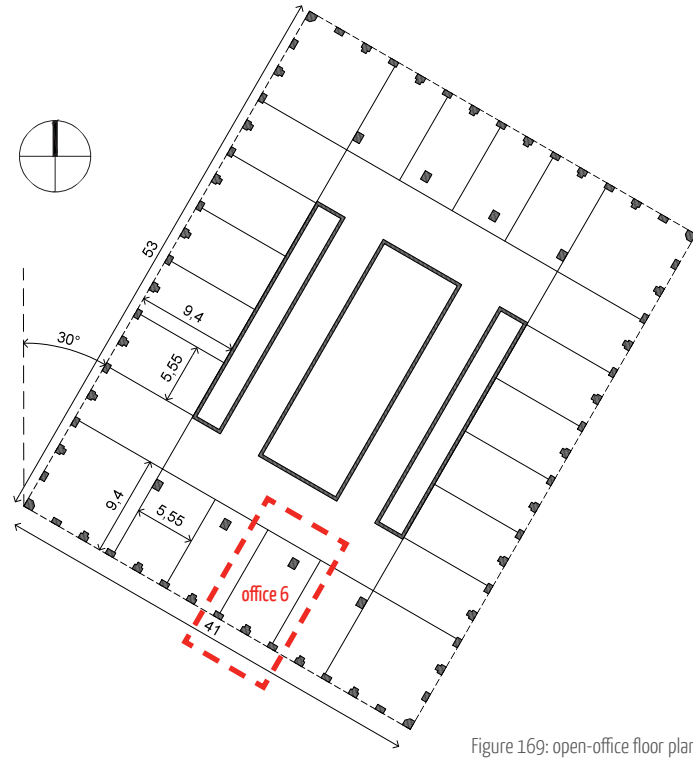


Figure 169: open-office floor plan

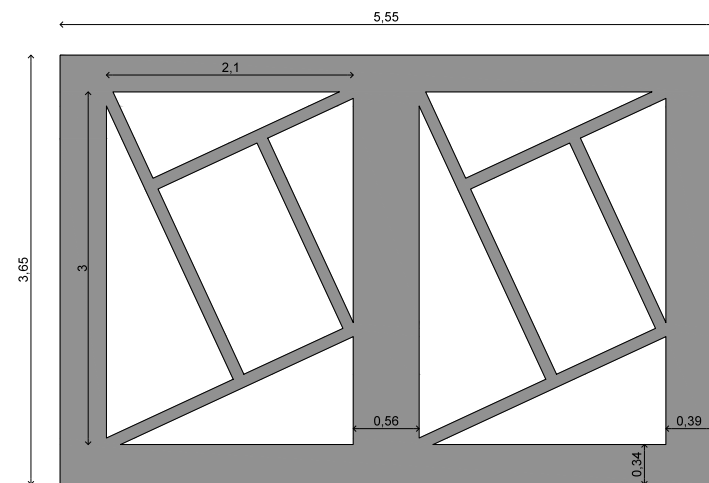


Figure 170: façade configuration simplified

cushions

As far as the ETFE cushions are concerned, since the THERM calculations had already been conducted the U-values that were obtained from the results will be used. In addition, a total solar transmission (SHGC) and a light transmission (Tvis) value should be set as well. In order to acquire more valid values, the WINDOW software was used, which works usually with the THERM software and has a windows database (materials list, ready glazing units etc). Therefore, ETFE was added as a new material to the list with both a 0.3 mm and 0.1 mm thickness, without and with a coating of 0.2 emissivity value. Then the whole unit was created with the three-layered inflated cushion and the two-layered vacuum element behind it. As it is shown in the figure below the WINDOW gave a U-value of 0.81 W/m²K, a SHGC of 0.572 and a Tvis of 0.623.

This light transmission value was expected as a single foil of ETFE has 0.9 so five layers give a value of $0.9^5 = 0.6$. As for the U-value, the average between the result from THERM (1.335 W/m²K) and the WINDOW (0.81 W/m²K) was inserted in Design Builder in the end, which is **1.09 W/m²K**.

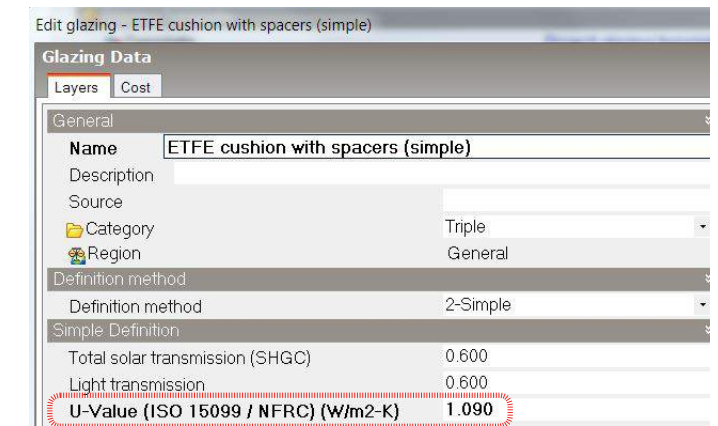


Figure 171: settings of 5-layered ETFE system in Design Builder

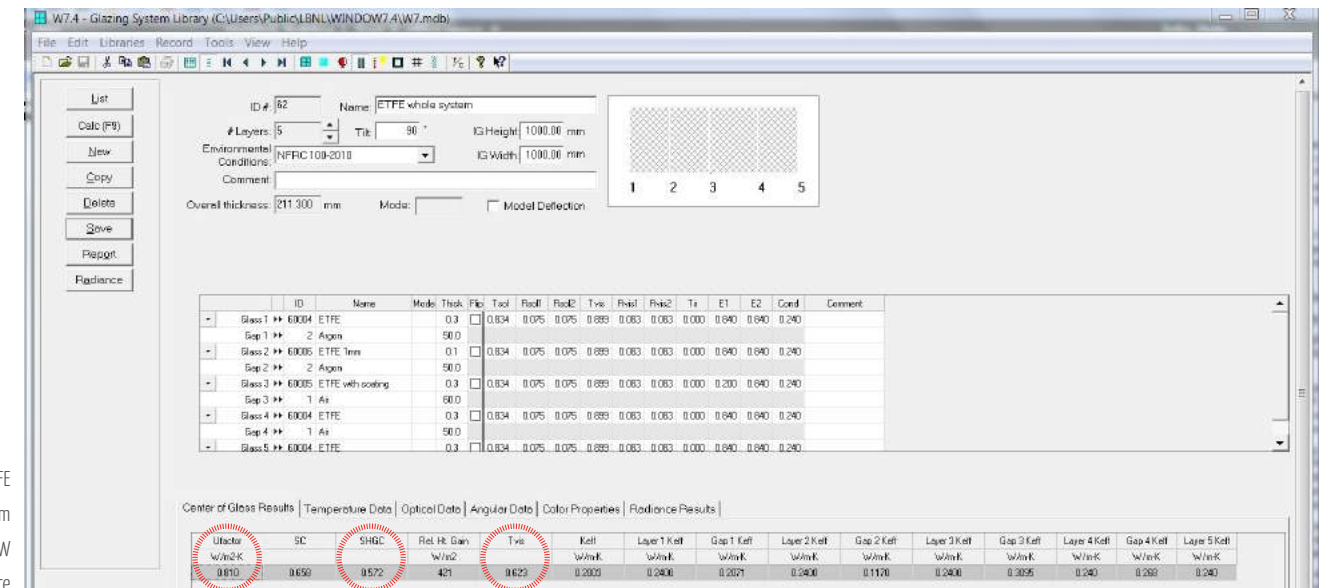


Figure 172: ETFE 5-layered system from WINDOW software

shading

As already mentioned, the shape of the cushions were simplified into triangles inside a rectangular opening. In figure 112 the surface area is shown for each one of them and since the two openings have identical “window” units they have also the same numbering. For the simulations an outside shading (low reflectance-low transmittance) was used since the cushion was set as a single element with given values for the solar (SHGC) and light transmission (Tvis), as well as U-values and thus the shading could be placed either inside or outside. The outside position was chosen in order to avoid overheating of the interior space. The shading was placed gradually in front of each cushion to explore the impact of it into the reduction of the total energy consumption and the indoor temperature when the cooling is turned off. So, the number that is being covered corresponds to a percentage of shading. More specifically:

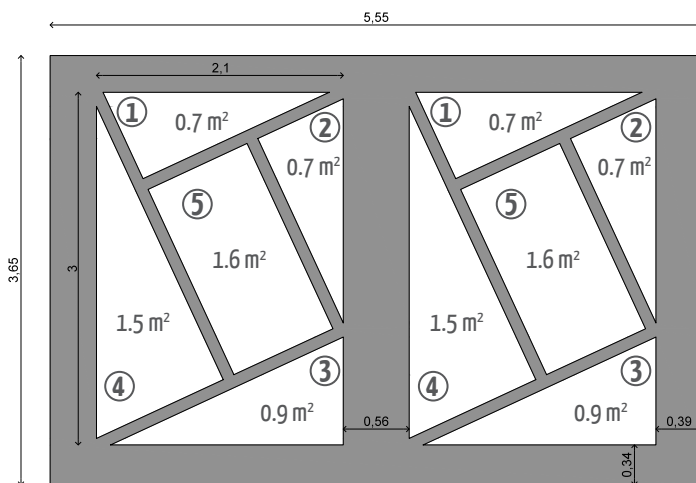


Figure 173: numbering and surface area

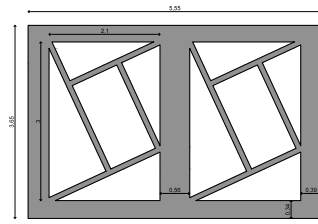


Figure 174:
0% shading

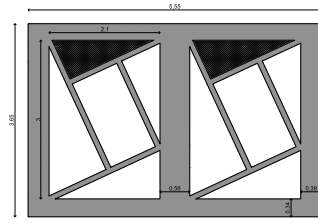


Figure 175:
1 = 20% shading

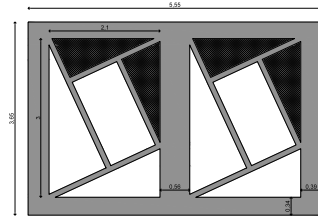


Figure 176:
2 = 40% shading

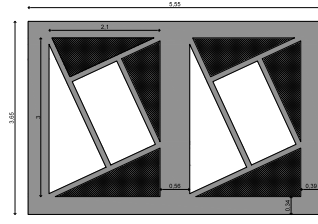


Figure 177:
3 = 60% shading

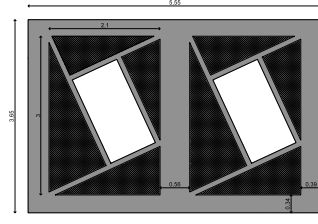


Figure 178:
4 = 80% shading

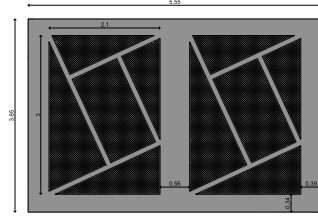


Figure 179:
5 = 100% shading

design builder settings

general

A number of settings were realised and will be described as shortly as possible. Extended information can be found in the Appendix (B). Firstly, the weather data file for Paris was loaded and then the orientation of the building was set (30° from the North as shown in figure 109, p.104). The design of three floors that was mentioned before was made in order to perform the simulations on a middle floor to avoid any heat gain or losses from the ground floor or the roof. Also, for time-saving purposes the Scope in the Model Data tab was then set to Zone to simulate only one office.

The case study constitutes an open-plan office building and thus the schedule wherever it's needed is set to office hours.

Furthermore, the density/occupancy had to be set and so 12m² were given to each person. The office spaces have a floor area of approx. 50m² which gives as a result 4 persons per office. So 12.5m² (=50/4) correspond to one person and the density can be calculated to 1/12.5 = 0.08.

Moreover, the value for the minimum fresh air had to be defined and so 9 l/s were appointed per person, which corresponds to 30m³/h per person. In addition, an infiltration rate of 0.3 ac/h was set (Construction tab > Airtightness > Model infiltration > Constant rate > 0.3 and Schedule > On 24/7), according to

building regulations for new constructions.

As far as the amount of energy consumed for the office equipment and lighting are concerned, the computers were turned on with 10 W/m² gain (Activity tab) and general lighting was turned on with a normalised power density of 1 W/m² per 100 lux (Lighting tab).

construction

The goal of the simulations was to test the performance of the façade element itself that was designed and its influence in the total energy consumption of the building. For this reason the exterior wall of the building was given a high insulating material (0.2m reinforced cast-dense concrete with a 0.3m EPS layer behind it), so as to play an insignificant role in the total energy consumption. Also, the internal floors were set to 100mm concrete slab for good thermal insulation performance.

openings

As already mentioned, the glazing type was set as the ETFE 5-layered system with the values that were described before, with 60% glazing and type as “Fill surface (100%)”. The component has an aluminum window frame (with thermal break) of 0.02m thick with 1 horizontal and 1 vertical divider of 0.01m wide each.

heating & cooling **on**

For the conduction of the simulations the worst case was taken into account, that of southern orientation (office 6, figure 109, p. 104) and two versions were tested. Firstly, a version with heating and cooling both turned on, along with mechanical ventilation, was performed without any shading and the purpose was to see the total energy consumption of the building. Subsequently, the same settings were used but with the gradual addition of shading this time.

The settings for cooling and heating are the following. In the

Activity tab > Environmental control the heating setpoint was set to 21°C with a heating set back to 15°C and the cooling setpoint to 25°C with a cooling set back to 28°C. In addition, the HVAC system was left to default which corresponds to a Fan Coil Unit (4-Pipe), Air cooled Chiller. As for the mechanical ventilation (HVAC tab) the Outside air definition method was set to **Min fresh air (per person)** with Open office hours schedule, which takes into account the data from the Activity tab. Lastly, the natural ventilation is off since the design doesn't include any operable windows.

	Annual energy per total building area (kWh/m ²)			Summer energy per total building area (kWh/m ²)			Winter energy per total building area (kWh/m ²)		
	Total (kWh/m ²)	District heating (kWh)	District cooling (kWh)	Total (kWh/m ²)	District heating (kWh)	District cooling (kWh)	Total (kWh/m ²)	District heating (kWh)	District cooling (kWh)
heating / cooling ON									
No shading	122.45	284.66	3156.63	83.57	0	2768.34	39.36	289.83	396.62
Shading									
20%	117.04	302.34	2884.45	79.24	0	2564.62	38.23	315.47	327.06
40%	112.36	320.4	2646.09	75.36	0	2381.94	37.41	333.47	270.58
60%	105.97	350.86	2314.91	69.8	0	2120.1	36.52	363.45	198.51
80%	96.65	426.64	1800.23	60.7	1.16	1690.65	36.09	432.7	109.19
100%	88.75	544.06	1310.77	51.71	10.14	1258.12	37.09	539.06	49.89

Figure 180: energy consumption when both heating and cooling are turned on

heating & cooling **off**

The next step was to turn off the cooling in order to see the maximum indoor air temperature that is being reached without any mechanical support. Two versions were examined here as well, one with no natural ventilation and one with. Also, these two versions were explored with and without shading so as to see again the maximum indoor air temperatures.

The settings that were made are the following. Firstly, in the Model Data tab the natural ventilation was turned on with the office hours schedule. In the Activity tab > ventilation setpoint temperature > indoor min. temperature control was set to 24°C. This value should be at least 2 degrees higher than the heating setpoint temperature (21°C) so as to prevent simultaneous heating and venting. In the HVAC tab, the mechanical ventilation is turned off and the natural ventilation is set **by zone** with 5 ac/h and again office hours schedule. In addition, the outdoor max. temperature control is set to 24°C, in order to prevent outside air hotter than 24°C to enter the building. Lastly, the Delta T limit is set to -50, because when the difference of the indoor temperature minus the outdoor is bigger than the Delta T the ventilation is not allowed.

	Annual energy per total building area (kWh/m ²)			Max summer temperature (°C)
	Total (kWh/m ²)	District heating (kWh)	District cooling (kWh)	
heating / cooling OFF				
Natural ventilation OFF				
No shading	55.08	269.59	0	53.96 (24 Aug)
Shading				
20%				51.84 (24 Aug)
40%				49.95 (24 Aug)
60%				47.21 (24 Aug)
80%				43.29 (25 Aug)
100%				39.31 (25 Aug)
Natural ventilation ON				
No shading	51.25	93.83	0	44.44 (22 Aug)
Shading				
20%				42.93 (21 Aug)
40%				41.71 (21 Aug)
60%				39.41 (25 Aug)
80%				37.47 (25 Aug)
100%				34.87 (25 Aug)

Figure 181: energy consumption and max. indoor temperatures when cooling is turned off | with and without ventilation

cooling off // graphs

At this point several graphs are presented that show the maximum temperatures during the summer period when cooling is turned off, with natural ventilation on and off, as well as with and without sun shading.

natural ventilation off

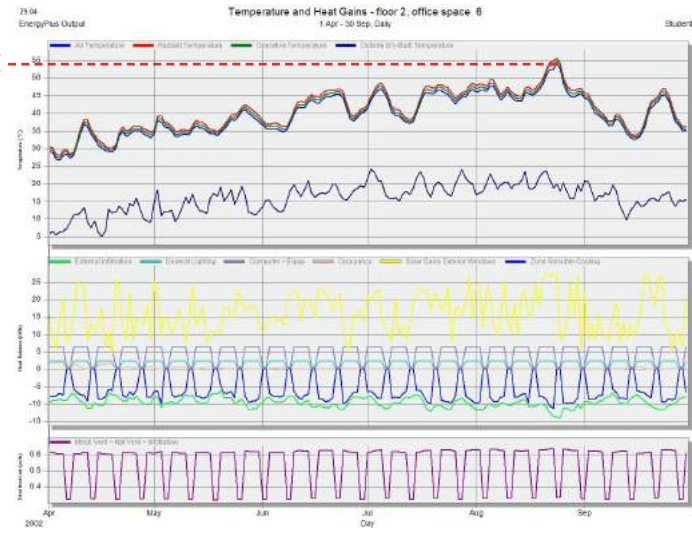


Figure 182: natural ventilation off // no shading

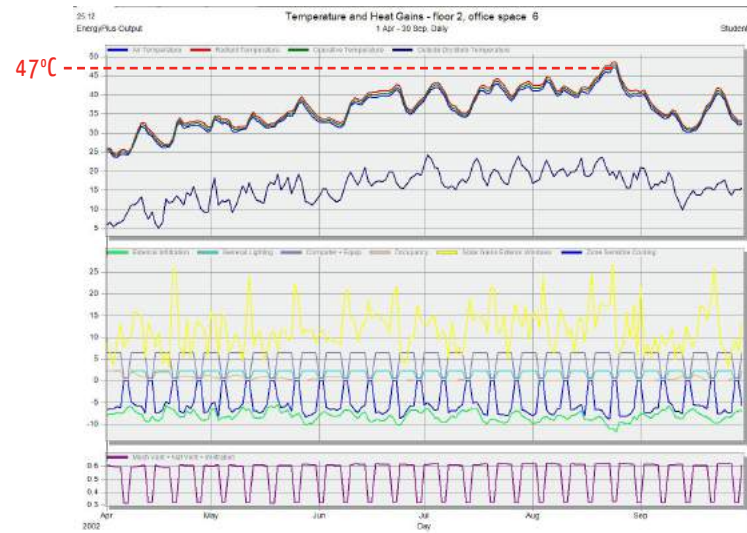


Figure 184: natural ventilation off // 60% shading

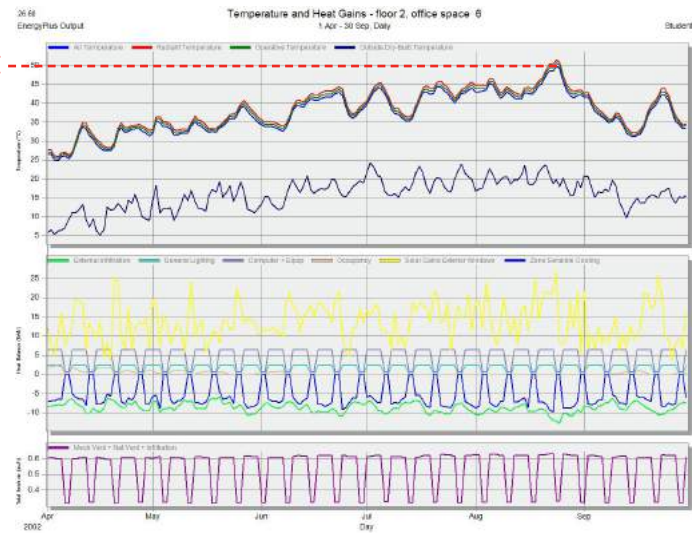


Figure 183: natural ventilation off // 40% shading

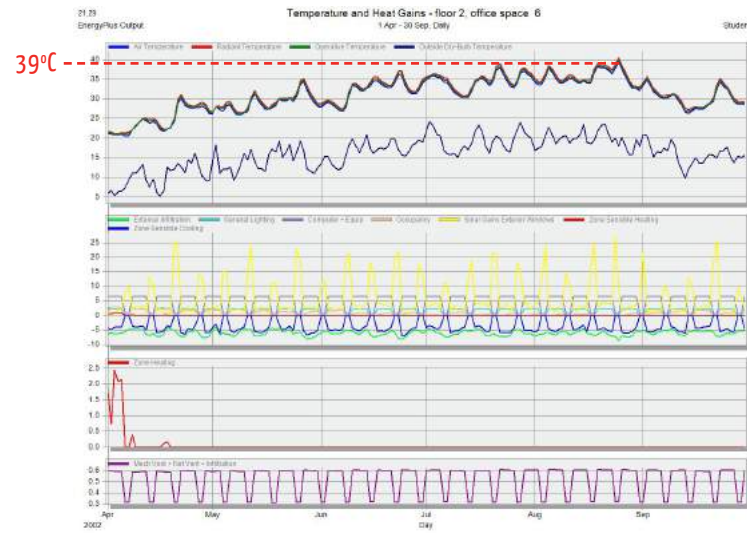


Figure 185: natural ventilation off // 100% shading

natural ventilation on

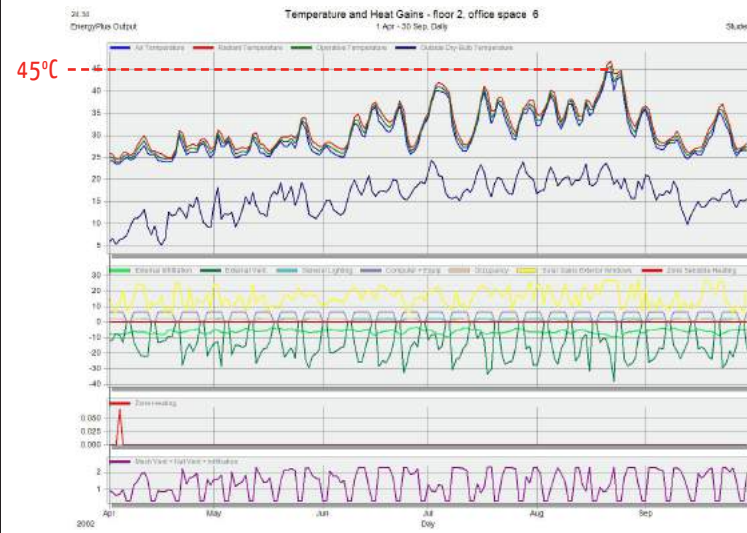


Figure 186: natural ventilation on // no shading

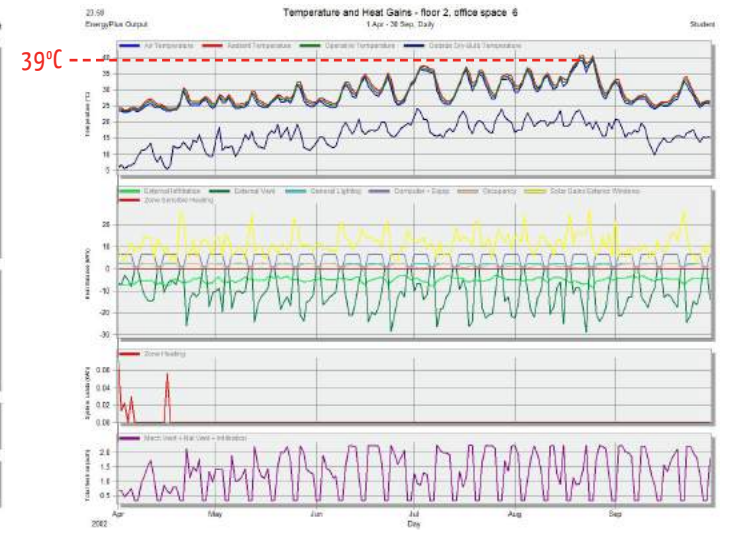


Figure 188: natural ventilation on // 60% shading

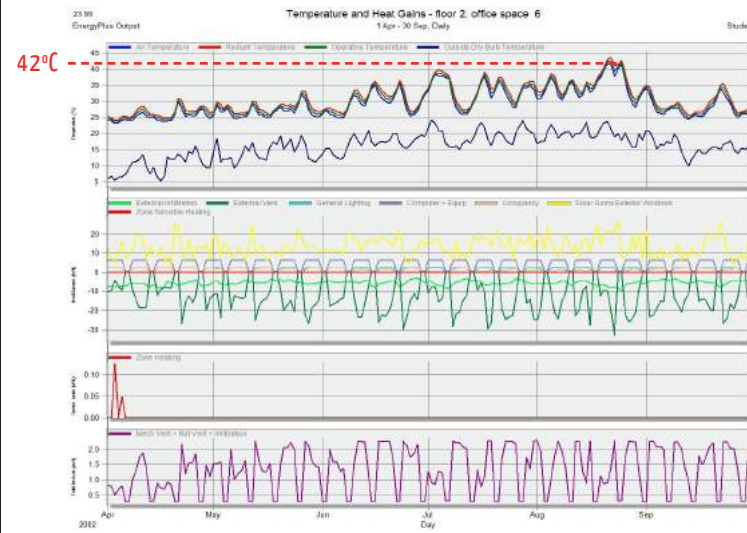


Figure 187: natural ventilation on // 60% shading

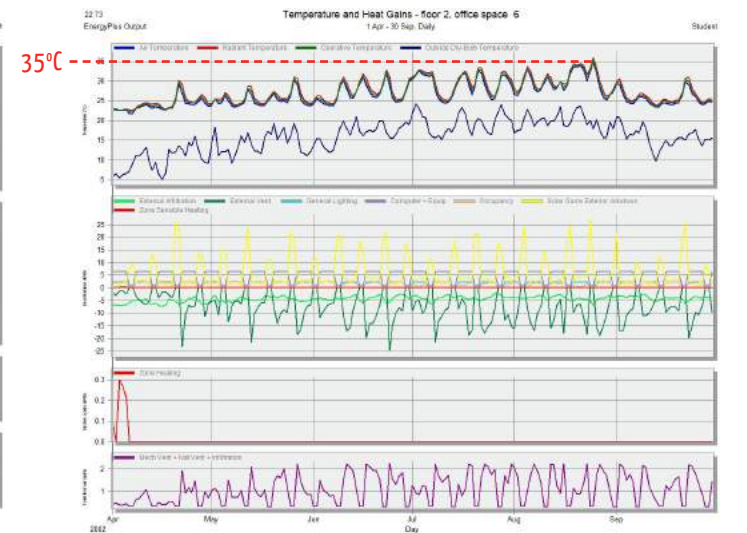


Figure 189: natural ventilation on // 100% shading

conclusions & further steps

Having completed the simulations described in the previous pages, several conclusions can be drawn. First of all, the total energy consumption of the building when both cooling and heating are turned on, without any shading, reaches the **122.45 kWh/m²**, with a number of **284.66 kWh** for district heating and **3156.63 kWh** for district cooling. Subsequently, shading is applied gradually and as the percentage grows higher the value for district heating is increasing, while the one for cooling is decreasing. When the whole window area is shaded (100%) the total energy consumption of the building drops to **88.75 kWh/m²**, which constitutes the **3/4** of the initial value, with a number of **544.06 kWh** (almost doubled) and **1310.77 kWh** (less than half) for district heating and cooling respectively.

Furthermore, when the cooling option is turned off, along with the natural ventilation as the designed façade doesn't provide any, the total energy consumption of the building reaches the **55.08 kWh/m²**, with **269.59 kWh** for cooling. The maximum indoor air temperature that can be found during the summer period is almost **54°C** and occurs on the 24th of August. Once again, with shading this temperature is decreasing with a minimum value of **39°C** on the 25th of August (100% shading). Afterwards, the version of having natural ventilation was investigated, in order to ascertain that in case of having that option, either with further development of this design or with

another façade design, the maximum indoor air temperatures will be lower than without any natural ventilation. Therefore, when natural ventilation is available without any shading, the total energy consumption of the building reaches the **51.25 kWh/m²**, with **93.83 kWh** for cooling, which is about 1/3 of the amount without natural ventilation. Also, the maximum indoor air temperature that can be found during the summer period is around **44°C** and occurs on the 22nd of August. When shading is applied, this number decreases with a minimum value of about **35°C** on the 25th of August (100% shading).

Different percentages of shading were applied for the simulations and it can be concluded that with the increase of shading the total energy consumption of the building is decreased, having the lowest value with 100% shading. However, the visual comfort should be taken into account and therefore the shading cannot obstruct completely the view towards the outside. Thus, an optimal amount for reducing the energy costs and at the same time permitting the visual contact of the users of the building with the outside, would be between 40%-60%, which corresponds to a shading area of **2.52 m²** and **3.78 m²** respectively per façade element.*

As already mentioned before, the HVAC system that was used for the simulations is **Fan Coil Unit (4-Pipe), Air cooled Chiller** (default) and gives the following results: the total energy

consumption of the building when both cooling and heating are turned on, without any shading, is **122.45 kWh/m²**, with a number of **284.66 kWh** for district heating and **3156.63 kWh** for district cooling. Another option to decrease this amount of energy consumption, apart from shading and natural ventilation, is to use a different HVAC system which would be much more efficient. Two simulations was conducted for both 1) a radiator heating, with boiler HV, mechanical ventilation supply and extract system and 2) a VAV, air-cooled chiller, fan-assisted reheat system. They both gave **67.76 kWh/m²** as the total energy consumption, which constitutes almost half of the Fan Coil unit value (122.45 kWh/m²), with **284.66 kWh** and **581.87 kWh** for heating and cooling respectively. This shows that the amount of cooling has been decreased dramatically (1/5 of the Fan Coil result: 3156.63 kWh).

Lastly, another option for the given situation would be to integrate a system that would generate energy and thus compensate for the energy needed for cooling purposes, which is rather important and cannot be ignored in any case.

* shading - surface area correlation:	100% --> 6.3 m ²
(the 100%=6.3 m ² corresponds -in the design- to the surface area of the whole façade element that the cushions cover without the outer frame)	80% --> 5.94 m ²
	60% --> 3.78 m ²
	40% --> 2.52 m ²
	20% --> 1.26 m ²

Such solution would be the integration of PV cells on the outer layer of the inflated membrane cushion. This is possible as technology has been improved towards this direction with the development of PV flexibles (films) that are compatible with membranes and can be easily integrated in them by a roll-to-roll technique that is used in order to place the PV cells in a multi-layer process on the foil. The result is a very thin and lightweight film, which is rather flexible and suitable for integration in membranes structures.

As it has been described already in the first chapter "membrane integrated photovoltaics", p. 26-27, the PV film is embedded between two ETFE foils in order to be protected from mechanical stresses, humidity and weathering. The position of the PV film on the outer layer of a cushion is preferable, as if placed in the middle, it would have limited power output due to refraction and heating effects. The laminated modules do not permit any light transmission though, as they are opaque, but they can be used as shading devices, reducing, thus, the solar heat gains and contributing to the reduction of cooling demands in the summer. For example, the "Flexible Organic Photovoltaic modules" that were mentioned in page 96 would be a nice solution as they are described to be independent from the sun's angle and they are efficient under diffuse light conditions as well.

Several rough calculations are presented here concerning the energy gains from the integration of PV films into the outer layer of the membrane cushions. As mentioned above, they can be used also for shading, while printing their negative pattern onto the middle movable layer in order to control the amount of sunlight that enters the building. So, the area of the PV films will be the same as the shading that was chosen previously, which means they will cover 40-60% of each façade element. For simplification reasons **50% = 3.15 m²** is chosen for the calculations.

energy gains from PV cells

Firstly, the efficiency of the PV flexibles or thin-film solar cells, as they are also called, had to be determined. “*The performance and potential of thin-film materials are high, reaching cell efficiencies of 12–20%*” (wikipedia¹), therefore 16% efficiency is taken into consideration, as it is assumed that the technological improvements will reach this percentage in the near future.

The Global Horizontal Irradiance (GHI) for Paris is **4.43 kWh/m²/day**,² so for the whole year it would be $4.43 \times 365 = 1617$ **kWh/m²/year**, which is the total amount of the solar radiation that is perceived per unit area by a surface that is always positioned in a horizontal direction³. However, a reduction

factor should be applied to this values, as the angle of the façade element in relation to the sun’s angle, as well as its orientation have a significant impact on the performance of the PV cells.

According to the orientation the reduction factors⁴ are the following (see table in the Appendix C):

South-West façade: 0.68
South-East façade: 0.66
North-West façade: 0.36
North-East façade: 0.36

And the corresponding solar radiation values that falls on each façade surface are:

South-West façade: 1617 x 0.68 = 1100 kWh/m²/year
South-East façade: 1617 x 0.66 = 1067 kWh/m²/year
North-West façade: 1617 x 0.36 = 582 kWh/m²/year
North-East façade: 1617 x 0.36 = 582 kWh/m²/year

sources:

1. https://en.wikipedia.org/wiki/Thin-film_solar_cell#Efficiencies
- 2,3. <https://solarenergylocal.com/states/arkansas/paris/>
4. <http://www.alforte.org/media/doc/NRG-systems/zonnepaneel%20reductie.pdf>

So, according to the efficiency of the PV films (16%) the energy gains for each façade surface are:

South-West façade: 1100 x 0.16 = 176 kWh/m²/year
South-East façade: 1067 x 0.16 = 170.7 kWh/m²/year
North-West façade: 582 x 0.16 = 93.1 kWh/m²/year
North-East façade: 582 x 0.16 = 93.1 kWh/m²/year

The next step is to multiply these results with the total surface area that the PV films will cover on every façade. The floor plan of the building is a rectangle of 41x53m=2173m² with 45 floors above the ground and with 40-60% coverage the total surface area for the PV films is calculated at 2271m² for the South-West and North-East and for the South-East and North-West at 2920m².

Therefore, the energy gains for the whole façade are:

South-West façade: 176 x 2271.36 = 399759 kWh/year
South-East façade: 170.7 x 2920.32 = 498489 kWh/year
North-West façade: 93.1 x 2920.32 = 271882 kWh/year
North-East façade: 93.1 x 2271.36 = 211464 kWh/year

giving a total number of **1.38 GWh/year** annual energy gains from integrated PV films in the façade for the whole building.

The last step would be to compare this result with the energy consumption values calculated from the Design Builder. The annual energy consumption with the default HVAC system, having both heating and cooling on, with 40% and 60% shading is **112.36 kWh/m²** and **105.97 kWh/m²** respectively. If we multiply these number with the total floor area of 45 floors (2173x45=97785m²) we get **10.99 GWh/year** (40% shading) and **10.36 GWh/year** (60% shading). The annual energy gains from the PV films calculated above constitute approximately the **1/10** of both consumption values.

If we consider now a more efficient HVAC system as mentioned before, the annual energy consumption becomes **67.76 kWh/m²**, with **60.984 kWh/m²** for 40% shading and **40.656 kWh/m²** for 60% shading. Multiplying again these numbers with the total floor area we get **5.96 GWh/year** (40% shading) and **3.98 GWh/year** (60% shading). The annual energy gains from PV films cover **23%** of the total energy consumption for the first case and **34%** for the second one.

7

AREVA

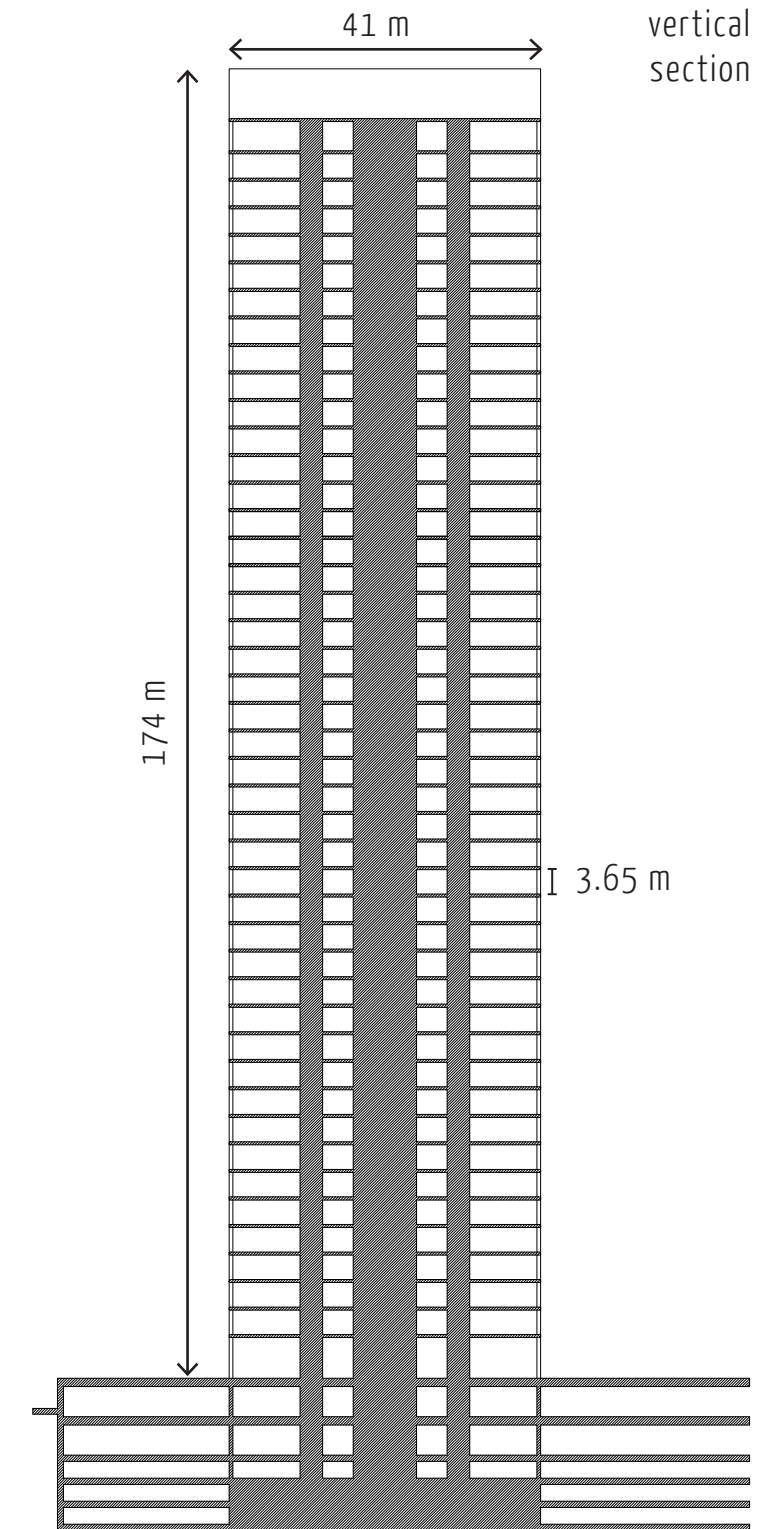
case study

tour areva

La Défense, Paris

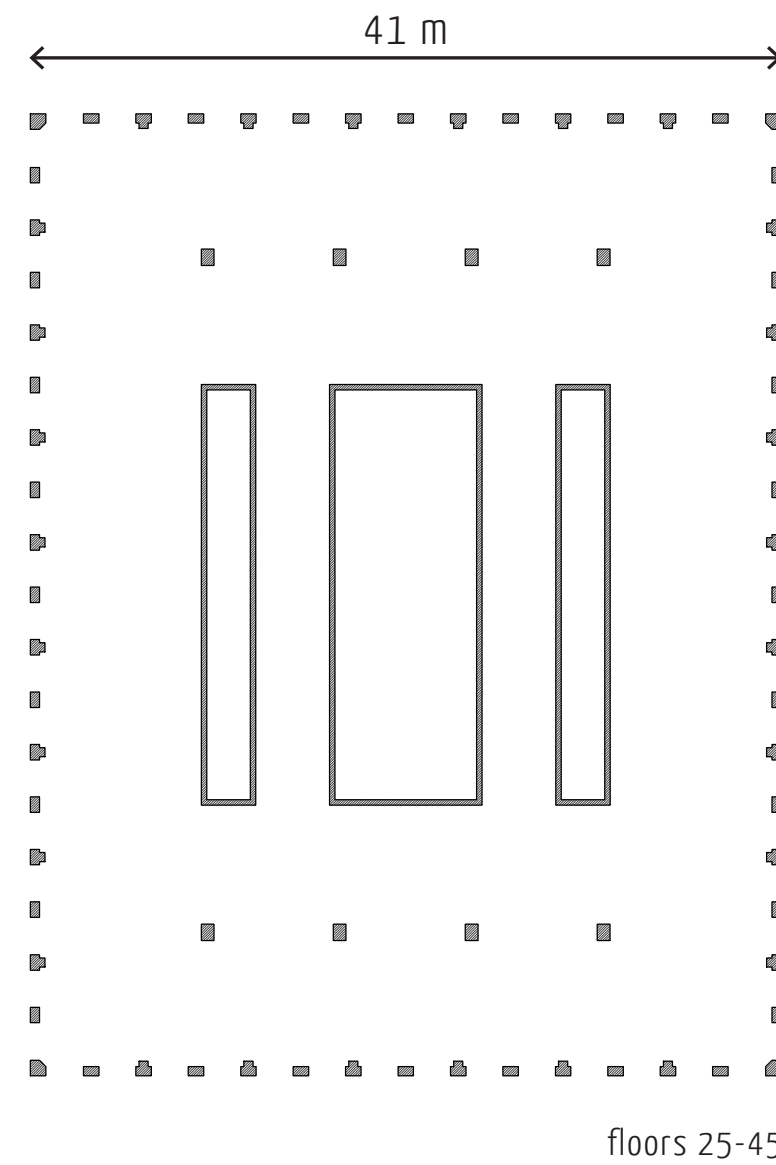
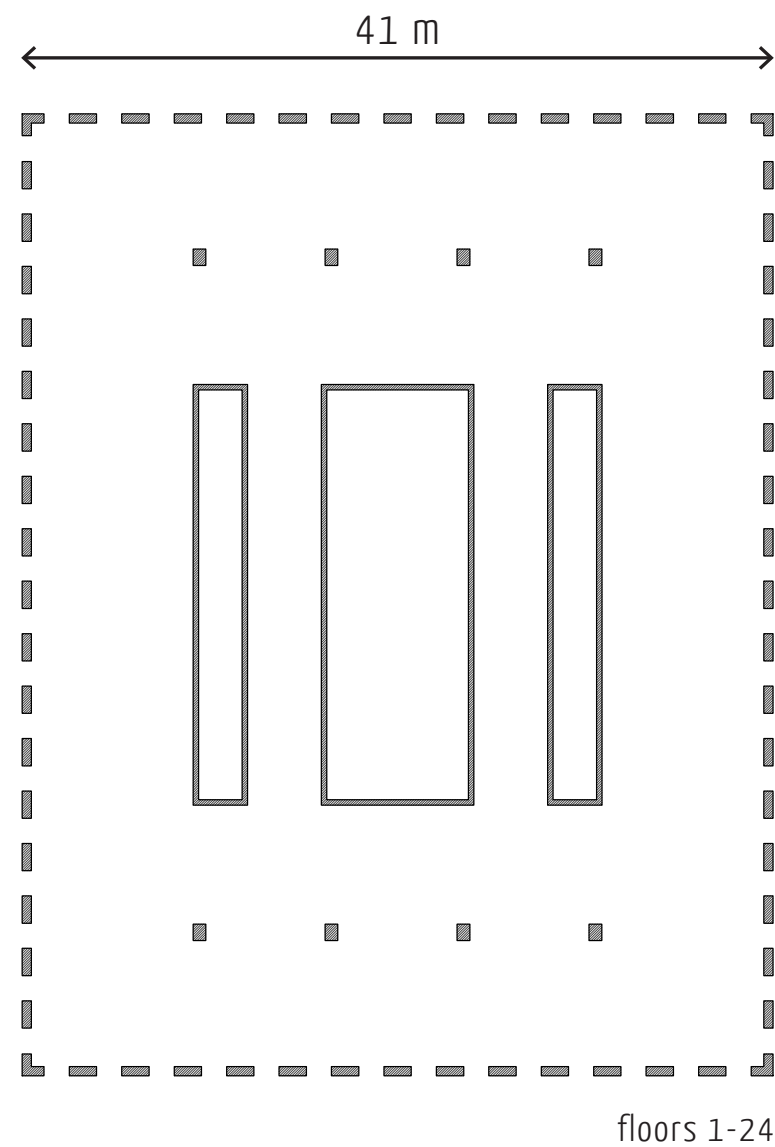
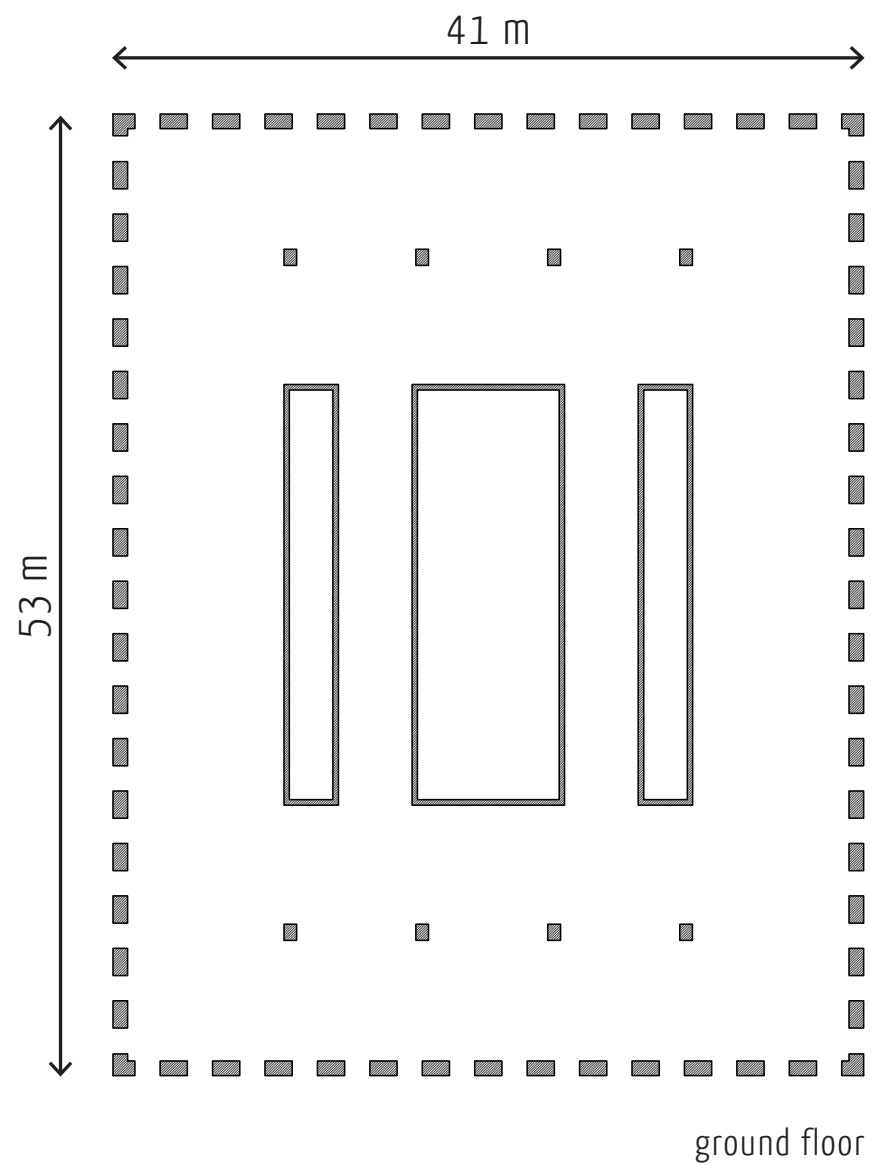
architects:	Roger Saubot, François Jullien and Skidmore, Owings & Merrill LLP
built:	1974
height:	174m from the ground floor
number of floors:	45 + 5 underground
ground floor surface:	53 x 41 m
structural material:	concrete
façade material:	granite cladding
façade system:	curtain wall
function:	offices / open-plan floor

The building that was chosen as a case study is situated in Paris, France and more specifically in the area of La Défense. It was built in 1974 by the collaboration of several architects (Roger Saubot, François Jullien and Skidmore, Owings & Merrill LLP) and constitutes an office building. Its total height reaches the 174m from the ground floor including 45 floors (each 3.65m high) and five underground levels. Its footprint is $53 \times 41 = 2173 \text{ m}^2$ and it has an open-plan floor organisation. The main structural material is concrete and granite cladding has been used for the façade that constitutes a standard curtain wall system. As it can be seen from the floor plans in the next pages, the structural system consists of a central concrete core and structural concrete elements are included in the façade as well. These elements become slenderer and the fixed windows taller, while going higher towards the top.



tour areva

La Défense, Paris





final design

position of the new façade

As it was mentioned before and it can also be seen from the floor plans, there are concrete structural elements in the façade of the existing building. Therefore, the question that was immediately generated was where the new membrane façade would be placed in relation to the old one. One option was to place it inside the existing openings, but then the rest of the façade elements should also be taken into account, in terms of thermal and acoustical insulation and water and airtightness as well. The other option was to place it in front of the existing one, so as to surround the whole building and thus the challenge would be to design a completely new façade consisting of membrane systems. The latter option was chosen (figure 190) as the purpose was to design a building envelope consisting exclusively out of membrane cushions.

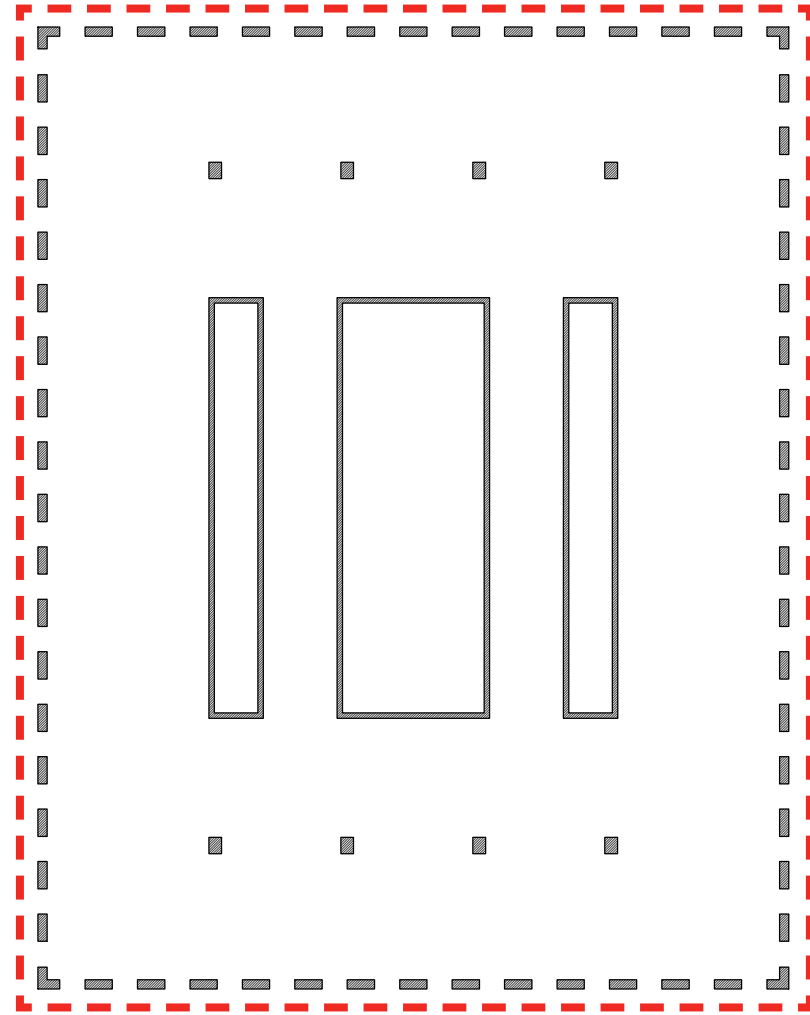


Figure 190: position of the new façade in relation to the existing building

design experiments

shape // patterns

The first step of the design process was to determine the pattern of the new façade, the grid that would be followed, the shading system's shape. In the beginning, a diagrid structure was investigated in order to create identical smaller cushions in between the structural elements that expand along the whole height of the building (in smaller parts of course but giving the impression of continuity). This option gives a

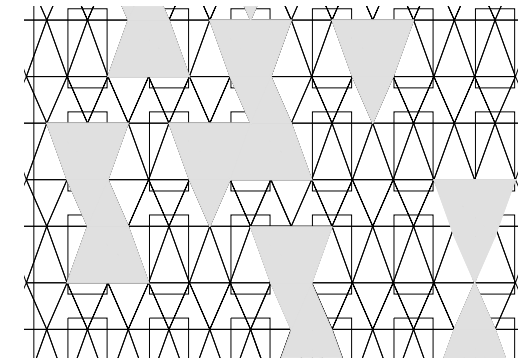


Figure 191: diagrid system and triangular shading layers

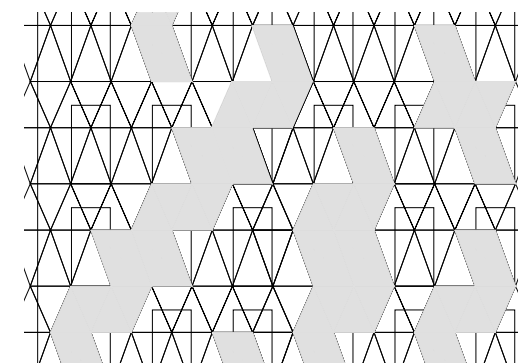


Figure 192: diagrid system and shading layers in irregular shapes

completely different result from the rectangular grid of the existing building and therefore it would be preferable to be placed in some distance from it, as the load-bearing concrete elements are really present and evident in the old façade. That creates new issues, such as how big this distance should be and what this new created space would be, in terms of use and function. Here, certain shapes and patterns are presented.

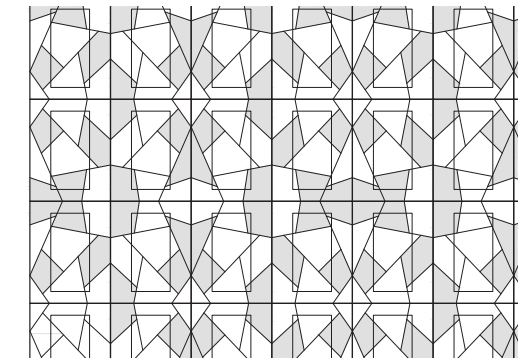


Figure 193: rectangular grid and cushions in irregular shapes

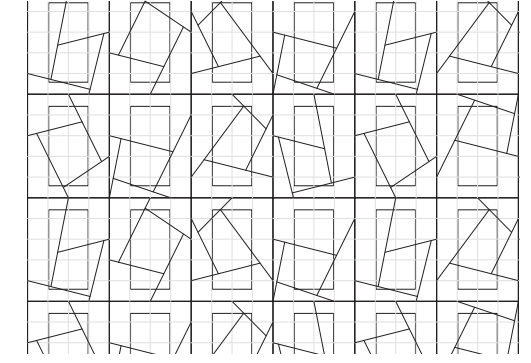


Figure 194: rectangular grid and cushions in irregular shapes

physical models

Subsequently, the grid of the existing façade was chosen to be explored. With this version the main structural elements would follow the rectangular arrangement of the concrete elements and inside this frame either a rectangular or a more irregular and random pattern would be followed to form the membrane cushions. Once again, the question about the

distance that should be given between the existing and the new façade and the space that was created in between had to be answered as well. At this point, several physical models were constructed in order to experiment in a more “realistic” context.

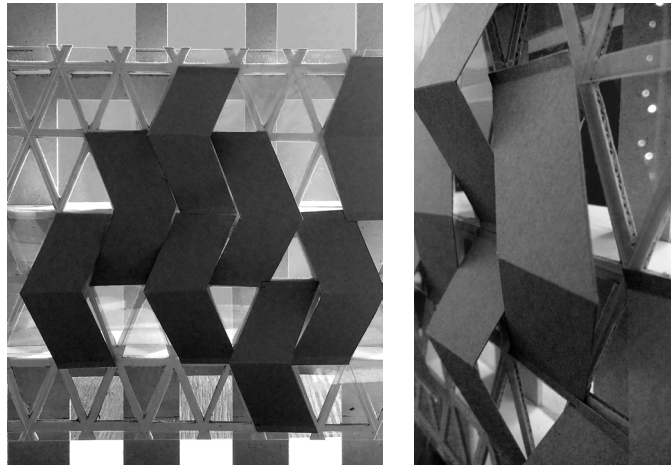


Figure 195: diagrid system

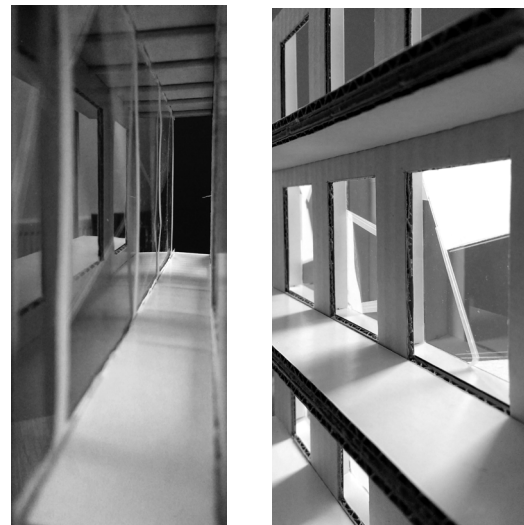


Figure 196: rectangular system

vacuum experiments

The next step was to experiment with the vacuum system since it was the less comprehensible, in the sense that it couldn't be easily neither imagined, nor predicted. Therefore, several experiments were made with a vacuum bag for storing clothes and a vacuum cleaner. Firstly, a big opening was tested but since the frame was not thick enough the two membrane

sides touched immediately one another. Next, some spacers were used and later on the opening was reduced to half. The spacers helped the sides not to touch but as the pressure was becoming lower the tension was higher until the bag was finally torn. Further research is needed for the integration of spacers into the vacuum element, which is elaborated later on.

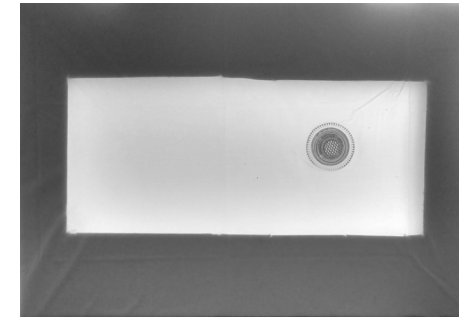


Figure 197: without spacers

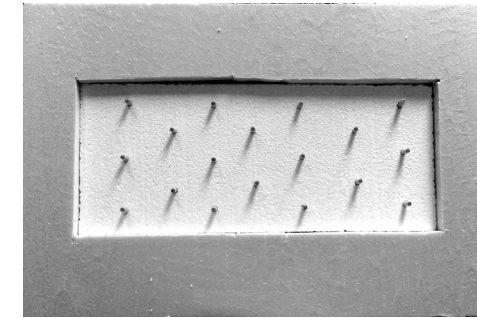


Figure 198: with spacers

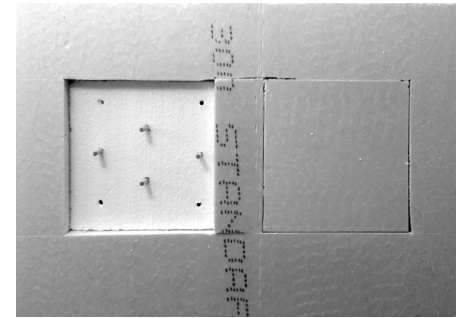


Figure 199: smaller opening with spacers

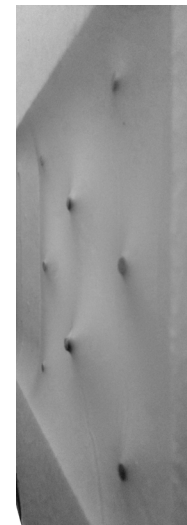


Figure 200: with spacers



Figure 201: with spacers and lower air pressure



Figure 202: with less spacers

design concept

Having completed the already described experiments the final design had to be defined. So, the concept that was chosen follows the orthogonal grid of the existing façade. More specifically, a rectangular stiff “wide” frame (aluminum or steel) surrounds various membrane cushions, whose frame is thinner and less “heavy” than the outer one. Furthermore, each façade element consists of both transparent and translucent parts depending on the insulation material (argon=transparent, aerogel=translucent) and the existence or absence of shading.

As far as the shading system is concerned, the outer layer of the inflated cushion (and of the whole component) is printed with a pattern, whose negative is printed in the middle layer of the same cushion. Therefore, by inflating and deflating the two air chambers alternately, the middle layer can move forwards and backwards. Thus, when the two patterns coincide the light transmission is blocked, otherwise light is permitted into the interior space (figure 204). Another alternative would be to integrate PV films into the outer layer with a specific pattern and to print its negative on the middle layer and follow the same logic as before.

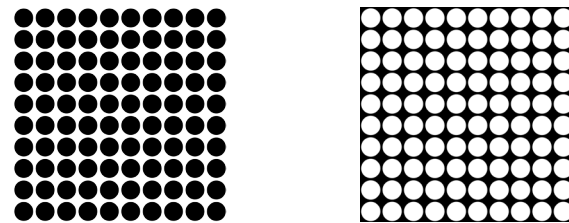
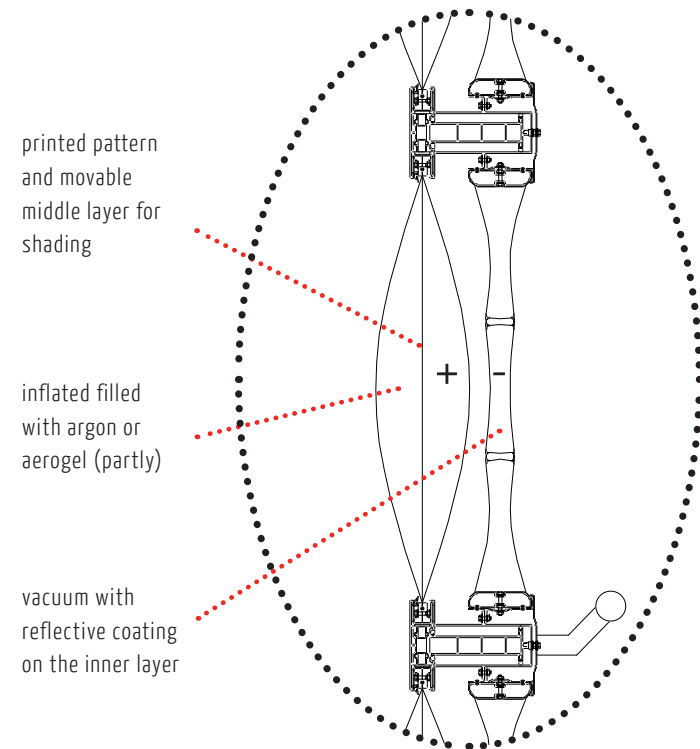


Figure 203: example of positive and negative printed pattern

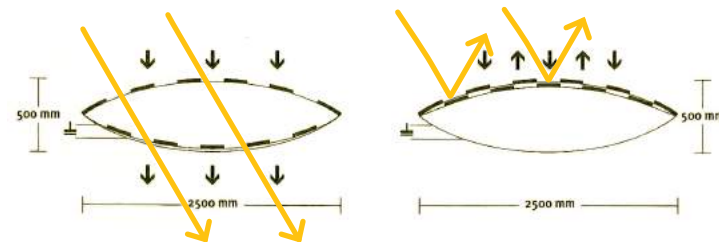


Figure 204: printed pattern on the outer and the movable middle layer for shading

inflated cushion

The inflated cushions consist of a 3-layers membrane system, whose cavities are independent from each other. The two outer layers of each cushion is from 300µm (0.3mm) thick ETFE foil and the middle layer has a thickness of 100µm (0.1mm). The reason for this is the fact that the outer layer is exposed to bigger loads (rain, wind, snow) and thus higher forces are developed onto its surface. On the contrary, the inner layer is subjected to a lower prestress and has a minimum contribution to the total carrying loads (Knippers, 2011).

As examined before in the building physics chapter, multi-layer cushions offer the possibility of improving the thermal insulation of the system as more air cavities are created. Furthermore, the shading system that is chosen requires independent pressure control of the two air chambers in order to achieve the movable middle layer. More specifically, by inflating the inner chamber and deflating the outer one the middle layer moves towards the outer membrane and therefore the two printed patterns coincide with each other blocking the light transmission. Following exactly the opposite procedure, light is permitted into the building. Hence, independent pipes' systems must be installed for the inflation/deflation of the two air chambers.

pressure level

As far as the pressure level is concerned, under normal circumstances (no storms, extreme wind etc.) it must be maintained at a constant situation of approximately 220 Pa. However, leaks are unavoidable due to the material itself, the joints (welded seams and edges) and the air supply connections. Therefore, the internal pressure must be controlled and adjusted constantly to compensate for the air losses (Knippers, 2011).

air supply systems

The air supply systems are not only used for inflating the cushions and maintaining the desired pressure, but also to ensure that the air inside the cushions is dry. Otherwise, condensation might occur and algae might grow. Therefore, filtering the air is necessary to avoid dust and dirt as well. The inflation units consist of a filter, a fan/compressor and a condenser drier or a dehumidification unit with a heating battery. Dehumidifying the air leads to a remarkable reduction of the energy consumption of the air supply system (Knippers, 2011).

There are two ways of arranging the pipes that connect the cushions to the inflation units: in a series or parallel (figure 205). The parallel system ensures a constant pressure level in all the cushions and in case of damage each cushion can be replaced independently without interfering with the rest. Moreover, the installation of a return air system leads to a bigger reduction of the energy consumption, as the dehumidification of the air is happening only when it is activated by the help of sensors.

A single inflation unit can support about 1000m² of ETFE cushions¹. So, as the total surface area of all the four façades of the Tour Areva is 10383m², it means that approximately 10 inflation units are needed. A standard size of an inflation unit is 1.20 x 1.20 x 0.90m (Architen Landrell).

As for the pipes' sizes, a common supply pipe has a diameter of 100-150mm and the branches 40-50mm. For maintaining the air pressure very small hose diameters of 10-20mm are suitable. Hoses from elastic polymers are preferred, such as ETFE hoses, because they need to resist UV radiation. Transparent PUR hoses with steel convolutions are commonly used (Knippers, 2011).

In addition, the width of each cushion is usually the 1/5 of the span (length)³. Lastly, the chosen material for the frame of the cushions is FRP because the idea is to have a lightweight inflated cushion as a whole that will be placed inside a "heavier" and bigger aluminum frame.

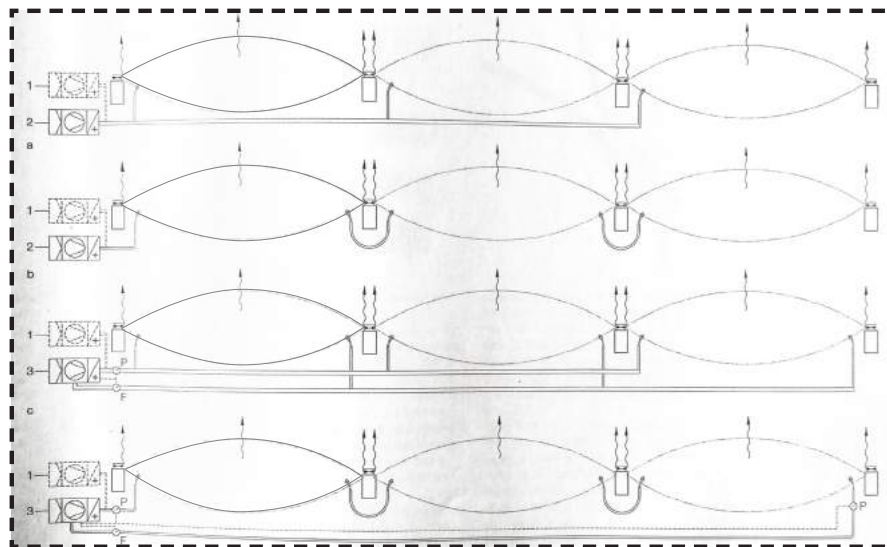


Figure 205: Air supply systems with parallel (a), series (b), return air & parallel (c), return air & series (d) connections

1. Backup supply
2. Primary air supply / filter / inflation unit / dehumidifier
3. Return air system with sensors (P = sensor for air pressure, F = sensor for humidity)

sources:

1. Bessey, R.P., 2012, Structural Design of Flexible ETFE Atrium Enclosures Using a Cable-Spring Support System, Brigham Young University - Provo, Master of Science thesis, page 24
2. <http://www.architen.com/articles/etfe-foil-a-guide-to-design/>
3. Watts, A., 2014, Modern Construction Envelopes, Birkhäuser

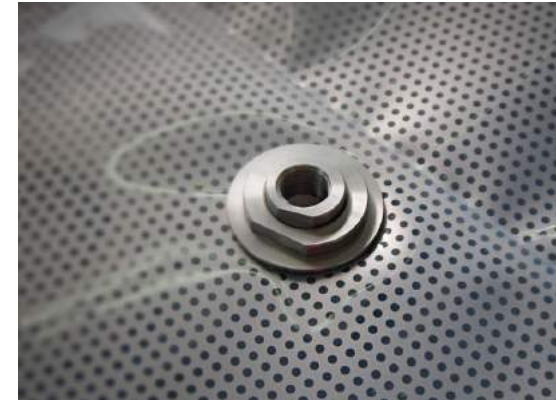


Figure 206: steel detail connection of ETFE cushion with pipes

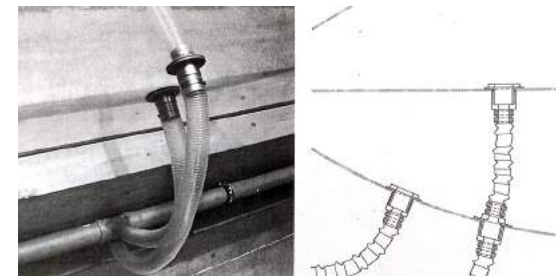


Figure 207: plastic hoses and steel convolutions of ETFE cushion

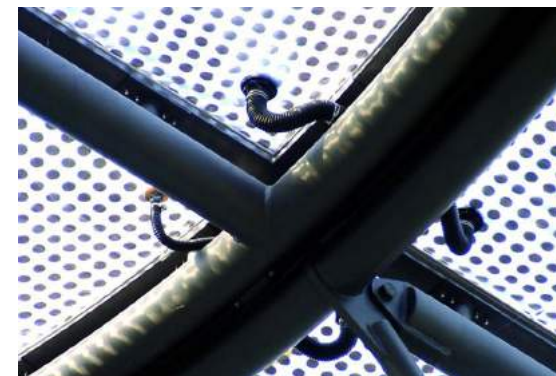


Figure 208: pipes and branches of an air supply system to ETFE cushions

vacuum system

The second component of the façade element consists of a vacuum system. A deflated unit has still a lot of potential for further development. The "deflateables" belong in the category of pneumatic constructions. As "vacuum" can be defined the absence of air, which impossible to be achieved in practice due to the very strong forces that are developed and the unavoidable leaks. So, it can be used for spaces having lower pressure than the atmospheric one (1 bar).

The vacuum system can have various advantages in the building technology field (Knaack, U., Klein, T., Bilow, M., 2008, p. 20):

- » The absence of air inhibits convection
- » The absence of air reduces the transfer of sound waves
- » The absence of air can have a impact on the acoustical performance of the vacuum unit

According to the pressure level there are four categories of vacuum:

- » Low or coarse vacuum (1 bar=atmospheric pressure to 10⁻³ bar)
- » Medium or fine vacuum (10⁻³ to 10⁻⁶ bar)
- » High vacuum (10⁻⁶ to 10⁻¹⁰ bar)
- » Ultra-high vacuum (less that 10⁻¹⁰ bar)

In the case of the designed façade element, a low vacuum is used of 10^{-1} bar (10^4 Pa). The element consists of two layers of 300µm (0.3mm) ETFE foil and several spacers in between them that are responsible for keeping the two membranes from touching each other. An elaboration on the spacers will be made later on.

physical properties of the vacuum

thermal behaviour

As it is known from building physics, heat transfer occurs through three ways: convection, conduction and radiation. The vacuum system has an impact on most of these and therefore it has also an impact on the transfer of the thermal energy.

convection

Convection characterises heat transfer through the flow of a liquid or a gaseous medium. In case of vacuum, where ideally there is no air and thus no medium, heat convection cannot occur. As mentioned before, though, absolute vacuum cannot be achieved, so even in a low vacuum situation less air exists and hence less heat transfer though convection is happening.

conduction

Heat transfer through conduction takes place by means of direct, successive collisions between molecules within a medium or between mediums in direct physical contact. The level of conduction depends on the type of the material and

its physical state (solid, liquid, gas). Gases are not good conductors as the distance between their molecules is bigger and thus fewer collisions occur and consequently less heat transfer by conduction. As far as air cavities are concerned, the wider the cavity the less the thermal conduction (figure 209) (Knaack, U., Klein, T., Bilow, M., 2008, p. 25).

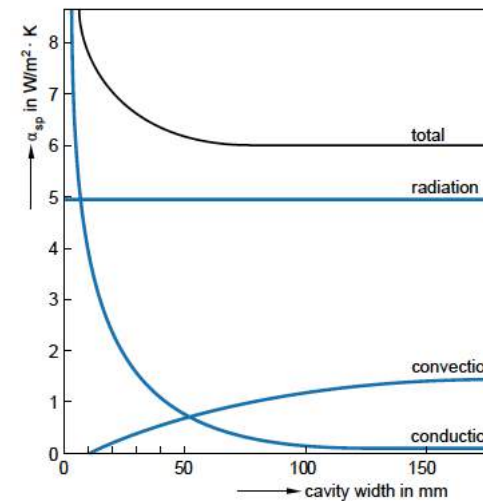


Figure 209: Heat transport through vertical air cavities through conduction, radiation and convection, depending on width of cavity: approximate indication of transfer coefficient a_{sp} (source: van der Linden, A.J., *Bouwfysica - Engels, Chapter 1. Heat, heat transport, thermal insulation, p. 7*)

sources:

1. Knaack, U., Klein, T., Bilow, M., (2008), *Deflateables*, Rotterdam, 010 Publishers
2. Vries, the J.E. (2011). Triple-layer membrane structures Sound insulation performance and practical solutions (Master Thesis TU Delft)

radiation

Radiation is the heat transfer through electromagnetic radiation and therefore no medium is needed for this to occur. As described previously in the building physics chapter, a way to reduce the heat transfer through radiation is the application of reflective coatings with low emissivity values on one or both sides of the cavity. So, the vacuum has absolutely no effect on the radiation passing through it.

acoustic behaviour

As for the acoustic behaviour of a vacuum system, it is known that sound needs a medium to be transmitted, since it constitutes a wave motion or vibration, and once again collisions between the molecules need to occur. In the ideal vacuum there is no air, thus no collisions are happening and consequently no sound can be transmitted.

For all these reasons mentioned above, the vacuum system was chosen as part of the façade element design mostly because of its acoustic insulation properties. Unfortunately, as described in the building physics chapter, the first physical model failed before the acoustic test and the second attempt was incomplete, as the desired pressure level was not reached, so it cannot be proved in practice, at least at this point.

As a cavity width a minimum of 50mm is chosen because as

it is shown in the figure 209 the wider the cavity the less conduction occurs. Also, the forces in the vacuum system are very high so the membranes have to be kept in a minimum distance from each other in order not to touch.

Moreover, the frame that is used to hold the membranes in place is again FRP, like in the inflated cushions, in order to sustain the idea of having lightweight cushions. However, the thickness of the cross section of the frame in the vacuum system is bigger than the inflated cushions because of the really high forces that are developed.

Lastly, the pipes' size that are used in the vacuum element is smaller than those for the cushions. A diameter of about 10mm is used in the designed element.



Figure 210: vacuum façade physical model (source: Knaack, U., Klein, T., Bilow, M., (2008), *Deflateables*, Rotterdam, 010 Publishers, p. 30)

façade patterns

The next step was to define the design and shape of the façade element. As mentioned before, the concept that was chosen follows the orthogonal grid of the existing façade. The goal was to have a rectangular stiff “wide” frame and on the inside various membrane cushions, whose frame would be thinner and less “heavy” than the outer one. Furthermore, each façade element consists of both transparent and translucent parts depending on either the insulation material (argon=transparent, aerogel=translucent) and/or the existence or absence of shading. Two options were examined, as shown in the following schemes, one with the cushions following the rectangular grid as well and one with a more irregular pattern for the cushions. Based on personal preference, the second option was chosen to be developed further.

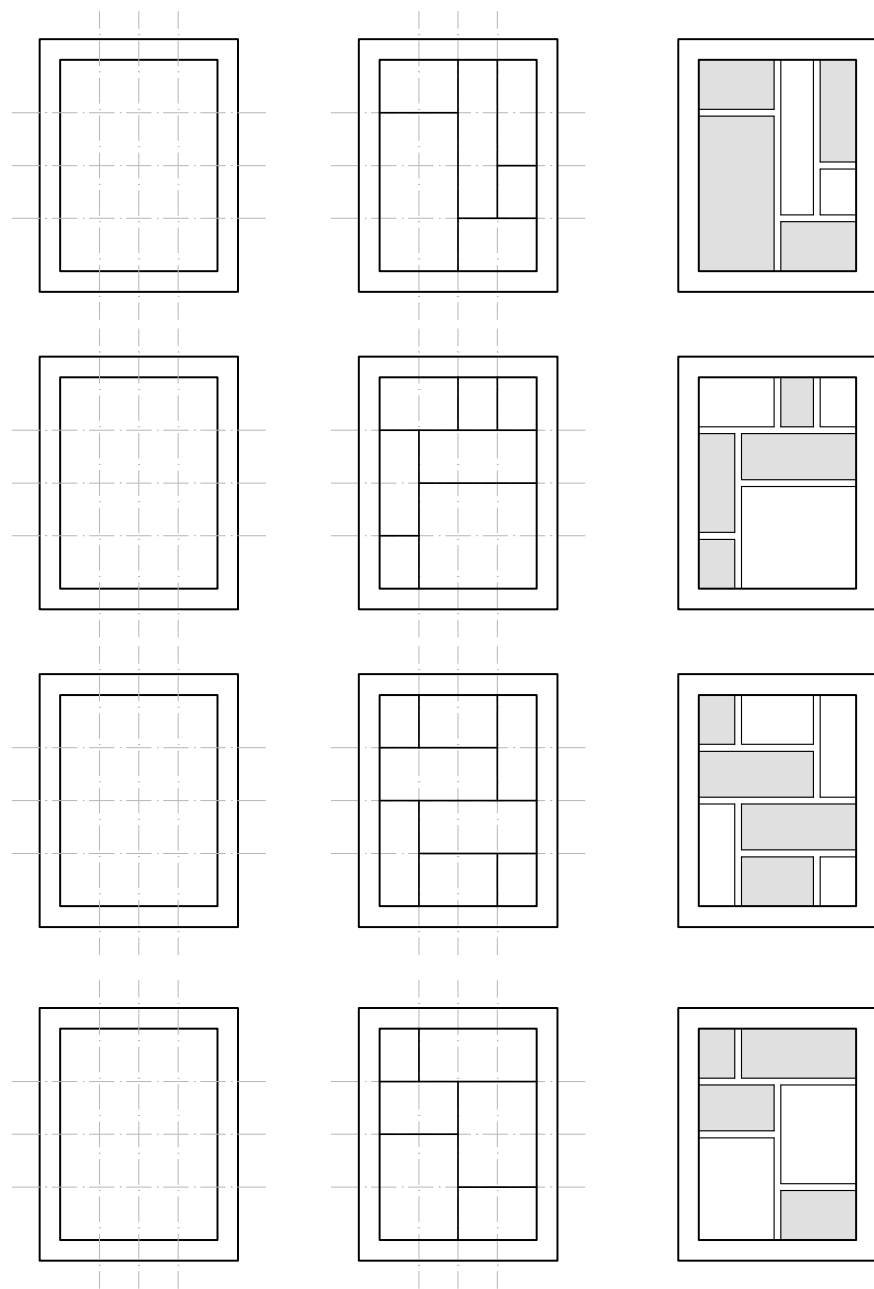


Figure 211: outer rectangular frame and inner rectangular pattern of cushions

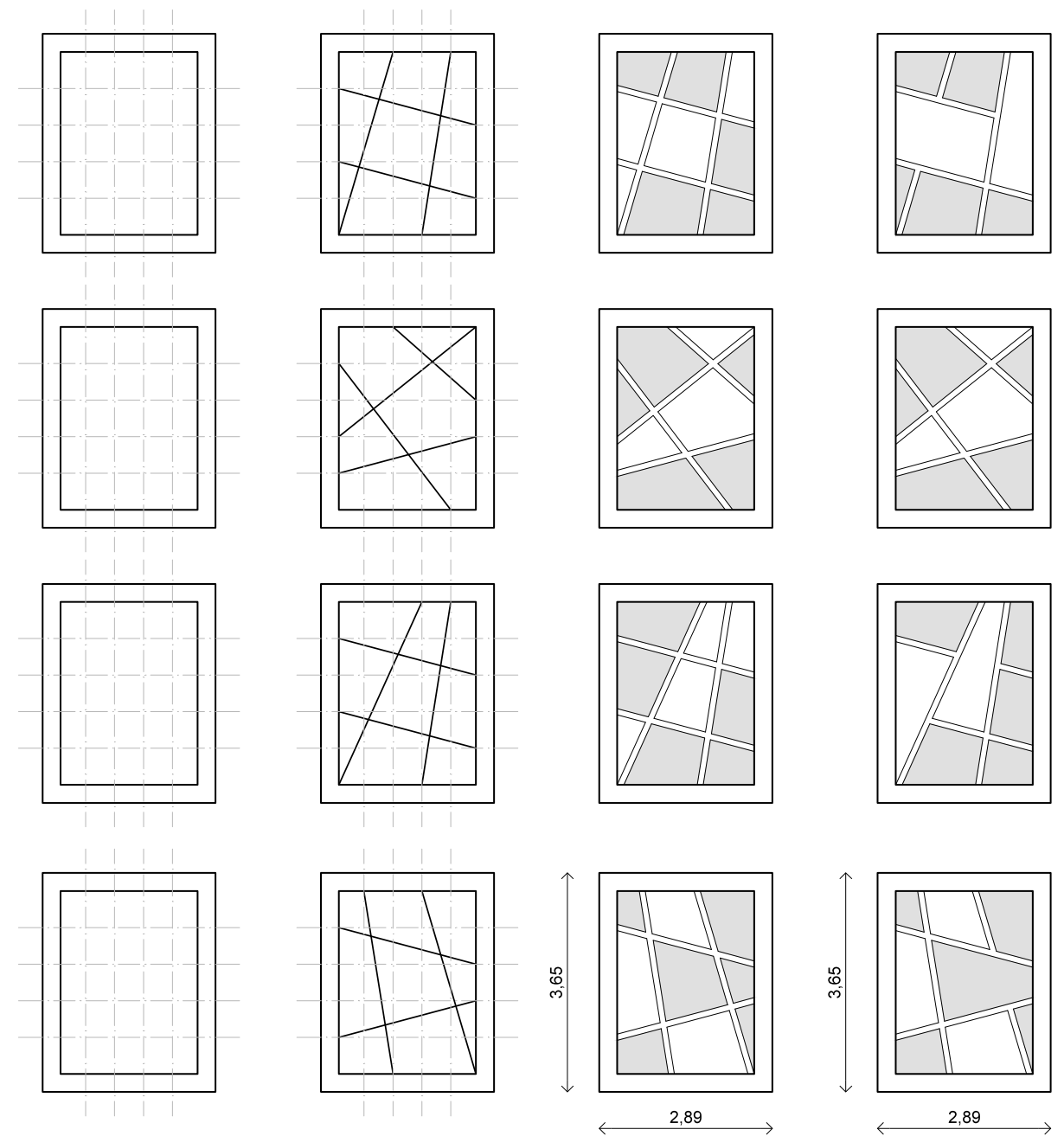


Figure 212: outer rectangular frame and inner irregular pattern of cushions

façade configurations

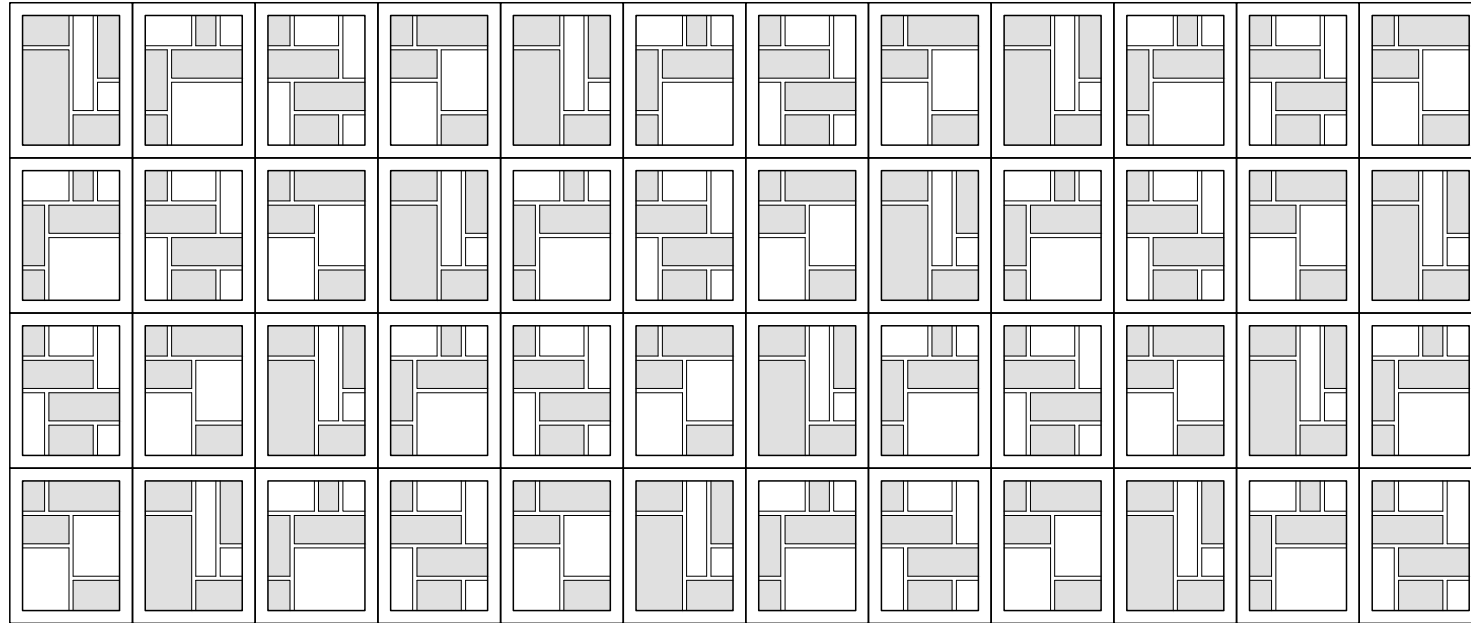


Figure 213: façade configuration 1 (regular cushions' grid)

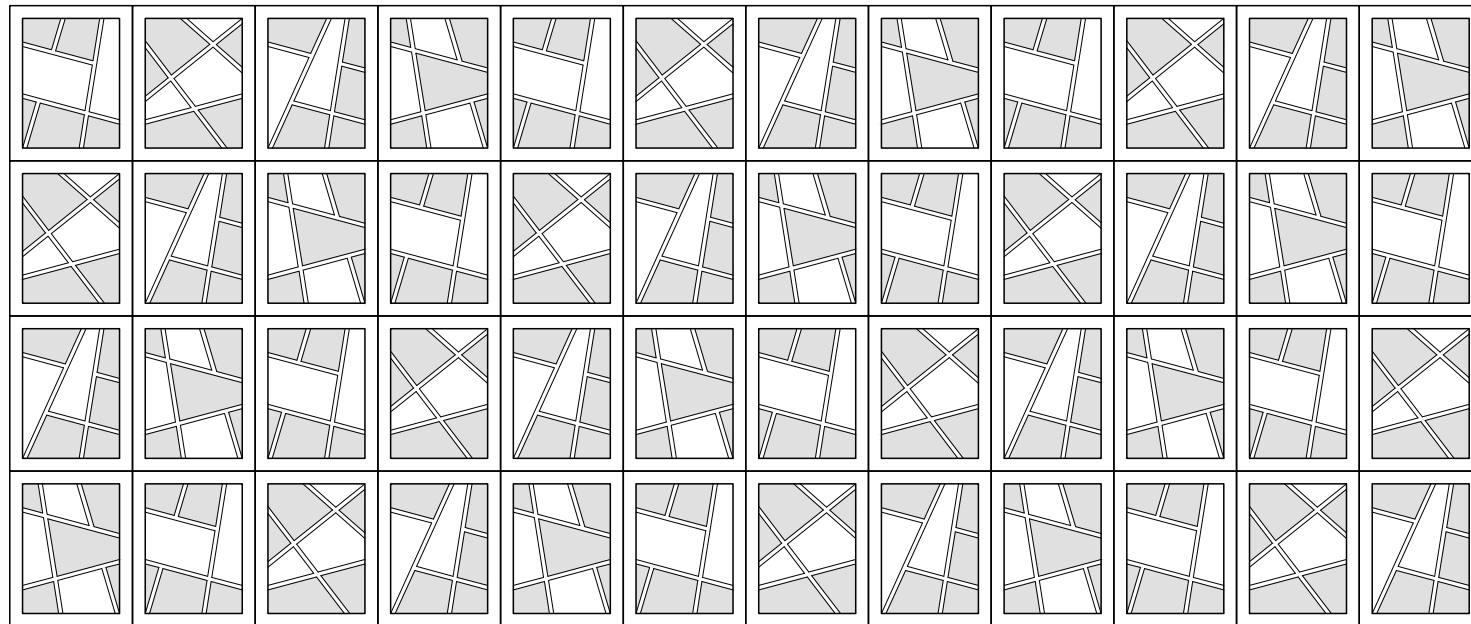


Figure 214: façade configuration 2 (irregular cushions' grid)

indicative elevations

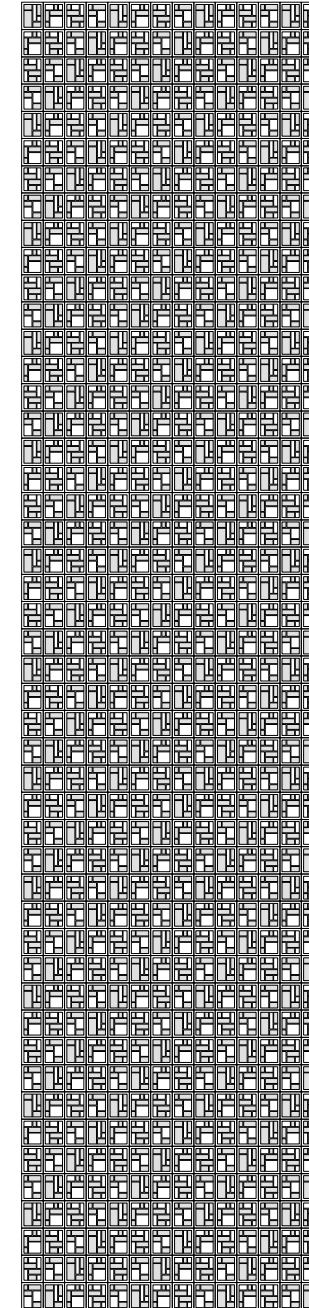


Figure 215: façade configuration 1 (regular cushions' grid)

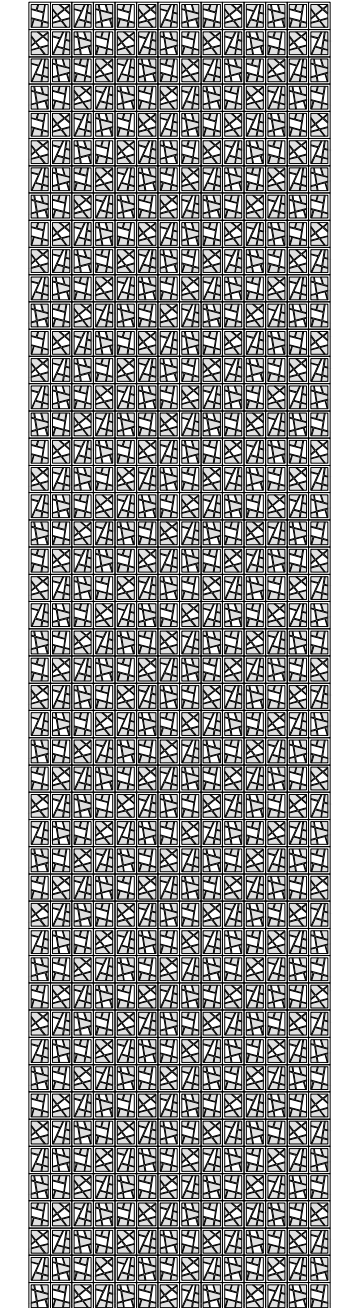


Figure 216: façade configuration 2 (irregular cushions' grid)

sections 1.50

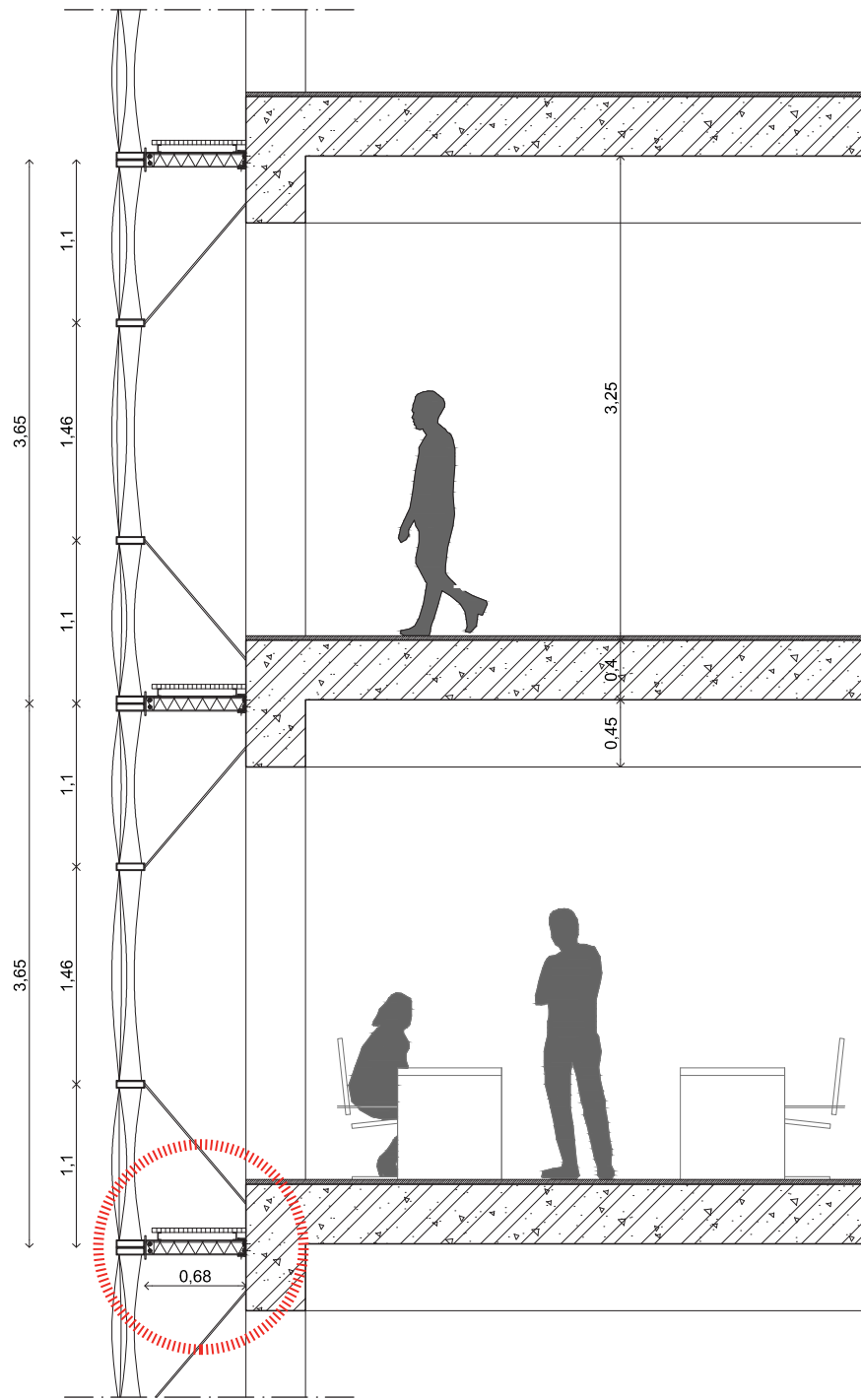
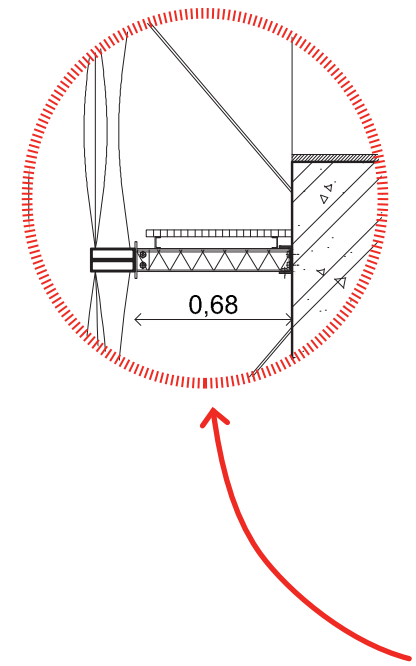


Figure 217: vertical section
1.50_version 1

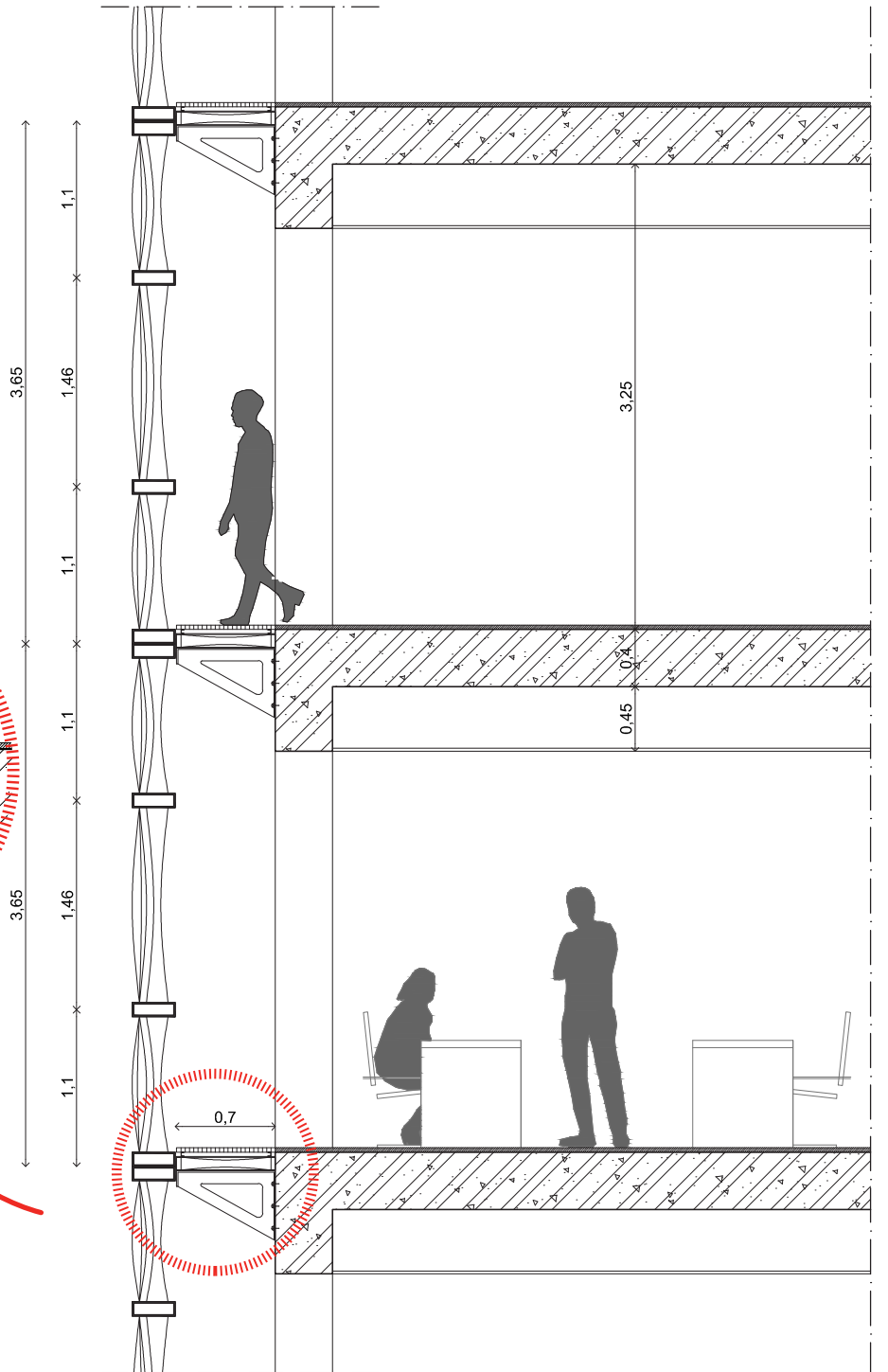
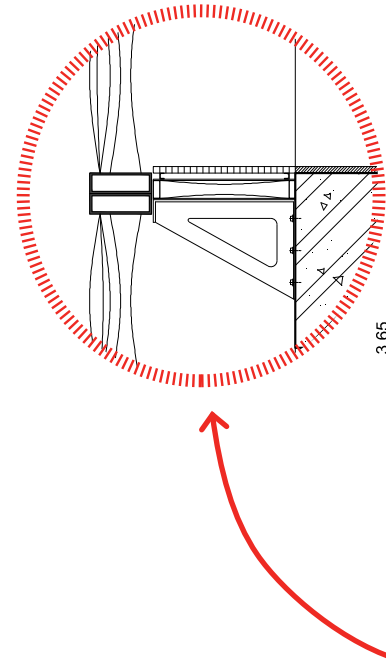


Figure 218: vertical section 1.50_version 2
(horizontally placed vacuum cushions in
between the floors)

sections 1.50

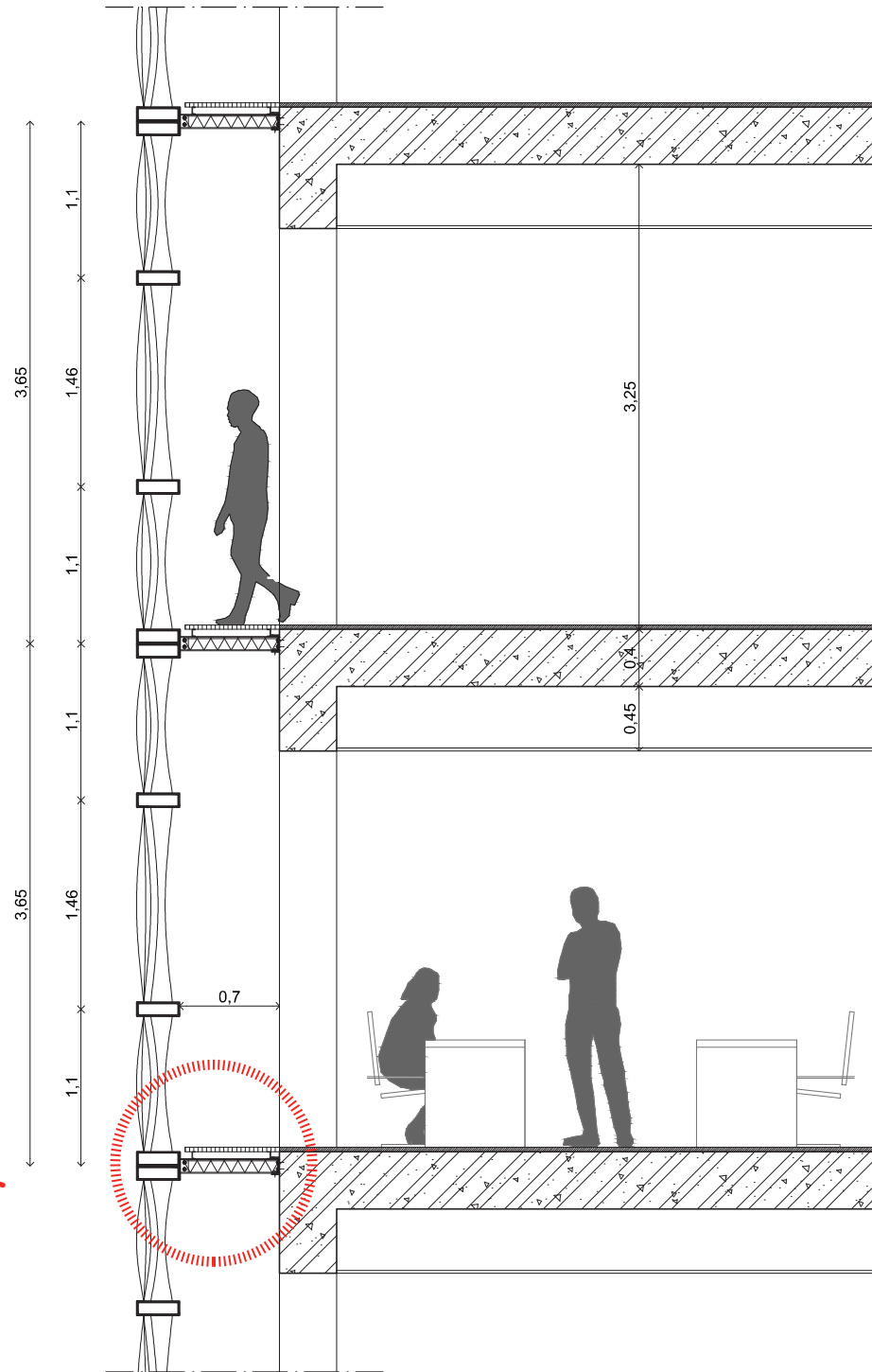


Figure 219: vertical section
1.50_version 3 (bigger frames)

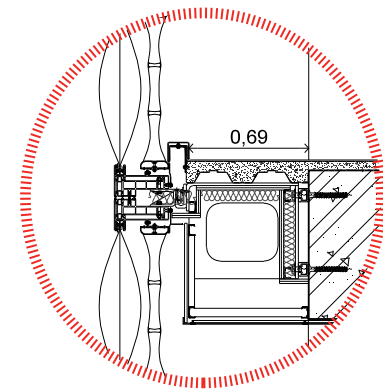
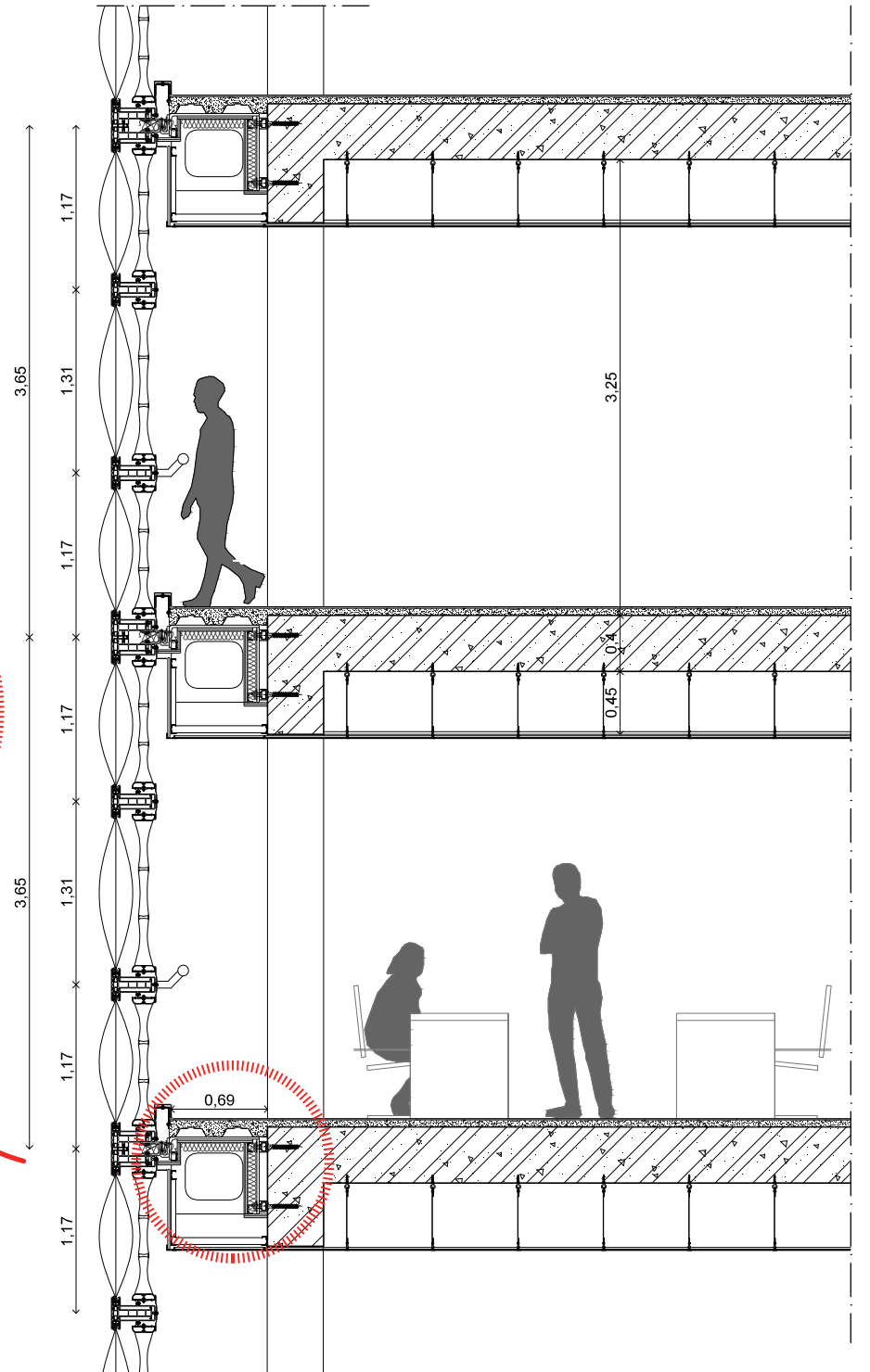


Figure 220: vertical section
1.50_final version



structural concept

The façade element described before spans from floor to floor and its dimensions are 2.90m (width) x 3.65m (height) (figure 221). It consists of two elements placed one behind the other, the inflated cushion and the vacuum system. The separate cushions vary in shape and size (from 0.6 to 2m.). The whole component is already pre-fabricated in the factory in order to save construction time and to ensure that the façade requirements are met, in terms of watertightness, airtightness and thermal bridges. Therefore, when the elements arrive on site they are ready to be assembled. The panels are suspended from their upper part and connected in their lower part, so the assembly process starts from the bottom to the top.

As far as the cushions are concerned, the inflated one consists of three layers of ETFE that are clamped together at the same point with a PVC keder and a clamping bar and then it is placed into a FRP frame all around. The vacuum, on the other hand, consists of an already sealed bag (welded), whose edges are rolled around a PVC keder. The whole bag is first placed around a FRP frame and then its edges are clamped with an additional cap (figures 223-224).

As for the air supply system, each inflated cushion needs two pipes for its two air chambers and the vacuum only one. So, three pipes are necessary in total for both elements. Since all the cushions are immediately connected with the outer frame all the tubes are guided inside it to end up to the upper corner, where the installations are placed and from there they can be guided further away to the pumps (figure 222).

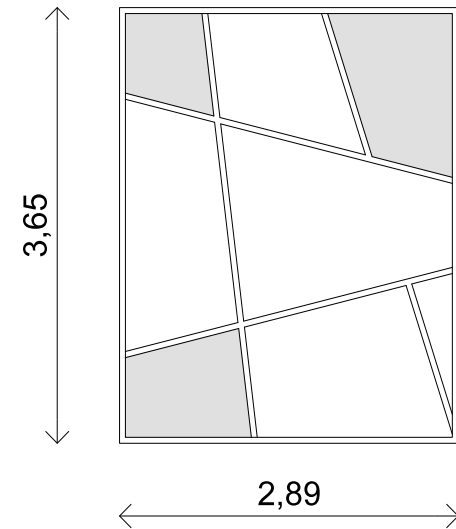


Figure 221: individual element

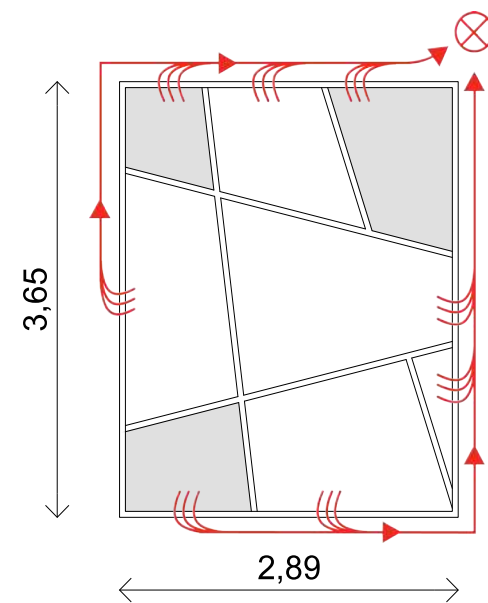


Figure 222: pipes system diagram

inflated cushion assembly

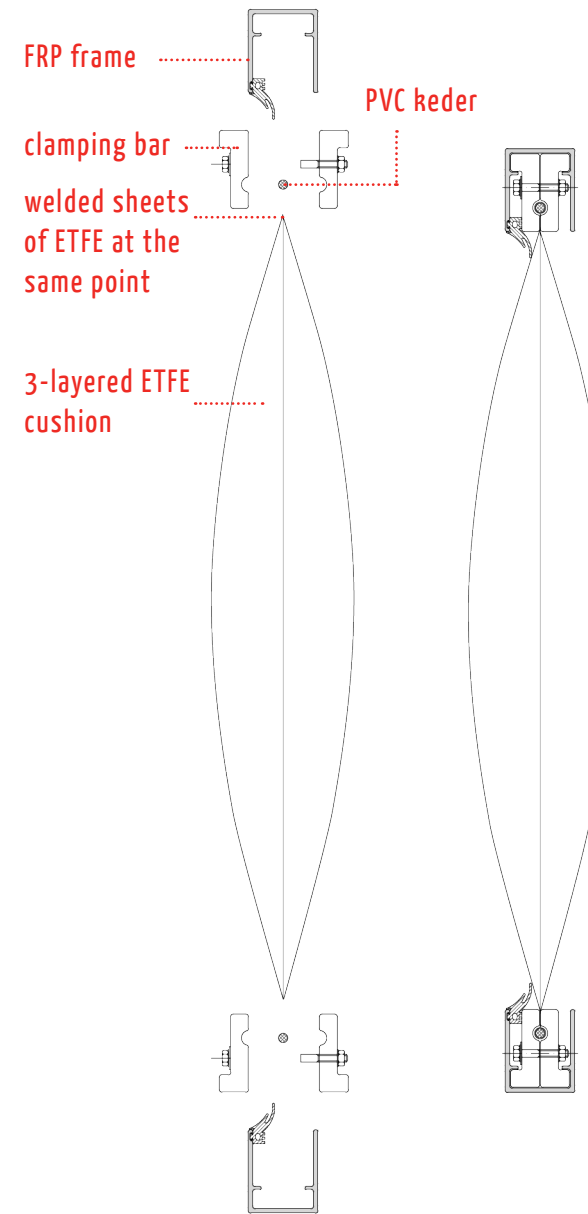


Figure 223: inflated cushion assembly

vacuum system assembly

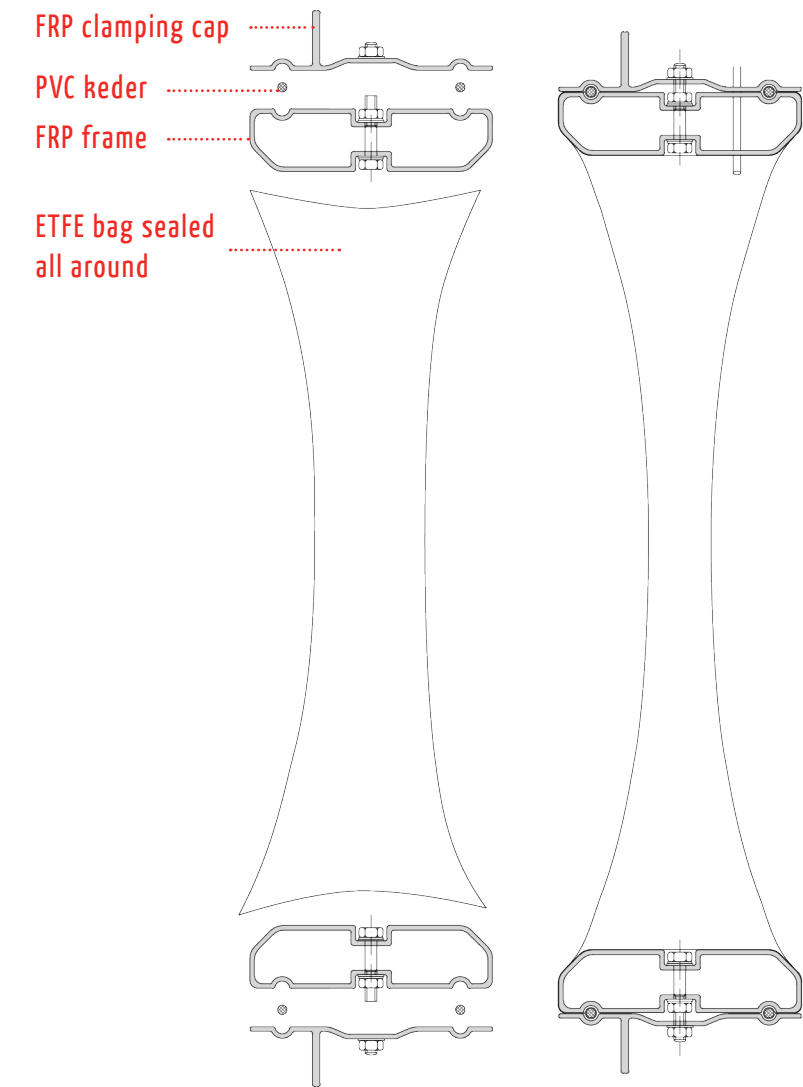


Figure 224: vacuum cushion assembly

forces calculations

In order to have a solid idea about the materials that should be used for the façade elements, several rough calculations were conducted concerning both the wind forces and the force on the frame that is developed due to the deflation in the vacuum system.

wind

When wind falls onto a surface the wind energy is transformed into pressure (P_{wind}) and subsequently that pressure is transformed into a force (F_{wind}). The annual average wind velocity in the region of Paris is **3.58m/s**. For safety reasons though, we take into account an extreme situation of wind speed of **9m/s**.

For the calculation of the load that falls onto the frame of each façade panel (3.65 x 2.9 m), the panel is divided into 4 parts with the same surface area, as it can be seen in figure 225. Since these parts have the same area, it can be assumed that the force that falls onto each one them corresponds to the 1/4 of the total force (F_{wind}) that is applied onto the whole panel. This force is transported afterwards to the correspondent frame part. Lastly, in order to calculate the uniform load applied to each frame part, the wind force ($F_{wind}/4$) is divided by the length of the frame.

The formulas that are used are the following with a drag coefficient $C_d = 2$ for buildings.

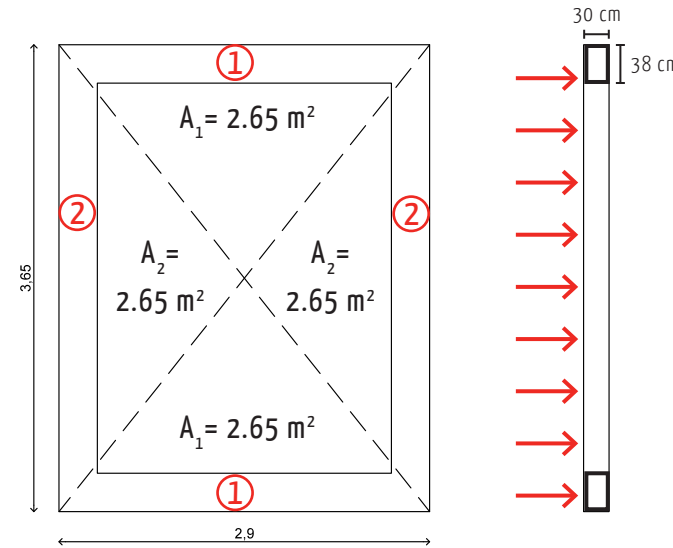


Figure 225: elevation and section of the façade panel

$$A_{tot} = 10.59 \text{ m}^2, \quad v_{maxW} = 9 \text{ m/s}, \quad C_d = 2 \text{ (for buildings)}$$

$$P_{wind} = 0.613 \times v_{maxW} = 50 \text{ N/m} \quad (1)$$

$$F_{wind} = A_{tot} \times P_{wind} \times C_d = 1059 \text{ N} \quad (2)$$

For one frame:

$$F_{wind} / 4 = 264.75 \text{ N} = 0.265 \text{ kN}$$

For frame 1 the uniform load is:

$$q_1 = F/l_1 = 0.265/3.65$$

$$= 0.07 \text{ kN/m}$$

For frame 2 the uniform load is:

$$q_2 = F/l_2 = 0.265/2.9$$

$$= 0.09 \text{ kN/m}$$

sources

- 1,2: <http://www.wikihow.com/Calculate-Wind-Load>
- 2: <http://www.constructiononline.eu/ligger.php>

materials:	load (kN/m)	length (mm)	elastic modulus (N/mm ²)	width (mm)	height (mm)	thickness (mm)	max stress (N/mm ²)	max deflection (mm)
steel								
vertical beam	0.07	3650	210000	380	300	5	0.2	0
						4	0.2	0
						3	0.3	0
						2	0.4	0
						4	0.2	0
						2	0.3	0
horizontal beam	0.09	2900	210000	380	300	5	0.1	0
						4	0.2	0
						3	0.2	0
						2	0.3	0
						4	0.2	0
						2	0.3	0
aluminum								
vertical beam	0.07	3650	71000	380	300	5	0.2	0
						4	0.2	0
						3	0.3	0
						2	0.4	0.1
						4	0.2	0
						2	0.3	0
horizontal beam	0.09	2900	71000	380	300	5	0.1	0
						4	0.2	0
						3	0.2	0
						2	0.3	0
						4	0.2	0
						2	0.3	0
FRP								
Glass FRP								
vertical beam	0.07	3650	40000	380	300	5	0.2	0
						4	0.2	0
						3	0.3	0.1
						2	0.4	0.1
						4	0.2	0
						2	0.3	0
horizontal beam	0.09	2900	40000	380	300	2	0.3	0
						2	0.3	0
						2	0.3	0
						2	0.3	0
						2	0.3	0
						2	0.3	0
Aramid FRP								
vertical beam	0.07	3650	100000	380	300	2	0.4	0
						2	0.4	0
horizontal beam	0.09	2900	100000	380	300	2	0.3	0
						2	0.3	0

Figure 226: calculation results from the excel file with the help of the online calculator "Simply supported beams calculations"

In the table above, several materials were investigated in order to calculate the deflection of the frames (1&2) for the resulted wind loads mentioned before. As it can be seen, the dimensions of the cross section of the frame of each façade element (38x30cm) are more than enough to withstand the wind forces and the deflection values are really small (0.1mm the maximum).

forces calculations

vacuum

In order to calculate the forces that are developed in the vacuum system, several parameters had to be taken into account. When the deflation of the elements takes place, forces start to appear due to the pressure difference. More specifically, the total load (q) that is applied onto each membrane surface is the difference (ΔP) of the external (P_{out}) and the internal (P_{in}) pressure. To calculate the force (H) that is applied onto each side of the frame, we first take into consideration the x direction and then the y direction, as it is shown in figure 227. The formulas that are used are the following.

For one side of the frame:

$$H = (w \times L^2) / (8 \times h) \text{ [kN]}^1$$

For both sides of the frame:

$$H (x2) \text{ [kN]}$$

For the whole length of the frame:

$$H_{tot} = H (x2) \times d \text{ [kN/m]}$$

with

$$P_{out} = 100\,000 \text{ Pa}, P_{in} = 10\,000 \text{ Pa}$$

$$\Delta P = 90\,000 \text{ Pa} = 90\,000 \text{ N/m}^2 = q$$

uniform load:

$$w = q \times d \text{ [N/m]}$$

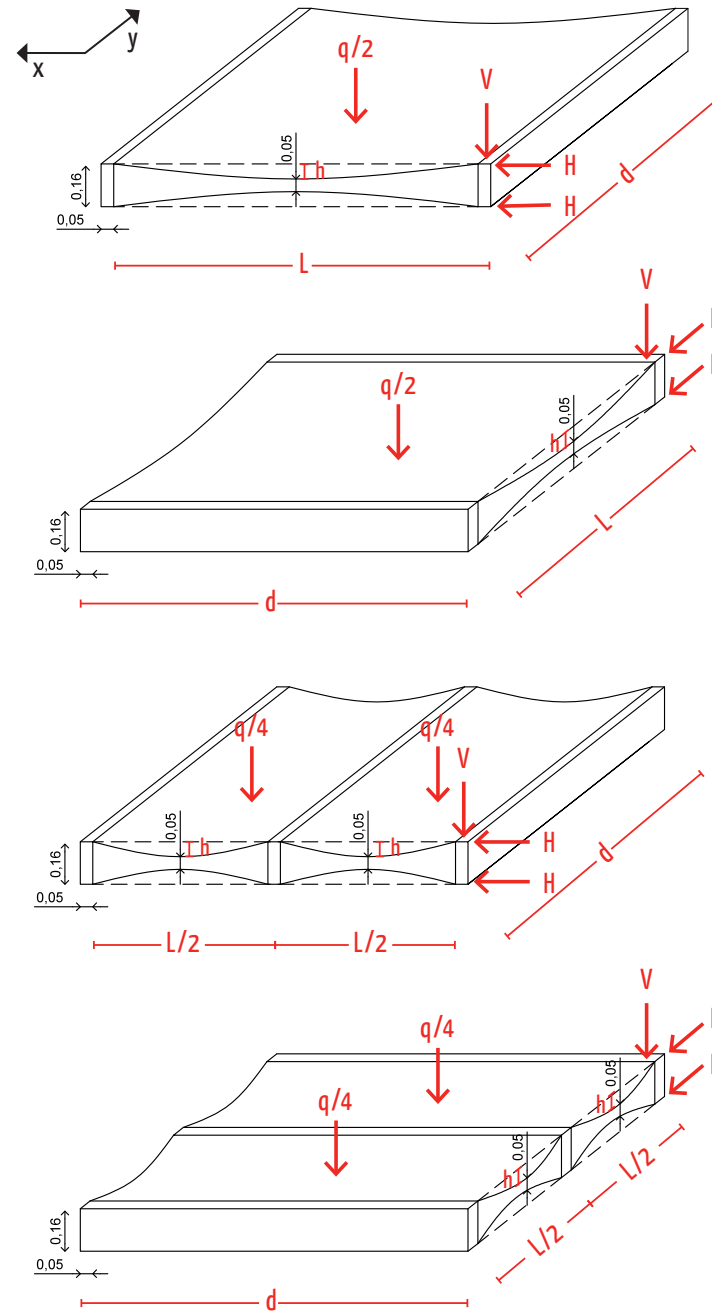


Figure 227: uniform loads and forces on the façade element (x & y directions)

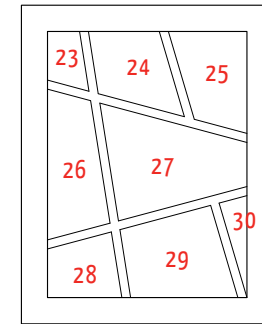
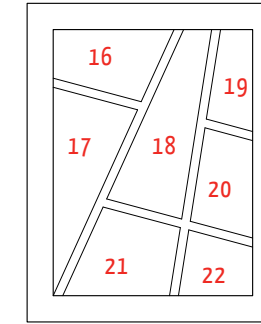
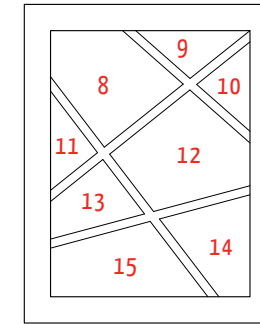
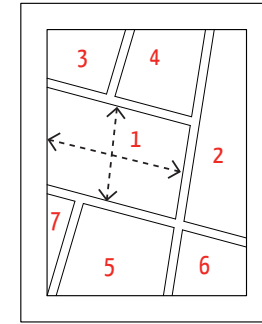


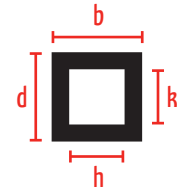
Figure 228: numbering of various façade elements with different cushions configurations

The next step was to take the four different configurations of the façade elements and conduct the calculations for each cushion separately. For reasons of simplification, the cushions are considered to have rectangular shape and as the two dimensions (length and width) the lengths of their two main central axis are taken into account (ex. cushion 1, figure 228). The goal was to calculate the maximum deflection of the frame that is the result of the uniform load (w) and consequently the force (H), which is developed on the edges. In the next pages, tables showing the values of the maximum deflections of each vacuum cushion are presented. The cross section of the frame that is used for the calculations is 160 x 50 mm with three different thicknesses of 4, 3 and 2 mm. Also, the number of divisions refers to how many times the length of the distance between two opposite frames is divided, and thus how many “spacers” are placed in the specific direction. For instance, 1 means there are no spacers, 2 means there is one spacer in between, 3 means there are two spacers etc. Lastly, after the calculation of the total force (H_{tot}) from the

formulas mentioned before, the Moment of Inertia had to be calculated for the specific cross section.

Moment of Inertia:

$$I = (b \cdot d^3) - (h \cdot k^3) / 12 \text{ [mm}^4\text{]}^2$$



Max. deflection:

$$\Delta_{max} = (5/384) \times \{(H_{tot} \cdot L^4) / (E \cdot I)\} \text{ [mm]}^3$$

where:

E = modulus of elasticity of the frame's material (N/mm²)

I = moment of inertia (mm⁴)

H_{tot} = total force on the frame (N/mm)

L = length of the frame (mm)

1. Charbonneau, L., (2011), Time-Dependent Tensile Properties of ETFE Foils, Waterloo, Ontario, Canada, page 23

2. http://www.engineersedge.com/beam_bending/beam_bending1.htm | <http://www.constructiononline.eu/ligger.php>

3. http://www.engineersedge.com/calculators/section_square_case_10.htm | <http://www.constructiononline.eu/ligger.php>

max. deflection calculations

As the material for the frame, the aramid FRP is chosen with a value for the elastic modulus of 100000 N/mm². The idea is to have a lightweight cushion system that will be placed afterwards into the stronger aluminum frame of the bigger façade element. Therefore, the selection of a composite polymer constitutes the best option to achieve this goal.

As already mentioned, the tables that follow in the next pages present the values of the maximum deflection of the frame of each vacuum cushion.

Number of panel	Panel		Frame		Number of divisions	H _{tot} (mm)	Cross section (mm)			Deflection (mm)
	length (m)	width (m)	length (m)	width (m)			b	h	w	
1	1.6	1.07	0.16	0.05	1	599.5	160	50	4	702.5
									3	5.5
									2	7
	1.07	1.6	0.16	0.05	1	599.5	160	50	4	140.5
									3	1.1
									2	1.4
2	2.3	0.6	0.16	0.05	1	389.5	160	50	4	1949.1
									3	15.2
									2	19.3
	0.6	2.3	0.16	0.05	1	389.5	160	50	4	27.6
									3	0.9
									2	1.1
3	0.85	0.8	0.16	0.05	1	94.6	160	50	4	9
									3	0.1
									2	0.1
	0.8	0.85	0.16	0.05	1	94.6	160	50	4	8.8
									3	11.2
									2	16
4	0.9	0.85	0.16	0.05	1	119.7	160	50	4	0.1
									3	0.1
									2	0.1
	0.8	0.85	0.16	0.05	1	94.6	160	50	4	6.9
									3	8.8
									2	12.6
5	1.14	1	0.16	0.05	1	265.8	160	50	4	0.1
									3	0.1
									2	0.2
	1	1.14	0.16	0.05	1	265.8	160	50	4	14.2
									3	20.3
									2	27.6
6	0.8	0.75	0.16	0.05	1	73.6	160	50	4	0.1
									3	0.1
									2	0.1
	0.75	0.8	0.16	0.05	1	73.6	160	50	4	17.8
									3	25.5
									2	31.2
7	1.16	0.16	0.16	0.05	1	7	160	50	4	0.1
									3	0.1
									2	0.1
	0.16	1.16	0.16	0.05	1	7	160	50	4	0.1
									3	0.1
									2	0.1
8	1.45	1.06	0.16	0.05	1	483.2	160	50	4	0.1
									3	0.1
									2	0.1
	1.06	1.45	0.16	0.05	1	483.2	160	50	4	381.9
									3	3
									2	3.8
9	1.3	0.55	0.16	0.05	1	104.6	160	50	4	5.4
									3	6.8
									2	9.8
	0.55	1.3	0.16	0.05	1	104.6	160	50	4	4.2
									3	5.3
									2	7.6

Figure 229: table of the frames' max. deflection_ part 1

Number of panel	Panel		Frame		Number of divisions	H _{tot} (mm)	Cross section (mm)			Deflection (mm)
	length (m)	width (m)	length (m)	width (m)			b	h	w	
1	0.85	0.9	0.16	0.05	1	119.7	160	50	4	11.2
									3	14.2
									2	20.3
	1.14	1	0.16	0.05	1	265.8	160	50	4	0.1
									3	0.1
									2	0.2
2	1.07	1.6	0.16	0.05	1	599.5	160	50	4	140.5
									3	1.1
									2	1.4
	1.6	1.07	0.16	0.05	1	599.5	160	50	4	1.1
									3	1.4
									2	2
3	2.3	0.6	0.16	0.05	1	389.5	160	50	4	1949.1
									3	15.2
									2	19.3
	0.6	2.3	0.16	0.05	1	389.5	160	50	4	27.6
									3	0.9
									2	1.1
4	0.85	0.8	0.16	0.05	1	94.6	160	50	4	9
									3	0.1
									2	0.1
	0.8	0.85	0.16	0.05	1	94.6	160	50	4	8.8
									3	11.2
									2	16
5	1.14	1	0.16	0.05	1	265.8	160	50	4	0.1
									3	0.1
									2	0.1
	1	1.14	0.16	0.05	1	265.8	160	50	4	17.8
									3	25.5
									2	31.2
6	0.8	0.75	0.16	0.05	1	73.6	160	50	4	0.1
									3	0.1
									2	0.1
	0.75	0.8	0.16	0.05	1	73.6	160	50	4	381.9
									3	3
									2	3.8
7	1.16	0.16	0.16	0.05	1	7	160	50	4	5.4
									3	6.8
									2	9.8
	0.16	1.16	0.16	0.05	1	7	160	50	4	4.2
									3	5.3
									2	7.6
8	1.45	1.06	0.16	0.05	1	483.2	160	50	4	0.1
									3	0.1
									2	0.1
	1.06	1.45	0.16	0.05	1	483.2	160	50	4	109.1
									3	0.9
									2	1.1
9	1.3	0.55	0.16	0.05	1	104.6	160	50	4	53.4
									3	0.4
									2	0.5
	0.55	1.3	0.16	0.05	1	104.6	160	50	4	0.8
									3	1.7
									2	0
10	1.3	0.55	0.16	0.05	1	104.6	160	50	4	0
									3	0
									2	0
	0.55	1.3	0.16	0.05	1	104.6	160	50	4	0
									3	0
									2	0

Figure 230: table of the frames' max. deflection_ part 2

Number of panel	Panel		Frame		Number of divisions	H _{tot} (mm)	Cross section (mm)			Deflection (mm)					
	length (m)	width (m)	length (m)	width (m)			b	h	w						
10	1	0.6	0.16	0.05	1	73.6	160	50	4	13.2					
						2	9.2	160	50	4	0.1				
						3				4	0.1				
	0.6	1	0.16	0.05	1	73.6	160	50	4	2	0.2				
										3	1.7				
										2	2.2				
11	1.14	0.54	0.16	0.05	1	77.5	160	50	4	23.4					
						2	9.7	160	50	4	0.2				
						3				4	0.2				
						2				4	0.3				
						1	77.5	160	50	4	1.2				
						3				4	1.5				
	0.54	1.14	0.16	0.05	1	77.5	160	50	4	2	2.1				
										3	0				
										2	9.7	160	50	4	0
										3				4	0
										2				4	0
										3				4	0
12	1.6	1.45	0.16	0.05	1	1100.9	160	50	4	1290.1					
						2	137.6	160	50	4	10.1				
						3				4	12.8				
						2				4	18.3				
						1	1100.9	160	50	4	870.2				
						3				4	6.8				
	1.45	1.6	0.16	0.05	1	1100.9	160	50	4	2	137.6				
										3				4	8.6
										2				4	12.3
										3				4	
										2				4	
										3				4	
13	1.07	0.76	0.16	0.05	1	135.3	160	50	4	31.7					
						2	16.9	160	50	4	0.2				
						3				4	0.3				
						2				4	0.4				
						1	135.3	160	50	4	8.1				
						3				4	0.1				
	0.76	1.07	0.16	0.05	1	135.3	160	50	4	2	16.9				
										3				4	0.1
										2				4	0.1
										3				4	0.1
										2				4	0.1
										3				4	0.1
14	1.22	1.13	0.16	0.05	1	388.7	160	50	4	154					
						2	48.6	160	50	4	1.2				
						3				4	1.5				
						2				4	2.2				
						1	388.7	160	50	4	113.3				
						3				4	0.9				
	1.13	1.22	0.16	0.05	1	388.7	160	50	4	2	48.6				
										3				4	1.1
										2				4	1.6
										3				4	
										2				4	
										3				4	

Figure 231: table of the frames' max. deflection_part 3

Number of panel	Panel		Frame		Number of divisions	H _{tot} (mm)	Cross section (mm)			Deflection (mm)					
	length (m)	width (m)	length (m)	width (m)			b	h	w						
15	1.9	0.95	0.16	0.05	1	666.4	160	50	4	1552.9					
						2	83.3	160	50	4	12.1				
						3				4	15.4				
						2				4	22				
						1	666.4	160	50	4	97.1				
						3				4	0.8				
	0.95	1.9	0.16	0.05	1	666.4	160	50	4	2	83.3				
										3				4	1
										2				4	1.4
										3				4	
										2				4	
										3				4	
16	1.26	0.78	0.16	0.05	1	197.6	160	50	4	89					
						2	24.7	160	50	4	0.7				
						3				4	0.9				
						2				4	1.3				
						1	197.6	160	50	4	13.1				
						3				4	0.1				
	0.78	1.26	0.16	0.05	1	197.6	160	50	4	2	24.7				
										3				4	0.1
										2				4	0.2
										3				4	0.1
										2				4	0.2
										3				4	0.2
17	2.3	0.63	0.16	0.05	1	429.5	160	50	4	2148.9					
						2	53.7	160	50	4	16.8				
						3				4	21.3				
						2				4	30.5				
						1	429.5	160	50	4	12.1				
						3				4	0.1				
	0.63	2.3	0.16	0.05	1	429.5	160	50	4	2	53.7				
										3				4	0.1
										2				4	0.1
										3				4	0.1
										2				4	0.2
										3				4	0.2
18	2.14	0.6	0.16	0.05	1	337.2	160	50	4	1264.6					
						2	42.2	160	50	4	9.9				
						3				4	12.5				
						2				4	17.9				
						1	337.2	160	50	4	7.8				
						3				4	0.1				
	0.6	2.14	0.16	0.05	1	337.2	160	50	4	2	42.2				
										3				4	0.1
										2				4	0.1
										3				4	0.1
										2				4	0.1
										3				4	0.1
19	1.14	0.45	0.16	0.05	1	53.8	160	50	4	16.3					
						3				4	20.6				
						2				4	29.5				
						1	53.8	160	50	4	0.1				
						3				4	0.2				
						2				4	0.2				
	0.45	1.14	0.16	0.05	1	53.8	160	50	4	2	53.8				
										3				4	0.4
										2				4	0.5
										3				4	0.7
										2				4	0
										3				4	0
1.14	0.45	0.16	0.05	1	53.8	160	50	4	2	6.7					
									3				4	0	
									2				4	0	
									3				4	0	
									2				4	0	
									3				4	0	

Figure 232: table of the frames' max. deflection_part 4

Number: of panel:	Panel		Frame		Number of divisions	H _{tot} (mm)	Cross section (mm)			Deflection (mm)	
	length (m)	width (m)	length (m)	width (m)			b	h	w		
20	1.09	0.65	0.16	0.05	1	102.7	160	50	4	25.9	
										32.9	
										47	
										0.2	
										0.3	
	0.65	1.09	0.16	0.05	1	102.7	160	50	4	3.3	
										4.2	
										5.9	
										0	
										0	
21	1.06	0.95	0.16	0.05	1	207.4	160	50	4	46.8	
										0.4	
										0.5	
										0.7	
										30.2	
	0.95	1.06	0.16	0.05	1	207.4	160	50	4	0.2	
										0.3	
										0.4	
										0	
										0	
22	0.8	0.65	0.16	0.05	1	55.3	160	50	4	4.1	
										5.1	
										7.4	
										0.1	
										1.8	
	0.65	0.8	0.16	0.05	1	55.3	160	50	4	2.2	
										3.2	
										0	
										0	
										0	
23	0.62	0.42	0.16	0.05	1	13.9	160	50	4	0.4	
										0.5	
										0.7	
										0	
										0.1	
	0.42	0.62	0.16	0.05	1	13.9	160	50	4	0.1	
										0.1	
										0.1	
										0	
										0	
24	0.9	0.9	0.16	0.05	1	134.2	160	50	4	15.7	
										20	
										28.6	
	2	16.8	160	50	2	0.2	0.2	0.2	0.2	0.2	
											0.3
											0.3
25	1.08	0.75	0.16	0.05	1	134.2	160	50	4	32.6	
										0.3	
										0.3	
										0.5	
										7.6	
	0.75	1.08	0.16	0.05	1	134.2	160	50	4	9.6	
										13.8	
										0.1	
										0.1	
										0.1	

Figure 233: table of the frames'
max. deflection_part 3

Number: of panel:	Panel		Frame		Number of divisions	H _{tot} (mm)	Cross section (mm)			Deflection (mm)
	length (m)	width (m)	length (m)	width (m)			b	h	w	
26	1.56	0.6	0.16	0.05	1	179.2	160	50	4	189.8
										22.4
										1.5
										1.9
										2.7
	0.6	1.56	0.16	0.05	1	179.2	160	50	4	4.2
										5.3
										7.5
										0
										0
27	1.58	0.9	0.16	0.05	1	413.6	160	50	4	460.9
										51.7
										3.6
										4.6
										6.5
	0.9	1.58	0.16	0.05	1	413.6	160	50	4	48.5
										0.4
										0.5
										0.7
										0
28	0.8	0.7	0.16	0.05	1	64.1	160	50	4	4.7
										6
										8.5
										0
										0
	0.7	0.8	0.16	0.05	1	64.1	160	50	4	2.8
										3.5
										5
										0
										0
29	1.14	1	0.16	0.05	1	265.8	160	50	4	80.3
										33.2
										0.6
										0.8
										1.1
	1	1.14	0.16	0.05	1	265.8	160	50	4	47.5
										0.4
										0.5
										0.7
										0.7
30	1.13	0.48	0.16	0.05	1	60.2	160	50	4	17.5
										22.3
										31.8
										0.1
										0.2
	0.48	1.13	0.16	0.05	1	60.2	160	50	4	0.6
										0.7
										1
										0
										0
2	7.5	160	50	4	0	0	0	0	0	
										0
										0
										0
										0

Figure 234: table of the frames'
max. deflection_part 4

spacers

As it can be seen in the previous tables, in order to achieve the smaller value of the maximum deflection that is permitted according to regulations, most of the distances between the two opposite frames had to be divided in 2 parts, which means that one row of spacers is needed in each direction of the vacuum cushion.

Following the idea of having a lightweight cushion, the material that is chosen for the spacers is **glass-fibre**, because of its high strength under compression and also its good thermal resistance, as it was described in the building physics chapter. Although the calculations were conducted by dividing the frame into smaller parts in both directions, which would give as a result a rectangular grid of “spacers” into each element (figure 238), the type of spacers that are chosen are glass-fibre rods that are placed in the meeting points of the rectangular grid (figure 239). The calculation of the diameter of the rods is beyond the scope of this graduation research, but for the sake of the design a diameter of 20mm is chosen, which is reduced to 15mm in the middle of each spacer. As described above, one row of spacers is needed in each direction, but since these rods are used instead of longer elements that would cover the whole length, for safety reasons more than one row can be used in the design if necessary. The tables (figures 235&236) present several technical information

PULTRUDED SOLID ROD & BAR SECTIONS				
MATERIAL PROPERTIES DATA				
THE FOLLOWING DATA WAS DERIVED FROM ASTM COUPON and FULL SECTION TESTING. Testing results are average values based on random sampling from production runs. The following tables are results from testing our Plexinate P-100 resin system for solid rods. PLEASE NOTE: ROD stock are manufactured from LONGITUDINAL REINFORCEMENT ONLY.				
PROPERTY (Coupon value)	ASTM Test	Units	65% Glass	73% Glass
MECHANICAL				
Tensile Strength (LW)	D638	MPa	689.0	825.7
Tensile Modulus (LW)	D638	GPa	41.4	41.4
Compressive Strength (LW)	D695	MPa	413.2	481.7
Flexural Strength (LW)	D790	MPa	689.0	825.7
Flexural Modulus (LW)	D790	GPa	41.4	41.4
Notched Izod IMPACT (LW)	D256	J/m	2135	2135
PHYSICAL				
Barcol Hardness	D2583		50 / 55	50 / 55
Water Absorption	D570	% Max	0.25	0.25
Density	D792	Mg / m3	2.01-2.10	2.01-2.10
Coefficient of Thermal Expansion (LW)	D696	10 ⁻⁶ K ⁻¹	5.5	5.5
ELECTRICAL				
Arc Resistance	D495	seconds	120	120
Dielectric Strength (LW)	D149	kV / mm	1.58	1.58
Dielectric Constant (PF)	D150	@60Hz	5.2	5.2
FIRE RESISTANCE				
Flammability Extinguishing	D635		self extinguishing	
UV. And CHEMICAL RESISTANCE				
Refer to our data sheets for full details.			Excellent	
(LW) = Lengthwise (PF) = Perpendicular to Laminate face				

Figure 235: table of glass-fibre rods properties data | source: <https://www.fibreglassshop.co.nz/products/fibreglass-rods>

	Units	Property Data
Tensile strength	MPa	550
Tensile Modulus	GPa	30
Density	g/cc	1.9
Electrical Strength	kV/mm	10
Thermal conductivity	W/m.K	0.35
Water absorption	% wt/wt	0.2%

Figure 236: table of glass-fibre rods' technical data sheet | source: <https://www.ecfibreglasssupplies.co.uk/product/white-polyester-fibreglass-rod-20mm-dia>

for the glass-fibre rods.

connection

The connection of the glass-fibre rods to the membrane sheets is shown in figure 237. An additional part is used, also made out of a composite, which is welded onto the membrane and its shape locks the spacer in between and holds it in place. The spacers, apart from reducing the forces that are developed on the frame, they are also responsible for preventing the two membrane sheets from touching each other.

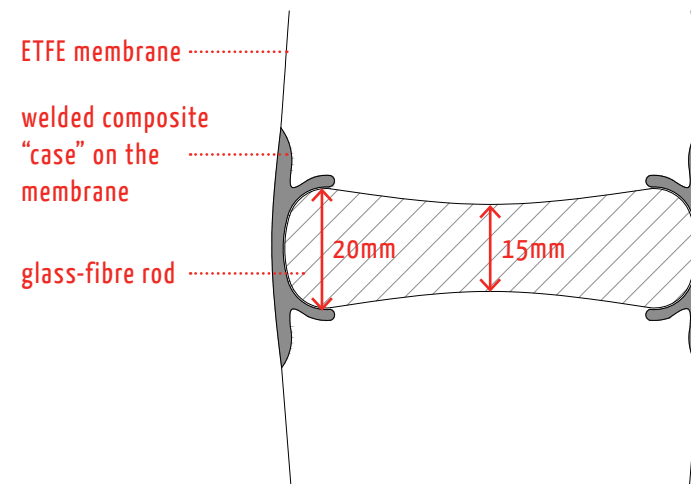


Figure 237: detail of the connection of the spacer with the membranes

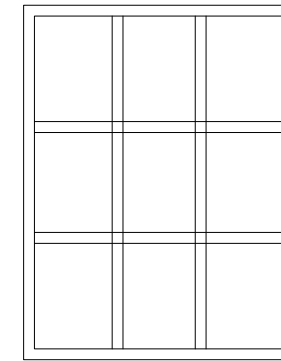


Figure 238: rectangular grid of longer elements as spacers

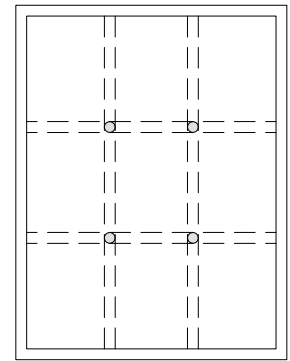


Figure 239: circular rods in the meeting points of the rectangular grid

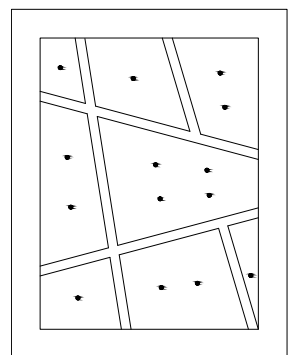
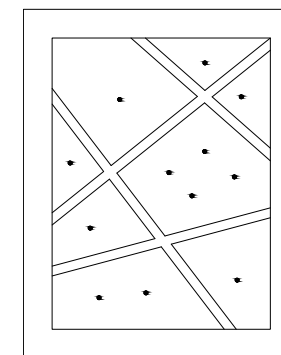
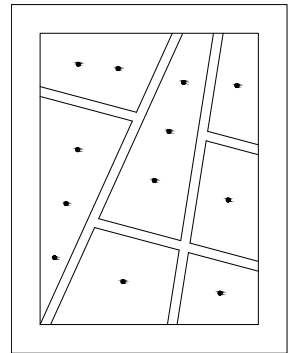
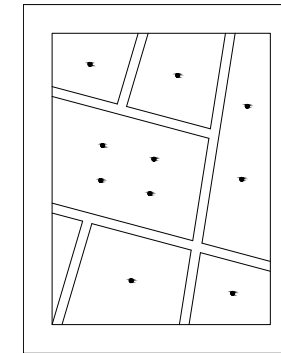


Figure 240: different configurations of façade elements with circular spacers

details 1.5

- | | | |
|----------------------------------|---|--|
| 1. aluminum extruded profile 4mm | 11. steel decking floor sheet | 19. weather protection foil |
| 2. aluminum extruded profile 2mm | 12. aluminum stud | 20. suspended ceiling |
| 3. GFRP extruded profile 3mm | 13. concrete floor 120mm for 90' fire delay | 21. inflation pipe $\varnothing 20\text{mm}$ |
| 4. valve | 14. steel console (550x630mm) | 22. deflation pipe $\varnothing 10\text{mm}$ |
| 5. EPDM linking gasket | 15. fireproof boards 12.5mm | 23. main pipe $\varnothing 50\text{mm}$ |
| 6. weather gasket | 16. thick mineral fibre insulation 60mm | 24. L-shaped steel profile 4mm |
| 7. hook bracket | 17. hard insulation | 25. railing |
| 8. anchor | 18. aluminum click cap 2mm | 26. glass-fibre rod $\varnothing 20\text{mm}$ (spacer) |
| 9. thermal break | | |
| 10. anchor channels | | |

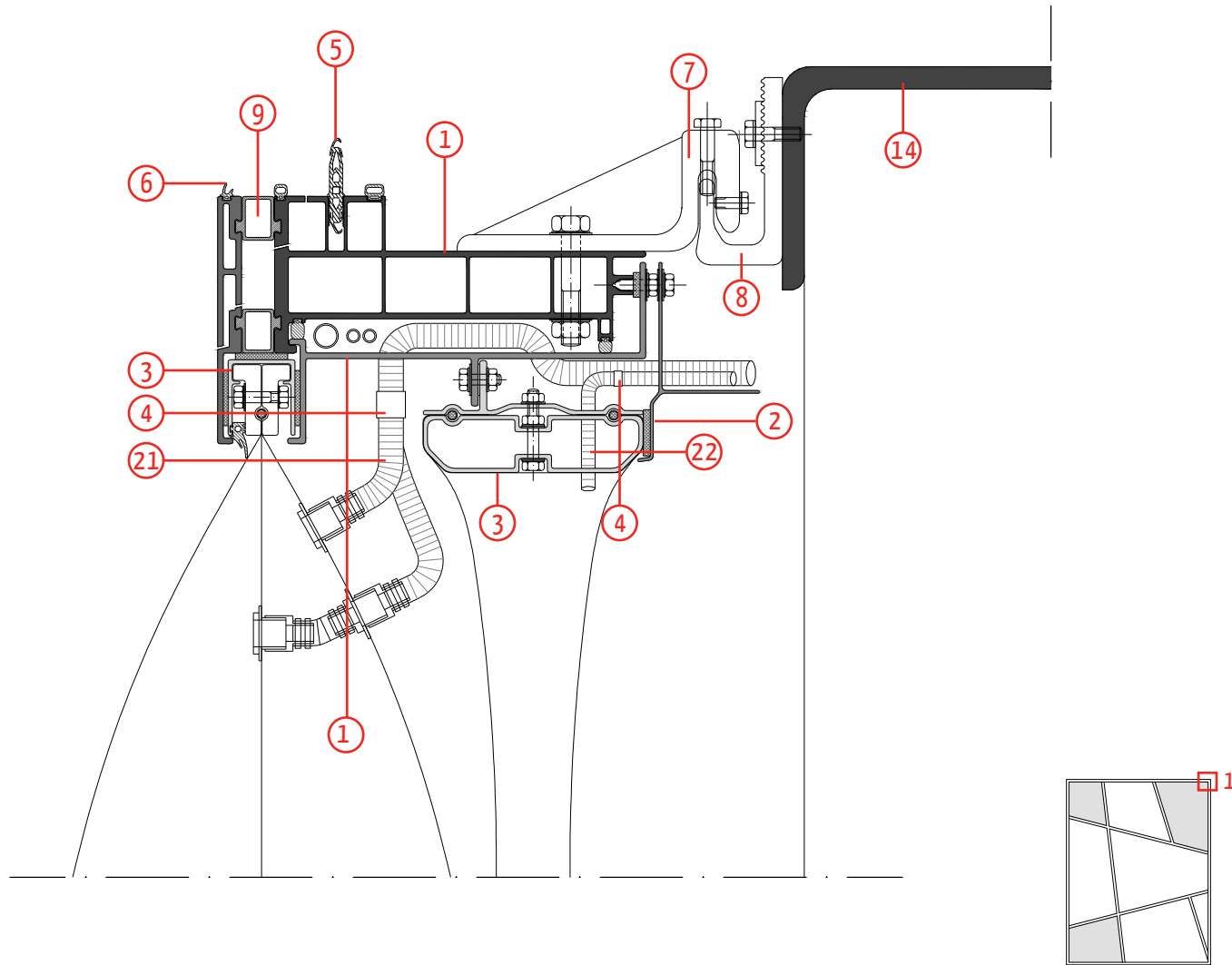


Figure 241: detail 1_connection of the upper part to the main construction

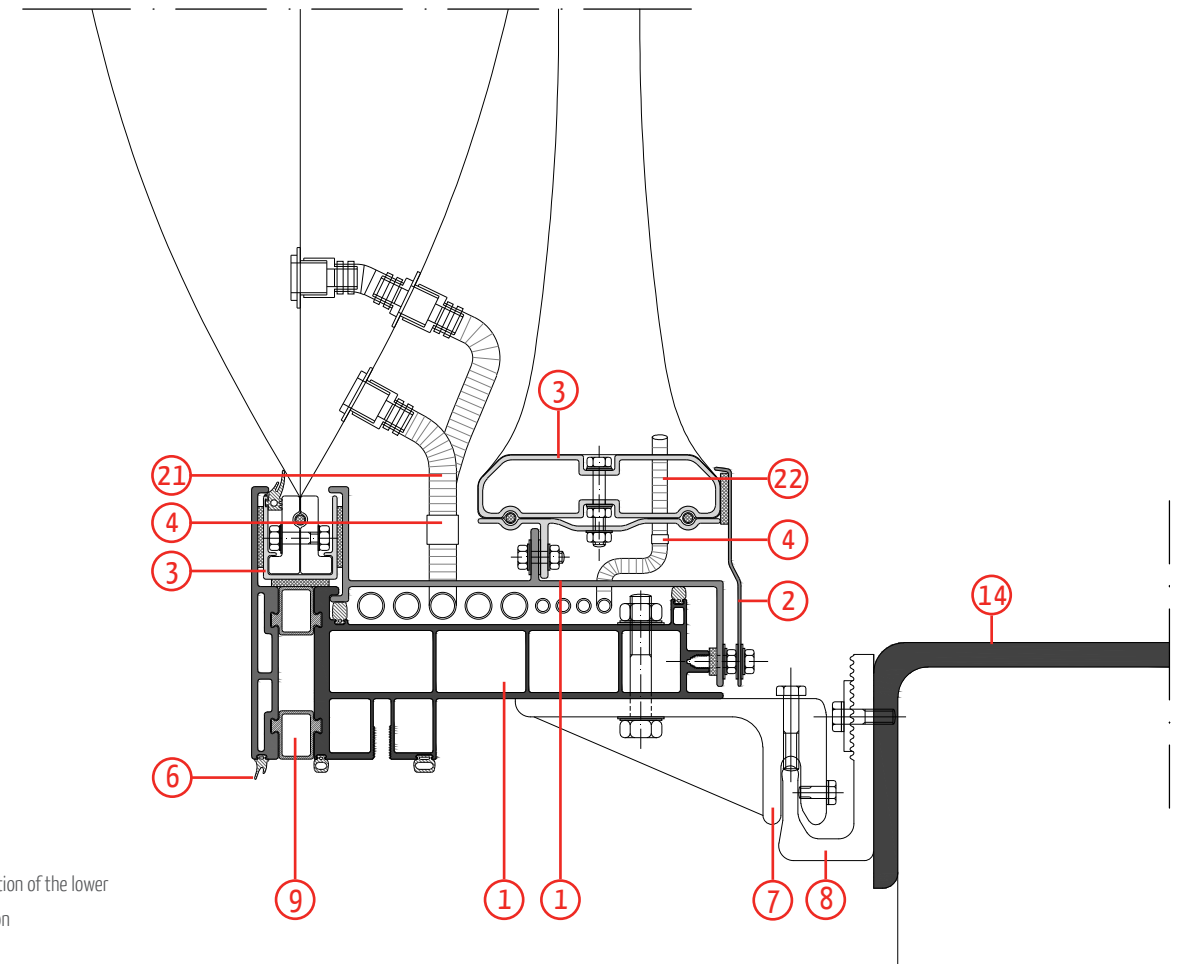
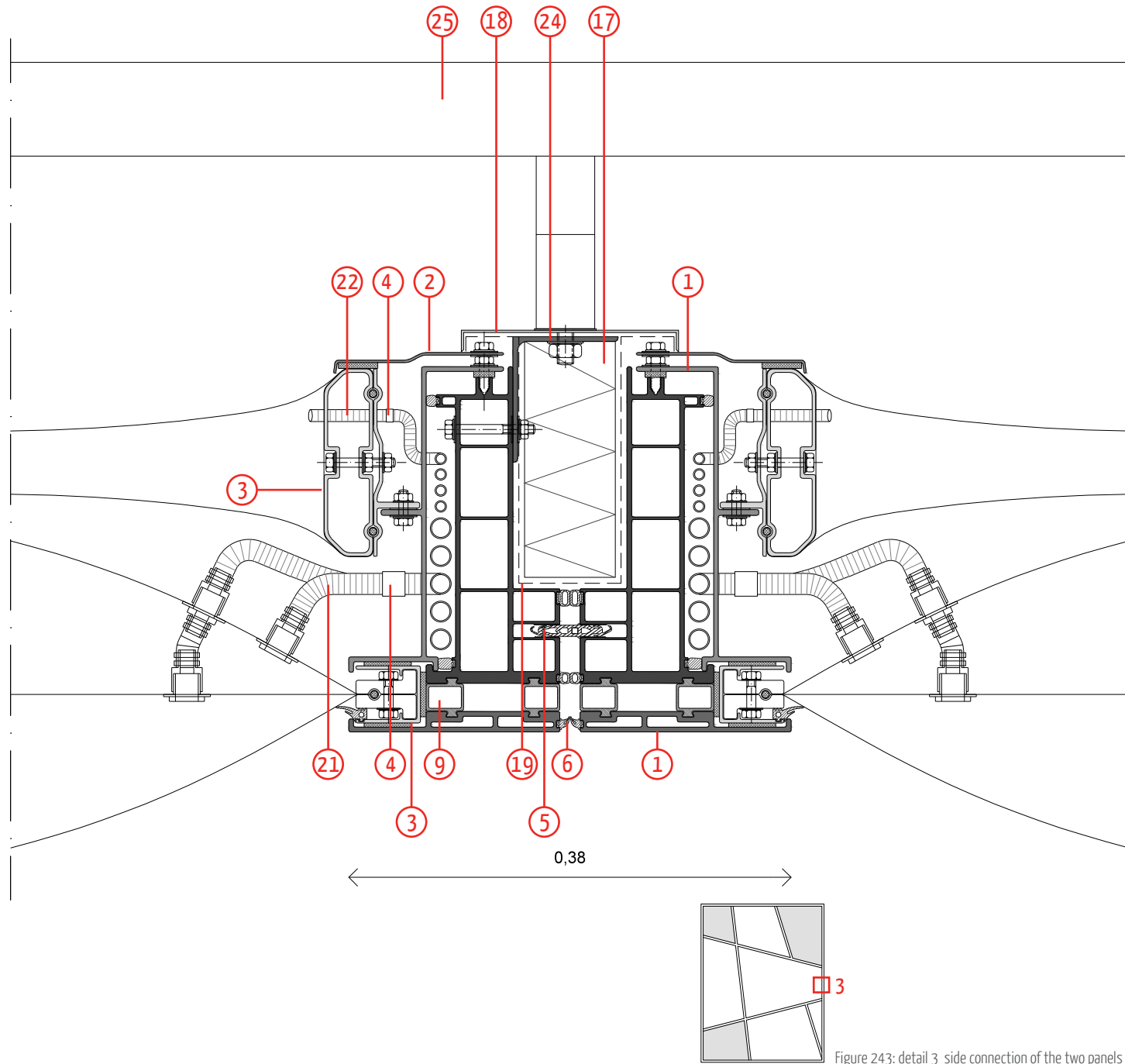


Figure 242: detail 2_connection of the lower part to the main construction

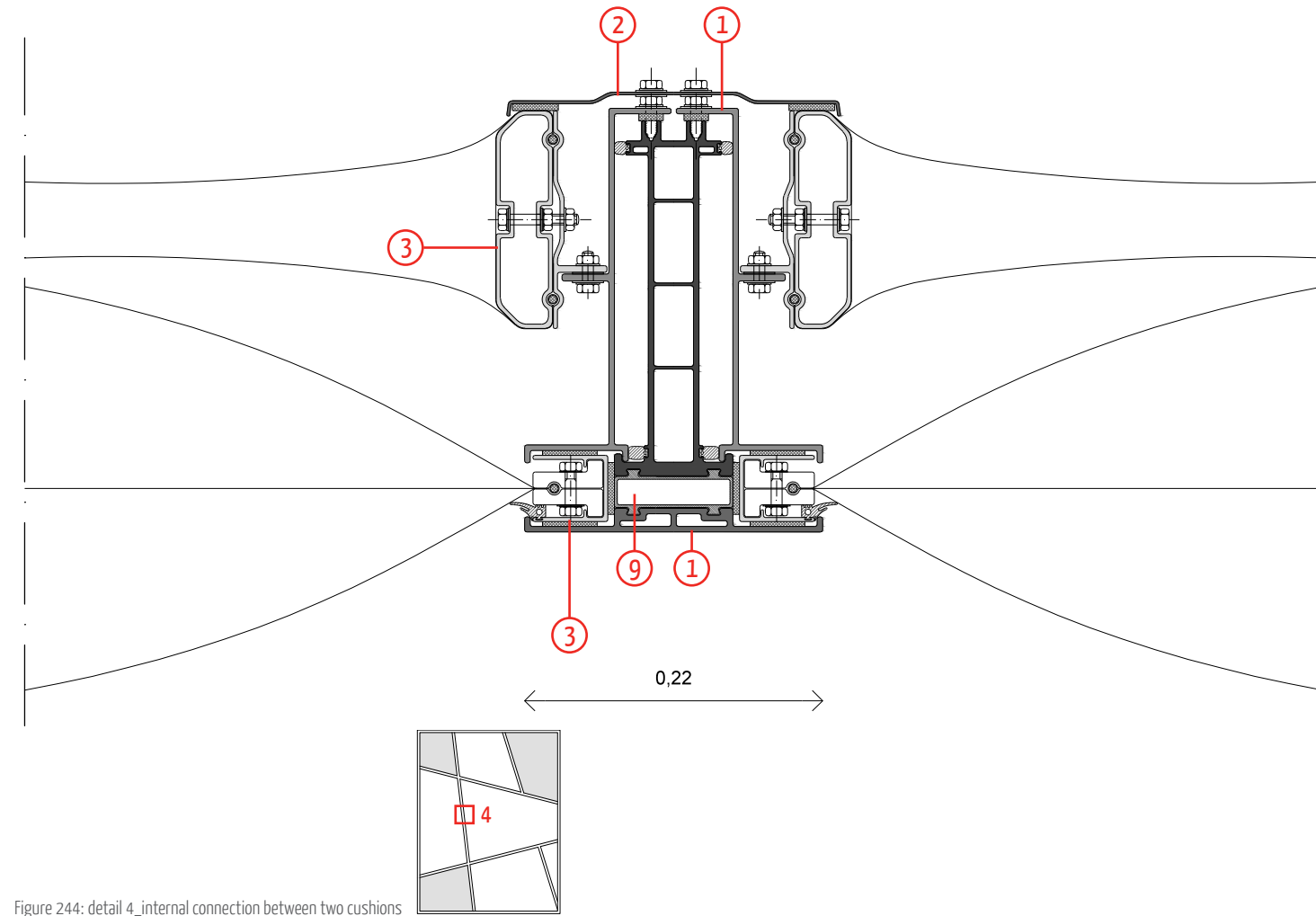
details 1.5



1. aluminum extruded profile 4mm
2. aluminum extruded profile 2mm
3. GFRP extruded profile 3mm
4. valve
5. EPDM linking gasket
6. weather gasket
7. hook bracket
8. anchor
9. thermal break

10. anchor channels
11. steel decking floor sheet
12. aluminum stud
13. concrete floor 120mm for 90' fire delay
14. steel console (550x630mm)
15. fireproof boards 12.5mm
16. thick mineral fibre insulation 60mm
17. hard insulation
18. aluminum click cap 2mm

19. weather protection foil
20. suspended ceiling
21. inflation pipe $\varnothing 20\text{mm}$
22. deflation pipe $\varnothing 10\text{mm}$
23. main pipe $\varnothing 50\text{mm}$
24. L-shaped steel profile 4mm
25. railing
26. glass-fibre rod $\varnothing 20\text{mm}$ (spacer)



details 1.5

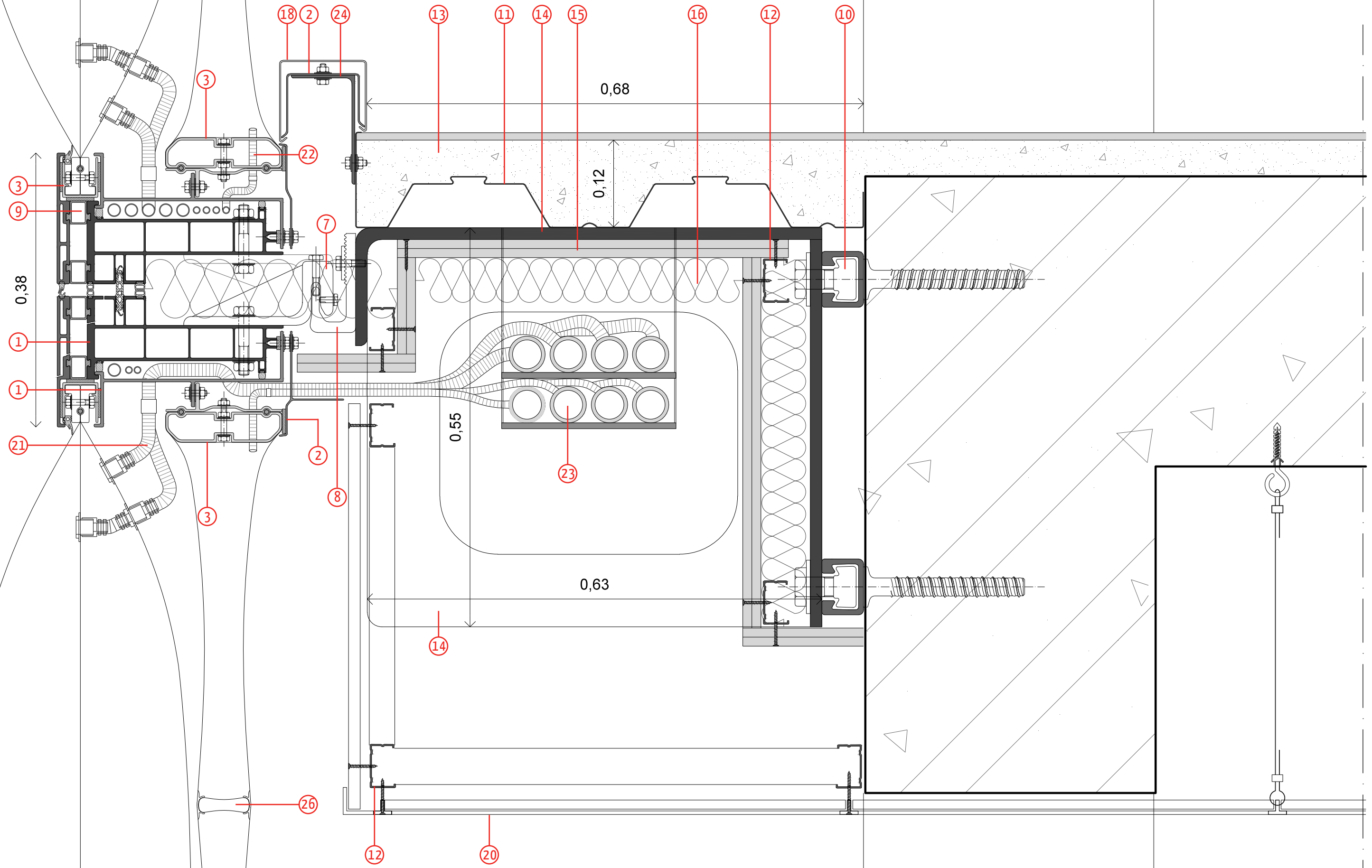


Figure 245: details 1&2_connection of the panel to the main construction

assembly concept

1

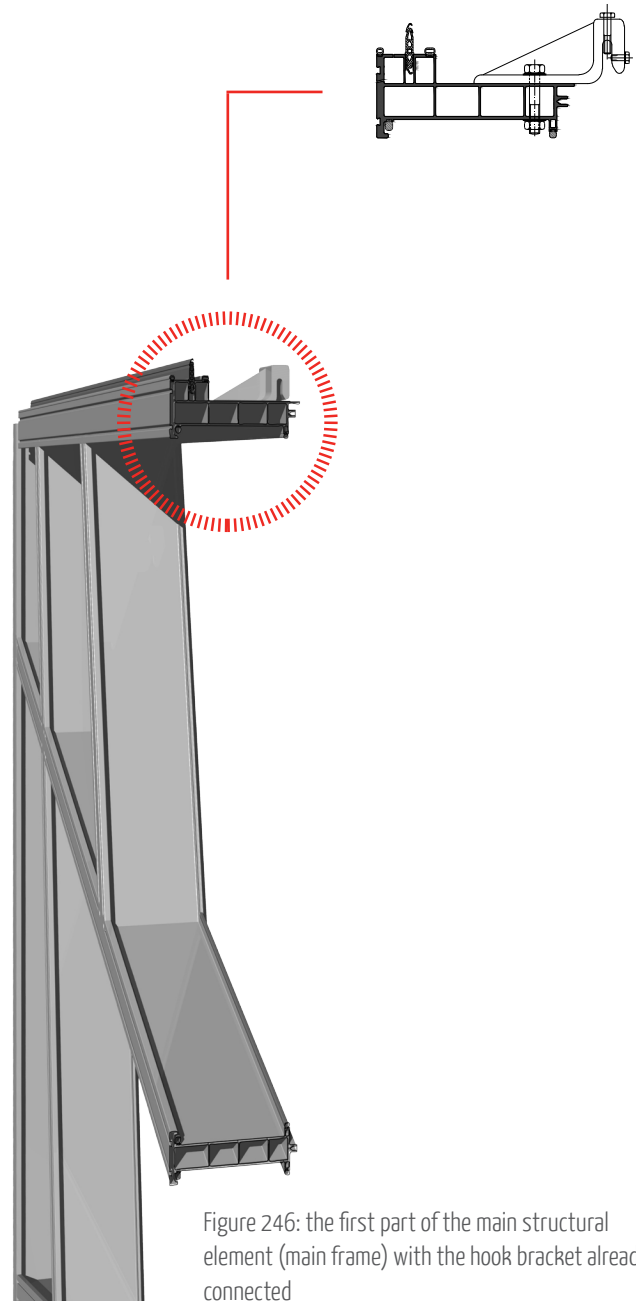


Figure 246: the first part of the main structural element (main frame) with the hook bracket already connected

2

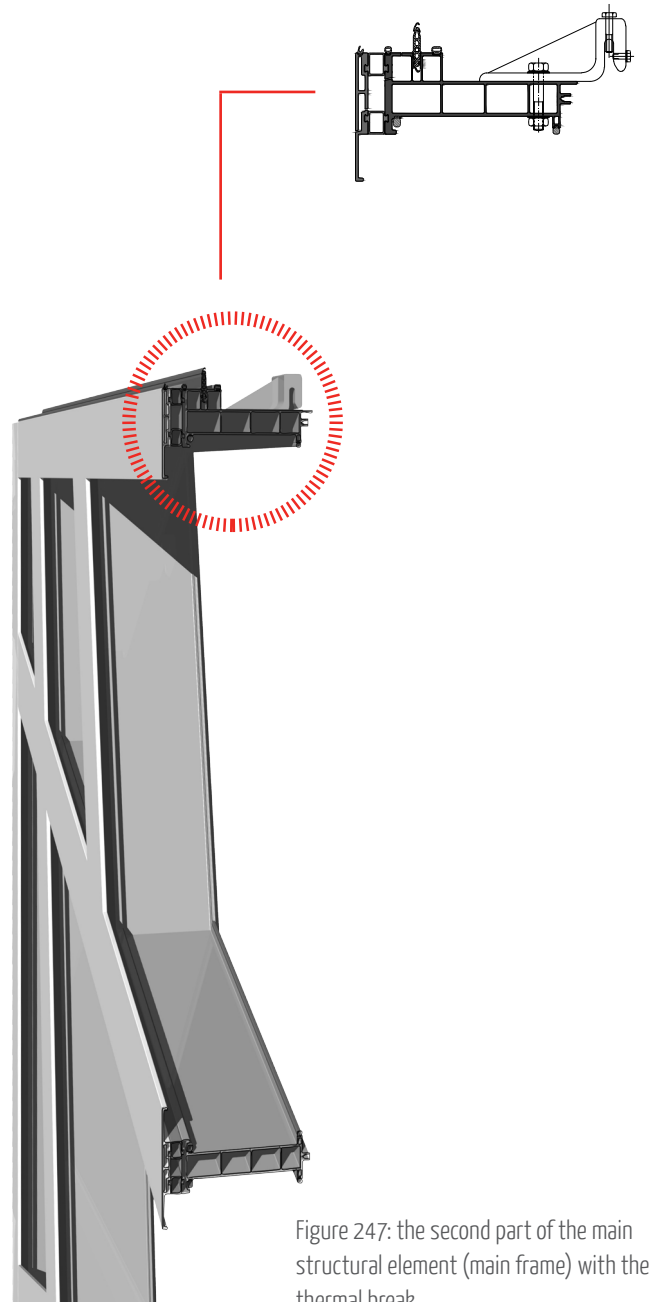


Figure 247: the second part of the main structural element (main frame) with the thermal break

3

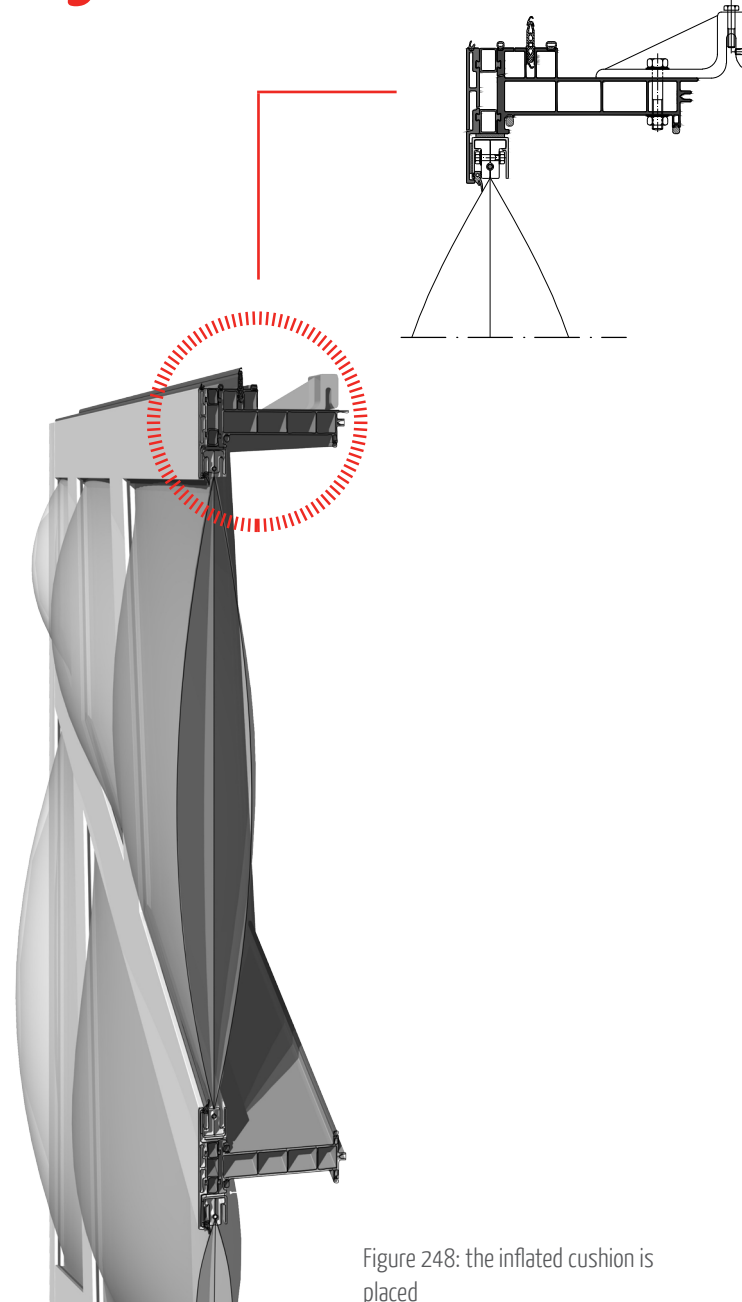


Figure 248: the inflated cushion is placed

4

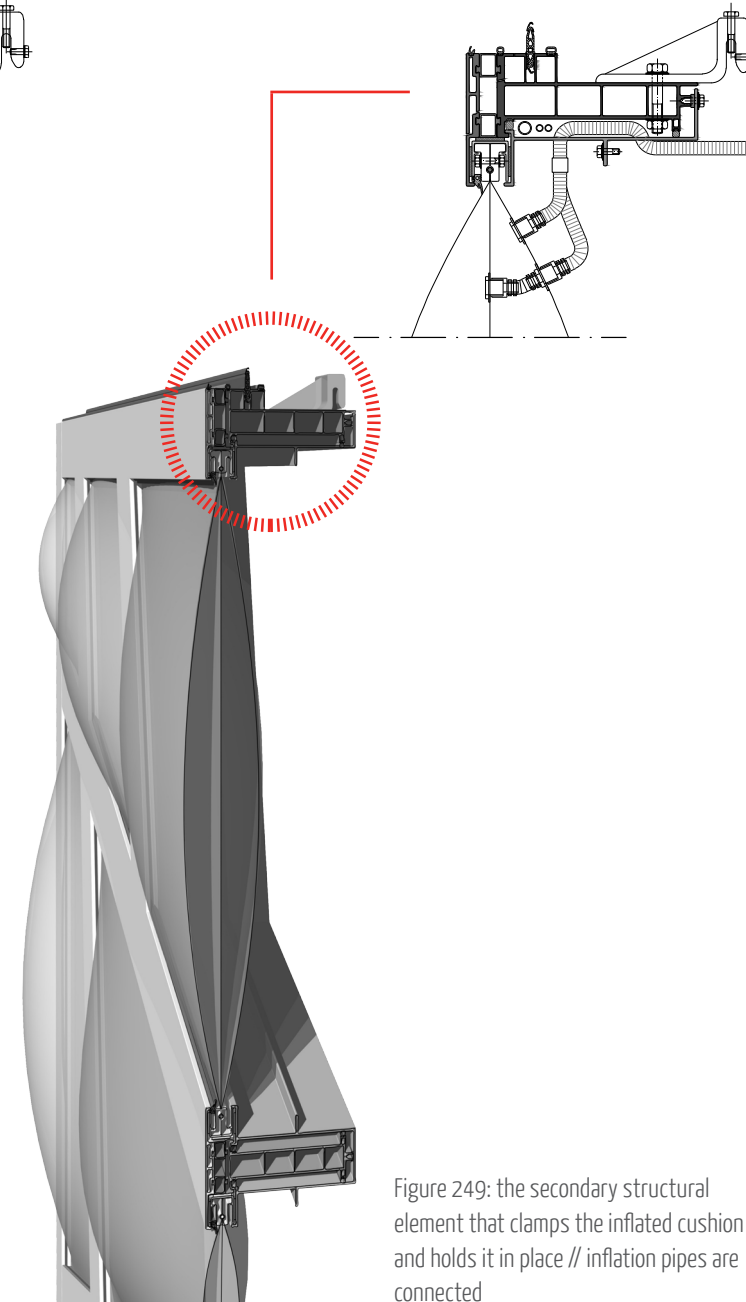


Figure 249: the secondary structural element that clamps the inflated cushion and holds it in place // inflation pipes are connected

assembly concept

5

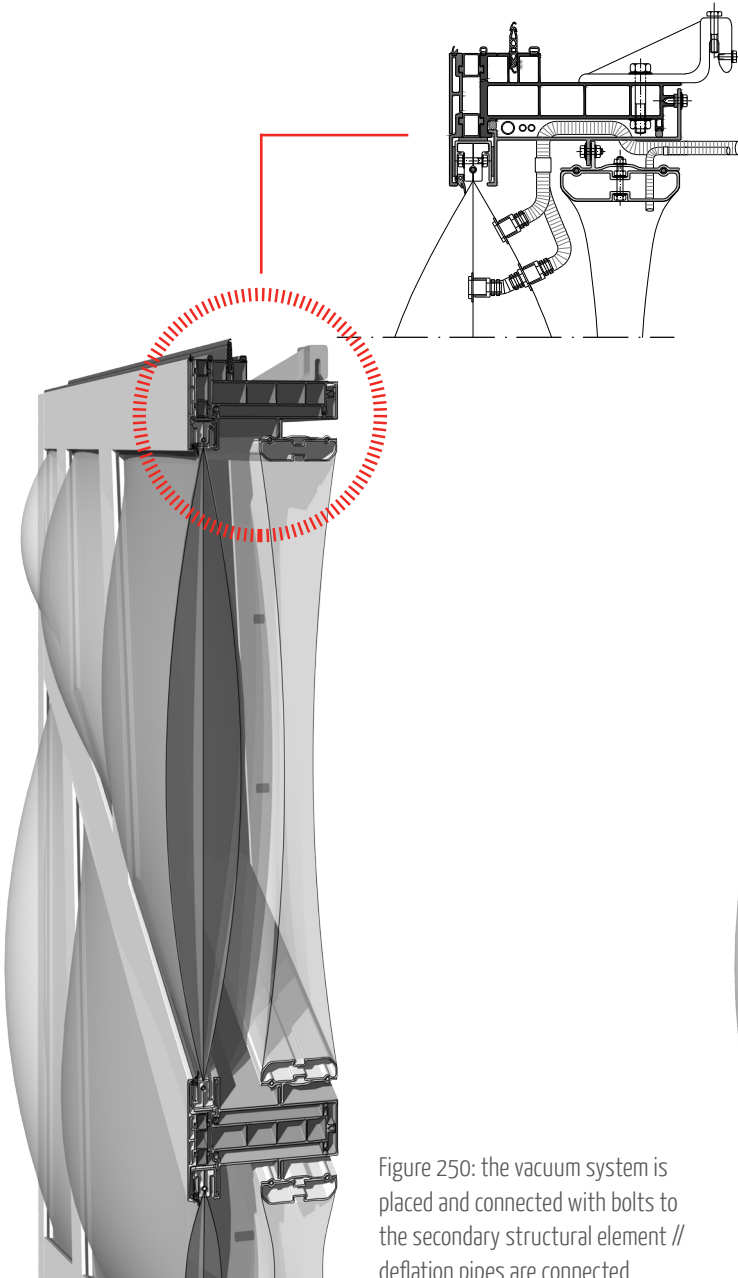


Figure 250: the vacuum system is placed and connected with bolts to the secondary structural element // deflation pipes are connected

6

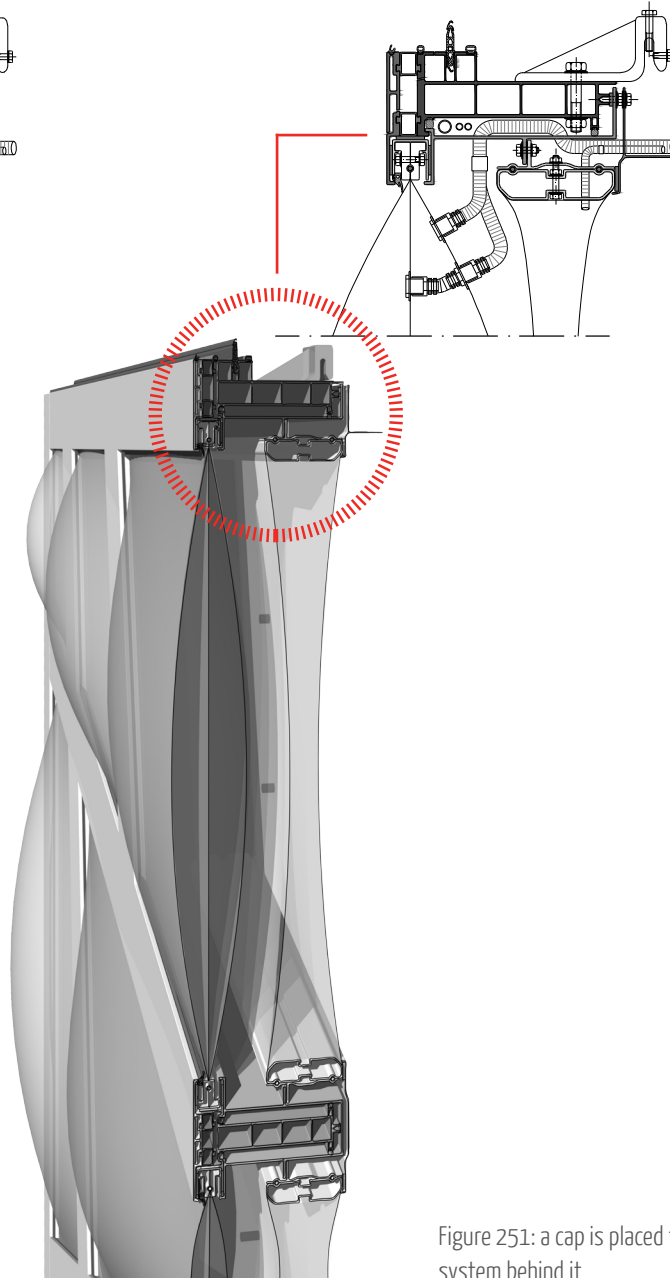


Figure 251: a cap is placed to cover the system behind it

7

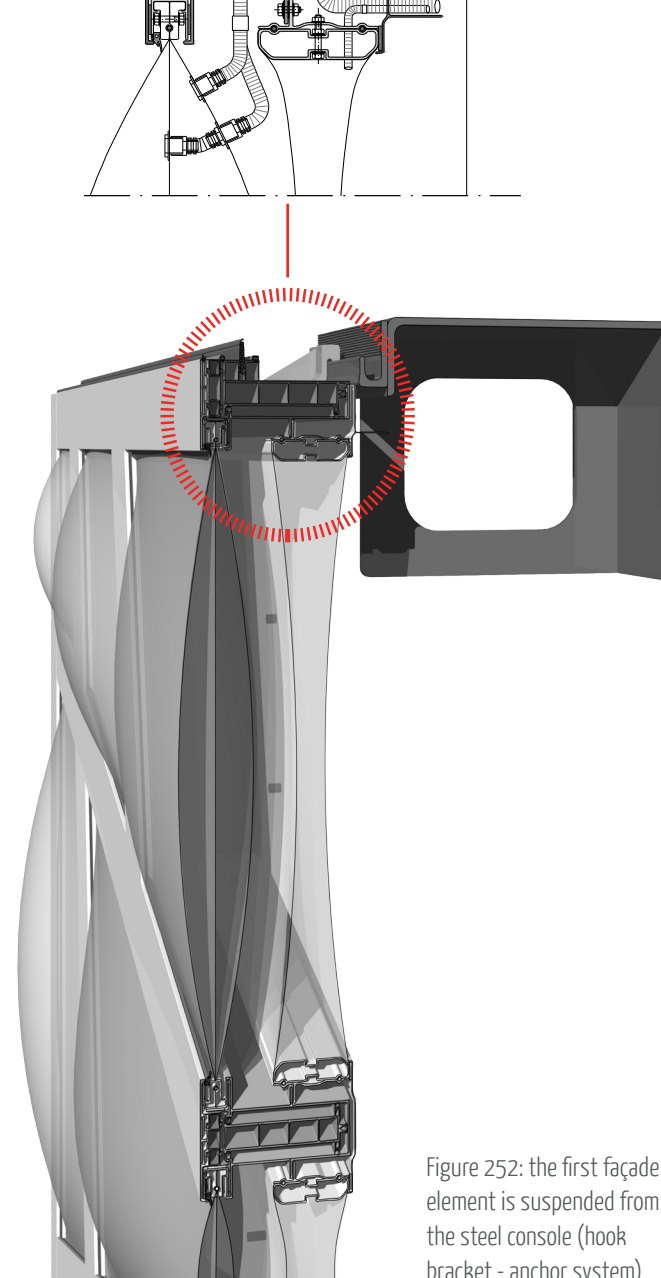


Figure 252: the first façade element is suspended from the steel console (hook bracket - anchor system)

8

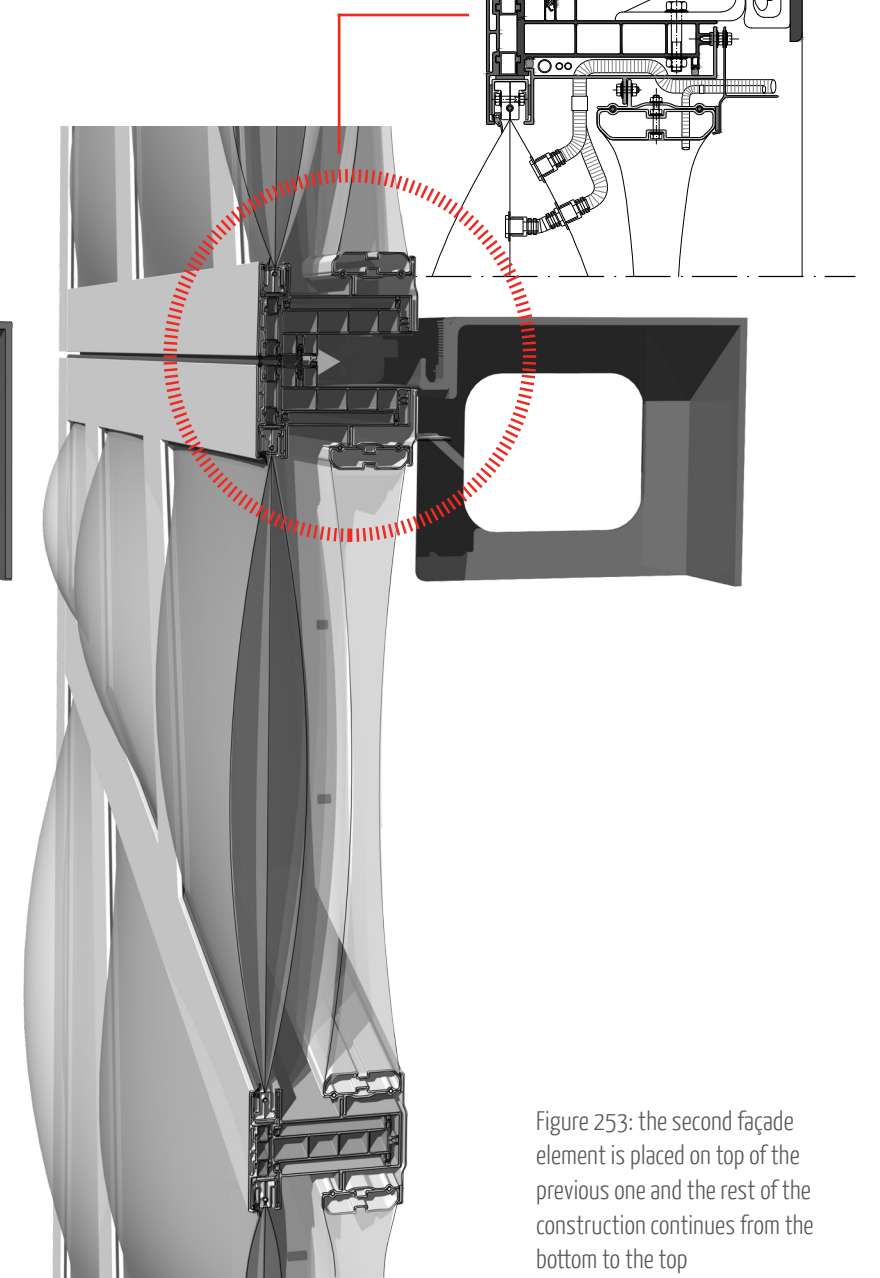
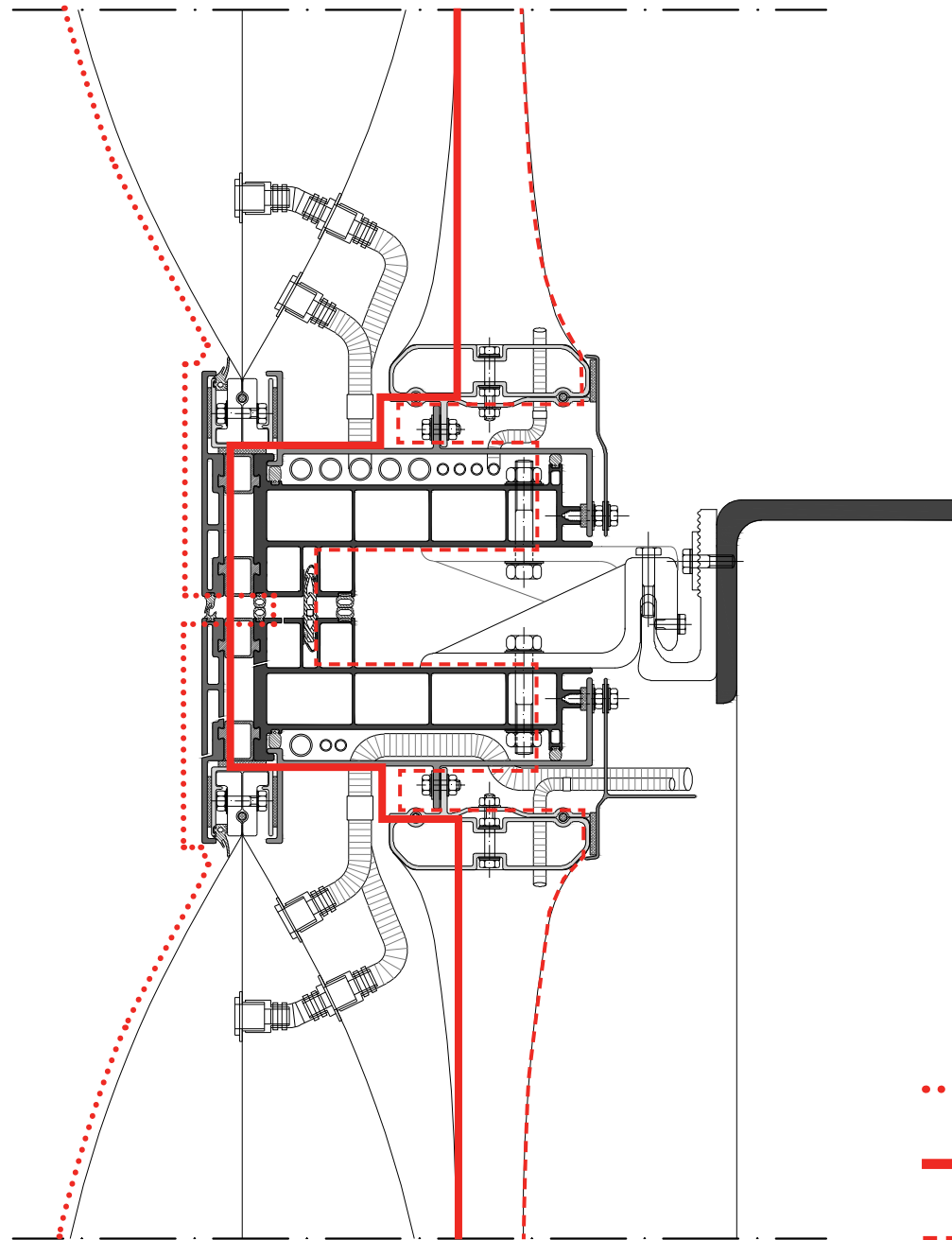


Figure 253: the second façade element is placed on top of the previous one and the rest of the construction continues from the bottom to the top

lines of defense



- watertight line
- insulation line
- - - - airtightness line

3D detail impression



3D impressions



Figure 254: view to the outside from the offices space

3D impressions

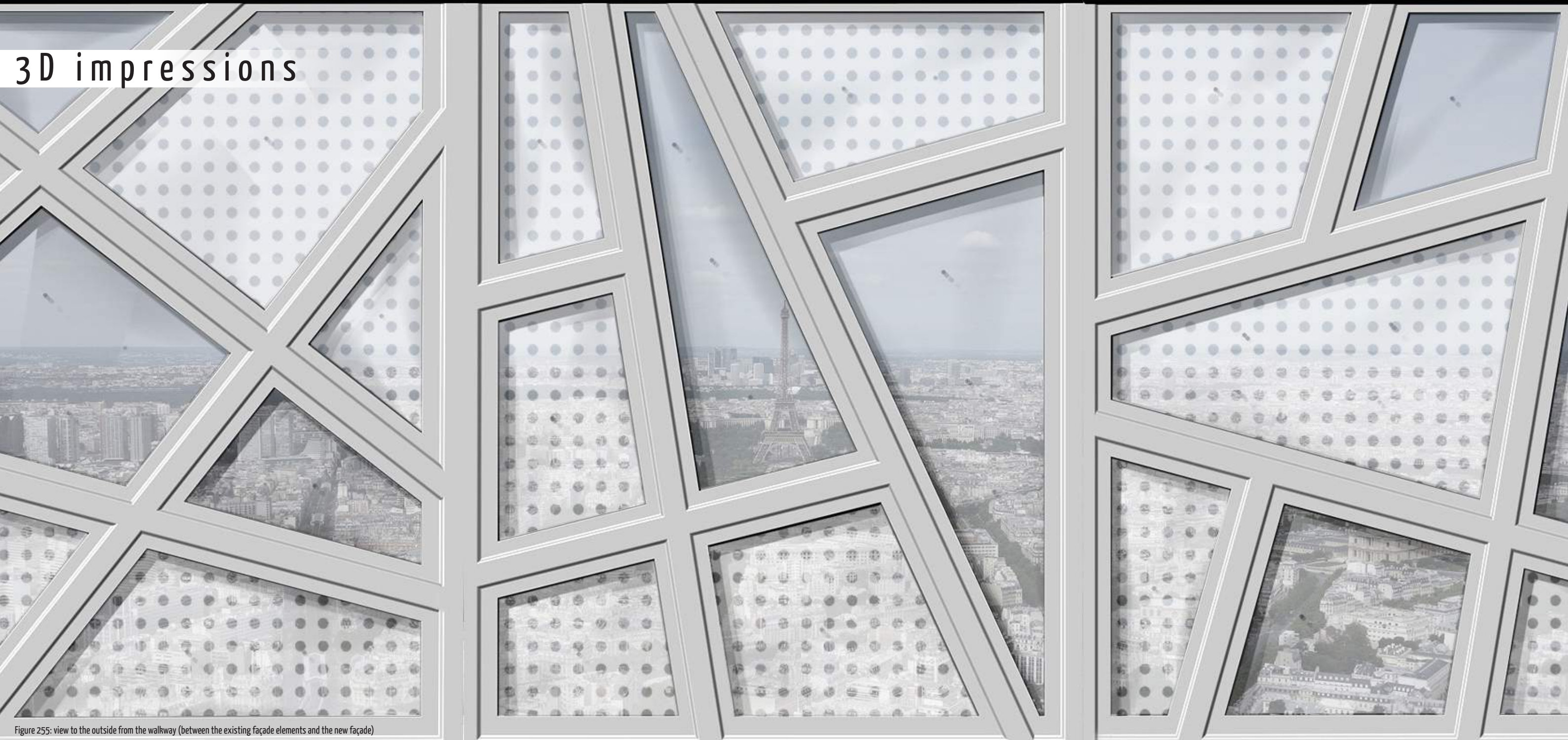


Figure 255: view to the outside from the walkway (between the existing façade elements and the new façade)

3D impressions

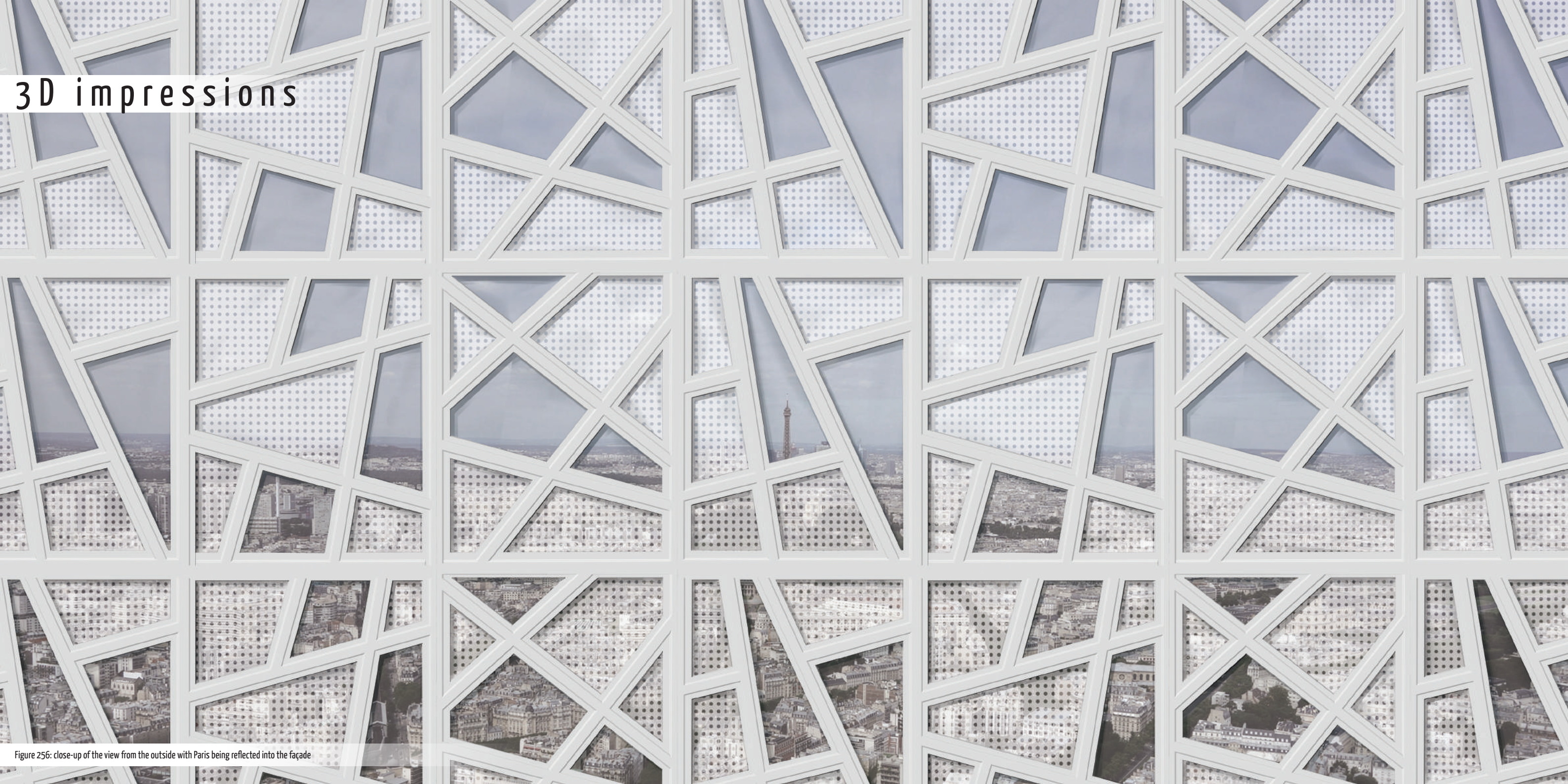


Figure 256: close-up of the view from the outside with Paris being reflected into the façade

physical model 1:10



Figure 257: cardboard base for the clay



Figure 258: clay forming "bubbles" placed in the cardboard base



Figure 259: internal parts are removed



Figure 260: clay forming "bubbles" placed in the cardboard base



Figure 261: vacuum forming of a plastic sheet with clay as a mould



Figure 262: inflated cushion and vacuum system formed



Figure 263: vacuum cushion back side



Figure 264: inflated cushion front side

safety & maintenance

safety of cushion structures

The inflated cushions function while maintaining the inner pressure level at a constant condition. However, there is a chance of failure that should be taken into account in order to avoid serious damages. There are two cases that should be considered: failure of the air supply and local damage of the membrane (holes). Neither of these situations has as a result the total failure of the structure. On the contrary, an overpressure is maintained in the cushions for some time and the only thing that is happening is that the membranes lose gradually their prestress. Most systems include sensors that control the pressure and prevent such problems of failure. Every inflation unit should include two fans that ensure the constant operation of the whole inflation system and also they are provided by backup generators as well (Knippers,2011) .

fire safety

When referring to a membrane structure, one of the first issues that occurs is that of fire safety. The positive argument for the ETFE foil is that it is self-distinguishing, meaning that under fire conditions it shrinks away allowing the smoke and the fire to be vented to the exterior.¹ Furthermore, the melted material solidifies quickly and so it's not "dripping".² It has low

flammability (270°C) and according to DIN 4102 it has been rated as fire class B1. However, in some cases it cannot be guaranteed that fire will reach the ETFE at the temperature that will cause its failure. Thus, it is advised to install automatic actuators in order to ventilate the space from the smoke.² Another solution would be to coat the membrane with a fire spray or a fire-resistant intumescent paint. Lastly, fire safety systems, like sprinklers and smoke exhaust, as mentioned above, are usually necessary for safety reasons.³



Figure 265: fire test of ETFE (source: Behling, S., Brensing, C., Fuchs, A., Ingenhoven, C., 20101, Innovative Design and Construction, DETAIL, page 49)

sources:

1. Charbonneau, L., (2011), Time-Dependent Tensile Properties of ETFE Foils, Waterloo, Ontario, Canada, page 3
2. Behling, S., Brensing, C., Fuchs, A., Ingenhoven, C., 20101, Innovative Design and Construction, DETAIL, page 49
3. <http://www.architen.com/articles/etfe-foil-a-guide-to-design/>
4. <http://architectureau.com/articles/practice-23/>

material's delicacy & safety barrier

Another crucial issue is that of safety/explosion risk. As a flexible material, ETFE foil can take very high loads for a short period of time, which makes it suitable for use in locations where there is a high risk of explosion. As far as vandalism is concerned, due to the fact that each cushion is independent from each other in terms of structure and air supply, if there is a damage in one of them it will not affect the rest. Also, the cushions will not break or fall out of their frames when damaged.³ Last but not least, users' safety is a priority and for this reason an internal railing is installed and connected to the main elements of the structure, so as to prevent the occupants from being in direct contact with the inflated/ deflated cushions.

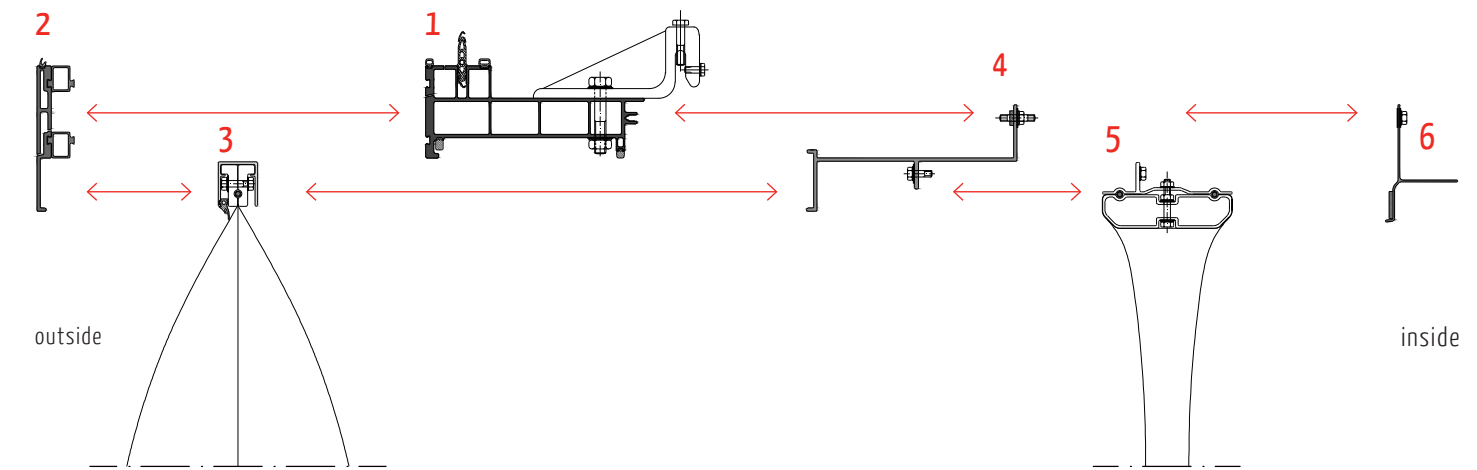


Figure 266: assembly/disassembly and replacement strategy

maintenance & replacement

In high-rises maintenance constitutes another critical aspect. Firstly, ETFE foil has self-cleaning properties, as already mentioned, which means that it requires less cleaning or even any at all. Moreover, the way the details are designed for the whole façade element makes the replacement possible from the inside for both the inflated cushions and the vacuum system. It is a demountable system that allows complete access to all of its parts from the interior. As it can be seen from the scheme below (figure 266), first the vacuum system can be taken out and subsequently the inflated cushion.

conclusions

conclusions

overall assessment

In order to draw several conclusions about the whole project, it will be useful to recall the main research question that was raised in the very beginning, along with the sub-questions.

main research question

“How can an adaptive, lightweight and flexible fabric façade be designed, a façade that will be responsible for meeting the requirements and improving the indoor comfort in terms of thermal and acoustical insulation, as well as shading and sun control in a high-rise in Paris?”

sub questions

1. Which are the main problems of high-rises that should be tackled? Which among them occur in the chosen location?
2. Which are the most suitable fabrics/textiles as a solution to the above problems? Do they meet the building envelope requirements?
3. Which is the most effective façade design that meets all the requirements?

4. How can the desired adaptivity be achieved? With what kind of mechanisms?

If all these questions can be answered in the end then it means that the project managed to provide a successful solution for the above aspects that required one.

1. Which are the main problems of high-rises that should be tackled? Which among them occur in the chosen location?

One of the main problems that high-rises have to deal with is the high wind forces that are developed at big heights. As it was proven from the rough calculations that were conducted in order to determine the wind loads on the designed façade elements, the chosen frames are able to withstand these forces and therefore the façade is successfully designed in that sense.

Furthermore, another issue of high-rises is the erection and the assembly process of the façade elements. Since the designed panel is firstly fully prefabricated and then transported and assembled on site, this results in less construction time, less auxiliary equipment and consequently it is cost-efficient.

Lastly, the maintenance of the façade is also an important

aspect, as well as the replacement of certain components in case of damage. As already described, the ETFE has self-cleaning properties and every part of the façade element is accessible from the interior space.

2. Which are the most suitable fabrics/textiles as a solution to the above problems? Do they meet the building envelope requirements?

After the research that was made in the literature part, the material that was chosen to be used for the specific project is the ETFE foil. The reasons for this decision are the following. Firstly, the ETFE has a high tensile strength compared to the other membrane materials that were investigated. It provides different levels of transparency (possible light transmittance of 90% and above) and a variety of colours. In addition, it has an excellent UV-resistance, with the suitable coatings it can be completely watertight and also it has self-cleaning properties, important aspect concerning its maintenance. Moreover, it offers the possibility of printing, something that can be used for sun shading for instance. As far as fire resistance is concerned, the ETFE is self-distinguishing and it has been rated as fire class B1 according to DIN 4102. Lastly, it allows for the formation of cushions, which means the creation of multiple air cavities that improve the thermal insulation of the inflated system.

3. Which is the most effective façade design that meets all the requirements?

As the project concerns a façade element, the design has to fulfill the building envelope requirements. More specifically, the designed panel has to provide thermal insulation, which is possible with the formation of multiple air chambers in the cushions system, as it was mentioned previously. Furthermore, the acoustic insulation is achieved with the cavities system, the same way that glass units provide airborne sound insulation and also with the vacuum system the sound insulation is supposed to be increased tremendously, as with the absence of air no sound transmission can occur.

Additionally, the air and watertightness are ensured from the total prefabrication of the façade elements that they only need to be assembled on site.

Lastly, the efficient replacement concept (having all the components accessible from the inside), constitutes a main advantage of this design solution.

4. How can the desired adaptivity be achieved? With what kind of mechanisms?

As far as the adaptivity aspect is concerned, there is an adaptive sun shading system integrated into several of the inflated cushions. The outer and middle layer of the cushion have opposite printed patterns and with the inflation and deflation of the two air chambers the middle layer can move towards the outer layer and backwards, blocking and letting respectively the light into the interior space. This constitutes a simple system with no additional mechanism and it can be adjustable to the occupants' needs, either automatically or manually.

It seems that all the questions that were set in the beginning of the graduation project are answered rather successfully and therefore the design proposal can be considered in general effective and successful as well.

further development

Although the designed solution was proved to be rather successful, further development can be made to improve certain features. Firstly, more structural calculations could be made with the use of FEM analysis software, for instance, in order to obtain more accurate results. As for the spacers in the vacuum system, more calculations could be conducted concerning point loads on the spacers from the membrane due to high pressures, as well as more research could be done about the spacers' material, the thermal and acoustical performance.

Moreover, the acoustic test for the vacuum element remained incomplete, as explained in the building physics chapter. It would be rather interesting, though, to reach the desired air pressure of 0.2 bar (or even lower if that is possible) and actually test the theory of having no sound transmission with no air present, but in order to achieve this the testing model has to be constructed professionally and also suitable equipment should be available. As it is already mentioned, the spacers play a significant role for the membranes to remain intact and thus they would have to be from the right material, formed into the correct shape, cut in the required size, smoothed

as much as possible, aligned perfectly perpendicularly to the foils and be provided with a solid solution in order to stay in place.

In addition, another aspect that was mentioned in the building physics chapter is the integration of openings into the façade element and thus the availability of natural ventilation. The version of having natural ventilation was investigated in the simulations with the Design Builder software and it was proved that the maximum indoor air temperatures, without having the cooling turned on, are significantly reduced than the case without any natural ventilation. Therefore, it would be interesting to investigate whether the integration of openings in the proposed design is possible or what could be altered in the design in order to include openings as well.

Lastly, another future proposal would be to integrate a system into the façade element that would generate energy and therefore compensate for the energy needed for cooling purposes, which is rather important and cannot be ignored in any case. Such solution would be the integration of PV cells in the outer layer of the inflated membrane cushion. This is

possible, as analysed previously, with the development of PV flexibles (films) that are compatible with membranes and can be easily integrated in them. The result is a very thin and lightweight film, which is rather flexible and suitable for use in membranes structures. The rough calculations that were conducted concerning the integration of PV films showed that with 16% efficiency, which concerns an improved version of PV films in the near future, the energy gains constitute approximately the 1/10 of the total consumed energy. Consequently, it is a solution that should be considered.

10

references

references

bibliography

1. Garbe, T., editors: Lang, W., McClain, A., *Tents, Sails, and Shelter: Innovations in Textile Architecture*, (based on a presentation by Dr. Jan Cremers)
2. Jeska, S., (2008), *Transparent Plastics, Design and technology*, Basel, Boston, Berlin, Birkhäuser
3. Knaack, U., Klein, T., (2010), *The future envelope 3: façades - the making of*, IOS Press and the Authors
4. Krippners, Herzog, R., Lang, T., Werner, (2004), *Facade Construction Manual*, Birkhäuser Verlag GmbH
5. Pohl, G., (2010), *Textiles, Polymers and Composites for Buildings*, Woodhead Publishing
6. Knippers, Cremers, Gabler, Lienhard, (2011), *Construction manual for polymers + membranes : materials semi-finished products form-finding design*, Basel, Boston, Berlin, Birkhäuser Verlag GmbH
7. Motro, R. (Ed.), (2013), *Flexible Composite Materials in Architecture, Construction and Interiors*, Basel, Birkhäuser Verlag GmbH
8. Llorens, J., (2015), *Fabric Structures in Architecture*, Cambridge UK, Woodhead Publishing
9. Knaack, U., Klein, T., Bilow, M., (2008), *Deflateables*, Rotterdam, 010 Publishers
10. Knaack, U., Klein, T., Bilow, M., (2008), *Imagine 01 – Façades*, Rotterdam, 010 Publishers
11. Eisele, J., Kloft, E., (2003), *High-Rise Manual: Typology and Design, Construction and Technology*, Basel, Boston, Berlin, Birkhäuser
12. Gräwe, C., Cachola Schmal, P., (2007), *Contemporary highrise architecture and the international highrise award 2006*, Jovis
13. Hemel, M., Kuit, B., (2010), *Supermodel: making one of the world's tallest tower*, nai010 publishers
14. Bessey, R.P., 2012, *Structural Design of Flexible ETFE Atrium Enclosures Using a Cable-Spring Support System*, Brigham Young University - Provo, Master of Science thesis
15. Watts, A., 2014, *Modern Construction Envelopes*, Birkhäuser
16. Charbonneau, L., (2011), *Time-Dependent Tensile Properties of ETFE Foils*, Waterloo, Ontario, Canada
17. Behling, S., Brensing, C., Fuchs, A., Ingenhoven, C., (2010), *Innovative Design and Construction*, DETAIL
18. Vries, the JJE. (2011). Triple-layer membrane structures Sound insulation performance and practical solutions (Master Thesis TU Delft). Consulted <https://repository.tudelft.nl/islandora/search/?collection=education>
19. Knaack, U., Klein, T., Bilow, M., Auer, T., (2007), *Façades: Principles of Construction*, Birkhäuser
20. Van de Koppel, W. J., & Van Dijck, S. H. M. (2013). *Rigidized inflatable structures: An innovative production method for structurally optimized elements*. (Master Thesis TU Eindhoven / Retrieved from <http://alexandria.tue.nl/extra2/afstversl/bwk/761286a.pdf>)
21. Gumm, M. (2008), *Integrating Photovoltaics Building Envelope Onto Surfaces* (Retrieved from <http://rci-online.org/wp-content/uploads/2008-12-gumm.pdf>)
22. Building Acoustics notes, chapter 4: Airbourne sound insulation of cavity constructions
23. Building Physics, chapter 2: Glazing properties and their effect on the insulation and heat admittance in a building

web sources

1. <http://www.rt-batiment.fr/batiments-neufs/reglementation-thermique-2012/presentation.html>
2. https://fr.wikipedia.org/wiki/Climat_de_Paris
3. <https://weather-and-climate.com/average-monthly-Rainfall-Temperature-Sunshine,Paris,France>
4. <http://www.detail-online.com/article/london-2012-olympic-shooting-venues-16398/>
5. <https://www.dezeen.com/2012/06/12/olympic-shooting-venue-by-magma-architecture/>
6. <http://www.archdaily.com/244370/olympic-shooting-venue-magma-architecture>
7. <https://www.festo.com/net/SupportPortal/Files/8574>
8. <https://www.dezeen.com/2010/04/27/german-pavilion-by-schmidhuber-partner/>
9. <http://www.e-architect.co.uk/shanghai/shanghai-expo-german-pavilion>
10. http://www.solardecathlon.gov/past/pdfs/07_talking_points/07_georgia_tech.pdf
11. <http://www.gmp-architekten.com/projects/olympic-stadium-reconstruction-and-roofing.html>
12. <http://www.e-architect.co.uk/berlin/olympic-stadium-building>
13. <http://www.e-architect.co.uk/dubai/burj-al-arab>
14. <https://www.dezeen.com/2008/02/06/watercube-by-chris-bosse/>
15. http://www.arup.com/projects/chinese_national_aquatics_center
16. <http://www.e-architect.co.uk/beijing/watercube-beijing>
17. <http://architectureau.com/articles/practice-23/>
18. https://en.wikipedia.org/wiki/List_of_tallest_buildings_and_structures_in_the_Paris_region

19. <http://www.citylab.com/design/2013/09/could-city-light-become-city-height/6953/>
20. <http://parispropertygroup.com/blog/2015/rise-paris-city-center-skyscrapers/>
21. http://faculty.arch.tamu.edu/media/cms_page_media/4433/TurningTorso.pdf
22. www.opvius.com
23. <https://www.electronics-cooling.com/2002/11/the-thermal-conductivity-of-air-at-reduced-pressures-and-length-scales/>
24. https://en.wikipedia.org/wiki/Thin-film_solar_cell#Efficiencies
25. <https://solarenergylocal.com/states/arkansas/paris/>
26. <http://www.alforte.org/media/doc/NRG-systems/zonnepaneel%20reductie.pdf>
27. <http://www.architen.com/articles/etfe-foil-a-guide-to-design/>
28. <http://www.wikihow.com/Calculate-Wind-Load>
29. <http://www.constructiononline.eu/ligger.php>
30. http://www.engineersedge.com/beam_bending/beam_bending1.htm | <http://www.constructiononline.eu/ligger.php>
31. http://www.engineersedge.com/calculators/section_square_case_10.htm | <http://www.constructiononline.eu/ligger.php>
32. <http://architectureau.com/articles/practice-23/>



11

appendix

Construction | Openings | Lighting | HVAC | Generation | Outputs | CFD

Glazing Template

Template **Project glazing template**

External Windows

Glazing type **ETFE cushion with SPACERS (simple)**

Layout **Preferred height 1.5m, 60% glazed**

Dimensions

Type **6-Fill surface (100%)**

Reveal

Frame and Dividers

Has a frame/dividers?

Construction **Aluminium window frame (with thermal break)**

Dividers

Type 1-Divided lite

Width (m) **0.0100**

Horizontal dividers 1

Vertical dividers 1

Outside projection (m) 0.000

Inside projection (m) 0.000

Glass edge-centre conduction ratio 1.000

Frame

Frame width (m) **0.0200**

Frame inside projection (m) 0.000

Frame outside projection (m) 0.000

Glass edge-centre conduction ratio 1.000

Shading

Window shading

Local shading

Airflow Control Windows

Airflow control

Free Aperture

Informal Windows

Sloped Roof Windows/Skylights

Dividers

Vents

Construction | Openings | Lighting | HVAC | Generation | Outputs | CFD

HVAC Template

Template **Fan Coil Unit (4-Pipe), Air cooled Chiller**

Mechanical Ventilation

On

Outside air definition method 2-Min fresh air (1Per person)

Operation

Schedule **Office_OpenOff_Occ**

Economiser (Free Cooling)

Heat Recovery

Auxiliary Energy

Heating

Heated

Fuel 2-Natural Gas

Heating system seasonal CoP 0.850

Type

Operation

Schedule **Office_OpenOff_Heat**

Cooling

Cooled

Cooling system **Default**

Fuel 1-Electricity from grid

Cooling system seasonal CoP 1.800

Supply Air Condition

Operation

Schedule **Office_OpenOff_Cool**

Humidity Control

DRW

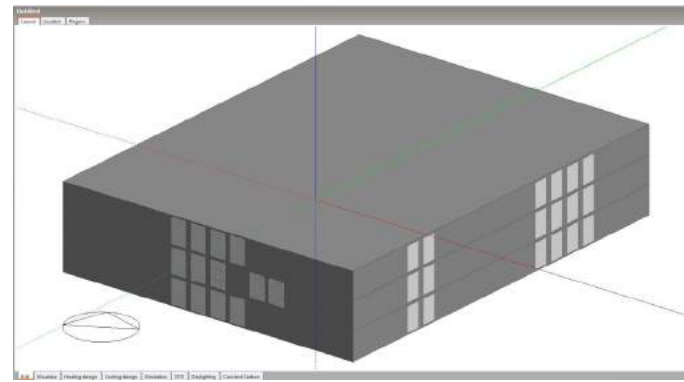
Natural Ventilation

On

Earth Tube

Air Temperature Distribution

Cost



Info, Data

Help | Close

Schedules

Data Report (Not Editable)

General

Office_OpenOff_Occ

Building: OFFICE Area OPEN PLAN OFFICE Occupancy schedule

UK NCM

Offices / Workshop/businesses

General

Region

Schedule type

2-Compact Schedule

Profiles

Schedule Compact

Office_OpenOff_Occ

Fraction

Through 31 Dec

For: Weekdays SummerDesignDay

Until: 07.00, 0

Until: 08.00, 0.25

Until: 09.00, 0.5

Until: 12.00, 1

Until: 14.00, 0.75

Until: 17.00, 1

Until: 18.00, 0.5

Until: 19.00, 0.25

Until: 24.00, 0

For: Weekends

Until: 24.00, 0

For: Holidays

Until: 24.00, 0

For: WinterDesignDay AllOtherDays

Until: 24.00, 0

W7A - Glass Library (C:\Users\Public\Documents\BIMBA\W7A.rvt)

EP 6007 Thickness: 38 mm

Name: EP6007

Product Name: EP6007

Manufacturer: Corning

City: Glastonbury

Country: GB

Type: Mirrored

Conductivity: 0.86 W/mK

Side

Trans. Front (Tco) 0.758

Trans. Back (Tcb) 0.758

Reflec. Front (Rco) 0.05

Reflec. Back (Rcb) 0.05

Visible

Trans. Front (Tco) 0.758

Trans. Back (Tcb) 0.758

Reflec. Front (Rco) 0.05

Reflec. Back (Rcb) 0.05

IR

Trans (Tco) 0.08

Emis. Front (Eco) 0.04

Emis. Back (Ecb) 0.04

Color: Blending Specular

Download

W7A - Glass Library (C:\Users\Public\Documents\BIMBA\W7A.rvt)

EP 6008 Thickness: 61 mm

Name: EP6008

Product Name: EP6008

Manufacturer: Corning

City: Glastonbury

Country: GB

Type: Mirrored

Conductivity: 0.74 W/mK

Side

Trans. Front (Tco) 0.634

Trans. Back (Tcb) 0.634

Reflec. Front (Rco) 0.05

Reflec. Back (Rcb) 0.05

Visible

Trans. Front (Tco) 0.634

Trans. Back (Tcb) 0.634

Reflec. Front (Rco) 0.05

Reflec. Back (Rcb) 0.05

IR

Trans (Tco) 0.08

Emis. Front (Eco) 0.04

Emis. Back (Ecb) 0.04

Color: Blending Specular

Download

W7A - Glass Library (C:\Users\Public\Documents\BIMBA\W7A.rvt)

EP 6007 Name: EP6007 Thickness: 38 mm

Product Name: EP6007

Manufacturer: Corning

City: Glastonbury

Country: GB

Type: Mirrored

Conductivity: 0.86 W/mK

Side

Trans. Front (Tco) 0.758

Trans. Back (Tcb) 0.758

Reflec. Front (Rco) 0.05

Reflec. Back (Rcb) 0.05

Visible

Trans. Front (Tco) 0.758

Trans. Back (Tcb) 0.758

Reflec. Front (Rco) 0.05

Reflec. Back (Rcb) 0.05

IR

Trans (Tco) 0.08

Emis. Front (Eco) 0.04

Emis. Back (Ecb) 0.04

Color: Blending Specular

Download

ID	Name	Mode	Thick	U	g	U	g	U	g	U	g	U	g	U	g	U	g	U	g
1	W7A - Glass Library	W7A	38	0.86	0.05	0.05	0.05	0.05	0.05	0.05	0.05	0.05	0.05	0.05	0.05	0.05	0.05	0.05	0.05
2	W7A - Glass Library	W7A	61	0.74	0.05	0.05	0.05	0.05	0.05	0.05	0.05	0.05	0.05	0.05	0.05	0.05	0.05	0.05	0.05

Construction | Openings | Lighting | HVAC | Generation | Outputs | CFD

Lighting Template

Template **Reference**

General Lighting

On

Normalised power density (W/m2-100 lux) **1.0000**

Schedule **Office_OpenOff_Light**

Luminaire type 1-Suspended

Radiant fraction 0.420

Visible fraction 0.180

Convective fraction 0.400

Lighting Control

On

Task and Display Lighting

On

Exterior Lighting

On

Cost

Edit construction - Concrete Wall Nick

Constructions Data

Layers | Surface properties | Image | Calculated | Cost | Condensation analysis

General

Name **Concrete Wall Nick**

Source

Category **Walls**

Region **General**

Definition

Definition method 1-Layers

Calculation Settings

Layers

Number of layers **2**

Outermost layer

Material **Concrete, cast - dense reinforced**

Thickness (m) **0.2000**

Bridged?

Innermost layer

Material **EPS Expanded Polystyrene (Standard)**

Thickness (m) **0.0300**

Bridged?

Model data

Insert layer | Delete layer

W7A - Glass Library (C:\Users\Public\Documents\BIMBA\W7A.rvt)

EP 6009 Thickness: 61 mm

Name: EP6009

Product Name: EP6009

Manufacturer: Corning

City: Glastonbury

Country: GB

Type: Mirrored

Conductivity: 0.74 W/mK

Side

Trans. Front (Tco) 0.634

Trans. Back (Tcb) 0.634

Reflec. Front (Rco) 0.05

Reflec. Back (Rcb) 0.05

Visible

Trans. Front (Tco) 0.634

Trans. Back (Tcb) 0.634

Reflec. Front (Rco) 0.05

Reflec. Back (Rcb) 0.05

IR

Trans (Tco) 0.08

Emis. Front (Eco) 0.04

Emis. Back (Ecb) 0.04

Color: Blending Specular

Download

W7A - Glass Library (C:\Users\Public\Documents\BIMBA\W7A.rvt)

EP 6010 Thickness: 61 mm

Name: EP6010

Product Name: EP6010

Manufacturer: Corning

City: Glastonbury

Country: GB

Type: Mirrored

Conductivity: 0.74 W/mK

Side

Trans. Front (Tco) 0.634

Trans. Back (Tcb) 0.634

Reflec. Front (Rco) 0.05

Reflec. Back (Rcb) 0.05

Visible

Trans. Front (Tco) 0.634

Trans. Back (Tcb) 0.634

Reflec. Front (Rco) 0.05

Reflec. Back (Rcb) 0.05

IR

Trans (Tco) 0.08

Emis. Front (Eco) 0.04

Emis. Back (Ecb) 0.04

Color: Blending Specular

Download

W7A - Glass Library (C:\Users\Public\Documents\BIMBA\W7A.rvt)

EP 6007 Name: EP6007 Thickness: 38 mm

Product Name: EP6007

Manufacturer: Corning

City: Glastonbury

Country: GB

Type: Mirrored

Conductivity: 0.86 W/mK

Side

Trans. Front (Tco) 0.758

Trans. Back (Tcb) 0.758

Reflec. Front (Rco) 0.05

Reflec. Back (Rcb) 0.05

Visible

Trans. Front (Tco) 0.758

Trans. Back (Tcb) 0.758

Reflec. Front (Rco) 0.05

Reflec. Back (Rcb) 0.05

IR

Trans (Tco) 0.08

Emis. Front (Eco) 0.04

Emis. Back (Ecb) 0.04

Color: Blending Specular

Download

ID	Name	Mode	Thick	U	g	U	g	U	g	U	g	U	g	U	g	U	g	U	g
1	W7A - Glass Library	W7A	38	0.86	0.05	0.05	0.05	0.05	0.05	0.05	0.05	0.05	0.05	0.05	0.05	0.05	0.05	0.05	0.05
2	W7A - Glass Library	W7A	61	0.74	0.05	0.05	0.05	0.05	0.05	0.05	0.05	0.05	0.05	0.05	0.05	0.05	0.05	0.05	0.05

cooling & heating on

Activity Construction Openings Lighting HVAC Outputs CFD

Activity Template: Generic Office Area

Zone type: 1-Standard

Zone multiplier: 1

Include zone in thermal calculations:

Include zone in Radiance daylighting calculations:

Floor Areas and Volumes

Density (people/m2): 0.0800

Schedule: Office_OpenOff_Occ

Metabolic

Generic Contaminant Generation

DRW

Environmental Control

Heating Setpoint Temperatures

Heating (°C): 21.0

Heating set back (°C): 15.0

Cooling Setpoint Temperatures

Cooling (°C): 25.0

Cooling set back (°C): 28.0

Humidity Control

Ventilation Setpoint Temperatures

Natural Ventilation

Minimum Fresh Air

Fresh air (l/s-person): 9.000

Mech vent per area (l/s-m2): 0.000

Lighting

Target illuminance (lux): 400

Default display lighting density (W/m2): 0

Computers

On

Gain (W/m2): 10.00

Schedule: Office_OpenOff_Equip

Radiant fraction: 0.200

Office Equipment

Miscellaneous

Gathering

Building 1, floor 2, office space 6

Activity Construction Openings Lighting HVAC Outputs CFD

Construction Template

Insulation: Typical ref, Energy code, Best practice

Thermal mass: Light, Medium, Heavy

Construction

External walls: Concrete Wall Nick

Below grade walls: Below grade wall - Typical reference - Medium weight (data)

Flat roof: Combined flat roof - Typical reference - Medium weight (data)

Pitched roof (occupied): Pitched roof - Typical reference - Medium weight (data)

Semi-Exposed

Semi-exposed ceiling: Combined semi-exposed roof - Typical reference - Medium w

Semi-exposed floor: Combined semi-exposed floor Typical reference - Medium we

Floors

Ground floor: Combined ground floor - Typical reference - Medium weight (

Basement ground floor: Combined ground floor - Typical reference - Medium weight (

External floor: Combined external floor - Typical reference - Medium weight (

Internal floor: 100mm concrete slab

Sub-surfaces

Walls: 100mm concrete slab

Internal: 100mm concrete slab

Roof: 100mm concrete slab

External door: Wooden door

Internal Thermal Mass

Construction: 100mm concrete slab

Exposed area (m2): 0.00

Adjoining

Geometry, Areas and Volumes

Surface Connection

Linear Thermal Bridging at Junctions

Activity Mass

Model mitigation

Constant rate (ach): 0.300

Schedule: On 24/7

Delta T and Wind Speed Coefficients

Cost

Building 1, floor 2, office space 6

Activity Construction Openings Lighting HVAC Outputs CFD

Template: Generic Office Area

Zone type: 1-Standard

Zone multiplier: 1

Include zone in thermal calculations:

Include zone in Radiance daylighting calculations:

Floor Areas and Volumes

Density (people/m2): 0.0800

Schedule: Office_OpenOff_Occ

Metabolic

Generic Contaminant Generation

DRW

Environmental Control

Heating Setpoint Temperatures

Heating (°C): 21.0

Heating set back (°C): 15.0

Cooling Setpoint Temperatures

Cooling (°C): 25.0

Cooling set back (°C): 28.0

Humidity Control

Ventilation Setpoint Temperatures

Natural Ventilation

Indoor min temperature control

Min temperature definition: 1-By value

Min temperature (°C): 24.0

Indoor max temperature control

Minimum Fresh Air

Fresh air (l/s-person): 9.000

Mech vent per area (l/s-m2): 0.000

Lighting

Target illuminance (lux): 400

Default display lighting density (W/m2): 0

Computers

On

Gain (W/m2): 10.00

Schedule: Office_OpenOff_Equip

no cooling & ventilation on

Building 1, floor 2, office space 6

Activity Construction Openings Lighting HVAC Outputs CFD

HVAC Template: Fan Coil Unit (4-Pipe), Air cooled Chiller

Mechanical Ventilation

On

Auxiliary Energy

Heating

Heated

Fuel: 2-Natural Gas

Heating system seasonal CoP: 0.850

Type: Operation

Schedule: Office_OpenOff_Heat

Cooling

Cooled

Humidity Control

DRW

Natural Ventilation

On

Outside air definition method: 1-By zone

Outside air (ach): 6.000

Operation

Schedule: Office_OpenOff_Occ

Outdoor Temperature Limits

Outdoor min temperature control

Outdoor max temperature control

Max temperature definition: 1-By value

Max temperature (°C): 24.0

Delta T Limits

Delta T limit control

Delta T definition: 2-By schedule

Delta T schedule: Indoor to Outdoor Delta T for Nat Vent Always -50

Delta T and Wind Speed Coefficients

Heat Mode Zone Equipment

Earth Tube

Air Temperature Distribution

Cost

Activity Construction Openings Lighting HVAC Outputs CFD

Glazing Template: Project glazing template

External Windows

Glazing type: ETFE cushion with spacers (simple)

Layout: Preferred height 1.5m, 60% glazed

Dimensions

Type: 5-Fill surface (100%)

Frame and Dividers

Has a frame/dividers?:

Construction: Aluminium window frame (with thermal break)

Dividers

Type: 1-Divided lite

Width (m): 0.0100

Horizontal dividers: 1

Vertical dividers: 1

Outside projection (m): 0.000

Inside projection (m): 0.000

Glass edge-centre conduction ratio: 1.000

Frame

Frame width (m): 0.0200

Frame inside projection (m): 0.000

Frame outside projection (m): 0.000

Glass edge-centre conduction ratio: 1.000

Shading

Window shading

Type: Low reflectance - low transmittance shade

Position: 3-Outside

Control type: 3-Schedule

Operation

Operation schedule: Office_OpenOff_Occ

Local shading

Airflow Control Windows

Free Aperture

Internal Windows

Sloped Roof Windows/Skylights

Doors

Building 1, floor 2, office space 6

Activity Construction Openings Lighting HVAC Outputs CFD

HVAC Template: Fan Coil Unit (4-Pipe), Air cooled Chiller

Mechanical Ventilation

On

Outside air definition method: 2-Min fresh air (Per person)

Operation

Schedule: Office_OpenOff_Occ

Economiser (Free Cooling)

Heat Recovery

Auxiliary Energy

Pump etc energy (W/m2): 0.0000

Schedule: Office_OpenOff_Occ

Heating

Heated

Fuel: 2-Natural Gas

Heating system seasonal CoP: 0.850

Type: Operation

Schedule: Office_OpenOff_Heat

Cooling

Cooled

Cooling system: Default

Fuel: 1-Electricity from grid

Cooling system seasonal CoP: 1.800

Supply Air Condition

Operation

Schedule: Office_OpenOff_Cool

Humidity Control

DRW

On

Natural Ventilation

On

Earth Tube

Air Temperature Distribution

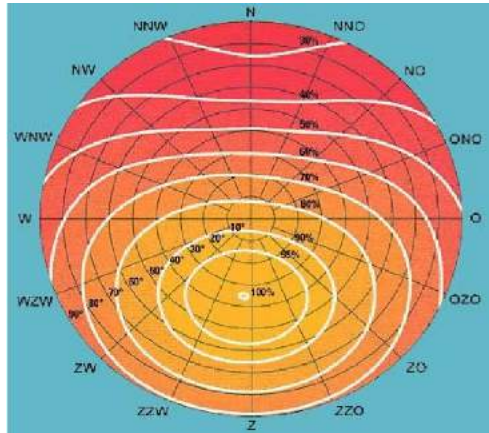
Cost

C. reduction factors for PV calculations



Reductiefactor De positie van het dak en de hellingshoek zijn van grote invloed op wat het geïnstalleerde zonnepaneel kan opbrengen. Het vermogen van het zonnepaneel hangt af van de positie van het dak en de hellingshoek. Onderstaande tabel geeft inzicht in de reductiefactor per specifieke situatie.

C



In de tabel zijn de rekeningen gehouden met de vermindering van de reductiefactor, waaronder:
 - warmtereductie
 - systeemverlies
 - schaduwwerking

dakpositie	dakhellingshoek in graden								
	10	20	30	40	50	60	70	80	90
Oost	0.85	0.83	0.80	0.77	0.73	0.67	0.63	0.56	0.50
* OZO									
* Zuid-oost	0.90	0.92	0.93	0.92	0.90	0.85	0.80	0.73	0.66
* ZZO									
Zuid	0.92	0.94	0.99	0.99	0.97	0.93	0.86	0.80	0.70
* ZZW									
* Zuid-west	0.91	0.93	0.95	0.94	0.92	0.87	0.82	0.75	0.68
* WZW									
West	0.86	0.85	0.82	0.80	0.75	0.70	0.65	0.60	0.55
* WNW									
* Noord-west	0.80	0.74	0.68	0.60	0.54	0.48	0.44	0.40	0.36
* NNW									
Noord	0.78	0.70	0.60	0.50	0.43	0.36	0.32	0.28	0.20
* NNO									
* Noord-oost	0.80	0.73	0.66	0.57	0.53	0.47	0.42	0.38	0.36
* ONO									

* De opbrengst van de zonnepanelen is het nominale vermogen van het zonnepaneel vermenigvuldigd met de reductiefactor.

D. several wind and vacuum forces calculations

Report - Simply supported beam

Input
 Length (l): 3650 mm
 Load (q): 0.07 kNm/m
 Material: Steel
 Profile: Rect. tube

Outside width b: 380 mm
 Outside height h: 300 mm
 Thickness w: 4 mm

Moment of Resistance Wx: 55462 mm³
 Moment of Inertia Ix: 83190 E+03 mm⁴
 Modulus of Elasticity E: 210000 N/mm²

Results
 Max. (bending) moment: 0.12 kNm
 Max. stress: 0.2 N/mm²
 Max. deflection distance: 0 mm

Report - Simply supported beam

Input
 Length (l): 3650 mm
 Load (q): 0.09 kNm/m
 Material: Steel
 Profile: Rect. tube

Outside width b: 380 mm
 Outside height h: 300 mm
 Thickness w: 2 mm

Moment of Resistance Wx: 282605 mm³
 Moment of Inertia Ix: 42391 E+03 mm⁴
 Modulus of Elasticity E: 210000 N/mm²

Results
 Max. (bending) moment: 0.09 kNm
 Max. stress: 0.3 N/mm²
 Max. deflection distance: 0 mm

Report - Simply supported beam

Input
 Length (l): 3650 mm
 Load (q): 0.09 kNm/m
 Material: Steel
 Profile: Rect. tube

Outside width b: 380 mm
 Outside height h: 300 mm
 Thickness w: 3 mm

Moment of Resistance Wx: 419913 mm³
 Moment of Inertia Ix: 62987 E+03 mm⁴
 Modulus of Elasticity E: 210000 N/mm²

Results
 Max. (bending) moment: 0.09 kNm
 Max. stress: 0.2 N/mm²
 Max. deflection distance: 0 mm

Report - Simply supported beam

Input
 Length (l): 3650 mm
 Load (q): 0.07 kNm/m
 Material: Aluminium
 Profile: Rect. tube

Outside width b: 380 mm
 Outside height h: 300 mm
 Thickness w: 2 mm

Moment of Resistance Wx: 282605 mm³
 Moment of Inertia Ix: 42391 E+03 mm⁴
 Modulus of Elasticity E: 100000 N/mm²

Results
 Max. (bending) moment: 0.12 kNm
 Max. stress: 0.4 N/mm²
 Max. deflection distance: 0 mm

Report - Simply supported beam

Input
 Length (l): 3650 mm
 Load (q): 0.07 kNm/m
 Material: Aluminium
 Profile: Rect. tube

Outside width b: 300 mm
 Outside height h: 150 mm
 Thickness w: 2 mm

Moment of Resistance Wx: 101453 mm³
 Moment of Inertia Ix: 7608979 mm⁴
 Modulus of Elasticity E: 71000 N/mm²

Results
 Max. (bending) moment: 0.12 kNm
 Max. stress: 1.1 N/mm²
 Max. deflection distance: 0.3 mm

Report - Simply supported beam

Input
 Length (l): 3650 mm
 Load (q): 0.07 kNm/m
 Material: Aluminium
 Profile: Rect. tube

Outside width b: 300 mm
 Outside height h: 150 mm
 Thickness w: 3 mm

Moment of Resistance Wx: 149579 mm³
 Moment of Inertia Ix: 11218 E+03 mm⁴
 Modulus of Elasticity E: 71000 N/mm²

Results
 Max. (bending) moment: 0.12 kNm
 Max. stress: 0.8 N/mm²
 Max. deflection distance: 0.2 mm

E. preliminary details

